

# GEOLOGIJA

2022 | št.: **65/1**



ISSN

Tiskana izdaja / Print edition: 0016-7789

Spletna izdaja / Online edition: 1854-620X

# GEOLOGIJA

65/1 – 2022



|                  |             |             |              |                  |
|------------------|-------------|-------------|--------------|------------------|
| <b>GEOLOGIJA</b> | <b>2022</b> | <b>65/1</b> | <b>1-123</b> | <b>Ljubljana</b> |
|------------------|-------------|-------------|--------------|------------------|



Izdajatelj: Geološki zavod Slovenije, zanj direktor MILOŠ BAVEC  
Publisher: Geological Survey of Slovenia, represented by Director MILOŠ BAVEC  
Financirata Javna agencija za raziskovalno dejavnost Republike Slovenije in Geološki zavod Slovenije  
Financed by the Slovenian Research Agency and the Geological Survey of Slovenia

**Glavna in odgovorna urednica / Editor-in-Chief: MATEJA GOSAR**

**Tehnična urednica / Technical Editor: BERNARDA BOLE**

#### **Uredniški odbor / Editorial Board**

DUNJA ALJINOVIC  
Rudarsko-geološki naftni fakultet, Zagreb  
MARIA JOÃO BATISTA  
National Laboratory of Energy and Geology, Lisbona  
MILOŠ BAVEC  
Geološki zavod Slovenije, Ljubljana  
MIHAEL BRENCIĆ  
Naravoslovnotehniška fakulteta, Univerza v Ljubljani  
GIOVANNI B. CARULLI  
Dip. di Sci. Geol., Amb. e Marine, Università di Trieste  
KATICA DROBNE  
Znanstvenoraziskovalni center SAZU, Ljubljana  
JADRAN FAGANELI  
Nacionalni inštitut za biologijo, MBP, Piran  
JANOS HAAS  
Etvös Lorand University, Budapest  
BOGDAN JURKOVŠEK  
Geološki zavod Slovenije, Ljubljana  
ROMAN KOCH  
Institut für Paläontologie, Universität Erlangen-Nürnberg

MARKO KOMAC  
Poslovno svetovanje s.p., Ljubljana  
HARALD LOBITZER  
Geologische Bundesanstalt, Wien  
MILOŠ MILER  
Geološki zavod Slovenije, Ljubljana  
RINALDO NICOLICH  
Università di Trieste, Dip. di Ingegneria Civile  
SIMON PIRC  
Naravoslovnotehniška fakulteta, Univerza v Ljubljani  
MIHAEL RIBIČIĆ  
Naravoslovnotehniška fakulteta, Univerza v Ljubljani  
NINA RMAN  
Geološki zavod Slovenije, Ljubljana  
MILAN SUDAR  
Faculty of Mining and Geology, Belgrade  
SAŠO ŠTURM  
Institut »Jožef Stefan«, Ljubljana  
MIRAN VESELIĆ  
Fakulteta za gradbeništvo in geodezijo, Univerza v Ljubljani

Naslov uredništva / Editorial Office: GEOLOGIJA Geološki zavod Slovenije / Geological Survey of Slovenia  
Dimičeva ulica 14, SI-1000 Ljubljana, Slovenija  
Tel.: +386 (01) 2809-700, Fax: +386 (01) 2809-753, e-mail: urednik@geologija-revija.si  
URL: <http://www.geologija-revija.si/>

GEOLOGIJA izhaja dvakrat letno. / GEOLOGIJA is published two times a year.  
GEOLOGIJA je na voljo tudi preko medknjižnične izmenjave publikacij. /  
GEOLOGIJA is available also on exchange basis.



#### **Izjava o etičnosti**

Izdajatelji revije Geologija se zavedamo dejstva, da so se z naglim naraščanjem števila objav v svetovni znanstveni literaturi razmahnil tudi poskusi plagiatorstva, zlorab in prevar. Menimo, da je naša naloga, da se po svojih močeh borimo proti tem pojavom, zato v celoti sledimo etičnim smernicam in standardom, ki jih je razvil odbor COPE (Committee for Publication Ethics).

#### **Publication Ethics Statement**

As the publisher of Geologija, we are aware of the fact that with growing number of published titles also the problem of plagiarism, fraud and misconduct is becoming more severe in scientific publishing. We have, therefore, committed to support ethical publication and have fully endorsed the guidelines and standards developed by COPE (Committee on Publication Ethics).

Baze, v katerih je Geologija indeksirana / Indexation bases of Geologija: Scopus, Directory of Open Access Journals, GeoRef, Zoological Record, Geoscience e- Journals, EBSCOhost

#### **Cena / Price**

Posamezni izvod / Single Issue  
Posameznik / Individual: 15 €  
Institucija / Institutional: 25 €

Letna naročnina / Annual Subscription  
Posameznik / Individual: 25 €  
Institucija / Institutional: 40 €

Tisk / Printed by: GRAFIKA GRACER d.o.o.

**Slika na naslovnih strani:** Antično rudišče Lavrion v Grčiji je vir kristalov pirita z najnižjo kubično 23 simetrijo. Fotografija prikazuje 1,3 × 1,3 mm velik kristal, ki je odraz dvojčenja dveh tetraederskih kristalov pirita s tako simetrijo. (Žorž in sod., članek v tej številki, Igor Dolinar).

**Cover page:** The ancient mine Lavrion in Greece is the source of pyrite crystals with the lowest cubic 23 symmetry. Photograph shows 1,3 × 1,3 mm crystal that reflects twinning of two tetrahedral pyrite crystals with that symmetry. (Žorž et al., paper in this issue, Igor Dolinar).

## VSEBINA – CONTENTS

|   |     |
|---|-----|
| <i>Žorž, M., Voudouris, P. &amp; Rieck, B.</i><br>Pyrite with lower cubic symmetry from Lavrion, Greece ..... 5<br>Pirit z nižjo kubično simetrijo iz Lavriona, Grčija  | 5   |
| <i>Elster, D., Szócs, T., Gál, N., Hansen, B., Voutchkova, D.D., Schullehner, J., Lions, J. Martarelli, L., Giménez-Forcada, E., Díaz-Muñoz, J.Á., Malcuit, E., Schubert, G., Hobiger, G. &amp; Rman, N.</i><br>Terminologies and characteristics of natural mineral and thermal waters in selected European countries ..... 21<br>Izrazoslovje in značilnosti naravnih mineralnih in termalnih voda v izbranih evropskih državah | 21  |
| <i>Ivšinović, J. &amp; Malvić, T.</i><br>Comparison of mapping efficiency for small datasets using inverse distance weighting vs. moving average, Northern Croatia Miocene hydrocarbon reservoir ..... 47<br>Primerjava učinkovitosti kartiranja za majhne podatkovne nize z uporabo metode inverzne utežene razdalje in metode drsečega povprečja v miocenskem rezervoarju ogljikovodikov, Severna Hrvaška                       | 47  |
| <i>Markič, M. &amp; Kanduč, T.</i><br>Carbon isotopic composition of methane and its origin in natural gas from the Petišovci-Dolina oil and gas field (Pannonian Basin System, NE Slovenia) – a preliminary study ..... 59<br>Izotopska sestava ogljika v metanu in njegov izvor v naravnem plinu na območju nafto-plinskega polja Petišovci-Dolina (Panonski bazenski sistem, SV Slovenija) – preliminarna raziskava            | 59  |
| <i>Kralj, P.</i><br>Rare earth elements and yttrium in cold mineral and thermal (~30-60 °C) waters from Tertiary aquifers in the Mura Basin, north-eastern Slovenia: A review ..... 73<br>Elementi redkih zemelj in itrij v hladnih mineralnih in termalnih (~30-60 °C) vodah iz terciarnih vodonosnikov Murskega bazena v severovzhodni Sloveniji: pregled dosedanjih raziskav   | 73  |
| <i>Diercks, M., Grützner, C., Vrabec, M. &amp; Ustaszewski, K.</i><br>Addendum to Diercks et al., 2021: A model for the formation of the Pradol (Pradolino) dry valley in W Slovenia and NE Italy ..... 93  | 93  |
| <i>Brajkovič, R., Gale, L. &amp; Djurić, B.</i><br>Multi-method study of the Roman quarry at Podpeč sedimentary succession and stone products ..... 101<br>Večmetodne raziskave sedimentarnega zaporedja in kamnitih izdelkov rimskodobnega kamnoloma v Podpeči   | 101 |
| Navodila avtorjem ..... 122   | 122 |
| Instructions for authors ..... 123  | 123 |





# Pyrite with lower cubic symmetry from Lavrion, Greece

## Pirit z nižjo kubično simetrijo iz Lavriona, Grčija

Mirjan ŽORŽ<sup>1</sup>, Panagiotis VOUDOURIS<sup>2</sup> & Branko RIECK<sup>3</sup>

<sup>1</sup>Prešernova 53, SI-1290 Grosuplje, Slovenia; e-mail: zorz@siol.net

<sup>2</sup>National and Kapodistrian University of Athens, Faculty of Geology & Geoenvironment,  
Department of Mineralogy and Petrology, University Campus-Zografou, 15784, Athens, Greece;  
e-mail: vourdouris@geol.uoa.gr

<sup>3</sup>Institut für Mineralogie und Kristallographie, Universität Wien, Althanstrasse 14, A-1090 Wien, Austria;  
e-mail: rieckb49@univie.ac.at

Prejeto / Received 4. 10. 2021; Sprejeto / Accepted 15. 7. 2022; Objavljeno na spletu / Published online 22. 7. 2022

*Key words:* Lavrion, pyrite, morphology, tetrahedral crystals, twins, point group 23, crystal structure

*Ključne besede:* Lavrion, pirit, morfoloģija, tetraedrski kristali, dvojčki, točkovna skupina 23, kristalna struktura

### Abstract

In this study, we examined the morphological, chemical, and structural details of tetrahedral pyrite crystals from the Jean Baptiste mine in Lavrion, Greece. Pyrite occurs in three generations. Tetrahedral crystals of the first generation are left- or right-handed with the lowest cubic  $23$  symmetry. In this generation, there are twins with higher cubic  $m\bar{3}$  and hexagonal  $6$  symmetry. All crystals of the second generation are primarily interpenetrated into twins with a cubic  $4m\bar{3}$  symmetry. Some, however, continue to twin up to crystals with the highest cubic  $m\bar{3}m$  and hexagonal  $6mm$  symmetry. Third-generation crystals overgrow second-generation crystals in a non-oriented manner. Chemical analysis confirms chemically pure pyrite, and single-crystal X-ray analysis of the first- and the second-generation crystals confirms the pyrite-specific  $m\bar{3}$  symmetry. The morphology of the single crystals and twins indicates that first generation of single pyrite crystals should have the lowest cubic  $23$  symmetry, which is not confirmed by the structural analysis. This discrepancy may be due to changed pT conditions and the consequent transformation of the original pyrite structure with symmetry  $23$  into a secondary structure with  $m\bar{3}$  symmetry, or to suboptimal conditions in determining the structure by X-ray diffraction.

### Izvleček

V tej študiji smo preučili morfološke, kemijske in strukturne podrobnosti tetraedrsko oblikovanih kristalov piritu iz rudnika Jean Baptiste v Lavrionu. Pirit se pojavlja v treh generacijah. Prvo predstavljajo tetraedrski levo oziroma desno sučni kristali z najnižjo kubično  $23$  simetrijo. V tej generaciji so dvojčki z višjo kubično  $m\bar{3}$  in heksagonalno  $6$  simetrijo. Vsi kristali druge generacije so že primarno zdvočeni do kubične  $4m\bar{3}$  simetrije. Nekateri pa se dvojčijo še naprej dokler ne dosežejo najvišje kubične  $m\bar{3}m$  ali heksagonalne  $6mm$  simetrije. Kristali tretje generacije neorientirano prekrivajo kristale druge generacije. Kemijska analiza potrjuje kemijsko čist pirit, monokristalna rentgenska analiza kristalov prve in druge generacije pa za pirit značilno  $m\bar{3}$  simetrijo. Očitno je torej, da morfološke oblike posameznih kristalov in dvojčkov kažejo na to, da imajo najnižjo kubično simetrijo, česar pa strukturna analiza ne potrjuje. Ta diskrepanca je lahko posledica spremenjenih pT pogojev in posledične transformacije prvotne strukture piritu s simetrijo  $23$  v sekundarno strukturo z  $m\bar{3}$  simetrijo ali pa neoptimalnih pogojev pri določitvi strukture z rentgensko difrakcijo.

### Introduction

Lavrion ore district, located about 50 km southeast of Athens (Greece), is famous for exploitation of silver-rich lead ore during ancient times (Marinos & Petrascheck, 1956). The district includes two extensive mining centers, Plaka and Kamariza, as well as several smaller ones, cov-

ering an outcrop area of about 150 km<sup>2</sup> (Fig. 1a). The Lavrion mines were operated almost continuously from the 4<sup>th</sup> millennium BC until the Late Roman period, and then until late 20<sup>th</sup> century (Conophagos, 1980; Morin & Photiades, 2012). The Lavrion ore district hosts a carbonate-replacement Pb-Zn-Ag-Au deposit (Marinos &

Petrascsek, 1956). It is well established that in addition to the carbonate-replacement style ores, four types of mineralization occur at Lavrion district: porphyry-type Mo-W ores in granodiorite, Cu-Fe-skarns, and Pb-Zn-Ag bearing breccias, and Pb-Zn-Ag-Au rich veins (Skarpelis,

2007; Voudouris et al., 2008; Bonsall et al., 2011; Scheffer et al., 2017, 2019). The ore deposits in Lavrion are structurally and lithologically controlled, and ore formation occurred under extensional kinematic conditions (Skarpelis, 2007; Berger et al., 2013; Scheffer et al., 2017, 2019).

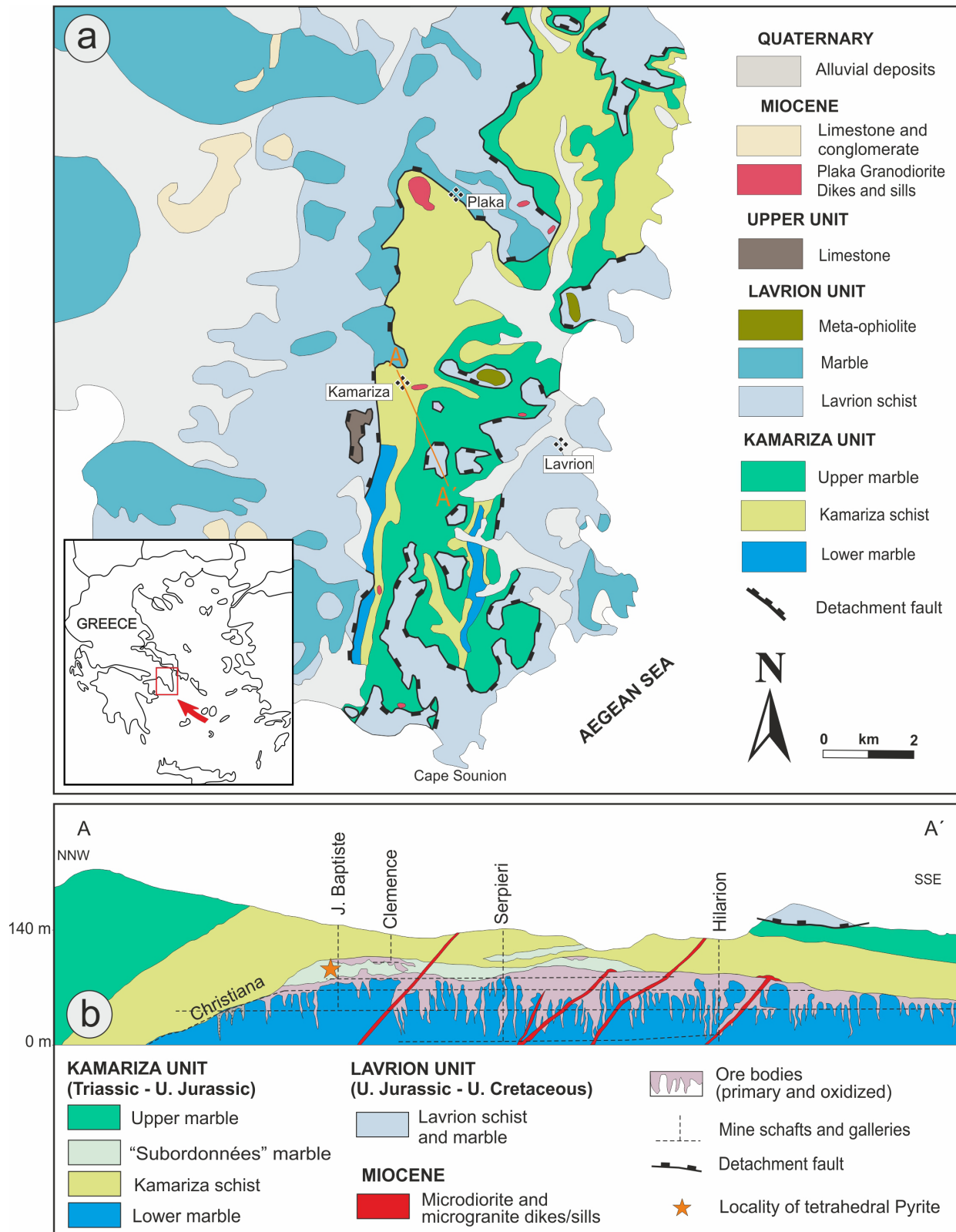


Fig. 1. (a) Simplified geological map of the Lavrion ore district (from Marinos and Petraschek 1956, Scheffer et al. 2016 and modified after Voudouris et al. 2021); (b) Cross-section A-A' of the Kamariza deposit (see geological map, figure 1a) (from Marinos and Petraschek 1956, modified after Voudouris et al. 2008).

Carbonate-replacement Pb-Zn-Ag±Au deposits at Kamariza are located in the central part of the district (Fig. 1a; Voudouris et al., 2008). The carbonate-replacement mineralization occurs in the form of stratabound massive sulfide replacement bodies (mantos) and chimneys, crosscutting with respect to layering in the host marble (Skarpelis, 2007; Voudouris et al., 2008; Bonsall et al., 2011, Scheffer et al., 2017 and 2019; Fig. 1b). Stratabound massive sulfide bodies (mantos) at Kamariza occur within the marbles as well as along the contacts of rocks with different permeabilities (marbles and schists). Ore deposition took place mainly from high-T magmatic fluids during the transitional ductile/brittle and brittle deformation stage of the host rocks (Bonsall et al., 2011; Scheffer et al., 2017, 2019). Beneath the individual manto orebodies, the rocks are cut by N-S to NE-SW, and NW-SE to E-W trending and steeply dipping veins that follow faults and fissures. The veins are usually zoned and brecciated, and in the breccias, the fragments are cemented by a sulfide-rich matrix. Pb-Zn-Ag veins are generally found below but also above the Lavrion detachment in the marbles of the Lavrion unit, in the Upper marble, in the Kamariza schists and at the interface between the Kamariza schists and the Lower marble. N-S trending veins crosscut the “Subordonnés” formation in the Jean Baptiste deposit (Fig. 1b). The veins are thought to be fluid pathways and feeder zones for the stratabound mineralization. The vein-style deposits were formed as the rock entered the brittle regime, by mixed seawater and meteoric fluids (Bonsall et al., 2011; Scheffer et al., 2017, 2019). The Jean Baptiste mine is located in the northwest area of the Kamariza district (Figs. 1a and b). Its mineralization consists of several vertical veins that have been the target of modern mining on the first level (and above) of the mine in the beginning of 20<sup>th</sup> century. The veins show ore zoning, whereby the crystallized minerals are present in the veins and in horizontal fissures. Tetrahedral pyrite crystals were found by chance in 2001 in a detached chamber within the Jean Baptiste mine that used to be a small ore prospect. It was obviously of no significant commercial value and consequently abandoned. Euhedral tetrahedral pyrite crystals grew within the banded marble and in the open ore veins hosting crystallized arsenopyrite, sphalerite, galena, calcite, dolomite, aragonite, and quartz.

Pyrite is the most widespread sulfide mineral that occurs in a wide range of morphological shapes. It comes in the form of single crystals

belonging to cubic  $m\bar{3}$  point group (symmetry further in text). The most frequent crystallographic forms are cube {100}, octahedron {111}, and pentagon dodecahedron, i.e. pyritohedron {210} that dictate the basic crystal morphology, which is further modified by many accessory crystallographic forms. Distorted, i.e. elongated single pyrite crystals are common appearances. Their symmetry depends on elongation direction. If they are elongated in (111)- and (100)-direction they develop 3-fold form with morphologic  $\bar{3}m$  symmetry and 2-fold form with morphologic  $mmm$  symmetry, respectively. All other orientations yield elongated crystals with 1-fold morphologic symmetry. Situation changes if the crystals are attached to a matrix. If they are attached with their [111]- and [110]-axis they develop chiral morphologic 3 and 2 symmetry, respectively. All other attachment possibilities result in chiral morphologic 1 symmetry, with a single exception of [001]-axis attachment that results in a non-chiral  $mm2$  morphology (Žorž, 2019). Pyrite basic  $m\bar{3}$  symmetry does not allow the existence of tetrahedral crystals. If this is the case then the octahedron {111} transforms either to positive  $t\{111\}$  or to negative  $t\{\bar{1}\bar{1}\bar{1}\}$  tetrahedrons with the resulting lower cubic  $\bar{4}m\bar{3}$  or  $23$  symmetries. Morphologic distortion of octahedral crystal morphology that would lead to a predominance of four octahedron faces and consequently to a tetrahedral crystal shape is not known.

Pyrite is often associated with other minerals in epitactic, i.e. in oriented growth relationships. Of them, the most frequent is epitaxy of pyrite on marcasite and vice versa. Richards et al. (1995) reported on oriented growth of single pyrite crystals with their {001} face on {010} face of a single marcasite crystal. In this case, pyrite crystals have two orientations with respect to the marcasite {010} face. The reason for that lies in non-alignment of 2-fold axes between pyrite in marcasite. Brock and Slater (1978) described another epitactic relationship, where marcasite (101)-twins grow on {001} face of a single pyrite crystal, whereby their (101)-twin planes are oriented perpendicularly with respect to pyrite {001} face. This time the 2-fold axes of both minerals coincide, which results in a single orientation of twinned marcasite on pyrite. In these two cases, the epitactic relationship was ascribed to alignment of Fe-S chains in the structures. Gait and Dumka (1986), and Gait et al. (1990) published the case of single pyrite crystals growth on a cyclic (101)-twinned marcasite. Miklavič et al. (2006) reported on oriented pyrite growth along

the twinning planes of the (101)-twinned marcasite. Orientation of pyrite with respect to marcasite and vice versa is in these two cases the same and results in a single pyrite orientation. Oriented growths of pyrite on arsenopyrite and pyrite on pyrrhotite were described by Zebec (2012). Pyrite is attached with its {001} face to {001} face of arsenopyrite. Non-alignment of 2-fold axes of both minerals again requires two different orientations of pyrite, which is observed on specimens from Trepča. Pyrite is attached with its {001} face to {001} face of pyrrhotite. Octahedral {111} face of pyrite has a chiral trifold symmetry without any mirror plane, whereas the pyrrhotite {001} face has a 6-fold symmetry with 6 mirror planes. For that reason pyrite can have six different orientations on the pyrrhotite that are rotated by 60°, of which four are spatially equivalent. The remaining two are rotated by 180° with respect to each other. Chiral symmetry of the octahedron face requires another two orientations of which one is left- and the other right-handed. In the end, four different orientations remain, of which two are left- and two right-handed, and at the same time rotated by 180°. The outcome is intergrown pyrite with the same surface symmetry as pyrrhotite. Zebec did not specify individual orientations of pyrite on arsenopyrite and pyrrhotite.

Twinned pyrite crystals are rare appearances. The most common are “iron-cross” twins formed by interpenetration of two crystals, rotated by 90° about [110]-axis with respect to each other. The twin acquires the highest cubic  $m\bar{3}m$  symmetry. The study of Donnay et al. (1977) found no evidence of impurity metals at the (110)-twin boundaries and that the twinning planes were actually irregular surfaces. The study of Rečnik et al. (2016), on the contrary, showed that a monolayer of Cu atoms was necessary to stabilize the {110} twin structure.

Goldschmidt (1922) published figures (No. 134 and No. 135) of pyrite crystals from Bösingsfelde near Lippe in Germany that are twinned in accordance with two other laws. The first twin type forms by 60°-rotation about the [111]-axis and acquires a hexagonal  $6/m$  symmetry. The second type is generated by mirroring in (110) plane with simultaneous 60°-rotation about [111]-axis and yields a twin with the highest trigonal  $\bar{3}m$  symmetry. Pabst (1971) reported on pyrite crystals with the unusual form that consist of a central pyrite crystal to which six other are presumably {001}-twinned. The composite crystal resembles a cruciform steacyite twin. In absence of morpho-

logical details, an X-ray determination revealed that they were single crystals.

Here, we report on five new twinning laws that were determined on the pyrite crystals from Jean Baptiste section in Lavrion mines.

## Methods

*In situ* sampling of pyrite specimens took place in the period between 2001 and 2020. Specimens for morphological determination with Olympus SZ-11 stereomicroscope were cleaned in an ultrasonic bath filled with a demineralized water. Morphology of single and twinned pyrite crystals was reconstructed using a program SHAPE 7.1.

Camera Sony Alpha III, equipped with LAOWA 25 mm, F 2.8 ultra macro lens was used to photograph specimens, using the focus stacking method.

Three pyrite crystals were chosen for quantitative chemical analysis. All samples were dissolved in hot *aqua regia*. Varian Spectra AA 110 instrument was used to determine Fe, Cu and Zn, and Agilent 7900 ICP-MS instrument was utilized to determine Bi.

Antimony content was analysed by means of electron micro probe analysis (EMPA). The working conditions were set at 20 kV, 10-nA beam current, 2- $\mu$ m beam size, and peak counting time of 20 s. Nine different crystals within the same polished section were analyzed.

A single crystal of the first generation and a twinned crystal of the second generation, free of visible sfalerite or quartz inclusions, were chosen for a single-crystal X-ray analysis that was conducted on Oxford Xcalibur3 single-crystal X-ray diffractometer equipped with a CCD detector (MoK $\alpha$ ).

## Results

### Quantitative chemical analysis

Table 1 summarizes results of iron, copper, zinc, bismuth, and antimony content obtained on samples of tetrahedral pyrite crystals from Jean Baptiste mine section. Iron content in the single crystal of the first generation is close to a theoretical pyrite composition. Contents of other metals are below 0,06 wt%. (001)-twins of the second generation are less pure, which is ascribed to mechanical inclusions of other minerals, especially sfalerite and quartz. Percentage of bismuth is low in all cases and antimony was determined below 0.1 wt % on the (001)-twin of the second generation.

Table 1. Percentage content of metals in pyrite from Jean Baptiste mine section. Sample 1 was a first generation crystal, prepared from the marble, free of microscopically visible sphalerite and quartz inclusions. Samples 2 and 3 were of the second generation and detached from the matrix covered with sphalerite and quartz crystals.

| Sample                                      | Fe (wt%)     | Cu (wt%)    | Zn (wt%)    | Bi (wt%)      | Sb (wt%)           |
|---|--------------|-------------|-------------|---------------|--------------------|
| Single crystal - 1 <sup>st</sup> generation | 45,9±0,5     | 0,052±0,001 | 0,055±0,001 | 0,035±0,0010  |                    |
| (001)-twin - 2 <sup>nd</sup> generation     | 43,0±0,5     | 0,113±0,009 | 0,944±0,009 | 0,0010±0,0001 |                    |
| (001)-twin - 2 <sup>nd</sup> generation     | 43,5±0,5     | 0,063±0,001 | 0,049±0,001 | 0,0007±0,0001 |                    |
| (001)-twin - 2 <sup>nd</sup> generation     |              |             |             |               | 0,06 (0,03 - 0,12) |
| <b>Theoretical content</b>                  | <b>46,56</b> |             |             |               |                    |

### Morphological analysis

#### First generation

Pyrite crystals of the first generation are imbedded in marble concordantly with respect to its banding and cover the walls of open veinlets that are perpendicular to the banding (Fig. 2). They are attached to thin crusts of quartz crystals. The smallest pyrite crystals (less than 1 mm) are combinations of strongly striated cube  $a\{100\}$  and pentagon dodecahedron  $d\{210\}$  faces (Fig. 3A).

Sizes of cube and dodecahedron faces on each single crystal vary greatly, giving the crystals the appearance of deformation. Those imbedded in the marble are fresh and have a strong luster on crystal faces, whereas those from the veins are golden brown due to oxidation. An increase in crystal dimensions is reflected in onset of tetrahedron  $t\{110\}$  faces. The larger are the crystals the more developed are the tetrahedrons and the narrower are cube  $a\{100\}$  and dodecahedron  $d\{210\}$

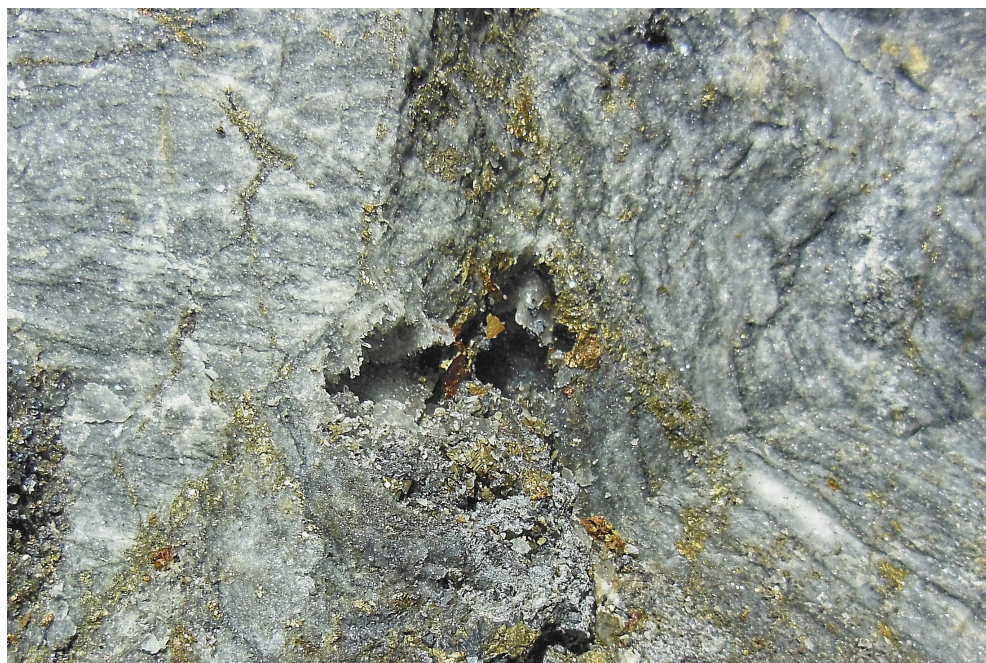


Fig. 2. *In situ* photograph of marble with mineralized ore vein in Jean Baptiste mine section. Pyrite crystals of the first generation are imbedded concordantly with respect to the marble banding and along the veinlets that are oriented more or less perpendicularly to the banding. Pyrite crystals of the second generation with a characteristic rugged pattern grow on quartz and sphalerite crystals in the ore vein. Field of view: 17 cm × 11 cm.

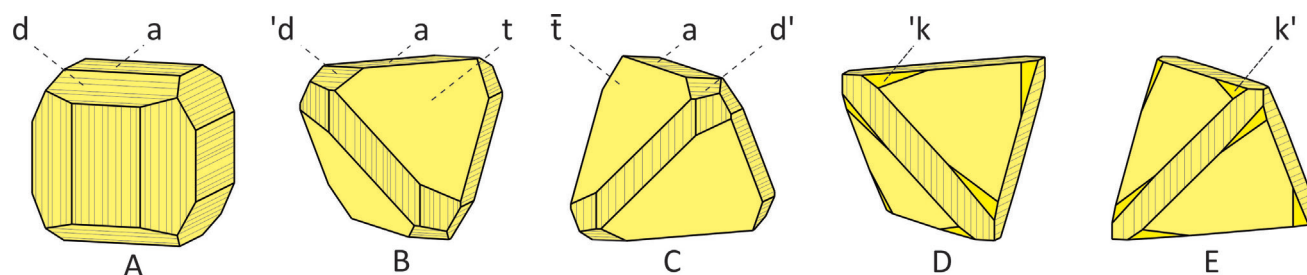


Fig. 3. Crystal morphology of the primary pyrite crystals. Smaller crystals are combinations of cube  $a\{100\}$  and pentagon dodecahedron  $d\{210\}$  faces. Their alternations are responsible for characteristic striations on crystal faces (A). Larger primary crystals are tetrahedral, and exhibit left- (B) or right-oriented striations on a and d faces (C). This is a reflection of the presence of positive  $t\{110\}$  or negative tetrahedron  $\bar{t}\{111\}$  faces. Symmetry-defining chiral class-specific forms of left  $k\{11.10.14\}$  (D) and right  $k'\{11.10.14\}$  (E) tetrahedral pentagon dodecahedron are frequently present on the crystals.

faces. Striations on cube faces that are the result of alternations of cube and dodecahedrons have a quality of enantiomorphism, which is reflected in crystals with left- or right-handedness. Crystals with positive tetrahedrons  $t\{111\}$  are left-handed and vice versa for those with negative  $\bar{t}\{\bar{1}\bar{1}\bar{1}\}$  tetrahedrons (Figs. 3B, 3C and Fig. 4). Consequently, the pentagon dodecahedron  $d$  gains on speci-

ficity by its transformation to class-specific left ' $d\{210\}$ ' or right ' $d\{120\}$ ' tetrahedral pentagon dodecahedron. Handedness of crystals is enhanced by a presence of highly reflective faces of a tetrahedral pentagon dodecahedron  $k\{11.10.14\}$ . This class-specific form clearly defines handedness of crystals by its left ' $k\{11.10.14\}$ ' or right ' $k\{\bar{1}.10.14\}$ ' analogue (Figs. 3D and E, and Figs. 4A and B).



Fig. 4. Single pyrite crystals of the first generation on quartz matrix. Calcite crystallized later. Pyrite morphology is defined by tetrahedron  $t$  and striated cube  $a$  faces. Photographs A and B show left-handed and right-handed crystal, respectively. Note the class-specific faces of the corresponding left ' $k\{11.10.14\}$ ' and right ' $k\{\bar{1}.10.14\}$ ' tetrahedral pentagon dodecahedron. Both crystals measure one mm on their edges.



Fig. 5. (001)-interpenetration twins of the first pyrite generation. Photograph A shows the twin (one mm in diameter) with a typical reentrant between tetrahedron  $t$  faces and characteristic striations on cube  $a$  faces. Better-developed twin on photograph B is 2-fold in all (100) planes. Note the orientations of striations on its cube  $a$  faces. Twin dimensions: 1.3 mm  $\times$  1.3 mm. Faces of dyakis-dodecahedron  $k$  are present on both crystals in mirror-symmetric positions with respect to (100) planes of symmetry.

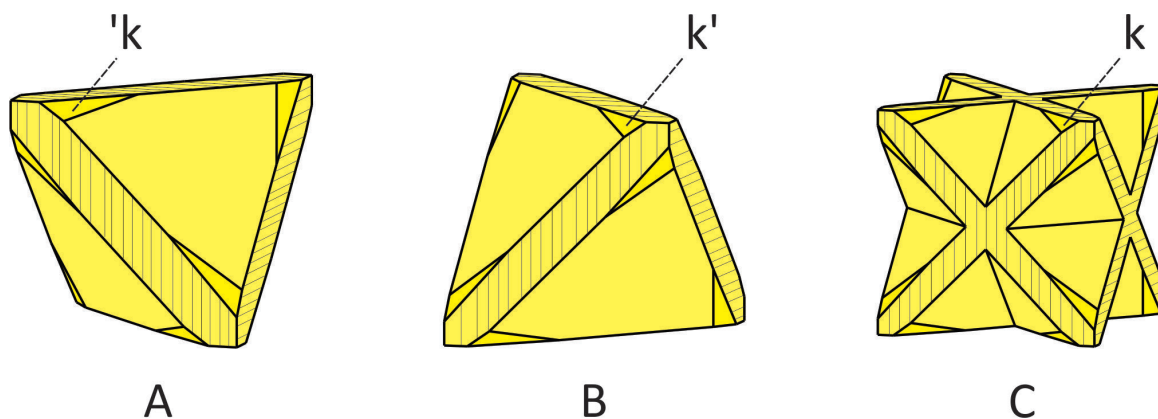


Fig. 6. (001)-interpenetration of single left- (A) and right-handed (B) tetrahedral crystals yields a twin (C). Chiral faces of tetrahedral pentagon dodecahedron forms 'k and k' transform to non-chiral dyakis-dodecahedron k (C).

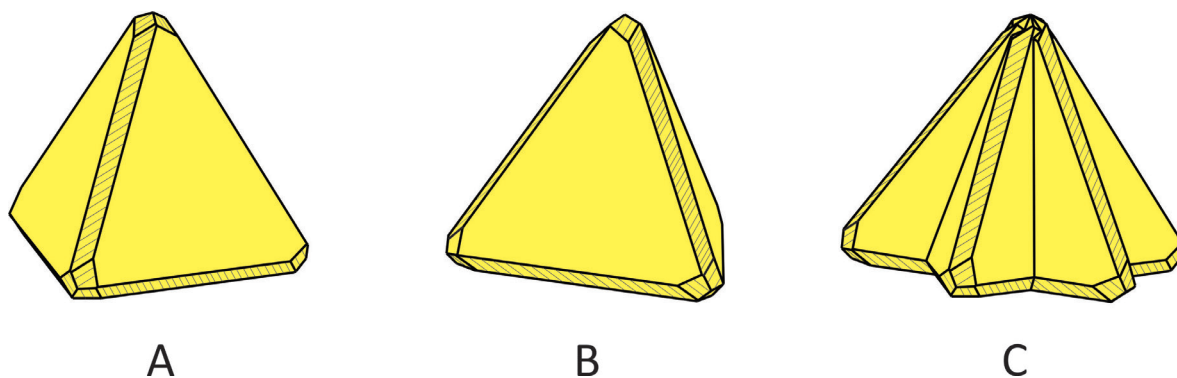


Fig. 7. 6-fold (111)-interpenetration twin (C) is a combination of two left- (shown in the drawing) or two right-handed tetrahedral single crystals, whereby one of them is simultaneously rotated by 60° (B) with respect to the other one (A).

Some of the first pyrite generation crystals are twinned. Two twinning possibilities are noted. The first is twinning by (001)-interpenetration of two tetrahedral crystals of which one is left- and the other right-handed. The resulting twin has deep re-entrants and characteristic orientation of striations on cube *a* faces. Tetrahedral pentagon dodecahedron faces 'k and k' are present in twinning positions, whereby they lose their chiral character and consequently transform to dyakis-dodecahedron *k* (diploid). These twins are rare (Figs. 5 and 6).

The second possibility is interpenetration of two left- or two right-handed tetrahedral crystals about [111]-axis by simultaneous 60°-rotation. The resulting twinned crystal is 6-fold and has a common face (pedion), composed of two tetrahedrons  $t\{111\}$  and deep re-entrants between all other tetrahedron faces. The twin retains the

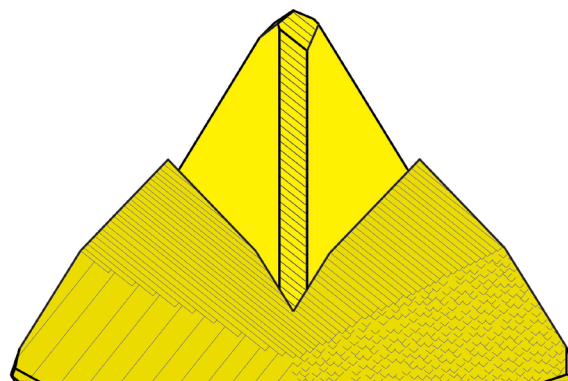
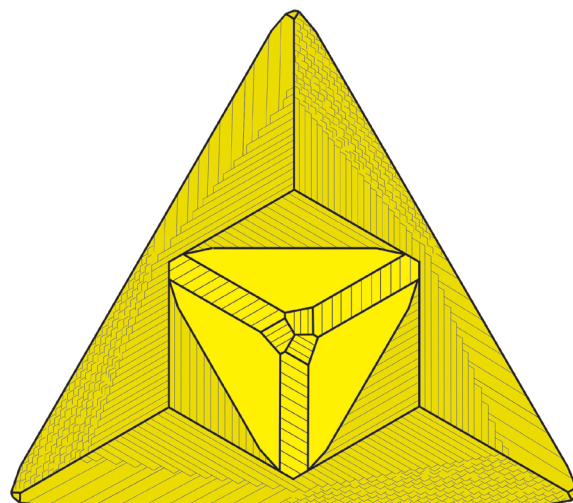


Fig. 8. (111)-interpenetration twins are never theoretically developed. Real crystals exhibit lower 3-fold symmetry, because of the incomplete development of the crystal that surrounds the central one. Drawings above and below show the projection of the right-handed twin along its [111]-twin axis and its projection perpendicularly to the same axis, respectively. Cube *a* faces are present only on the central crystal. Note the characteristic chiral-specific patterns.



Fig. 9. A group of (111)-interpenetrated twins of the first pyrite generation. Twins in the middle-left and at the top are right-handed and that in the middle-right is left-handed. Heavily striated cube faces are present on the central crystals only. Surrounding crystals are without them - note their sharp tetrahedral edges. The largest twin measures three mm on its edge.

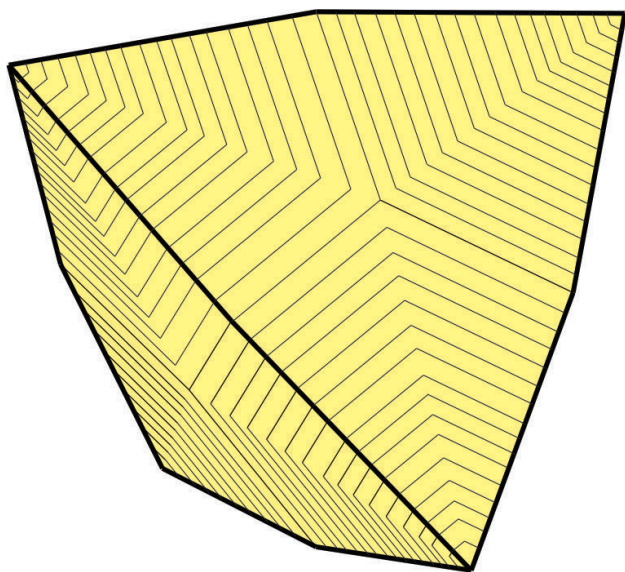


Fig. 10. Pyrite crystals of the second generation have a simple tetrahedral morphology and exhibit characteristic 3-fold mirror symmetric pattern on their faces.

handedness of the interpenetrated single crystals. Faces of tetrahedral pentagon dodecahedron **k** are not present on (111)-twinned crystals. Typical chiral-specific striations appear on tetrahedrons as the result of alternations between tetrahedron **t** and tetrahedral pentagon dodecahedron **d** faces (Figs. 7, 8 and 9). This twinning type may take place on any tetrahedron face, which leads to the formation of more common multiple twins.

#### Second generation

Pyrite crystals of the second generation have a dull luster and grow only on the walls of the open veins (Fig. 2). If the crystals of the first generation are present, then those of the second generation may overgrow them. They also have a tetrahedral morphology and reach up to 20 mm on their edges. Crystals are sharp-edged due to absence of cube **a**, and dodecahedron **d** faces and lack any traces of handedness. Instead of that,



Fig. 11. Pyrite crystals of the second generation with characteristic 3-fold mirror-symmetric rugged pattern on their faces. The largest crystal measures six mm on its edge.

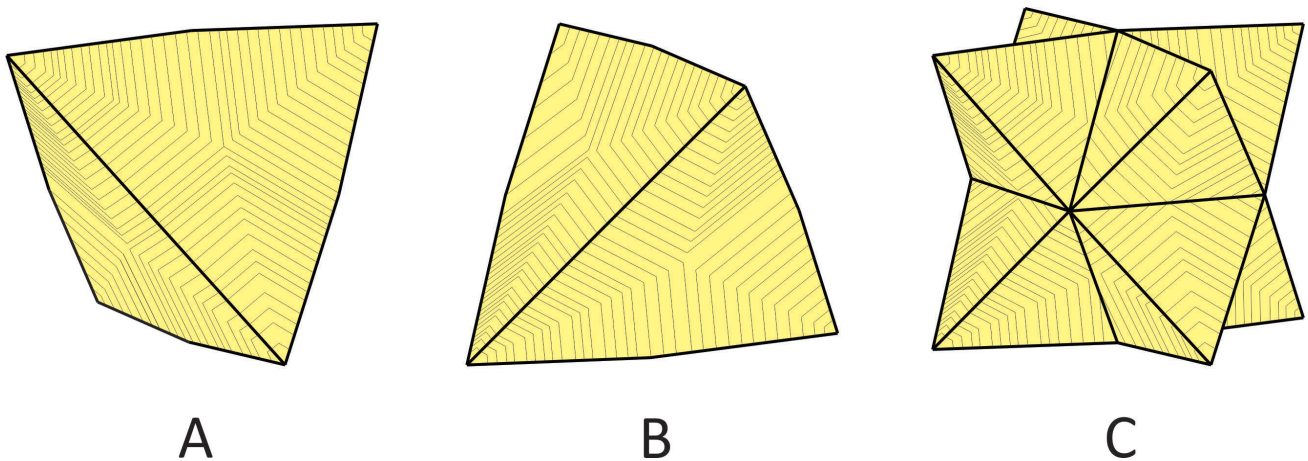


Fig. 12. (001)-interpenetration of two tetrahedral crystals of the second pyrite generation. Crystal B simultaneously rotates by  $90^\circ$  with respect to crystal A. The resulting twin has deep reentrants between tetrahedrons and a mirror-symmetric pattern along all symmetry planes (C).

they exhibit a characteristic mirror-symmetric 3-fold rugged pattern on their tetrahedral faces (Figs. 10 and 11).

Twinned crystals occur in the second generation as well. Again, two twinning possibilities are present. The first is an interpenetration along [001]-axis. Twin is composed of two character-

istically patterned tetrahedral crystals and has deep reentrants between them. All patterns are mirror-symmetric in all (100) planes of the twin (Figs. 12 and 13).

The second possibility is an interpenetration along [111]-axis that yields a 6-fold twin that has a common pedion face composed of two tetra-



Fig. 13. (001)-interpenetration twins of the second pyrite generation. Photograph A shows the twin, measuring three mm on its edge, with a typical reentrant between tetrahedron faces. Mirror-symmetric pattern on its faces is present but less-pronounced. Twin photographed along its 4-fold [100]-axis, is presented on photograph B. Its diameter is two mm.

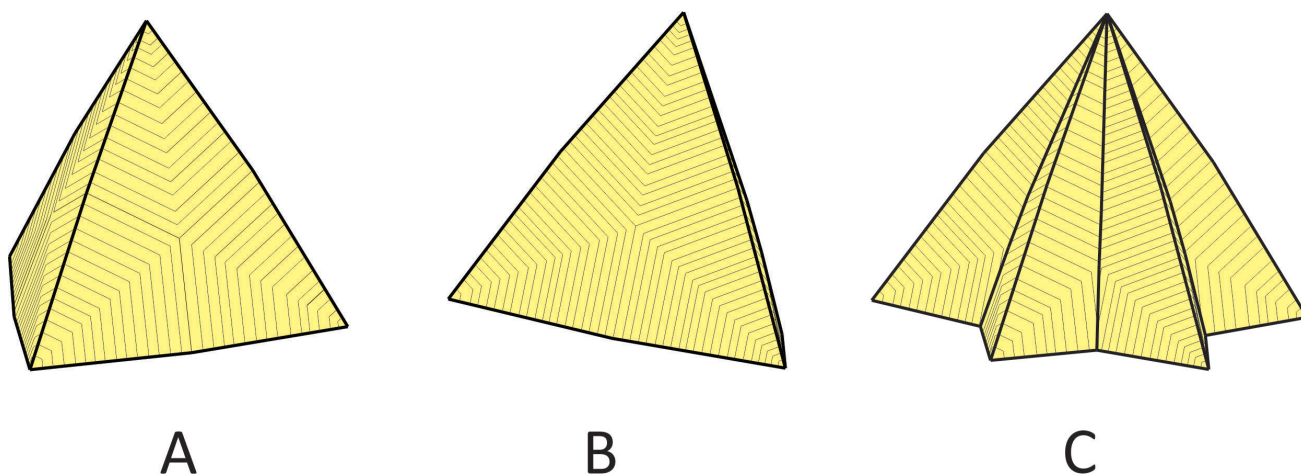


Fig. 14. 6-fold (111)-interpenetration twin (C) is a combination of two tetrahedral crystals, whereby one of them (B) is rotated by  $60^\circ$  with respect to the other one (A). Twin has deep reentrants between tetrahedrons. Note the mirror-symmetric pattern in all symmetry planes of the twin.

hedron faces and with deep reentrants between all other faces. Characteristic mirror-symmetric rugged pattern is present on all faces as well (Figs. 14, 15 and 16). Multiple (111)-interpenetration twinning is very frequent with crystals of this generation (Fig. 16).

#### Third generation

Pyrite crystals of the third generation do not exceed three mm on their edges. They are oxidized, striated, and composed of cube **a**, pentagon dodecahedron **d**, and exceptionally octahedron **o**{111} faces (Fig. 17). They cover partially or completely pyrite crystals of the second generation. Crystals of the third generation are

preferentially attached with their cube faces in parallel with respect to tetrahedron faces of the second-generation crystals, yet in a completely random manner (Fig. 18).

#### Single-crystal X-ray analysis

All the collected reflections obtained with this structure-discerning method belonged to the common pyrite structure defined by an  $m\bar{3}$  point group. No evidence of tetrahedrite inclusions and twin-related reflections were observed neither on the crystal of the first nor on the (001)-twinned crystal of the second generation, after the refinement of the structure to  $R = 2\%$ .

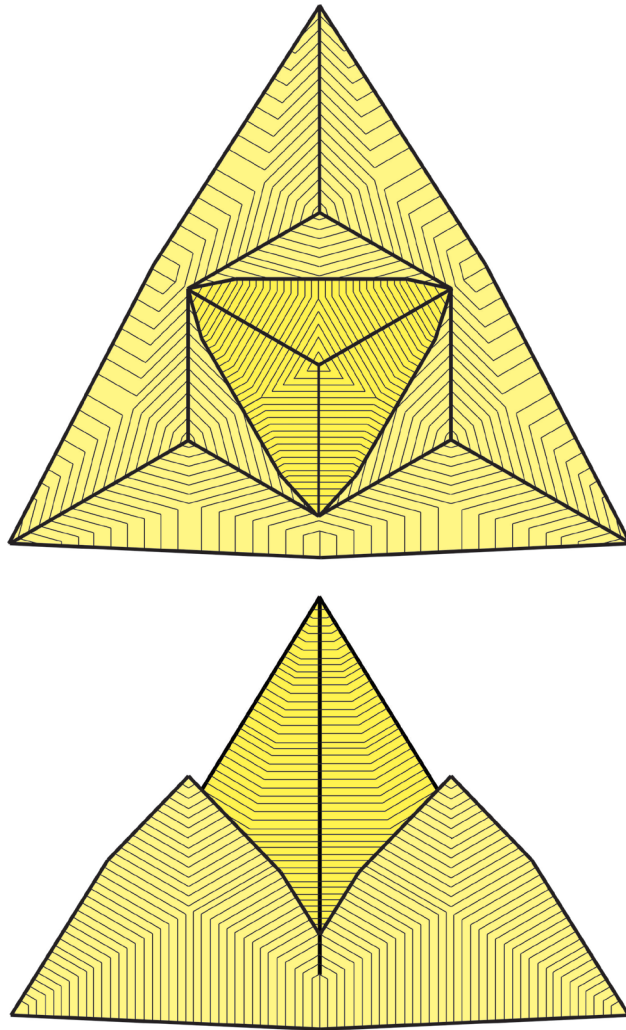


Fig. 15. (111)-interpenetration twins of the second generation are never theoretically developed. Real crystals exhibit lower 3-fold symmetry, because of the incomplete development of the crystal that surrounds the central one. Drawings above and below show the projection of the twin along its [111]-twin axis and its projection perpendicular to the same axis, respectively. Note the characteristic mirror-symmetric patterns.



Fig. 16. (111)-interpenetration twins of the second pyrite generation. Photograph A shows a typical twin (lower right) with the central crystal and less-developed surrounding crystal. It measures six mm on its lower edge. Twin at the top left shows its pedion face. Crystals are partially covered with thin gypsum crusts. Photograph B shows a multiple (111)-interpenetration twin attached to quartz and sphalerite crystals. A sharp tetrahedral edge of the central crystal protrudes out of the surrounding crystals. Height of the twin is five mm. Characteristic mirror-symmetric rugged pattern is present on all crystals.

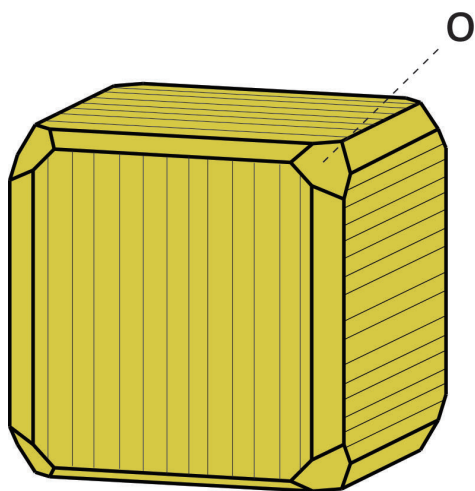


Fig. 17. Pyrite crystals of the third generation have a cubic morphology that is slightly modified by pentagon dodecahedron **d** and octahedron **o**{111} faces.



Fig. 18. Oxidized pyrite crystals of the third generation cover pyrite crystals of the second generation. Note their random orientations on the tetrahedron faces of the secondary generation. The largest crystal measures 11 mm on its tetrahedral edge. Bluish-white coatings are aragonite crystals.

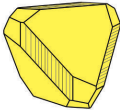
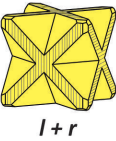
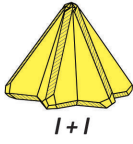
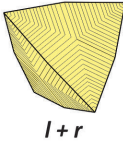
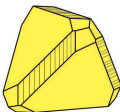
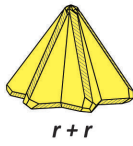
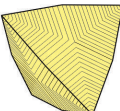
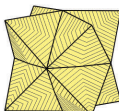
| Starting symmetry     |   | Twin symmetry   |  |   |   |   |
|-----------------------|---|---|--|---|---|---|
|                       |   | $m\bar{3}$  | $6$  | $\bar{4}m3$   | $m\bar{3}m$   | $6mm$   |
| $l-23$                |  |  | <br>$l+l$ | <br>$l+r$ |   |   |
| $r-23$                |  | $l+r$   | <br>$r+r$ | $l+r$   |   |   |
| $\bar{4}m3$           |  |   |  |   |  |  |
| Twin generation       |   | $1^{\text{st}}$   |  | $2^{\text{nd}}$   |   |   |
| Interpenetration mode |   | (100)   | (111)  | (110)   | (100)   | (111)   |

Fig. 19. Schematic presentation of the observed pyrite crystals from Jean Baptiste section with respect to starting symmetry, generation, and interpenetration mode. Pyrite crystals of the first generation appear as single tetrahedral crystals with left- or right-handed  $23$  symmetry, as twins with isometric  $m\bar{3}$  symmetry and as simple or multiple twins with left- or right-handed hexagonal  $6$  symmetry. The second pyrite generation is primarily twinned and has the corresponding  $\bar{4}m3$  symmetry. Crystals of this generation appear as tetrahedrons, as twins with the highest isometric  $m\bar{3}m$  symmetry and as simple or multiple twins with hexagonal  $6mm$  symmetry.

## Discussion

The first to report on pyrite crystals with tetrahedral morphology from Lavrion mine was Mügge in 1895 and 1903. His drawings show left- and right-handed tetrahedral pyrite crystals of the first generation. Crystallographic forms of cube  $a\{100\}$ , tetrahedral pentagon dodecahedron  $d\{210\}$ , and tetrahedron  $t\{111\}$  define the crystal morphology, with chiral-specific striations on a faces. The third drawing shows a crystal of the second generation. The apparent low symmetry of the crystals is, in accordance with his opinion, the result of a pyrite pseudomorph after tetrahedrite, whereby he could not detect any traces of tetrahedrite within the crystals, and chemical analysis was negative for copper. Evident tetartohedral symmetry of the pyrite would require its twinning in accordance with “iron cross” in order to adapt to a higher point group of tetrahedrite, which is  $\bar{4}m3$ , but no signs of such twinning on the primary crystals existed. He concluded therefore, that the evident morphologic tetartohedry could lead to a wrong opinion that the pyrite crystals from this location should have such a low symmetry and stressed that the exact pyrite symmetry was already known at that time beyond any doubt. Mügge (1895) also added that the pyrite crystals appear together with quartz and prismatic arsenopyrite in single and (101)-twinned crystals. The proposed oriented growth of pyrite on tetrahedrite can be understood as a contact of pyrite octahedron  $\{111\}$  face with a tetrahedron  $\{111\}$  face of tetrahedrite. Symmetry of the tetrahedron face is 3-fold with three mirror planes. This symmetry requires left- and right-handed orientation of pyrite. In this way, pyrite acquires the same planar symmetry on its  $\{111\}$  face, i.e. 3-fold with three symmetry planes. Tetrahedrite  $\{111\}$  face, completely overgrown with pyrite in the discussed orientation, could indeed exhibit twinned structure as observed on the second generation of pyrite from Jean Baptiste section. However, it is very likely that the scattered pyrite crystals would only partially cover the tetrahedral faces of real tetrahedrite crystals in two distinctly recognizable chiral orientations, which is not the case here. Oriented growths of pyrite on tetrahedrite or vice versa are not known.

Since then, no new works on the subject, and no new material had appeared until 2001, when a group of researchers from Athens rediscovered the location and collected new specimens (Voudouris et al., 2004). A preliminary SEM analysis was performed to determine which mineral

the tetrahedral crystals belonged to. It turned out that they were pure pyrite without indication for replacement of another mineral.

It is clear that Mügge described the primary crystals from exactly the same location, because the tetrahedral pyrite crystals from the new find have the same morphology and come together with arsenopyrite in single and (101)-twinned crystals. Besides that, no other location with tetrahedral pyrite crystals has ever been encountered in Lavrion mines. It has to be stressed that the pyrite crystals of the first generation exhibit the evident morphological lowermost cubic symmetry  $23$ . ICP-MS analysis of primary crystals confirmed the purity of the first-generation pyrite crystals with respect to their Cu, Zn, and Bi content. EMPA analysis of the second-generation pyrite crystals showed the comparably low antimony content (see Table 1). Single-crystal X-ray analysis excluded tetrahedrite inclusions in single and in twinned crystals.

Discovery of different interpenetration twin types on the new material sheds a completely new light on the trivial symmetry of the tetrahedral pyrite crystals at Jean Baptiste location. Formation of (001)-interpenetration twins, exhibiting a cubic  $m\bar{3}$  symmetry as presented in Figure 5, is not possible unless the starting symmetry is the lowermost isometric  $23$  (tetartohedry). Figure 6 shows the formation of such a twin. (111)-interpenetration twins are another proof of lower primary symmetry, because they are chiral and retain the handedness of the twinned single crystals, which is only possible if the starting symmetry is  $23$ . The resulting twins with symmetry  $6$  are for that reason either left- or right-handed (see Fig. 7). Real twinned crystals of this type exhibit lower, but evidently chiral  $3$  symmetry as the outcome of the incomplete interpenetration (Figs. 8 and 9).

All tetrahedral pyrite crystals of the second generation have a characteristic 3-fold mirror-symmetric pattern on tetrahedron faces. This fact reflects a higher symmetry, which is the result of (110)-interpenetration in which two tetrahedral crystals of the opposite handedness interpenetrate (Fig. 19).

All pyrite crystals of the second generation are therefore twins with  $\bar{4}m3$  symmetry, which enables further twinning by (001)-interpenetration yielding a twin with the highest cubic  $m\bar{3}m$  symmetry. Twins of this type exhibit sharp tetrahedral edges and characteristic rugged pattern on their faces that is mirror-symmetric along all (100) and (110) planes of symmetry (Figs. 12 and 13).

The highest twin symmetry appears when two crystals of the second pyrite generation are (111)-interpenetrated by simultaneous 60°-rotation about the [111]-axis. The resulting twin has a hemimorph  $6mm$  symmetry with a characteristic pattern on all tetrahedral faces that is mirror symmetric along six mirror planes that are parallel to the twin's main 6-fold axis (Fig. 14). Real crystals exhibit lower symmetry due to incomplete interpenetration (Figs. 15 and 16A). Multiple twinning of this type is frequent (Fig. 16B). Figure 19 shows a schematic presentation of all described twinning possibilities.

Pyrite crystals of the third generation are cubes that are slightly moderated by pentagon dodecahedron  $\mathbf{d}$  and octahedron  $\mathbf{o}\{111\}$  faces on cube corners. There are no twinning signs on them, which confirms their trivial  $m\bar{3}$  symmetry.

The cubic  $m\bar{3}$  symmetry of the first-generation single crystals as well as of the (110)-twinned crystals of the second generation derives from the findings of the single-crystal X-ray analysis conducted on them. It is therefore evident, that the results of morphological and structural analysis do not match. It is not the aim of this study to specify the environmental and structural details leading to the formation of the observed twins. To explain this discrepancy, we may only propose that the pyrite crystals of the first generation crystallized under conditions that favored their initial low isometric  $23$  symmetry, and consequently the formation of tetrahedral crystals and twins. Crystallization conditions might change in the course of time and the initial symmetries (crystal structures) of all single and twinned crystals of the first and the second generation transformed to structures with higher  $m\bar{3}$  symmetry, whereas their morphologies remained unchanged.

The other explanation might consider a possible insufficient specificity of the single-crystal X-ray analysis. Namely, pyrite trivial  $m\bar{3}$  point group ranks to a group of centrosymmetric Laue classes. Two crystals measured in this study, on the contrary, belong to morphologically evident non-centrosymmetric  $23$  and  $\bar{4}m\bar{3}$  point groups that may mimic the centrosymmetric  $m\bar{3}$  one if a resonant scattering (anomalous dispersion) was negligible or not detected.

Future work on this topic should therefore go into direction of determining conditions during the formation and growth of three pyrite generations, which would include the determination of physico-chemical growth parameters, fluid inclusions in crystal paragenesis and into the op-

timization and refinement of the single-crystal X-ray analysis.

### Acknowledgements

We truly thank to Luca Bindi from Dipartimento di Scienze della Terra Università degli Studi di Firenze, who conducted the single-crystal X-ray analysis, and to Radmila Milačič from Department of Environmental Sciences, Jožef Stefan Institute, Ljubljana, for the chemical analysis. Our sincere thank goes to Igor Dolinar from Ljubljana, for his efforts in photographing the samples.

### References

- Berger, A., Schneider, D. A., Grasemann, B. & Stockli, D. 2013: Footwall mineralization during Late Miocene extension along the West Cycladic Detachment System, Lavrion, Greece. *Terra Nova*, 25: 181-191.
- Bonsall, T. A., Spry, P. G., Voudouris, P., Tombros, S., Seymour, K. & Melfos, V. 2011: The Geochemistry of Carbonate Replacement Pb-Zn-Ag Mineralization in the Lavrion District, Attica, Greece, Fluid Inclusion, Stable Isotope, and Rare Earth Element Studies. *Econ. Geol.*, 106: 619-651.
- Brock, K. J. & Slater L.D. 1978: Epitaxial marcasite on pyrite from Rensselaer, Indiana. *American Mineralogist*, 63: 210-212.
- Conophagos, C. 1980: The Lavrion and the ancient Greek techniques for silver production. Athens, Ekdotiki Athinion: 458 p.
- Gait, R. I. & Dumka, D. 1986: Morphology of pyrite from the Nanisivik mine, Baffin Island, Northwest territories. *Canadian Mineralogist*, 24/4: 685-688.
- Gait, R. I., Robinson, G. V., Bailey, K. & Dumka, D. 1990: Minerals of the Nanisivik Mine, Baffin Island, Northwest Territories. *Mineralogical Record*, 21/6: 515-534.
- Goldschmidt, V. M. 1922: Atlas Der Krystallformen, Bd. VI. Verlag Winters, Heidelberg.
- Marinos, G. & Petrascheck, W. E. 1956: Lavrion: geological and geophysical research. *Inst. Geol. Subsurf. Res.* 4: 246.
- Miklavič, B., Žorž, M. & Schmidt, G. 2006: Markazit in pirit izpod Prisojnika. In monograph: Mineralna bogastva Slovenije. Scopolia, Suppl. 3: 439-443.
- Morin, D. & Photiades, A. 2012: L'exploitation des gisements métallifères profonds dans l'Antiquité. Les mines du Laurion (Grèce).

- Eckart Olshausen/Vera Sauer (Hg.) Die Schätze der Erde – Natürliche Ressourcen in der antiken Welt. Stuttgarter Kolloquium zur Historischen Geographie des Altertums 10, 2008. *Geographica Historica* 28. Franz Steiner Verlag Stuttgart 2012: 28-335. CD-Rom Illustrations. ISBN 978-3-515-10143-1.
- Mügge, O. 1895: Regelmässige Verwachsung von Pyrit mit Fahlerz in Pseudomorhosen nach letzteren. *Neues Jahrbuch für Mineralogie, Geologie und Palaentologie, I. Band*: 103-105.
- Mügge, O. 1903: Die regelmässige Verwachsungen von Mineralien verschiedener Art. *Neues Jahrbuch für Mineralogie, Geologie und Palaentologie, XVI. Beilage – Band*: 340-341.
- Pabst, A. 1971: Pyrite of unusual habit simulating twinning from the Green River Formation of Wyoming. *American Mineralogist*, 56/1-2: 133-145.
- Rečnik, A., Zavašnik, J., Jin, L., Čobić, A. & Daneu, N. 2016: On the origin of “iron-cross” twins of pyrite from Mt. Katarina, Slovenia. *Mineralogical Magazine*, 80/6: 937-948. <https://doi.org/10.1180/minmag.2016.080.073>
- Richards, R. P., Clopton, E. L. & Jaszczak, J. A. 1995: Pyrite and marcasite intergrowths from northern Illinois. *Mineralogical Record*, 26/2: 129-138.
- Scheffer, C., Tarantola, A., Vanderhaeghe, O., Voudouris, P., Rigaudier, T., Photiadis, A., Morin, D. & Alloucherie, A. 2017: The Lavrion Pb-Zn-Fe-Cu-Ag detachment-related district (Attica, Greece): Structural control on hydrothermal flow and element transfer-deposition. *Tectonophysics*, 717/16: 607-627. <https://doi.org/10.1016/j.tecto.2017.06.029>
- Scheffer, C., Tarantola, A., Vanderhaeghe, O., Voudouris, P., Spry, P.G., Rigaudier, T. & Photiades, A. 2019: The Lavrion Pb-Zn-Ag-rich Vein and Breccia Detachment-Related Deposits (Greece): Involvement of Evaporated Seawater and Meteoric Fluids during Post-Orogenic Exhumation. *Economic Geology*, 114/7: 1415-1442. <https://doi.org/10.5382/econgeo.4670>
- Skarpelis, N. 2007: The Lavrion deposit (SE Attica, Greece): geology, mineralogy and minor elements chemistry. *Neues Jahrbuch für Mineralogie Abhandlungen*, 183/3: 227-249. <https://doi.org/10.1127/0077-7757/2007/0067>
- Voudouris, P., Tsolakos, A., Papanikitas, A. & Solomos, Ch. 2004: Nicht nur Micromounts Neufunde aus Lavrion. *Lapis*, 4: 13-15.
- Voudouris, P., Melfos, V., Spry, P.G., Bonsall, T., Tarkian, M. & Solomos, Ch. 2008: Carbonate-replacement Pb-Zn-Ag±Au mineralization in the Kamariza area, Lavrion, Greece: Mineralogy and thermochemical conditions of formation. *Mineral. Petrol.*, 94/1-2: 85-106. <https://doi.org/10.1007/s00710-008-0007-4>
- Voudouris, P., Melfos, V., Mavrogonatos, C., Photiades, A., Moraiti, E., Rieck, B., Kolitsch, U., Tarantola, A., Scheffer, C., Morin, D., Vanderhaeghe, O., Spry, P.G., Ross, J., Soukis, K., Vaxevanopoulos, M., Pekov, I.V., Chukanov, N.V., Magganas, A., Kati, M., Katerinopoulos, A. & Zaimis, S. 2021: The Lavrion Mines: A Unique Site of Geological and Mineralogical Heritage. *Minerals*, 11/1: 76. <https://doi.org/10.3390/min11010076>
- Zebec, V. 2012: Trepča/Stari trg, Zagreb: 415 p.
- Žorž, M. 2019: The Symmetry System, 2<sup>nd</sup> edition, Ljubljana: 212 p.





# Terminologies and characteristics of natural mineral and thermal waters in selected European countries

## Izrazoslovje in značilnosti naravnih mineralnih in termalnih voda v izbranih evropskih državah

Daniel ELSTER<sup>1</sup>, Teodóra SZÓCS<sup>2</sup>, Nóra GÁL<sup>2</sup>, Birgitte HANSEN<sup>3</sup>, Denitza D. VOUTCHKOVA<sup>3</sup>, Jörg SCHULLEHNER<sup>4</sup>, Julie LIONS<sup>5</sup>, Lucio MARTARELLI<sup>6</sup>, Elena GIMÉNEZ-FORCADA<sup>7</sup>, José Ángel DÍAZ-MUÑOZ<sup>7</sup>, Eline MALCUIT<sup>5</sup>, Gerhard SCHUBERT<sup>1</sup>, Gerhard HOBIGER<sup>1</sup> & Nina RMAN<sup>8</sup>

<sup>1</sup>Geological Survey of Austria – GBA, Neulinggasse 38, 1030 Vienna, Austria;

e-mail: daniel.elster@geologie.ac.at, gerhard.schubert@geologie.ac.at, gerhard.hobiger@geologie.ac.at

<sup>2</sup>Mining and Geological Survey of Hungary – MBFSZ, Columbus utca 17-23, 1145 Budapest, Hungary;

e-mail: szocs.teodora@mbfsz.gov.hu, gal.nora@mbfsz.gov.hu

<sup>3</sup>Geological Survey of Denmark and Greenland – GEUS, C.F. Møllers Allé 8, 8000 Aarhus C, Denmark;

e-mail: bgh@geus.dk, dv@geus.dk,

<sup>4</sup>Geological Survey of Denmark and Greenland – GEUS, C.F. Møllers Allé 8, 8000 Aarhus C, Department of Public Health, Aarhus University, Bartholins Allé 2, 8000 Aarhus C, Denmark; e-mail: jsc@geus.dk

<sup>5</sup>Geological Survey of France – BRGM, 3 Av. Claude Guillemin, 45100 Orléans, France;

e-mail: j.lions@brgm.fr, e.malcuit@cfg.brgm.fr

<sup>6</sup>Geological Survey of Italy – ISPRA, Via Vitaliano Brancati 48, 00144 Rome, Italy;

e-mail: lucio.martarelli@isprambiente.it

<sup>7</sup>Instituto Geológico y Minero de España – CN-IGME CSIC, 28003 Madrid, Spain;

e-mail: e.gimenez@igme.es, j.diaz@igme.es

<sup>8</sup>Geological Survey of Slovenia – GeoZS, Dimičeva ulica 14, 1000 Ljubljana, Slovenia; e-mail: nina.rman@geo-zs.si

Prejeto / Received 16. 11. 2021; Sprejeto / Accepted 15. 7. 2022; Objavljeno na spletu / Published online 22. 7. 2022

*Key words:* hydrogeology, regulatory framework, hydrogeochemical composition, natural mineral water, thermal water, Europe

*Ključne besede:* Hidrogeologija, zakonodajno okolje, hidrogeokemična sestava, naravna mineralna voda, termalna voda, Evropa

### Abstract

This study discusses 1) the national legislative frameworks, terminologies, and criteria for the recognition of natural mineral waters and thermal waters in selected European countries (Austria, Bosnia and Herzegovina, Denmark, France, Hungary, Iceland, Italy, Lithuania, Poland, Portugal, Romania, Serbia, Slovenia, and Spain), and 2) it provides a first extensive multi-national overview of hydrogeological and hydrogeochemical characteristics of numerous water sources from those regions.

Natural mineral waters are well defined and regulated in the European Union by the Directives 2009/54/EC and 2003/40/EC that are implemented by national law regulations. In contrast, no legal definition exists for thermal waters on an EU level and national definitions commonly differ or are not present. Defining thermal waters by water temperatures of at least 20 °C at the outlet is commonly found (6 out of 15 countries), but other definitions like considering the difference to the average air temperature are also present. Furthermore, no definitions on a national level are quite frequent (5 out of 15 countries), those countries preferentially refer to expert recognitions.

We considered 678 natural mineral waters and 2,390 thermal waters in this study and collected information on practical use, hydrogeological settings and hydrogeochemical conditions. The comparison of the datasets shows commonalities like a predominance porous aquifers, especially sandy aquifers, and sedimentary carbonate rock aquifers (limestone, dolomite, chalk). Furthermore, natural mineral waters commonly show TDS contents of less than 1 g/l and alkaline-earth-HCO<sub>3</sub> water types. Surprisingly, 21 % of the considered sources bear water temperatures above 20 °C and could be considered as thermal waters as well. Thermal waters – the majority (above 30 °C) is found in Hungary - usually show water temperatures between 20 and 70 °C and TDS contents between 1 and 14.5 g/l. The hydrogeochemical properties show a larger variation in contrast to natural mineral waters, but Na-(HCO<sub>3</sub>, Cl) waters seem to be most commonly found.

## Izveček

Študija razpravlja o: 1) nacionalnih zakonodajnih okvirjih, izrazoslovju in kriterijih za priznavanje naravnih mineralnih in termalnih voda v izbranih evropskih državah (Avstrija, Bosna in Hercegovina, Danska, Francija, Madžarska, Islandija, Italija, Litva, Poljska, Portugalska, Romunija, Srbija, Slovenija in Španija), ter 2) predstavlja prvi pregledni več-nacionalni pregled hidrogeoloških in hidrogeokemijskih značilnosti številnih vodnih virov v teh regijah.

Naravne mineralne vode v Evropski uniji so definirane in regulirane z Direktivama 2009/54/EC in 2003/40/EC, implementiranima z nacionalno zakonodajo. Nasprotno, na nivoju EU ne obstaja zakonodajna definicija za termalne vode, nacionalne definicije so različne ali pa celo ne obstajajo. Kot termalna voda so običajno opredeljene vode s temperaturo iztoka vsaj 20 °C (v 6 od 15 držav), vendar obstajajo tudi definicije, ki upoštevajo odstopanje od povprečne letne temperature zraka. Nadalje, ponekod nacionalnih definicij nimajo (5 od 15 držav), tam jih običajno priznavajo na podlagi strokovnih mnenj.

V raziskavo smo vključili 678 naravnih mineralnih voda ter 2.390 termalnih voda in zbrali podatke o rabi, hidrogeoloških osnovah in hidrogeokemijskih pogojih. Primerjava podatkov je pokazala, da prevladujejo medzrnski, še posebej peščeni vodonosniki, in vodonosniki v sedimentnih karbonatnih kamninah (apnenec, dolomit, kreda). Nadalje, naravna mineralna voda ima najpogosteje manj kot 1 g/l skupnih raztopljenih snovi ter je zemeljskoalkalijsko- $\text{HCO}_3$  tipa. Presenetljivo lahko kar 21 % naravnih mineralnih voda uvrstimo tudi med termalne vode, saj imajo temperaturo nad 20 °C. Termalne vode imajo temperaturo običajno med 20 in 70 °C in TDS med 1 in 14,5 g/l, večino (z nad 30 °C) pa najdemo na Madžarskem. Hidrogeokemične lastnosti termalnih voda so bolj spremenljive kot pri naravnih mineralnih vodah, najpogosteje pa so vode Na-( $\text{HCO}_3$ , Cl) tipa.

## Introduction

Thermal and mineral waters are special types of groundwater. They are well known for thousands of years and have an important role in society, well-being and health (e.g. EuroGeoSurveys, 2016; Stober & Bucher, 2012; Lund, 2001). From prehistoric use of natural thermal waters to Roman public baths – the evolution of societies is always accompanied by these waters. Today, as these waters are widely used in our society for societal and economic purposes, regulations have been drawn up at the national and international levels.

Today, natural mineral waters have an important role in the bottled water industry among EU's member states. According to the non-profit trade association, "Natural Mineral Waters Europe", 97 % of all bottled water sold in Europe comes from a natural mineral water or spring water source (Natural Mineral Waters Europe, 2021). The EU average consumption was approximately 118 liters per capita in 2019; and Italy, Germany, Portugal, Hungary and Spain were biggest consumers.

Thermal waters or geothermal waters – the water temperature is elevated due to geothermal heat and they are a source of clean energy as well as a valuable product with therapeutic, balneotherapeutic and recreational properties (Sowizdzal, 2018). For centuries, they are used for balneological purposes and wellness. There are numerous examples for famous spas in Europe, like Gellert, Széchenyi and Rudas in Hungary, Baden-Baden in Germany, Karlovy Vary in Czech Republic or Grindavik in Iceland, while natural mineral water sites e.g. Rogaška Slatina in Slove-

nia were used for drinking treatments for centuries. Furthermore, the geothermal energy sector has continuously grown over the last decades and geothermal water is directly used for heating and electric power generation. For example, already 1,028 megawatt (MWe) comes from 57 geothermal power plants across Europe (EGEC, 2019) and the Pannonian basin is one of most prominent and historic geothermal places (Rman et al., 2020).

Several studies about the hydrogeology and hydrochemistry of mineral and thermal waters have been published on a national level in recent years, e.g. Haas et al., 2018; Elster et al. 2016, 2018; Eftimi & Frasheri, 2016; Miošić & Samardžić, 2016; Rosca et al., 2016; Todorović et al., 2016; Burić et al., 2016; Benderev et al., 2016; Borović et al., 2016; Eggenkamp & Marques, 2013; Dinelli et al., 2012; Brenčič et al. 2010; Lourenço et al. 2010; Käss & Käss, 2008; Lapanje, 2006; Zötl & Goldbrunner, 1993; Minissale, 1991. However, less studies describe and compare sources from multiple countries and regions in Europe (Porowski, 2019; Bräuer, et al. 2016; Papić, 2016; Balderer et al., 2014; Borszédi, 2013; Szocs et al. 2013; Gros, 2003; LaMoreaux & Tanner, 2001; Albu et al., 1997; Michel, 1997; Carlé, 1975). Furthermore, the comprehensive study on European Bottled Waters by Reimann & Birke (2010) focuses on Natural Mineral Waters to some extent, as well as books by Evina (1992) and Kirschner (2009).

Certainly, extensive literature is available to deepen the understanding of this topic. However, used terminologies vary between countries and can lead to misinterpretations. Divergent or missing national legislative frameworks are commonly the reason besides legal adaptations in

time. The generally used glossary comprises a large number of technical terms including mineral water, healing/curative water, natural mineral water and spring water in the bottling industry, and thermal water that have to be clearly distinguished.

This study aims to assess first the national legislative frameworks, terminologies, and criteria for the recognition of natural mineral waters and thermal waters in the following European and neighbouring countries: Austria, Bosnia and Herzegovina, Denmark, France, Hungary, Iceland, Italy, Lithuania, Poland, Portugal, Romania, Serbia, Slovenia, and Spain. All were involved in Hydrogeological processes and Geological settings over Europe controlling dissolved geogenic and anthropogenic elements in groundwater of relevance to human health and the status of dependent ecosystems GeoERA (HOVER) project. Second, it provides a first extensive multi-national overview of hydrogeological and hydrochemical characteristics of numerous water sources from those regions.

### Methodology

An overview of the legal recognition of thermal and natural mineral waters was provided within the project GeoERA HOVER by the national geological surveys based on the analysis of each relevant national legislation (see supplement information).

Furthermore, a database with a harmonized structure was set up to collect the hydrogeological and hydrochemical information at a multi-national scale (Table 1 and supplement information). A focus was given to available vocabulary standards of Inspiring New Scientific Perspective in Research and Ethics (INSPIRE) and Geoscience Markup Language (GEOSCIML) to increase the level of transparency. The data collection comprises hydrogeological and hydrochemical information (names of sources, locations, type of sources, use, borehole depths, aquifer media and type, aquifer lithology and age, hydrochemistry and groundwater age) (see Table 1 for details). Only representative single hydrochemical analysis were collected instead of data series assuming stable hydrochemical conditions with negligible variations for both types of special groundwaters (thermal and natural mineral waters). Stable conditions are a prerequisite requirement of a natural mineral water definition, and in most cases observed at thermal waters also. However, the selection of the representative analysis is based on expert evaluation. Post processing of the dataset comprised a general data curation, critical checks for outliers and anomalies, ion balance calculations of representative analysis (charge balance error (%) =  $100 \times \frac{(\sum \text{cations} - \sum \text{anions})}{(\sum \text{cations} + \sum \text{anions})}$ ; see Freeze and Cherry, 1979) and water type calculations (cations and anions > 20 eq%). Analyses

Table 1. Collected hydrogeological and hydrochemical information in the dataset.

| General information   |
|---|
| <ul style="list-style-type: none"> <li>name of source and country</li> <li>classification: thermal water, natural mineral water (Directive 2009/54/EC), natural mineral water (national law recognition)</li> <li>type of water source: single well, well field, single artesian well, artesian well field, single captured spring, captured spring group, single gallery, gallery group, single spring, combination of sources</li> <li>use: bottled natural mineral water, natural mineral water publicly available, thermal water for balneology, thermal water for heating, thermal water for electricity production, other; multiple answers (up to 3) were possible.</li> <li>yield classes in l/s: &lt;5, 5-25, &gt;25</li> <li>borehole depth and screen depths in m (true vertical depths)</li> <li>Aquifer media type according to INSPIRE: <a href="http://inspire.ec.europa.eu/codelist/AquiferMediaTypeValue">http://inspire.ec.europa.eu/codelist/AquiferMediaTypeValue</a></li> <li>Aquifer type according to INSPIRE: <a href="http://inspire.ec.europa.eu/codelist/AquiferTypeValue">http://inspire.ec.europa.eu/codelist/AquiferTypeValue</a></li> <li>Lithology of the aquifer according to INSPIRE: <a href="http://inspire.ec.europa.eu/codelist/LithologyValue">http://inspire.ec.europa.eu/codelist/LithologyValue</a></li> <li>Proportion of the lithology according to GEOSCIML: <a href="http://resource.geosciml.org/classifier/cgi/proportionterm">http://resource.geosciml.org/classifier/cgi/proportionterm</a></li> <li>Aquifer age according to INSPIRE: <a href="http://inspire.ec.europa.eu/codelist/GeochronologicEraValue/">http://inspire.ec.europa.eu/codelist/GeochronologicEraValue/</a></li> </ul> |
| Location  |
| <ul style="list-style-type: none"> <li>the location is derived from 1 km and 10 km grids, <a href="https://www.eea.europa.eu/data-and-maps/data/eea-reference-grids-2">https://www.eea.europa.eu/data-and-maps/data/eea-reference-grids-2</a> and no exact coordinates are provided</li> </ul>  |
| Information of a representative hydrochemical analysis  |
| <ul style="list-style-type: none"> <li>water temperature classes at the outlet of the source in °C: &lt;15, 15-20, 20-30, 30-40, 40-50, 50-60, 60-70, 70-80, 80-90, 90-100, &gt;100. We chose those classes to provide detailed information on water temperature distributions. They may not connect to national legislative frameworks.</li> <li>total dissolved solids (g/l): &lt;1, 1-14.5, &gt;14.5</li> <li>field parameters specific conductivity (µS/cm; 25°C), pH, redox potential (Eh), O<sub>2</sub> (mg/l)</li> <li>hydrochemical compounds in mg/l: Na, K, Ca, Mg, Sr, Ba, Fe, Mn, NH<sub>4</sub>, HCO<sub>3</sub>, CO<sub>3</sub>, F, Cl, Br, I, SO<sub>4</sub>, NO<sub>3</sub>, HS, Al, Sb, As, Be, Pb, Cd, Cs, Cr, Co, Cu, Li, Mo, Ni, Hg, Rb, Se, U, V, Zn, Sn, H<sub>2</sub>SiO<sub>3</sub>, H<sub>2</sub>BO<sub>3</sub></li> <li>gas phase dominance: Methane (CH<sub>4</sub>), Carbon dioxide (CO<sub>2</sub>), Nitrogen (N<sub>2</sub>), Hydrogen sulphide (H<sub>2</sub>S)</li> <li>Apparent residence time: younger than 60, 60-10,000 years, older than 10,000 years. Those threshold values for groundwater ages were estimated by available isotope data or estimated expert judgements, however no raw data on relevant isotopes for groundwater age dating was collected. The categories were chosen by common criteria connected to isotope interpretation: e.g. presence of <sup>3</sup>H, <sup>14</sup>C.</li> </ul>  |

with a charge balance error above 10 % were not considered in the further data evaluation. Shares of hydrochemical analyses below detection limit (DL) were treated by DL/2 to consider them in basic statistical figures (e.g. boxplots).

## Results

### EU and national legislations

#### Natural mineral waters

The exploitation and marketing of natural mineral waters in the European Union is regulated in Directive 2009/54/EC (see Annex 1- legal norms) and it can be clearly distinguished from ordinary drinking water by the following criteria:

1. by its nature, which is characterised by its mineral content, trace elements or other constituents and, where appropriate, by certain effects;
2. by its original purity and constant level of minerals.

This Directive shall not apply to:

3. waters which are medicinal products within the meaning of Directive 2001/83/EC on the Community code relating to medicinal products for human use;
4. natural mineral waters used at source for curative purposes in thermal or hydromineral establishments.

An underground origin and protection from all risks of pollution are required to meet those criteria. The hydrochemical composition, tem-

perature and other essential characteristics of natural mineral waters shall remain stable in time ( $\pm 20$  %) and should only show natural fluctuation. Furthermore, the extraction rate should also not affect the composition.

Expert practice prior to Directive 2009/54/EC (see also Directive 80/777/EEC, no longer in force and adopted before from some states cooperating in the project become EU Members) was that the requirement for the legal recognition was different especially for some of the States not yet EU Members at that time and dependent on the level of total dissolved solids (TDS) or the content of carbonic acid. Traditionally, mineral water source needed to show pharmacological, physiological and clinical properties or TDS of at least 1,000 mg/l at the source and after bottling or a minimum of 250 mg/l of free carbon dioxide.

Directive 2003/40/EC established a list of recognized sources that is regularly updated and sets concentration limits for public health purposes, labelling requirements and limited possibilities for water treatment (5 types of treatments are permitted). Natural mineral waters and spring waters may be treated at source to remove unstable elements and some undesirable constituents in compliance with the provisions laid down in Article 4 of Directive 2009/54/EC. Table 2 and 3 provide an overview of natural constituents, indications, and criteria for water quality. Finally, it should be mentioned that the hydrochemical composition needs to be present on the label of a bottled water as well.

Table 3. Criteria for natural mineral water indications according to Annex III of Article 9 in Directive 2009/54/EC.

| Indications                                 | Criteria   |
|---|--|
| Low mineral content                         | Mineral salt content, calculated as a fixed residue, not greater than 500 mg/l |
| Very low mineral content                    | Mineral salt content, calculated as a fixed residue, not greater than 50 mg/l  |
| Rich in mineral salts                       | Mineral salt content, calculated as a fixed residue, greater than 1,500 mg/l   |
| Contains bicarbonate                        | Bicarbonate content greater than 600 mg/l                                      |
| Contains sulphate                           | Sulphate content greater than 200 mg/l   |
| Contains chloride                           | Chloride content greater than 200 mg/l   |
| Contains calcium                            | Calcium content greater than 150 mg/l  |
| Contains magnesium                          | Magnesium content greater than 50 mg/l   |
| Contains fluoride                           | Fluoride content greater than 1 mg/l   |
| Contains iron                               | Bivalent iron content greater than 1 mg/l                                      |
| Acidic                                      | Free carbon dioxide content greater than 250 mg/l                              |
| Contains sodium                             | Sodium content greater than 200 mg/l   |
| Suitable for the preparation of infant food | —  |
| Suitable for a low-sodium diet              | Sodium content less than 20 mg/l   |
| May be laxative                             | —  |
| May be diuretic                             | —  |

Table 2. Constituents naturally present in natural mineral waters and maximum limits which, if exceeded, may pose a risk to public health according to Annex I in Directive 2003/40/EC.

| Constituents | Maximum limit in mg/l |
|--------------|-----------------------|
| Antimony     | 0.005                 |
| Arsenic      | 0.01 (as total)       |
| Barium       | 1                     |
| Boron        | not fixed             |
| Cadmium      | 0.003                 |
| Chromium     | 0.050                 |
| Copper       | 1.0                   |
| Cyanide      | 0.07                  |
| Fluorides    | 5.0                   |
| Lead         | 0.010                 |
| Manganese    | 0.50                  |
| Mercury      | 0.001                 |
| Nickel       | 0.02                  |
| Nitrates     | 50                    |
| Selenium     | 0.01                  |

In 2021, 2,098 trade descriptions of natural mineral waters are recognised by member states including Northern Ireland (UK) and countries in the European Economic Area (EEA countries). Natural mineral waters are subject to an authorization procedure carried out by the competent authorities of the EU countries. The lists of natural mineral waters officially recognised are published by the European Commission in the Official Journal of the European Union. These

lists are regularly updated. It has to be added that trade name can be associated with multiple sources (e.g. boreholes or springs). Germany leads the ranking with 827 accepted trade descriptions, followed by Italy (305), Hungary (173), Spain (160) and France (101). Another interesting note is that member states can recognize natural mineral water sources in third countries, for example Germany has accepted places of exploitation in Armenia, Bosnia and Herzegovina, Canada, China, Croatia, India, Iran, Kosovo, Macedonia, New Zealand, Russia, Serbia, Switzerland and Turkey. Therefore, sources of registered natural mineral waters in Europe can be imported from outside of Europe.

To avoid misunderstandings of used terms, natural mineral waters regulated by Directive 2009/54/EC have to be clearly separated from the following groundwater types:

- Bottled spring waters. They are intended for human consumption, usually from a single non-polluted groundwater source, are bottled at source and comply with the present drinking water regulations (Directive 2020/2184). However, the original purity may vary, what means that hydrochemical compositions do not need to remain stable as requested for mineral water ( $\pm 20\%$  of variation not relevant) over a lengthy period of time. Certain provisions of the previously mentioned Directive 2009/54/EC are also applicable to

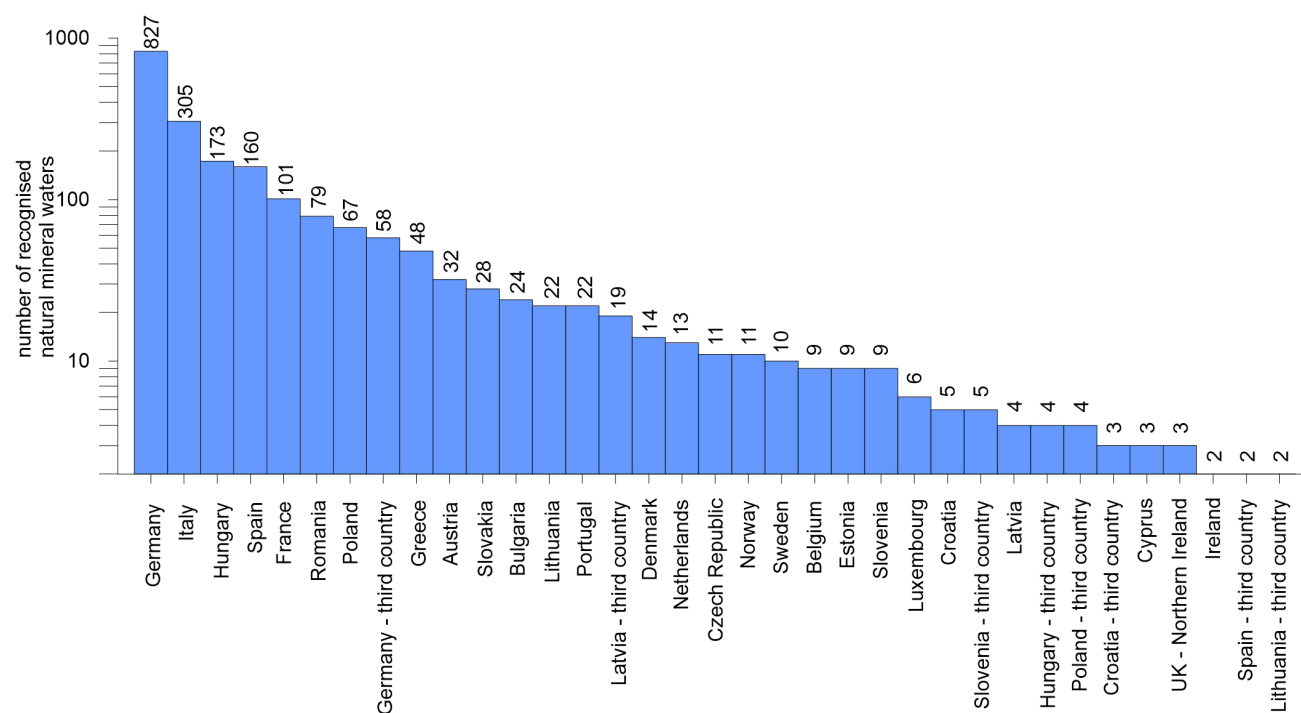


Fig. 1. List of natural mineral waters recognised by member states, United Kingdom (Northern Ireland) and EEA countries according to Directive 2003/40/EC, update from April 9th 2021 (see legal norms).

- spring waters such as the microbiological parameters and labelling requirements.
- Bottled drinking water: A bottled drinking water not necessarily has to have an underground source, therefore bottling at a spring or borehole is not a requirement (Directive 98/83/EC) and additional water treatment are allowed to modify water quality. Its quality has to comply with the drinking water regulations.
- Healing/curative/therapeutic and geothermal or thermomineral water: There is no Directive applicable, but national legislative frameworks may consider from nation-to-nation divergent definitions for those types of groundwaters that are commonly based on specific criteria (e.g. TDS content, hydrochemical compounds and temperature, pharmacological, physiological and clinical properties).

The following national legal norms regulate natural mineral waters in selected countries of the dataset (see also Annex 1: Legal norms; no information was delivered for Iceland and Lithuania):

|                               |   |
|-------------------------------|---|
| <b>Austria</b>                | In Austria, natural mineral waters are defined in the mineral water and spring water regulation: Mineral- and spring water regulation, BGBl. II, Nr. 309/1999 However, the following laws and regulations have to be considered as well: 1) water rights act: WRG 1959, BGBl. Nr. 215/1959 idgF. 2) drinking water ordinance: TWV, BGBl. II Nr. 304/2001 idgF. 3) Health- and nutrition security law: GESG, BGBl. I Nr. 63/2002 idgF. 4) food security and consumer protection law: LMSVG, BGBl. I Nr. 13/2006 idgF. 5) Food labelling regulation: LMKV, BGBl. Nr. 72/1993 idgF. Relevant threshold values are found in the previously mentioned mineral water and spring water regulation and the Austrian food code: Chapter B 17 „Bottled waters“ (BMGF-75210/0005-II/B/13/2016).  |
| <b>Bosnia and Herzegovina</b> | Natural mineral waters are defined in the Waters Act - Rulebook on natural mineral water, spring water and table water (Official Gazzette of the Bosnia and Herzegovina No. 26/10, 40/10).  |
| <b>Denmark</b>                | The groundwater source has to be approved by the Danish Veterinary and Food Administration under the Ministry of Environment and Food of Denmark and the following national legislation is relevant: 1) BEK nr 38 of 12/01/2016 Bekendtgørelse om naturligt mineralvand, kildevand og emballeret drikkevand; 2) VEJ nr 9105 of 10/04/2008 Vejledning om mærkning af naturligt mineralvand, kildevand og emballeret drikkevand.  |
| <b>France</b>                 | It is defined by transposition of the EU Directive 2009/54/EC into the Public Health Code (articles L1322-1 to 13 et R.1322-1 to 1322-44-23) and in the following regulations: Decree No 2007-49 of 11 January 2007 on the safety of water intended for human consumption. Supplemented by five orders relating to the constitution of the authorisation application files for public interest declaration, assignment of a protection perimeter, water quality criteria, analyses of sanitary control and water monitoring, etc. Before the application of the EU Directive, french mineral waters were also recognised for their therapeutic properties by the French Academy of Medicine. By regulation, mineral water can be used packaged (bottled), distributed in a public water supply (buvette publique) or used for therapeutic uses in a spa establishment, each usage is cover by a strict legislation to ensure water quality and public health (maximum limits, water treatment).   |
| <b>Hungary</b>                | Mineral water according to Hungarian law LVII from 1995 on water management is defined as water which originates from a natural aquifer, which has a typically different mineral composition compared to those used as a source for regular human drinking water, and its water composition meets the (biological and chemical) criteria defined in the relevant legislation. The 65/2004 (IV. 27.) FVM-ESzCsM-GKM common ministerial decree (with its update according to the 59/2006 (VIII. 14.) FVM-EüM-SZMM common ministerial decree) defines the requirements of bottled natural mineral water, spring water, drinking water, and enriched, flavoured, or enriched and flavoured bottled water. This decree is the law adopting and implementing the 80/777/EEC, 96/70/EC and 2003/40/EC EU laws. This decree does not regulate those non-bottled natural mineral waters which are used at their abstraction location or are used for medicinal purposes in balneological, health recuperation institutes. Those waters which are recognised as medicinal waters, including recognised medicinal mineral waters, are regulated by the 74/1999 (XII. 25.) EüM ministerial decree on natural medical factors. |
| <b>Italy</b>                  | In Italy, natural mineral water is defined in the Italian Legislative Decree N.176 of 8 October 2011, which adopts the EU Directive 2009/54/EC. Article 2.1 defines it as water which originated from a groundwater body, crops out at one or more natural of artificial springs and has peculiar purity conditions and health relevant properties.   |
| <b>Poland</b>                 | In Poland, natural mineral water is defined as groundwater which differs from water used for human consumption in its original chemical and microbiological purity, its characteristic stable mineral composition and, in certain cases, its properties can have beneficial effects on human health. The above definition of water comes from Act of 25 August 2006 on Food and Nutrition Safety (Jour. of Law 2006 No 171 item 1563). The requirements concerning the composition and physical properties of natural mineral water are set out in the Regulation of 31 March 2011 on natural mineral water, spring water and table water (Jour. of Law 2011 No 85 item 466).   |
| <b>Portugal</b>               | In Portugal, natural mineral water is defined in Law no° 54/2015 of 22 June (Geological Resources Law) and the following specific regulations: Decree-Law no. 86/90 of 16 March (natural mineral waters) and Decree-Law no. 84/90 of 16 March (spring water).   |
| <b>Romania</b>                | In Romania, natural mineral water is a pure microbiological water, originating in an underground aquifer, protected from any possible risk of pollution according to Annex no. 1 from Government Decision 1020/2005. It is exploited by one or more natural sources and it is characterized by a stable composition, temperature and other characteristics within the limits of natural fluctuation and in terms of source flow variations.   |

|                 |   |
|-----------------|---|
| <b>Serbia</b>   | In Serbia, natural mineral water is defined in the “Regulation on Quality and Other Requirements for Natural mineral water, Spring Water and Bottled Drinking Water” (Official Gazette of Serbia and Montenegro, number 53/05). Furthermore, the “Regulation on the Hygienic Acceptability of Potable Water (Official Gazette of FR Y, number 42/98 and 44/99) have to be considered.   |
| <b>Slovenia</b> | In Slovenia, natural mineral water is defined in the Rules on natural mineral water, spring water and table water (Official Gazette of Rep. of Slovenia No. 50/04, 75/05 in 45/08 – ZKme-1). Article 4 defines it as water which beside microbiological requirements from the 5th article also: has a source in a subsurface water source (is groundwater), protected from any possibility of contamination, and springs or is pumped at a spring from one or more natural outflows or wells; has properties which clearly distinguish it from drinking water and may be connected to content of dissolved solids, trace elements or other ingredients, and may have certain nutritional and physiological effects; has the same purity as at the source. The deviation from the mean annual measured values for the main constituents specific to the individual natural mineral water may not exceed $\pm 20\%$ .                                     |
| <b>Spain</b>    | Natural mineral waters are regulated by the following legislation: 1) Law of Mines 22/1973, 21 of July (BOE number 189, de 24-07-1973); 2) Royal Law 2857/1978, 25 of August (BOE number 295, de 11-12-1978). Furthermore, natural mineral waters are also regulated by the Royal Law 1798/2010 regarding the exploitation and commercialization of bottled drinking natural mineral waters and spring waters. From the interpretation of this legislation, it can be understood that depending on the use or destination, mineral-medicinal waters could be classified into: 1) Natural mineral waters: Those are microbiologically-free and with a constant chemical composition over time regardless of the water flow. They have a specific mineral and trace elements composition and are characterized for its original purity and 2) Spring waters: Those are microbiologically-free but no constant chemical composition over time is required. |

### Thermal waters

In opposition to natural mineral waters, no European directives exist to define thermal waters. Most definitions for thermal water are based on water temperatures at the outlet. However, thermal waters are not recognized or defined by an EU legislative framework. National laws or directives may set the criteria.

Results from this study show, that the majority of countries define a thermal water by a minimum temperature of 20°C at the outlet of the source (Table 4). However, several member states don't have any criteria on temperature, but apply expert / professional recognitions according to different water properties.

Detailed Information about the national legislation frameworks in considered countries is found in Annex 1- Legal norms. No legislation framework for the definition of thermal waters is present in Lithuania, Portugal and Iceland. In Denmark, no thermal waters are present as all groundwaters show temperatures at the outlet below 15 °C.

|                               |   |
|-------------------------------|---|
| <b>Austria</b>                | In Austria, sources of thermal waters are not defined by a federal law, but by Acts on natural health-promoting substances and spas for each state in Austria except Vorarlberg. However, they share the definition that groundwaters with a temperature of 20°C or higher at the outlet are considered as thermal water.   |
| <b>Bosnia and Herzegovina</b> | In Bosnia and Herzegovina thermal waters are defined in the Waters Act - Rolebook on the categorization, classification, the budget reserve of ground water and management of records about them (Official Gazette of the Bosnia and Herzegovina No. 47/11). Thermal waters are defined by a total mineralization <1 g/l and a water temperature greater than the mean annual air temperature of the area where the source is located. Thermal waters with a total mineralization > 1g/l are considered as thermomineral waters. Several additional regulatory frameworks and laws are relevant for the definition of thermal waters.   |
| <b>France</b>                 | In France, national regulations of thermal waters are based on the Public Health Code and the Decree 2007-49 11 January 2007 on the health safety of water intended for human consumption. There is no definition according to temperature at the outlet. A thermal water is defined as a natural mineral water used in a thermal establishment for its therapeutic properties (article R. 1322-52). Exploitation of thermal mineral water is covered by a legal authorisation and strict water quality controls overseen by the health authorities and covered by the Public Health Code. Thermal water is used on site or by direct adduction, for the internal or external treatment of the curists diseases, water from one or more regularly authorized mineral sources and/or sludges and/or gases. The therapeutic properties are recognized by the medicinal authorities (Académie de Médecine).                                  |
| <b>Hungary</b>                | In Hungary, thermal water according to the Hungarian law LVII from 1995 on water management is defined as (having its source from an aquifer) groundwater with an outflow temperature (at the surface) of 30°C or above. Its use is regulated as already mentioned under natural mineral waters, those waters which are recognised as medicinal waters, including recognised medicinal mineral waters, are regulated by the 74/1999 (XII. 25.) EüM ministerial decree on natural medical factors. Thermal water resource management, the management of used thermal water is regulated by the 147/2010. (IV. 29.) Government Decree under the general rules on the use, protection and damage control of waters, and water utilities. The Hungarian law XLVIII from 1993 on mining regulates when a geothermal energy usage requires concession rights, and defines the criteria for mining royalties related to geothermal energy usage. |
| <b>Italy</b>                  | In Italy, thermal water is mentioned in the Italian Governmental Law N.323 of 24 October 2000 but this act deals only with the exploitation permits and not with technical-scientific issues and, consequently, there is not a definition according to temperature at the outlet.   |
| <b>Poland</b>                 | In Poland, thermal water is defined as groundwater with a temperature at the outflow not lower than 20°C. The above definition of thermal water comes from Act of 9 June 2011 Geological and Mining Law (Jour. of Law 2018 item 1563)   |
| <b>Romania</b>                | In Romania, thermal water is defined in the Governmental Decision no. 1154/2004.  |

|                 |   |
|-----------------|---|
| <b>Serbia</b>   | In Serbia, thermal water is groundwater which temperature is higher than the average annual temperature of a given place. To be considered as a thermal groundwater, it should meet certain requirements: to have a stable regime and to be heated from the temperature of the Earth's crust, not from the Sun's heat, which means that its temperature should be a consequence of geothermal processes in the Earth's crust. Nevertheless, in practice groundwater with an outlet water temperature > 20°C are commonly considered as thermal water. There are no precise terms from national laws or rulebooks.   |
| <b>Slovenia</b> | In Slovenia, thermal water is defined in the Waters Act (Official Gazette of Rep. of Slovenia No. 67/02, 2/04 – ZZdrI-A, 41/04 – ZVO-1, 57/08, 57/12, 100/13, 40/14, 56/15). Row 6. of the article 7 defines it as a groundwater from a well, spring or a capture which is heated in geothermal processes in Earth's crust and has the temperature at the spring or wellhead at least of 20 °C.   |
| <b>Spain</b>    | In Spain, thermal waters are regulated by the following legislation: 1) Law of Mines 22/1973, 21 of July (BOE number 189, de 24-07-1973); 2) Royal Law 2857/1978, 25 of August (BOE number 295, de 11-12-1978). Furthermore, according to the Article 23.1 and 23.2 of the 22/173 Law of Mines and the Article 38.1 of the 2857/1978 Royal Law, thermal waters are defined as a Mineral Resource and are classified as a special type of “mineral water”. In detail, mineral water is considered as thermal water when the outlet water temperature is 4°C greater than the mean annual air temperature in the same location where the water source is located. |

Table 4. Minimum water temperatures at the outlet (°C) to define thermal waters in selected countries.

| Minimum water temperatures at the outlet (°C) to define thermal water                                  | number of countries | names   |
|--|---------------------|---|
| Average water temperature has to differ 4 °C in relation to average air temperature                    | 1                   | Spain   |
| water temperature greater than the mean annual air temperature of the area where the source is located | 1                   | Bosnia and Herzegovina                                    |
| 20   | 6                   | Austria, Czech Republic, Italy, Poland, Romania, Slovenia |
| 30   | 2                   | Hungary, Lithuania  |
| no definition  | 5                   | France, Iceland, Latvia, Portugal, Serbia                 |

### Constitution of the dataset

The dataset comprises hydrogeological and hydrochemical information from 3,068 sources (e.g. springs or wells) from selected countries: Austria, Bosnia and Herzegovina, Denmark, France, Hungary, Iceland, Italy, Lithuania, Poland, Portugal,

Romania, Serbia, Slovenia and Spain including Catalonia (see Table 5 and Fig. 3).

Limited data availability and missing rights of data uses are the restricting reasons for a complete dataset in some countries and regions leading to the consideration of 2,390 thermal

Table 5. Overview of considered sources in the dataset. Natural mineral waters trade descriptions recognised by member states derived from 2013/C95/03 (updated May 25th 2021).

| Sources in countries   | classification of considered sources in the dataset & data availability in the provided dataset |               |  |                              | Natural mineral waters trade descriptions recognised by member states (2013/C95/03) |
|------------------------|---|---------------|--|------------------------------|---|
|                        | Natural mineral water (Directive 2009/54/EC)  | Thermal water | Natural mineral water (Directive 2009/54/EC) | Thermal water                |   |
| Austria                | 40  | 62            | All  | Yes                          | 32  |
| Bosnia and Herzegovina | 0   | 28            |  | Yes                          | None  |
| Denmark                | 17  | 0             | All  | No thermal waters in Denmark | 14  |
| France                 | 33  | 240           | partially                                    | Yes                          | 101   |
| Hungary                | 224   | 1,432         | all  | partially                    | 173   |
| Iceland                | 0   | 3             | none   | Yes                          | 1   |
| Italy                  | 0   | 241           | none   | Yes                          | 305   |
| Lithuania              | 21  | 0             | all  |                              | 22  |
| Poland                 | 126   | 46            | all  | Yes                          | 89  |
| Portugal               | 17  | 121           | partially                                    | Yes                          | 22  |
| Romania                | 0   | 14            | none   | Yes                          | 79  |
| Serbia                 | 30  | 82            | all?   | Yes                          | none  |
| Slovenia               | 9   | 33            | all  | Yes                          | 9   |
| Spain                  | 161   | 88            | all  | Yes                          | 160   |
| <b>Total</b>           | <b>678</b>  | <b>2,390</b>  |  |                              |   |

water sources and 678 natural mineral waters in this dataset. In a few cases – like in Hungary or France – natural mineral water sources can be also thermal waters if recognised according to Directive 2009/54/EC. Those waters are counted as natural mineral water source in the dataset.

Most important, no information on natural mineral waters is available for Italy and Romania and partial information is only available for France and Portugal. Also, no hydrochemical information, but TDS is reported for Hungarian thermal water sources. As it concerns Italy, this information is not reported here since it is not managed by the Geological Survey of Italy.

### Hydrogeological characteristics of natural mineral waters

The natural mineral waters considered in the dataset are mostly used for bottling ( $n=565$  out of 678), other uses like a public easements (free public access to a natural mineral water source;  $n=21$ ) are rarely found (Fig. 2). The yield of the sources is usually below 5 l/s ( $n=320$ ) or 5 to 25 l/s ( $n=219$ ). Extraction rates above 25 l/s are rarely found ( $n=16$ ), but present in Spain, Austria, Serbia and France.

Sources of groundwater extraction are usually single wells ( $n=300$  out of 678), followed by well fields ( $n=169$ ) and single artesian wells

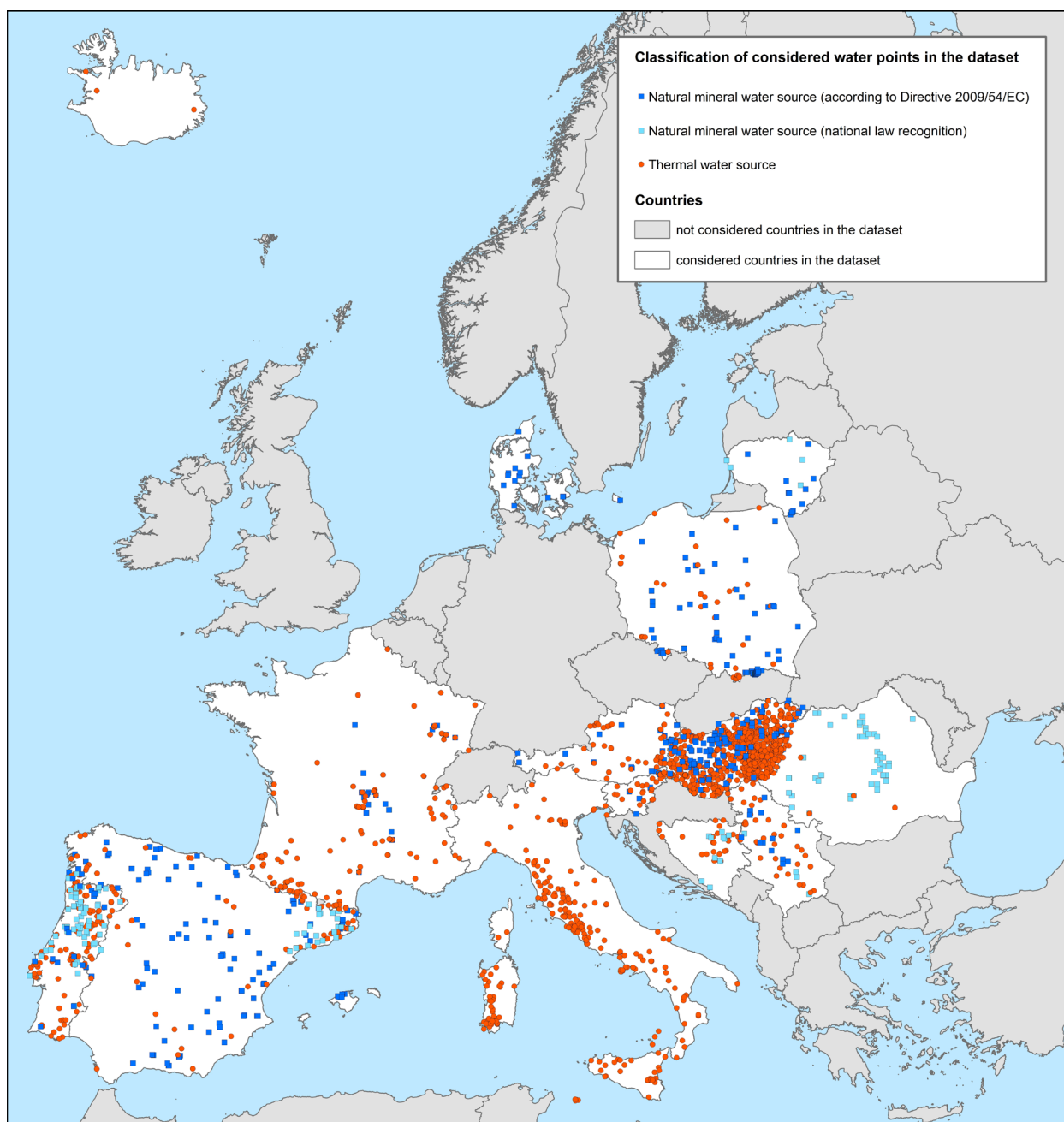


Fig. 2. Map of natural mineral waters and thermal waters found in the dataset.

( $n=74$ ). Captured springs ( $n=54$ ) or captured spring groups are less widespread ( $n=16$ ), which is expected as stable composition should prevail. Depths of wells are usually between approx. 85 and 250 m. Many sources are confined sub-artesian ( $n=299$ ) and artesian ( $n=114$ ). Unconfined conditions are uncommon ( $n=24$ ) as they are not suitable to meet the regulation criteria on geological and hydrogeological conditions for mineral water: water characteristics have to be preserved intact because of the underground origin of such groundwater, which has been protected from all risk of pollution.

The aquifer media type (primary and secondary porosity) is in most cases porous ( $n=275$  out of 678) or a combination of porous and fractured ( $n=99$ ). Karstic and fractured ( $n=78$ ), fractured ( $n=31$ ) and entirely karstic ( $n=2$ ) are less abundant. Karstic aquifers often have issues with microbiological pollution due to fast inflow of freshwater, therefore they rarely supply natural mineral waters resources. Porous aquifers with higher self-purification capabilities most often provide stable composition which is required for natural mineral waters.

The lithologies of the aquifers are often clastic sediments ( $n=264$  out of 678) and sandy aquifers are prevailing. Carbonate sedimentary rock aquifers ( $n=202$ ) are also numerous containing limestone, dolomite and chalk. Sources associated with pyroclastic rocks ( $n=65$ ), metamorphic rocks ( $n=27$ ), igneous rocks ( $n=24$ ) or clastic sedimentary rocks ( $n=17$ ) are less present. Most common aquifer ages are Neogene ( $n=133$  of 678), Mesozoic ( $n=120$ ) and Quaternary ( $n=103$ ).

Most sources have temperatures of  $<15$  °C at the outlet ( $n=312$  out of 678) and 132 sources

show temperatures between 15 and 20 °C (Table 7 and Fig. 3). Elevated temperatures above 20 °C are found for 117 natural mineral water sources, mainly in Hungary ( $n=71$ ) and less frequent in Serbia ( $n=16$ ), Spain. ( $n=14$ ), Portugal ( $n=7$ ), France ( $n=4$ ), Austria ( $n=3$ ), Slovenia ( $n=1$ ) and Poland ( $n=1$ ).

TDS are commonly below 1 g/l ( $n=342$ ), less sources show a range between 1-14.5 g/l ( $n=171$ ) and highly mineralized groundwaters with  $>14.5$  g/l are very rare ( $n=10$ ). Those highly mineralized natural mineral waters are entirely found in Hungary. The pH is usually in a range between 6.5 and 7.5 and EC mostly between 500 and 2,000  $\mu\text{S}/\text{cm}$  (25 °C); green color intensity to show higher numbers / percentages.

Calculations of the water types ( $>20\text{eq}\%$ ) of major cations and anions for 462 sources show, that (Ca, Mg)- $\text{HCO}_3$  waters are dominating ( $n=164$ ), followed by Na- $\text{HCO}_3$  waters ( $n=55$ ), Ca- $\text{HCO}_3$  waters ( $n=43$ ) and (Ca, Mg, Na)- $\text{HCO}_3$  waters ( $n=26$ ). 30 different water types were identified in the dataset proving a wide range of hydrochemical characteristics. Exclusively Na bearing types are found for 91 sources. Furthermore, non  $\text{HCO}_3$  types are rarely found ( $n=15$  for Cl;  $n=2$  for  $\text{SO}_4$ ). An overview of available hydrochemical analyses is found in Annex 2.

Under consideration of the indications of Directive 2009/54/EC for special labeling, 38 % of the sources are suitable for a low-Na diet, 33 % contain  $\text{HCO}_3$ , 31 % contain Fe, 26 % contain Na, 23 % contain Ca and Mg, 16 % contain F, 12 % contain Cl and 9 % contain  $\text{SO}_4$ .

Qualitative information on groundwater residence times is unfortunately scarce. Most sources show groundwater retention times above 60

Table 6. Natural mineral waters found in countries according to their temperatures at the outlet. Elevated numbers are visualized by green color intensity.

| Temperature class at the outlet (°C) (n=561 of 678) | <15 | 15-19.9 | 20-29.9 | 30-39.9 | 40-49.9 | 50-59.9 | 60-69.9 | 70-79.9 | Total number |
|---|-----|---------|---------|---------|---------|---------|---------|---------|--------------|
| Austria   | 33  | 4       | 1       | 2       |         |         |         |         | 40           |
| Denmark   | 14  |         |         |         |         |         |         |         | 14           |
| France  | 16  | 10      | 4       |         |         |         |         |         | 30           |
| Hungary   | 66  | 81      | 37      | 12      | 12      | 4       | 3       | 3       | 218          |
| Lithuania   | 20  | 1       |         |         |         |         |         |         | 21           |
| Poland  | 125 |         |         |         | 1       |         |         |         | 126          |
| Portugal  | 1   | 9       | 6       | 1       |         |         |         |         | 17           |
| Serbia  | 4   | 10      | 14      | 2       |         |         |         |         | 30           |
| Slovenia  | 7   | 1       | 1       |         |         |         |         |         | 9            |
| Spain   | 26  | 16      | 9       | 1       | 1       | 3       |         |         | 56           |
| Total number  | 312 | 132     | 72      | 18      | 14      | 7       | 3       | 3       | 561          |

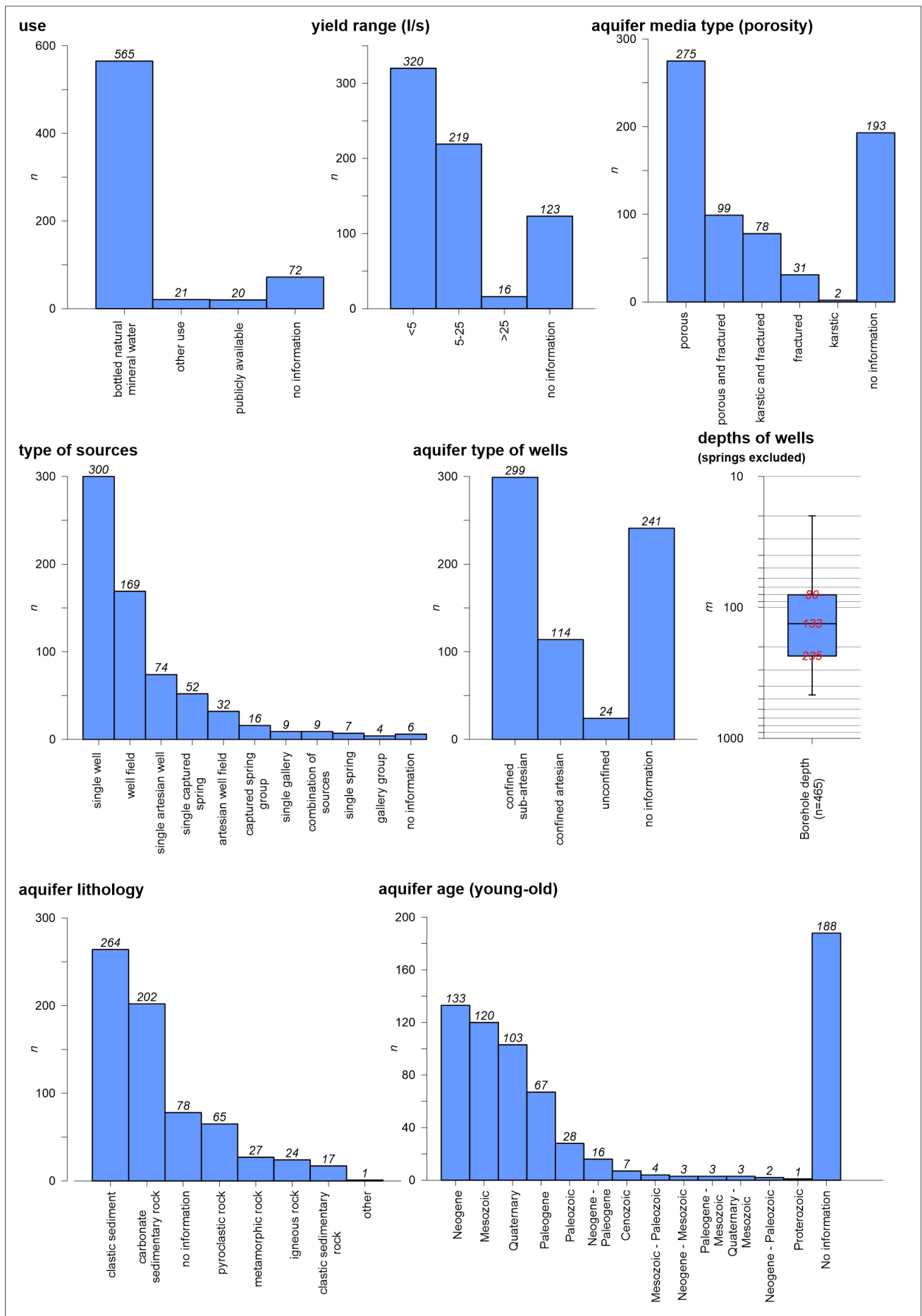


Fig. 3. Characteristics of natural mineral waters found in the dataset.

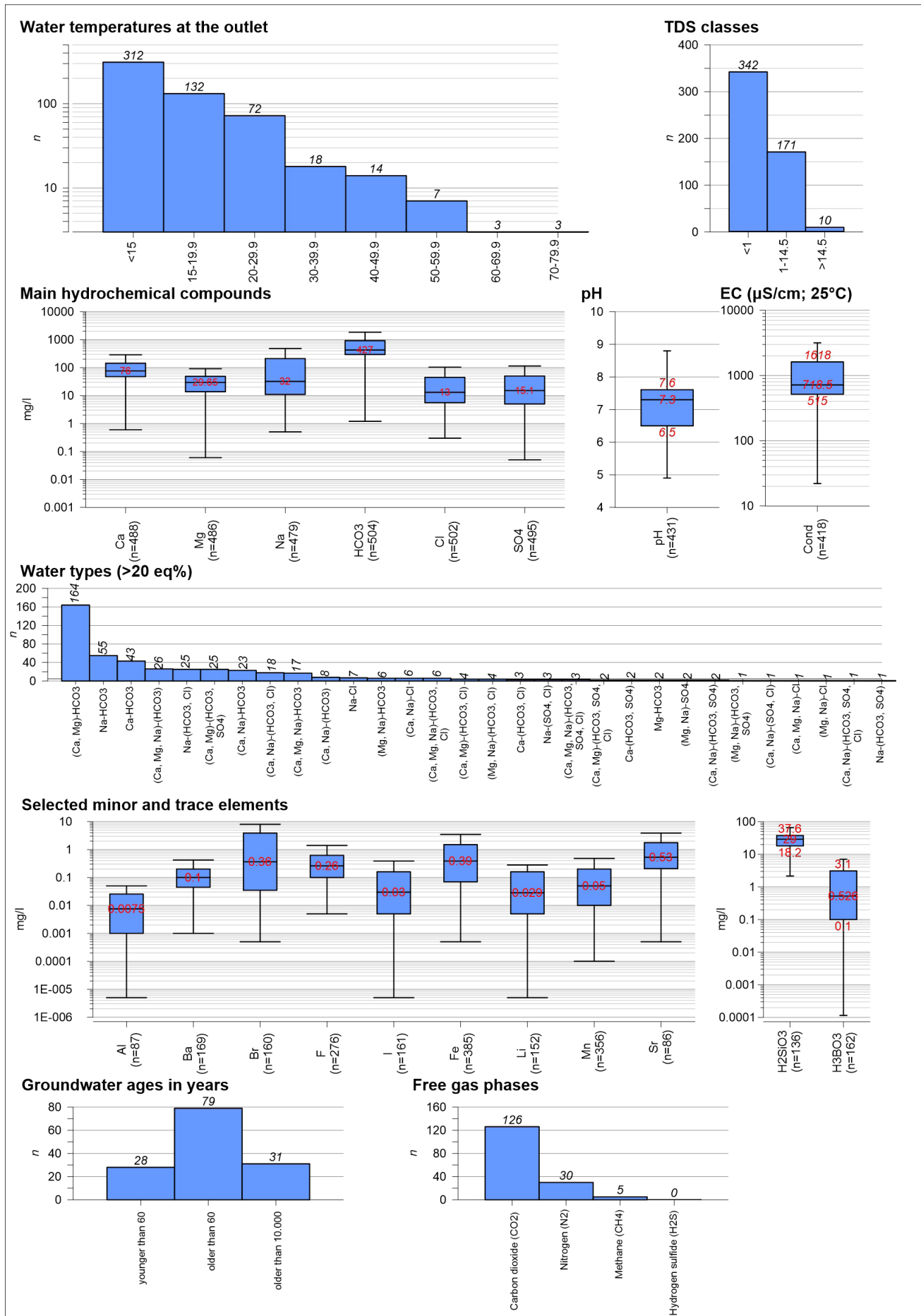


Fig. 4. Hydrochemical characteristics of natural mineral waters found in the dataset.

years ( $n=79$ ), however old groundwaters with ages above 10,000 years ( $n=31$ ) are present as well as groundwaters with less than 60 years ( $n=28$ ).

Data availability is also limited for free gas phases, however, groundwaters rich in carbon dioxide seem to be relatively common ( $n=126$ ). This is expected as historically mineral waters were enriched in  $\text{CO}_2$ .

### Hydrogeological characteristics of thermal waters

Thermal waters found in the dataset (not including waters above 20 °C from the natural mineral water dataset) are mainly used for balneological purposes ( $n=859$  out of 2,390) and heating ( $n=380$ ). However, other uses ( $n=512$ ) are very common. Sources that are entirely used for energy production are not present except for one site in Italy. Other uses may comprise agricultural purposes, aquaculture or in rare cases drinking water if no other water resource are available. Agricultural purpose is not uniformly classified by all countries as some included this use into the heating category. Extraction rates between 5 and 25 l/s ( $n=1,011$ ) outweigh the yield class <5 l/s ( $n=598$ ) and rates above 25 l/s ( $n=288$ ). This may occur as yield information is uncertain due to variable values with time.

Sources of thermal groundwater extraction are mostly wells ( $n=946$  out of 2,390) or artesian wells ( $n=860$ ). Captured springs ( $n=302$ ), captured spring groups ( $n=98$ ) and uncaptured springs ( $n=78$ ) are less common. The true vertical depth of wells is usually within the range of

465 to 1,298 m (25<sup>th</sup> to 75<sup>th</sup> percentile); it has to be added that absolute numbers were collected for data on borehole depths. The deepest artesian well that is used for heating is found in Poland with a depth of 3,943 m, however thermal water is extracted from a screen between 2,960 and 2,776 m at this site. Accordingly, the majority of sources are confined artesian ( $n=902$ ) or sub-artesian ( $n=694$ ).

The abundant aquifer media type (primary and secondary porosity) is porous ( $n=1,185$  out of 2,390) and a combination of porous and fractured ( $n=127$ ) is less common compared to the previously described natural mineral water sources. Karstic and fractured ( $n=316$ ), fractured ( $n=246$ ) and compound ( $n=167$ ) are also frequently present, but entirely karstic ( $n=16$ ) is rarely found.

The lithologies of aquifers are predominated by clastic sediments ( $n=1,383$  of 2,390), especially by sandy aquifers. Carbonate sedimentary rock aquifers ( $n=460$ ) containing limestones, dolomites and chalk are followed by clastic sedimentary rocks ( $n=356$ ), mainly sandstones. Sources associated with igneous rocks ( $n=267$ ) and metamorphic rocks ( $n=138$ ) are less present and other types like chemical sedimentary (evaporitic materials) ( $n=17$ ), tuffite ( $n=10$ ), pyroclastic rocks ( $n=5$ ) and biogenic sediments ( $n=2$ ) are rarely found. Most common aquifer ages are Neogene ( $n=1,064$  of 2,390), Mesozoic ( $n=362$ ) and Quaternary ( $n=187$ ).

Most frequent classes of water temperatures at the outlet are 30-40 °C ( $n=638$ ), 40-50 °C ( $n=424$ ) and 20-30 °C ( $n=355$ ) (Fig. 5). A distribution of

Table 7. Thermal waters found in countries according to their temperatures at the outlet; green colour intensity shows higher numbers.

| Temperature class at the outlet (°C) (n=2,340 of 2,390) | <15 | 15-19.9 | 20-29.9 | 30-39.9 | 40-49.9 | 50-59.9 | 60-69.9 | 70-79.9 | 80-89.9 | 90-99.9 | >100 | Total number |
|---|-----|---------|---------|---------|---------|---------|---------|---------|---------|---------|------|--------------|
| Austria   |     |         | 18      | 17      | 12      | 2       | 4       | 2       | 4       |         | 3    | 62           |
| Bosnia and Herzegovina                                  | 1   | 11      | 8       | 4       |         | 3       |         |         |         | 1       |      | 28           |
| France  | 39  | 26      | 37      | 38      | 32      | 29      | 14      | 4       | 1       |         |      | 220          |
| Hungary   |     |         | 88      | 466     | 312     | 199     | 167     | 87      | 63      | 47      | 3    | 1,432        |
| Iceland   |     |         |         |         |         |         |         | 1       | 1       |         | 1    | 3            |
| Italy   |     |         | 121     | 58      | 34      | 13      | 3       | 4       | 4       | 3       |      | 240          |
| Poland  | 2   |         | 21      | 2       | 4       | 5       | 5       | 6       | 1       |         |      | 46           |
| Portugal  | 1   | 96      | 16      | 2       |         |         |         |         |         |         |      | 115          |
| Romania   |     |         |         | 1       | 5       | 2       |         | 1       | 1       | 2       | 2    | 14           |
| Serbia  |     |         | 24      | 22      | 6       | 8       | 8       | 10      |         |         |      | 78           |
| Slovenia  |     |         | 7       | 9       | 3       | 5       | 8       | 1       |         |         |      | 33           |
| Spain   | 2   | 4       | 16      | 19      | 16      | 11      |         | 1       |         |         |      | 69           |
| Total number  | 45  | 137     | 356     | 638     | 424     | 277     | 209     | 117     | 75      | 53      | 9    | 2,340        |

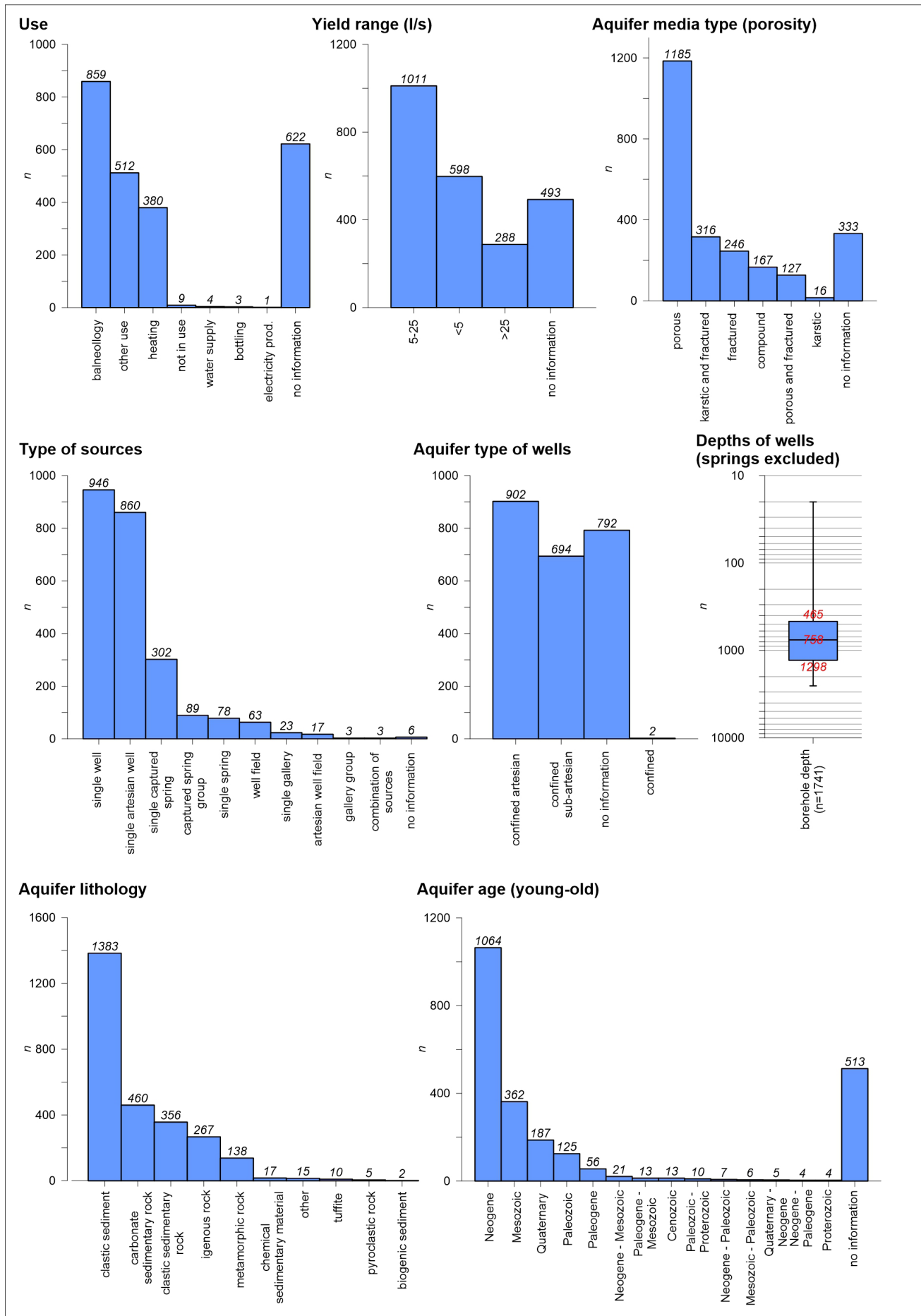


Fig. 5. Characteristics of thermal waters found in the dataset.

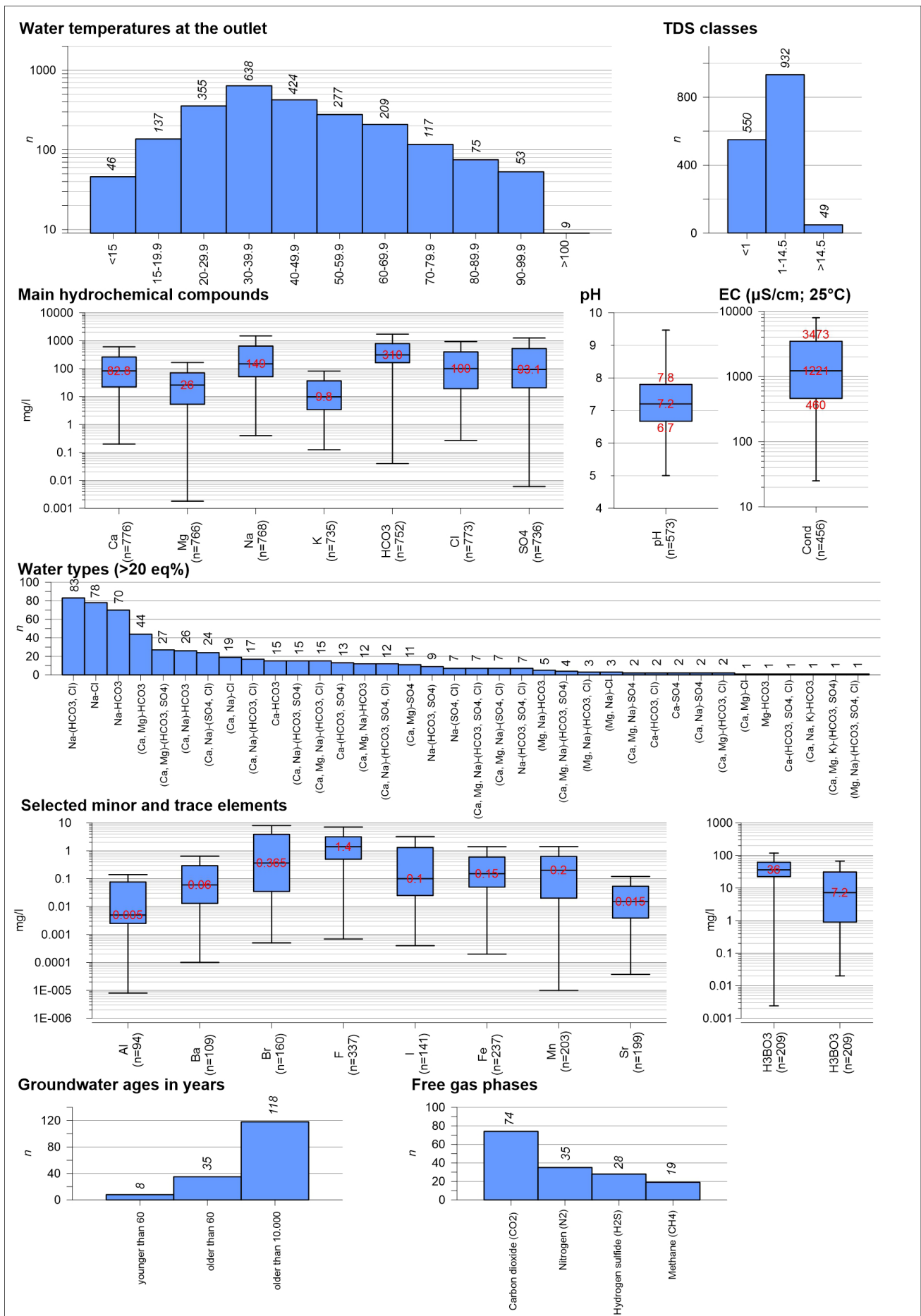


Fig. 6. Hydrochemical characteristics of thermal waters found in the dataset.

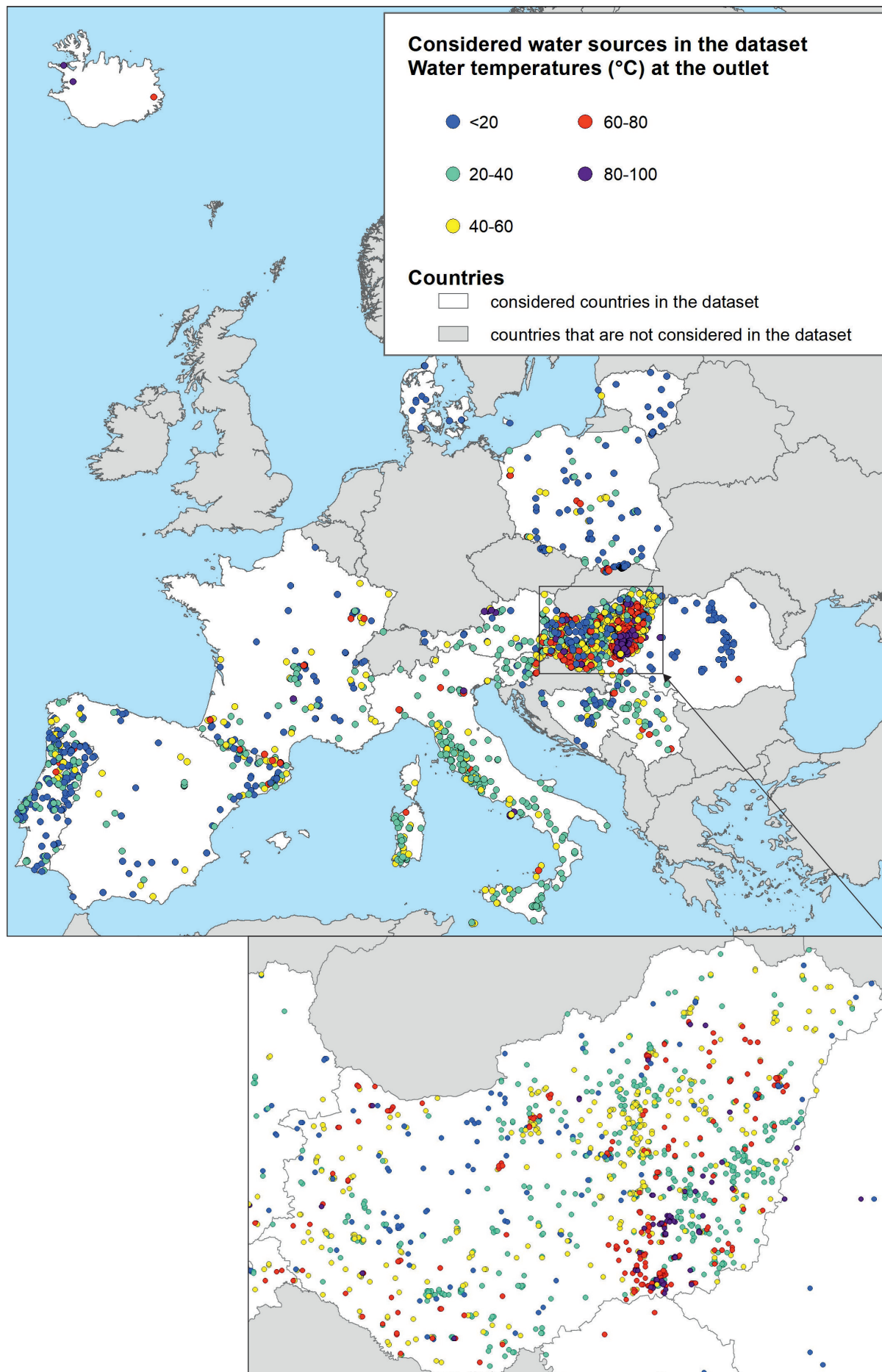


Fig. 7. Water temperatures at the outlet of sources found in the dataset of thermal and natural mineral waters; due to better visualisation, the classes are 20 degrees and not 10, as discussed in tables and text.

the temperature classes is found in Table 6 and it shows that the majority of sources are found in Hungary ( $n=1,432$ ). Sources with a temperature below 15 °C are included due to national criteria in some countries. Rarely existing thermal waters with >100 °C ( $n=9$ ; no exact temperature was gathered, only ranges) at the outlet are reported from Austria, Hungary, Romania and Iceland and can be usually associated with deep boreholes with depths between 1,500 and 2,800 m. However, a captured spring group in Iceland extracting from a basalt aquifer is an exception.

The common TDS range is 1 to 14.5 g/l ( $n=932$ ) and thermal waters with a mineralisation below 1 g/l ( $n=550$ ) are less prevailing. Highly mineralized thermal brines with a TDS content above 14.5 g/l are rather rare ( $n=49$ ), located in several countries: Austria, Spain, Romania, Bosnia and Herzegovina, Poland, Italy and Hungary. The common EC range of the considered thermal waters is overall between approx. 450 and 2,700  $\mu\text{S}/\text{cm}$  (25 °C) and pH is usually neutral to slightly alkaline.

Calculations of the water types (>20eq%) excluding the Hungarian dataset where no information is available show, that Na-( $\text{HCO}_3$ , Cl) waters ( $n=83$ ) are most common followed by Na-Cl waters ( $n=78$ ), Na- $\text{HCO}_3$  ( $n=70$ ) and (Ca, Mg)- $\text{HCO}_3$  ( $n=44$ ). However, the hydrochemical composition of the considered sources is highly diverse, this is shown by 34 present water types in the dataset. An overview of available hydrochemical analyses is found in Annex 2.

Qualitative information on groundwater residence times is rare. Most sources show ages above 10,000 years ( $n=118$ ) and groundwaters older than 60 years but younger than 10,000 years ( $n=35$ ) are

less frequent. Data availability is also limited for free gas phases, however, groundwaters rich in  $\text{CO}_2$  seem to be common ( $n=126$ ).

## Discussion

Natural mineral waters are well defined and regulated in the European Union by the Directives 2009/54/EC and 2003/40/EC. Those directives are implemented by national law regulations.

Datasets for natural mineral and thermal waters comprise a large number of data, but also exhibit large numbers of missing or partially missing information due to missing data availability or limited data access. For example, data on trace elements and groundwater retentions times are not available in most cases. However, considering available information, the comparison of the datasets from a hydrogeological point of view shows common characteristics but also obvious differences.

Porous aquifer media types are dominant in both datasets and aquifer lithologies are mostly clastic sediments, especially sandy aquifers followed by carbonate sedimentary rocks that may contain limestones, dolomites and chalk. Most important, unconfined conditions are rarely present in the dataset. They are due to faster recharge and more responsive dynamics less capable of providing ground waters with stable composition or warmer water.

Temperatures at the outlet of thermal waters are commonly between 20 and 70 °C (82 %) and temperatures above 70 °C are less common (11 %) (Table 8). Furthermore, only 7% of sources that are classified as thermal waters show temperatures below 20 °C. In comparison, 79 % of natural

Table 8. Comparison of the datasets of natural mineral and thermal waters regarding temperatures at the outlet and total dissolved solids; green colour intensity to show higher percentages.

|                           | TDS (g/l)             | T (°C) at the outlet of source |         |         |         |         |         |         |         |         |         |      | % of <i>n</i> sources |     |
|---------------------------|-----------------------|--------------------------------|---------|---------|---------|---------|---------|---------|---------|---------|---------|------|-----------------------|-----|
|                           |                       | <15                            | 15-19.9 | 20-29.9 | 30-39.9 | 40-49.9 | 50-59.9 | 60-69.9 | 70-79.9 | 80-89.9 | 90-99.9 | >100 |                       |     |
| natural mineral water     | <1                    | 35                             | 18      | 9       | 2       | 1       | 0       | 0       | 0       | 0       | 0       | 0    | 0                     | 64  |
| (Directive 2009/54/EC)    | 1-14,5                | 21                             | 4       | 4       | 1       | 2       | 1       | 1       | 1       | 0       | 0       | 0    | 0                     | 35  |
| ( $n=490$ out of 678)     | >14,5                 | 0,4                            | 0,2     | 0       | 0,2     | 0,2     | 0       | 0       | 0       | 0       | 0       | 0    | 0                     | 1   |
|                           | % of <i>n</i> sources | 56,4                           | 22,2    | 13      | 3,2     | 3,2     | 1       | 1       | 1       | 0       | 0       | 0    | 0                     | 100 |
| thermal waters            | <1                    | 0,2                            | 5       | 8       | 13      | 6       | 2       | 1       | 1       | 0       | 0       | 0    | 0                     | 36  |
| ( $n=1,523$ out of 2,390) | 1-14,5                | 0,3                            | 1,2     | 7       | 11,5    | 12,5    | 9,4     | 9       | 4,3     | 3,1     | 2,4     | 0,3  | 0,3                   | 61  |
|                           | >14,5                 | 0                              | 0,3     | 1,2     | 0,3     | 0,3     | 0,5     | 0,2     | 0,1     | 0,2     | 0,1     | 0,1  | 0,1                   | 3   |
|                           | % of <i>n</i> sources | 0,5                            | 6,5     | 16,2    | 24,8    | 18,8    | 11,9    | 10,2    | 5,4     | 3,3     | 2,5     | 0,4  | 0,4                   | 100 |

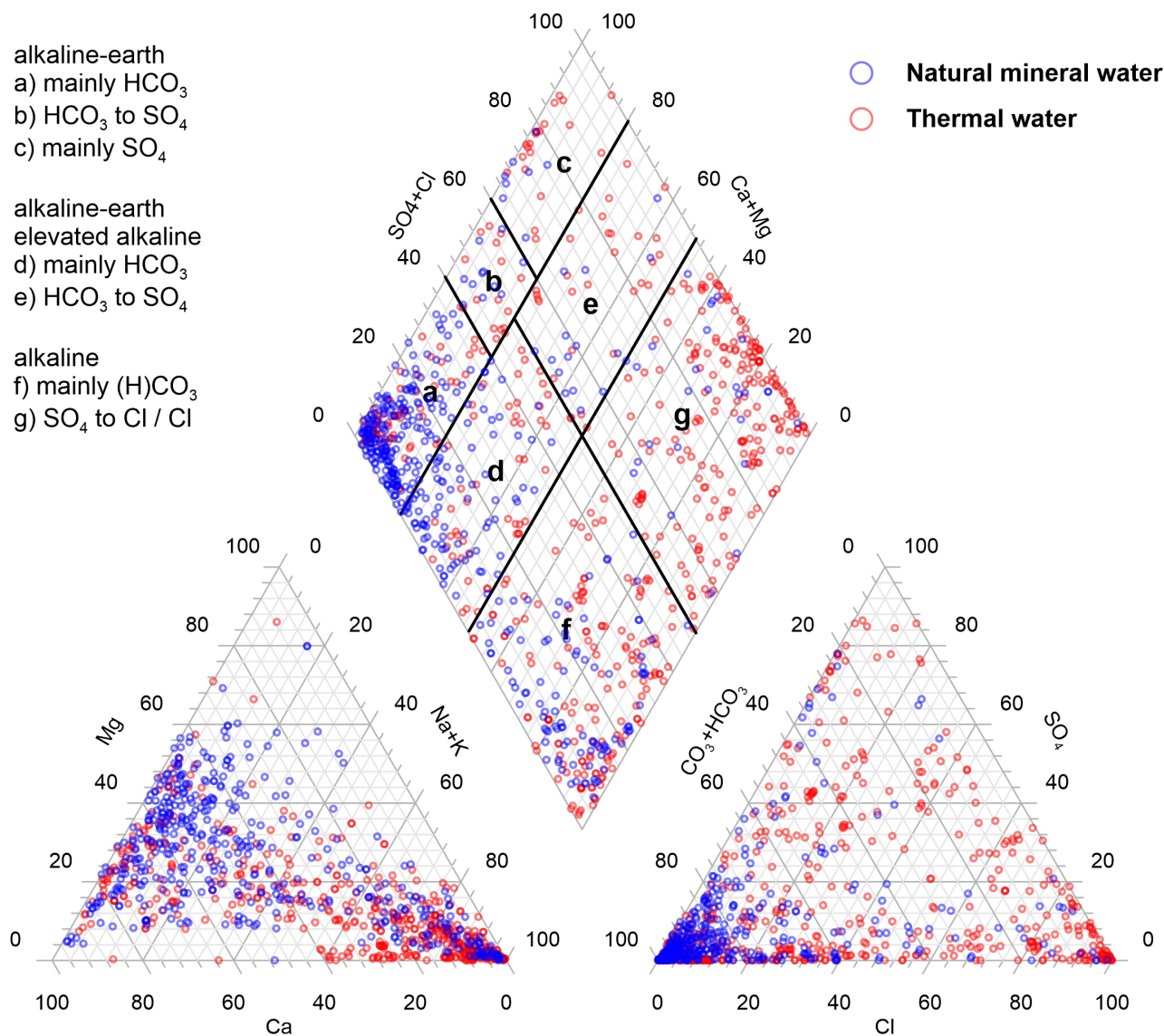


Fig. 8. Piper diagram to compare the datasets of natural mineral waters ( $n=423$  out of 678) and thermal waters ( $n=518$  of 2,390).

Table 9. Water types versus water temperatures at the outlet of natural mineral waters; green colour intensity to show higher percentages.

| Natural mineral waters<br>( $n= 423$ out of 678)   | Water temperature at the outlet ( $^{\circ}\text{C}$ ) |         |         |         |         |         |         |         | % of $n$ sources |
|--|--|---------|---------|---------|---------|---------|---------|---------|------------------|
|  | <15  | 15-19.9 | 20-29.9 | 30-39.9 | 40-49.9 | 50-59.9 | 60-69.9 | 70-79.9 |                  |
| (Ca)-(HCO <sub>3</sub> )                           | 7,1  | 0,9     | 0,5     | 0,0     | 0,0     | 0,0     | 0,0     | 0,0     | 8,5              |
| (Ca)-(HCO <sub>3</sub> ,Cl)                        | 0,5  | 0,0     | 0,0     | 0,0     | 0,0     | 0,0     | 0,0     | 0,2     | 0,7              |
| (Ca)-(HCO <sub>3</sub> ,SO <sub>4</sub> )          | 0,2  | 0,0     | 0,0     | 0,0     | 0,0     | 0,0     | 0,0     | 0,0     | 0,2              |
| (Ca,Mg)-(HCO <sub>3</sub> )                        | 19,4   | 12,8    | 3,5     | 1,2     | 0,2     | 0,0     | 0,0     | 0,0     | 37,1             |
| (Ca,Mg)-(HCO <sub>3</sub> ,Cl)                     | 0,2  | 0,2     | 0,0     | 0,0     | 0,0     | 0,0     | 0,0     | 0,0     | 0,5              |
| (Ca,Mg)-(HCO <sub>3</sub> ,SO <sub>4</sub> )       | 3,1  | 0,7     | 0,7     | 0,7     | 0,0     | 0,0     | 0,0     | 0,0     | 5,2              |
| (Ca,Mg)-(HCO <sub>3</sub> ,SO <sub>4</sub> ,Cl)    | 0,0  | 0,0     | 0,2     | 0,2     | 0,0     | 0,0     | 0,0     | 0,0     | 0,5              |
| (Ca,Mg,Na)-(Cl)                                    | 0,0  | 0,2     | 0,0     | 0,0     | 0,0     | 0,0     | 0,0     | 0,0     | 0,2              |
| (Ca,Mg,Na)-(HCO <sub>3</sub> )                     | 3,1  | 3,8     | 1,2     | 0,0     | 0,2     | 0,0     | 0,2     | 0,0     | 8,5              |
| (Ca,Mg,Na)-(HCO <sub>3</sub> ,Cl)                  | 0,2  | 0,2     | 0,5     | 0,5     | 0,0     | 0,0     | 0,0     | 0,0     | 1,4              |
| (Ca,Mg,Na)-(HCO <sub>3</sub> ,SO <sub>4</sub> ,Cl) | 0,2  | 0,0     | 0,0     | 0,0     | 0,5     | 0,0     | 0,0     | 0,0     | 0,7              |
| (Ca,Na)-(Cl)                                       | 1,7  | 0,0     | 0,0     | 0,0     | 0,0     | 0,0     | 0,0     | 0,0     | 1,7              |
| (Ca,Na)-(HCO <sub>3</sub> )                        | 4,3  | 1,4     | 1,2     | 0,0     | 0,2     | 0,0     | 0,0     | 0,0     | 7,1              |
| (Ca,Na)-(HCO <sub>3</sub> ,Cl)                     | 2,1  | 0,2     | 0,7     | 0,2     | 0,0     | 0,0     | 0,2     | 0,2     | 3,8              |
| (Ca,Na)-(HCO <sub>3</sub> ,SO <sub>4</sub> )       | 0,2  | 0,0     | 0,2     | 0,0     | 0,0     | 0,0     | 0,0     | 0,0     | 0,5              |

|  |             |             |             |            |            |            |            |            |              |
|--|-------------|-------------|-------------|------------|------------|------------|------------|------------|--------------|
| (Ca,Na)-(SO <sub>4</sub> ,Cl)                | 0,2         | 0,0         | 0,0         | 0,0        | 0,0        | 0,0        | 0,0        | 0,0        | 0,2          |
| (Mg)-(HCO <sub>3</sub> )                     | 0,0         | 0,5         | 0,0         | 0,0        | 0,0        | 0,0        | 0,0        | 0,0        | 0,5          |
| (Mg,Na)-(Cl)                                 | 0,0         | 0,2         | 0,0         | 0,0        | 0,0        | 0,0        | 0,0        | 0,0        | 0,2          |
| (Mg,Na)-(HCO <sub>3</sub> )                  | 0,5         | 0,2         | 0,5         | 0,0        | 0,0        | 0,0        | 0,0        | 0,0        | 1,2          |
| (Mg,Na)-(HCO <sub>3</sub> ,Cl)               | 0,2         | 0,0         | 0,2         | 0,0        | 0,0        | 0,0        | 0,0        | 0,0        | 0,5          |
| (Mg,Na)-(HCO <sub>3</sub> ,SO <sub>4</sub> ) | 0,0         | 0,0         | 0,2         | 0,0        | 0,0        | 0,0        | 0,0        | 0,0        | 0,2          |
| (Na)-(Cl)                                    | 0,2         | 0,7         | 0,0         | 0,0        | 0,0        | 0,2        | 0,0        | 0,0        | 1,2          |
| (Na)-(HCO <sub>3</sub> )                     | 3,5         | 5,0         | 3,3         | 0,0        | 0,9        | 0,2        | 0,2        | 0,0        | 13,2         |
| (Na)-(HCO <sub>3</sub> ,Cl)                  | 0,0         | 0,5         | 2,1         | 0,5        | 1,2        | 1,2        | 0,0        | 0,2        | 5,7          |
| (Na)-(HCO <sub>3</sub> ,SO <sub>4</sub> )    | 0,2         | 0,0         | 0,0         | 0,0        | 0,0        | 0,0        | 0,0        | 0,0        | 0,2          |
| (Na)-(SO <sub>4</sub> ,Cl)                   | 0,2         | 0,0         | 0,0         | 0,0        | 0,0        | 0,0        | 0,0        | 0,0        | 0,2          |
| <b>% of n sources</b>                        | <b>47,5</b> | <b>27,7</b> | <b>15,1</b> | <b>3,3</b> | <b>3,3</b> | <b>1,7</b> | <b>0,7</b> | <b>0,7</b> | <b>100,0</b> |

Table 10. Water types versus water temperatures at the outlet of thermal waters; green colour intensity to show higher percentages.

| <b>thermal waters<br/>(n= 518 out of 2,390)</b>    | <b>&lt;15</b> | <b>15-<br/>19.9</b> | <b>20-<br/>29.9</b> | <b>30-<br/>39.9</b> | <b>40-<br/>49.9</b> | <b>50-<br/>59.9</b> | <b>60-<br/>69.9</b> | <b>70-<br/>79.9</b> | <b>80-<br/>89.9</b> | <b>90-<br/>99.9</b> | <b>&gt;100</b> | <b>% of n<br/>sources</b> |
|--|---------------|---------------------|---------------------|---------------------|---------------------|---------------------|---------------------|---------------------|---------------------|---------------------|----------------|---------------------------|
| (Ca)-(HCO <sub>3</sub> )                           | 0,6           | 0,6                 | 1,5                 | 1,2                 | 0,4                 | 0,0                 | 0,0                 | 0,0                 | 0,0                 | 0,0                 | 0,0            | 4,2                       |
| (Ca)-(HCO <sub>3</sub> ,Cl)                        | 0,2           | 0,0                 | 0,0                 | 0,0                 | 0,0                 | 0,0                 | 0,0                 | 0,0                 | 0,0                 | 0,0                 | 0,0            | 0,2                       |
| (Ca)-(HCO <sub>3</sub> ,SO <sub>4</sub> )          | 0,8           | 0,0                 | 0,6                 | 0,0                 | 0,4                 | 0,2                 | 0,0                 | 0,0                 | 0,0                 | 0,0                 | 0,0            | 1,9                       |
| (Ca)-(HCO <sub>3</sub> ,SO <sub>4</sub> ,Cl)       | 0,0           | 0,2                 | 0,0                 | 0,0                 | 0,0                 | 0,0                 | 0,0                 | 0,0                 | 0,0                 | 0,0                 | 0,0            | 0,2                       |
| (Ca)-(SO <sub>4</sub> )                            | 0,0           | 0,0                 | 0,2                 | 0,0                 | 0,2                 | 0,0                 | 0,0                 | 0,0                 | 0,0                 | 0,0                 | 0,0            | 0,4                       |
| (Ca,Mg)-(HCO <sub>3</sub> )                        | 2,1           | 0,6                 | 3,1                 | 1,9                 | 0,2                 | 0,0                 | 0,6                 | 0,0                 | 0,2                 | 0,0                 | 0,0            | 8,7                       |
| (Ca,Mg)-(HCO <sub>3</sub> ,Cl)                     | 0,0           | 0,0                 | 0,0                 | 0,0                 | 0,2                 | 0,0                 | 0,0                 | 0,0                 | 0,0                 | 0,0                 | 0,0            | 0,2                       |
| (Ca,Mg)-(HCO <sub>3</sub> ,SO <sub>4</sub> )       | 1,0           | 0,6                 | 1,5                 | 0,8                 | 0,4                 | 0,2                 | 0,0                 | 0,0                 | 0,0                 | 0,2                 | 0,0            | 4,6                       |
| (Ca,Mg)-(SO <sub>4</sub> )                         | 0,0           | 0,2                 | 0,2                 | 0,6                 | 0,0                 | 0,0                 | 0,0                 | 0,0                 | 0,0                 | 0,0                 | 0,0            | 1,0                       |
| (Ca,Mg,K)-(HCO <sub>3</sub> )                      | 0,0           | 0,0                 | 0,2                 | 0,0                 | 0,0                 | 0,0                 | 0,0                 | 0,0                 | 0,0                 | 0,0                 | 0,0            | 0,2                       |
| (Ca,Mg,Na)-(HCO <sub>3</sub> )                     | 0,2           | 0,2                 | 0,8                 | 0,6                 | 0,0                 | 0,2                 | 0,0                 | 0,0                 | 0,0                 | 0,0                 | 0,0            | 1,9                       |
| (Ca,Mg,Na)-(HCO <sub>3</sub> ,Cl)                  | 0,0           | 0,4                 | 1,5                 | 0,4                 | 0,0                 | 0,0                 | 0,0                 | 0,0                 | 0,0                 | 0,0                 | 0,0            | 2,3                       |
| (Ca,Mg,Na)-(HCO <sub>3</sub> ,SO <sub>4</sub> )    | 0,0           | 0,0                 | 0,6                 | 0,0                 | 0,2                 | 0,0                 | 0,0                 | 0,0                 | 0,0                 | 0,0                 | 0,0            | 0,8                       |
| (Ca,Mg,Na)-(HCO <sub>3</sub> ,SO <sub>4</sub> ,Cl) | 0,0           | 0,2                 | 0,0                 | 0,8                 | 0,0                 | 0,0                 | 0,0                 | 0,0                 | 0,0                 | 0,0                 | 0,0            | 1,0                       |
| (Ca,Mg,Na)-(SO <sub>4</sub> )                      | 0,0           | 0,0                 | 0,0                 | 0,0                 | 0,0                 | 0,0                 | 0,0                 | 0,2                 | 0,0                 | 0,0                 | 0,0            | 0,2                       |
| (Ca,Mg,Na)-(SO <sub>4</sub> ,Cl)                   | 0,0           | 0,0                 | 0,2                 | 0,8                 | 0,0                 | 0,0                 | 0,0                 | 0,0                 | 0,0                 | 0,0                 | 0,0            | 1,0                       |
| (Ca,Na)-(Cl)                                       | 0,0           | 0,0                 | 0,2                 | 0,6                 | 1,9                 | 0,6                 | 0,0                 | 0,2                 | 0,2                 | 0,0                 | 0,0            | 3,7                       |
| (Ca,Na)-(HCO <sub>3</sub> )                        | 0,2           | 0,8                 | 2,3                 | 0,6                 | 0,0                 | 0,2                 | 0,6                 | 0,0                 | 0,0                 | 0,0                 | 0,0            | 4,6                       |
| (Ca,Na)-(HCO <sub>3</sub> ,Cl)                     | 0,4           | 0,2                 | 1,5                 | 0,6                 | 0,0                 | 0,0                 | 0,0                 | 0,4                 | 0,0                 | 0,0                 | 0,0            | 3,1                       |
| (Ca,Na)-(HCO <sub>3</sub> ,SO <sub>4</sub> )       | 0,0           | 0,0                 | 0,6                 | 0,4                 | 1,7                 | 0,0                 | 0,0                 | 0,0                 | 0,0                 | 0,0                 | 0,0            | 2,7                       |
| (Ca,Na)-(HCO <sub>3</sub> ,SO <sub>4</sub> ,Cl)    | 0,2           | 0,2                 | 0,4                 | 0,6                 | 0,4                 | 0,6                 | 0,0                 | 0,0                 | 0,0                 | 0,0                 | 0,0            | 2,3                       |
| (Ca,Na)-(SO <sub>4</sub> )                         | 0,0           | 0,0                 | 0,0                 | 0,0                 | 0,2                 | 0,2                 | 0,0                 | 0,0                 | 0,0                 | 0,0                 | 0,0            | 0,4                       |
| (Ca,Na)-(SO <sub>4</sub> ,Cl)                      | 0,6           | 0,0                 | 1,2                 | 1,2                 | 1,2                 | 0,4                 | 0,0                 | 0,4                 | 0,2                 | 0,0                 | 0,0            | 5,0                       |
| (Ca,Na,K)-(HCO <sub>3</sub> )                      | 0,0           | 0,0                 | 0,0                 | 0,2                 | 0,0                 | 0,0                 | 0,0                 | 0,0                 | 0,0                 | 0,0                 | 0,0            | 0,2                       |
| (Mg)-(HCO <sub>3</sub> )                           | 0,0           | 0,2                 | 0,0                 | 0,0                 | 0,0                 | 0,0                 | 0,0                 | 0,0                 | 0,0                 | 0,0                 | 0,0            | 0,2                       |
| (Mg,Na)-(Cl)                                       | 0,0           | 0,0                 | 0,2                 | 0,0                 | 0,2                 | 0,0                 | 0,0                 | 0,0                 | 0,0                 | 0,0                 | 0,0            | 0,4                       |
| (Mg,Na)-(HCO <sub>3</sub> )                        | 0,0           | 0,0                 | 0,0                 | 0,6                 | 0,4                 | 0,0                 | 0,0                 | 0,0                 | 0,0                 | 0,0                 | 0,0            | 1,0                       |
| (Mg,Na)-(HCO <sub>3</sub> ,Cl)                     | 0,0           | 0,0                 | 0,6                 | 0,0                 | 0,0                 | 0,0                 | 0,0                 | 0,0                 | 0,0                 | 0,0                 | 0,0            | 0,6                       |
| (Na)-(Cl)  | 0,4           | 1,0                 | 4,2                 | 1,7                 | 1,9                 | 2,9                 | 1,4                 | 0,8                 | 0,6                 | 0,2                 | 0,0            | 15,1                      |
| (Na)-(HCO <sub>3</sub> )                           | 0,4           | 1,2                 | 2,5                 | 3,1                 | 1,4                 | 1,7                 | 1,2                 | 1,0                 | 0,2                 | 0,0                 | 0,0            | 12,5                      |
| (Na)-(HCO <sub>3</sub> ,Cl)                        | 0,0           | 0,2                 | 4,1                 | 3,9                 | 2,5                 | 1,7                 | 1,5                 | 0,2                 | 0,4                 | 0,2                 | 0,6            | 15,3                      |
| (Na)-(HCO <sub>3</sub> ,SO <sub>4</sub> )          | 0,0           | 0,0                 | 0,4                 | 0,2                 | 0,4                 | 0,4                 | 0,4                 | 0,2                 | 0,0                 | 0,0                 | 0,0            | 1,9                       |
| (Na)-(HCO <sub>3</sub> ,SO <sub>4</sub> ,Cl)       | 0,0           | 0,0                 | 0,6                 | 0,4                 | 0,2                 | 0,0                 | 0,0                 | 0,0                 | 0,0                 | 0,0                 | 0,0            | 1,2                       |
| (Na)-(SO <sub>4</sub> ,Cl)                         | 0,2           | 0,0                 | 0,4                 | 0,0                 | 0,6                 | 0,0                 | 0,0                 | 0,0                 | 0,0                 | 0,0                 | 0,0            | 1,2                       |
| <b>% of n sources</b>                              | <b>7,1</b>    | <b>6,6</b>          | <b>29,5</b>         | <b>20,8</b>         | <b>14,9</b>         | <b>9,3</b>          | <b>5,6</b>          | <b>3,3</b>          | <b>1,7</b>          | <b>0,6</b>          | <b>0,6</b>     | <b>100,0</b>              |

mineral waters possess water temperatures below 20 °C, but the remaining 21 % of source bear temperatures above 20 °C and could be considered as thermal waters as well. However, those sources are evaluated as natural mineral waters in our approach. The mineralisation of natural mineral waters is usually below 1 g/l (64 %), whereas 1–14.5 g/l are common for thermal waters (61 %). Highly mineralized waters above 14.5 g/l are very rare in both datasets.

Natural mineral waters show primarily alkaline-earth bicarbonate water types (Fig. 7). In detail, 37 % of (Ca, Mg)-HCO<sub>3</sub> water type and 8.5 % a Ca-HCO<sub>3</sub> types are present (Table 9). On the other hand, Na-HCO<sub>3</sub> type waters are less abundant (13 %). The hydrochemical compositions of thermal water found in the dataset clearly exhibit a larger variation compared to natural mineral waters, but Na-Cl as well as Na-(HCO<sub>3</sub>, Cl) types are commonly found (43 %). This indicates that more complex hydrochemical settings – e.g. ion exchange waters and diluted brines are often found.

## Conclusions

This overview paper discussed legal framework and criteria for recognition of natural mineral water and thermal water in selected countries in Europe. It pointed out that especially for thermal waters, there is no uniform approach, despite the fact that most countries are within the European Union. This might cause misunderstandings not only among consumers of such goods but also for scientific research, due to varying definitions of classifications and threshold limits. In contrast, for natural mineral water it has to be mentioned that the definition is based on legislative definitions (Directive 2009/54/EC and Directive 2003/40/EC within the European Union, and national legislations in Bosnia and Herzegovina, Serbia).

This research provides a summary including a geological-hydrogeological statistical overview of recognised sources of natural mineral and thermal waters where comparison of both types reveals evident differences. Natural mineral waters are, usually, colder and less mineralized as thermal, but some can also be classified as thermal due to national definitions. Both are mostly tapped from confined aquifers, providing enough stable chemical composition. (Ca, Mg)-HCO<sub>3</sub> water type is prevailing at natural mineral water group while Na-(HCO<sub>3</sub>, Cl) at thermal waters. This latter is a result of more pronounced and

longer water-rock interaction having older water ages and hotter which results also in higher mineralization, while in some cases can represent diluted brines.

The collected and classified dataset is freely published at a webservice developed within the GeoERA project HOVER: [https://data.geus.dk/egdi/?mapname=hover\\_wp3\\_d35c#baslay=baseMapGEUS&extent=-4366900,-1320100,11512740,6181370](https://data.geus.dk/egdi/?mapname=hover_wp3_d35c#baslay=baseMapGEUS&extent=-4366900,-1320100,11512740,6181370). We strongly encourage to use this research as a basis for further data collection which can be later supplemented to this webportal.

## Acknowledgement and data availability statement

This research was funded by the European Union's Horizon 2020 research and innovation program (GeoERA Groundwater HOVER) under grant agreement number 731166. N. Rman participation was supported by the Slovenian Research Agency, research program P1-0020 Groundwaters and Geochemistry. The participation of D. Voutchkova, B. Hansen and J. Schullehner was supported with the "Innovation Fund Denmark (funding agreement number 8055-00073B)".

Members of the National Geological Surveys that were involved in HOVER WP3 and contributed data used for this publication: Austria (D. Elster; Geological Survey of Austria), Bosnia and Herzegovina (F. Skopljak; Federal Geological Survey BiH), Denmark (D. Voutchkova, B. Hansen, J. Schullehner; Geological Survey of Denmark and Greenland), Hungary (T. Szócs, N. Gál; Mining and Geological Survey of Hungary), Iceland (D. Þorbjörnsson; Iceland Geosurvey), Italy (L. Martarelli, B. Dessi; Geological Survey of Italy), Lithuania (J. Arustienė; Lithuanian Geological Survey), Poland (A. Felter; Polish Geological Institute), Portugal (A. Pereira; J. Sampaio; National Laboratory of Energy and Geology), Romania (A. Mercan, D. Perşa; Geological Institute of Romania), Serbia (T. Petrović Pantić; Geological Survey of Serbia), Slovenia (N. Rman; Geological Survey of Slovenia), Spain including Catalonia (E. Giménez Forcada; Instituto Geológico y Minero de España; G. Arnó; Cartographical and Geological Institute of Catalonia),

The Final Report for HOVER WP3.1 is available here: [https://repository.europe-geology.eu/egdidocs/hover/hover\\_d3-1\\_report\\_v2.pdf](https://repository.europe-geology.eu/egdidocs/hover/hover_d3-1_report_v2.pdf)

The webservice for natural mineral and thermal waters (HOVER WP3.5) is available here: [https://data.geus.dk/egdi/?mapname=hover\\_wp3\\_d35c#baslay=baseMapGEUS&extent=-4366900,-1320100,11512740,6181370](https://data.geus.dk/egdi/?mapname=hover_wp3_d35c#baslay=baseMapGEUS&extent=-4366900,-1320100,11512740,6181370)

## References

- Albu, M., Banks, D. & Nash, H. 1997: Mineral and Thermal Groundwater Resources. Springer, Dordrecht: 447 p. <https://doi.org/10.1007/978-94-011-5846-6>
- Balderer, W., Porowski, A., Idris, H. & Lamoreaux, J. W. 2014: Thermal and Mineral Waters. Origin, Properties and Applications. Springer, Berlin: 135 p. <https://doi.org/10.1007/978-3-642-28824-1>
- Borović, S., Marković, T., Larva, O., Brkić, Z. & Mraz, V. 2016: Mineral and Thermal Waters in the Croatian Part of the Pannonian Basin. In: Papić, P. (ed.): Mineral and Thermal Waters of Southeastern Europe. Springer, Berlin: 31-45. [https://doi.org/10.1007/978-3-319-25379-4\\_2](https://doi.org/10.1007/978-3-319-25379-4_2)
- Borszéli, B. (eds.) 2013: Mineral and medicinal waters of the Carpathian Basin (in Hungarian). Budapest: 320 p.
- Bräuer, K., Geissler, W.H., Kämpf, H., Niedermann, S. & Rman, N. 2016: Helium and carbon isotope signatures of gas exhalations in the westernmost part of the Pannonian Basin (SE Austria/NE Slovenia): Evidence for active lithospheric mantle degassing. *Chemical Geology*, 422/1: 60-70. <https://doi.org/10.1016/j.chemgeo.2015.12.016>
- Brenčić, M., Ferjan, T. & Gosar, M. 2010: Geochemical survey of Slovenian bottled waters. *Journal of Geochemical Exploration*, 107/3: 400-409. <https://doi.org/10.1016/j.gexplo.2010.09.007>
- Burić, M., Nikić, Z. & Papić, P. 2016: Mineral Waters of Montenegro. In: Papić, P. (ed.): Mineral and Thermal Waters of Southeastern Europe. Springer, Berlin: 65-79, [https://doi.org/10.1007/978-3-319-25379-4\\_4](https://doi.org/10.1007/978-3-319-25379-4_4)
- Carlé, W. 1975: Die Mineral- und Thermalwässer von Mitteleuropa. Stuttgart, Wiss. Verlagsgesellschaft mbH: 643 p.
- Dinelli, E., Lima, A., Albanese, S., Birke, M., Cicchella, D., Giaccio, L. et al. 2012: Comparative study between bottled mineral and tap water in Italy. *Journal of Geochemical Exploration*, 112, 368-389. <https://doi.org/10.1016/j.gexplo.2011.11.002>
- Eftimi, R. & Frashëri, A. 2016: Thermal Waters of Albania. In: Papić, P. (ed.): Mineral and Thermal Waters of Southeastern Europe. Springer, Berlin: 115-130. [https://doi.org/10.1007/978-3-319-25379-4\\_7](https://doi.org/10.1007/978-3-319-25379-4_7)
- EGEC, 2019: EGEC Geothermal Market Report, Full Report. European Geothermal Energy Council 2019, Brussels: 58 p.
- Eggenkamp, H. G. M. & Marques, J. M. 2013: A comparison of mineral water classification techniques: Occurrence and distribution of different water types in Portugal (including Madeira and the Azores). *Journal of Geochemical Exploration*, 132: 125-139. <https://doi.org/10.1016/j.gexplo.2013.06.009>
- Elster, D., Goldbrunner, J., Wessely, G., Niederbacher, P., Schubert, G., Berka, R., Philippitsch, R. & Hörhan, T. 2016: Erläuterungen zur geologischen Themenkarte Thermalwässer in Österreich 1:500.000. Geologische Bundesanstalt, Wien: 296 p.
- Elster, D., Fischer, L., Hann, S., Goldbrunner, J., Schubert, G., Berka, R., Hobiger, G., Legerer, P. & Philippitsch, R. 2018: Österreichs Mineral- und Heilwässer. Geologische Bundesanstalt, Wien: 448 p.
- EuroGeoSurveys, 2016: "Wonder water - the value of water", A geological journey around Europe's mineral springs, spas and thermal baths. Brussels, Belgium: 135 p.
- Evina, E. 1992: La Guide du Buveur d'Eau. Solar, France: 263 p.
- Freeze, A. & Cherry, J. 1979: Groundwater, 604 p.
- Gros, N. 2003: The comparison between Slovene and Central European mineral and thermal waters. *Acta Chimica Slovenica*, 50/1: 57-66.
- Haas, J., Brezsnýánszky, K., Budai, T., Fodor, L., Gál, N., Gombárné Forgács, G., Gyalog, L., Katona, G., Kovács, G., Kövér, Sz., Lesták, F., Nádor, A., † Nagymarosy, A., Prakfalvi, P., Rotárné Szalkai, Á., Scharek, P., Síkhegyi, F., Szepessy, G., Szócs, T., Török, Á., Vatai, J., Viktor, Zs. & Zilahi-Sebess, L. 2018: Geology. In: Kocsis, K. (ed.): National Atlas of Hungary: Natural environment. Budapest, MTA CSFK Geographical Institute: 16-35.
- Käss, W. & Käss, H. 2008: Deutsches Bäderbuch. Vereinigung für Bäder- und Klimakunde e.V., Schweizerbart, Stuttgart: 232 p.
- Kirschner, C. 2009: Glossar Kur, Heilbad, Rehabilitation = Glossary Cure, Spa, Rehabilitation. Schweizerbart Verlag, Germany: 352 p.
- LaMoreaux, P. & Tanner, J. 2001: Springs and Bottled Waters of the World: Ancient History, Source, Occurrence, Quality and Use. Springer, Berlin: 315 p. <https://doi.org/978-3-642-56414-7>
- Lapanje, A. 2006: Origin and chemical composition of thermal and thermomineral waters in Slovenia. *Geologija*, 49/2: 347-370. <https://doi.org/10.5474/geologija.2006.025>

- Lourenço, C., Ribeiro, L. & Cruz, J. 2010: Classification of natural mineral and spring bottled waters of Portugal using Principal Component Analysis. *Journal of Geochemical Exploration*, 107/3: 362-372. <https://doi.org/10.1016/j.gexplo.2010.08.001>
- Lund, J. 2001: Balneological use of thermal waters. In: *International Geothermal Days Germany 2001, Bad Urach, Germany*.
- Michel, G. 1997: *Mineral- und Thermalwässer. Allgemeine Balneogeologie*. Borntraeger, Stuttgart: 398 p.
- Minissale, A. 1991: Thermal springs in Italy: their relation to recent tectonics. *Applied Geochemistry*, 6/2: 201-212. [https://doi.org/10.1016/0883-2927\(91\)90030-S](https://doi.org/10.1016/0883-2927(91)90030-S)
- Miošić, N. & Samardžić, N. 2016: Mineral, Thermal and Thermomineral Waters of Bosnia and Herzegovina. In: Papić, P. (ed.): *Mineral and Thermal Waters of Southeastern Europe*. Springer, Berlin: 147-171. [https://doi.org/10.1007/978-3-319-25379-4\\_9](https://doi.org/10.1007/978-3-319-25379-4_9)
- Natural Mineral Waters Europe, 2021: <https://naturalmineralwaterseurope.org/> (25.10.2021)
- Nikić, Z. & Papić, P. 2016: Thermal Waters in Bulgaria. In: Papić, P. (ed.): *Mineral and Thermal Waters of Southeastern Europe*. Springer, Berlin: 47-64. [https://doi.org/10.1007/978-3-319-25379-4\\_3](https://doi.org/10.1007/978-3-319-25379-4_3)
- Papić, P. (ed.) 2016: *Mineral and Thermal Waters of Southeastern Europe*. Environmental Earth Sciences. Springer Verlag, Berlin: 174 p.
- Porowski, A., Rman, N., Fórizs, I. & LaMoreaux, J. 2019: Introductory Editorial Thematic Issue: "Mineral and thermal waters". *Environmental Earth Sciences*, 78/16: 2p. [https://doi.org/10.1007/978-1-4939-2493-6\\_978-1](https://doi.org/10.1007/978-1-4939-2493-6_978-1)
- Reimann, C. & Birke, M. (eds.) 2010: *Geochemistry of European Bottled Water*. Borntraeger, Stuttgart: 268 p.
- Rman, N., Bălan, L., Bobovečki, I., Gál, N., Jolović, B., Lapanje, A., Marković, T., Milenić, D., Skopljak, F., Rotár-Szalkai, Á., Samardžić, N., Szőcs, T., Šolaja, D., Toholj, N., Vijdea A. & Vranješ, A. 2020: Geothermal sources and utilization practice in six countries along the southern part of the Pannonian basin. *Environmental Earth Sciences*, 79/1. <https://doi.org/10.1007/s12665-019-8746-6>
- Rosca, M., Bendea, C. & Vijdea, A. 2016: Mineral and Thermal Waters of Romania. In: Papić, P. (ed.): *Mineral and Thermal Waters of Southeastern Europe*. Springer, Berlin: 97-114. [https://doi.org/10.1007/978-3-319-25379-4\\_6](https://doi.org/10.1007/978-3-319-25379-4_6)
- Sowizdzal, A. 2018: Geothermal energy resources in Poland – Overview of the current state of knowledge. *Renewable and Sustainable Energy Reviews*, 82/3: 4020-4027. <https://doi.org/10.1016/j.rser.2017.10.070>
- Stober, I. & Bucher, K. 2012: *Geothermie*. Springer Verlag, Berlin: 287 p. <https://doi.org/10.1007/978-3-642-24331-8>
- Szocs, T., Rman, N., Süveges, M., Palcsu, L., Tóth, G. & Lapanje, A. 2013: The application of isotope and chemical analyses in managing transboundary groundwater resources. *Applied Geochemistry*, 32: 95-107. <https://doi.org/10.1016/j.apgeochem.2012.10.006>
- Todorović, M., Štrbački, J., Čuk, M., Andrijašević, J., Šišović, J. & Papić, P. 2016: Mineral and Thermal Waters of Serbia: Multivariate Statistical Approach to Hydrochemical Characterization. In: Papić, P. (ed.): *Mineral and Thermal Waters of Southeastern Europe*. Springer, Berlin: 81-95, [https://doi.org/10.1007/978-3-319-25379-4\\_5](https://doi.org/10.1007/978-3-319-25379-4_5)
- Zötl, J. & Goldbrunner, J. E. 1993: *Die Mineral- und Heilwässer Österreichs. Geologische Grundlagen und Spurenelemente*. Springer, Wien: 331 p. <https://doi.org/10.1007/978-3-7091-6652-9>

## Annex 1 - Legal norms

### Europe

- Directive 2009/54/EC of the European Parliament and of the Council of 18 June 2009 on the exploitation and marketing of natural mineral waters. Internet: <https://eur-lex.europa.eu/legal-content/EN/ALL/?uri=celex%3A32009L0054> (25.10.2021)
- Directive 2020/2184 of the European Parliament and of the Council of 16 December 2020 on the quality of water intended for human consumption. Internet: <https://eur-lex.europa.eu/legal-content/EN/ALL/?uri=CELEX:32020L2184> (25.10.2021)
- Directive 80/777/EEC of 15 July 1980 on the approximation of the laws of the Member States relating to the exploitation and marketing of natural mineral waters. Internet: <https://eur-lex.europa.eu/legal-content/EN/ALL/?uri=CELEX%3A31980L0777> (25.10.2021)
- Directive 98/83/EC of 3 November 1998 on the quality of water intended for human consumption. Internet: <https://eur-lex.europa.eu/legal-content/EN/TXT/?uri=celex%3A31998L0083> (25.10.2021)
- Directive 2003/40/EC of 16 May 2003 establishing the list, concentration limits and labelling requirements for the constituents of natural mineral waters and the conditions for using ozone-enriched air for the treatment of natural mineral waters and spring waters. Internet: <https://eur-lex.europa.eu/legal-content/EN/ALL/?uri=CELEX%3A32003L0040> (25.10.2021)
- List of natural mineral waters recognised by member states. Internet: [https://eur-lex.europa.eu/legal-content/EN/TXT/HTML/?uri=CELEX:52013XC0403\(04\)&from=EN](https://eur-lex.europa.eu/legal-content/EN/TXT/HTML/?uri=CELEX:52013XC0403(04)&from=EN) (25.10.2021)

### Austria

- Austrian food code: Chapter B 17 „bottled waters“ BMGF-75210/0005-II/B/13/2016. Internet: <https://www.lebensmittelbuch.at/lebensmittelbuch/b-17-abgefuellte-waesser.html> (25.10.2021)
- Drinking water regulation – TWV, BGBl. II Nr. 304/2001 idgF. Internet: <https://www.ris.bka.gv.at/GeltendeFassung.wxe?Abfrage=Bundesnormen&Gesetzesnummer=20001483> (25.10.2021)
- Food labelling regulation:– LMKV, BGBl. Nr. 72/1993 idgF. Internet: <https://www.ris.bka.gv.at/GeltendeFassung.wxe?Abfrage=Bundesnormen&Gesetzesnummer=10010723&FassungVom=2014-12-12> (25.10.2021)
- Health- and nutrition security law– GESG, BGBl. I Nr. 63/2002 idgF. Internet: <https://www.ris.bka.gv.at/GeltendeFassung.wxe?Abfrage=Bundesnormen&Gesetzesnummer=20001896> (25.10.2021)
- Mineral and spring water regulation, BGBl. II, Nr. 309/1999. Internet: <https://www.ris.bka.gv.at/GeltendeFassung.wxe?Abfrage=Bundesnormen&Gesetzesnummer=20000003> (25.10.2021)
- Wasserrechtsgesetz 1959 – WRG 1959, BGBl. Nr. 215/1959 idgF. Internet: <https://www.ris.bka.gv.at/GeltendeFassung.wxe?Abfrage=Bundesnormen&Gesetzesnummer=10010290> (25.10.2021)
- Medicinal occurrence and health resort law of Burgenland (state in Austria). HeiKuG, LGBL. Nr. 15/1963, zuletzt geändert durch LGBL. Nr. 79/2013. Internet: <https://www.ris.bka.gv.at/GeltendeFassung.wxe?Abfrage=LrBgld&Gesetzesnummer=10000048> (25.10.2021)
- Medicinal occurrence and health resort law of Carinthia (state in Austria). LGBL. Nr. 157/1962, zuletzt geändert durch LGBL. Nr. 85/2013. Internet: <https://www.ris.bka.gv.at/GeltendeFassung.wxe?Abfrage=LrK&Gesetzesnummer=10000024> (25.10.2021)
- Medicinal occurrence and health resort law of Lower Austria (state in Austria). LGBL. Nr. 272/1978, zuletzt geändert durch LGBL. Nr. 219/2001. Internet: <https://www.ris.bka.gv.at/GeltendeFassung.wxe?Abfrage=LrNO&Gesetzesnummer=20000627> (25.10.2021)
- Medicinal occurrence and health resort law of Upper Austria (state in Austria). LGBL. Nr. 47/1961, zuletzt geändert durch LGBL. Nr. 90/2013. Internet: <https://www.ris.bka.gv.at/GeltendeFassung.wxe?Abfrage=LrOO&Gesetzesnummer=10000048> (25.10.2021)
- Medicinal occurrence and health resort law of Salzburg (state in Austria). LGBL. Nr. 101/1997, zuletzt geändert durch LGBL. Nr. 106/2013. <https://www.ris.bka.gv.at/GeltendeFassung.wxe?Abfrage=LrSbg&Gesetzesnummer=10001039> (25.10.2021)
- Medicinal occurrence and health resort law of Styria (state in Austria). LGBL. Nr. 161/1962, zuletzt geändert durch LGBL. 87/2013. Internet: <https://www.ris.bka.gv.at/GeltendeFassung.wxe?Abfrage=LrStmk&Gesetzesnummer=20000421> (25.10.2021)
- Medicinal occurrence and health resort law of Tyrol (state in Austria). LGBL. Nr. 24/2004, zuletzt geändert durch LGBL. Nr. 130/2013. Internet: <https://www.ris.bka.gv.at/GeltendeFassung.wxe?Abfrage=LrT&Gesetzesnummer=20000191> (25.10.2021)

Medicinal occurrence and health resort law of Vienna (state in Austria). LGBl. Nr. 29/2013. Internet: <https://www.ris.bka.gv.at/GeltendeFassung.wxe?Abfrage=LrW&Gesetzesnummer=20000303> (25.10.2021)

### **Bosnia and Herzegovina**

Waters Act - Rulebook on natural mineral water, spring water and table water. Official Gazette of the Bosnia and Herzegovina No. 26/10, 40/10.

The law on Waters. Official Gazette of the Federation BiH No. 70/06.

The law on Geological Surveys. Official Gazette of FBiH, No. 9/10.

The law on Bottled Water in Bosnia and Herzegovina, No. 45/04.

The law on Concessions on Water and Public Property. Official Gazette of the Federation BiH, No. 8/00.

Rulebook on natural mineral and natural spring waters. Official Gazette of BiH No. 26/10

Rulebook on the categorization, classification, calculation of groundwater reserves and keeping records on them. Official Gazette of the FBiH, No. 47/11.

Rulebook on conditions for determining sanitary protection zones and protective measures for water sources used or planned to be used for drinking. Official Gazette of the Federation BiH, No. 51/02.

Rulebook on minimum technical, technological and personnel requirements for the production of refreshing soft drinks, fruit juices and syrups and bottled waters. Official Gazette of the Federation BiH, no. 81/06.

Rulebook on table water. Official Gazette of BiH No. 40/10.

Rulebook on the health safety of drinking water. Official Gazette of BiH No. 40/10.

Rulebook on the manner of keeping records and creating Cadastre of deposits of mineral raw materials, geological phenomena and approved investigative areas. Official Gazette of the Federation of BiH, no.38/11.

### **Denmark**

Executive Order on natural mineral water, spring water and bottled drinking water: BEK nr 38 of 12/01/2016. Internet: <https://www.retsinformation.dk/eli/lta/2016/38> (25.10.2021)

Guidance on the labeling of natural mineral water, spring water and bottled drinking water: VEJ nr 9105 of 10/04/2008. Internet: <https://www.retsinformation.dk/eli/retsinfo/2008/9105> (25.10.2021)

### **France**

Public Health Codes, articles L1322-1 to 13 et R.1322-1 to 1322-44-23

Safety of water intended for human consumption, Decree No 2007-49 of 11 January 2007

[https://www.legifrance.gouv.fr/codes/article\\_lc/LEGIARTI000021940425/](https://www.legifrance.gouv.fr/codes/article_lc/LEGIARTI000021940425/)

[https://www.legifrance.gouv.fr/codes/article\\_lc/LEGIARTI000021940425/2010-02-26/](https://www.legifrance.gouv.fr/codes/article_lc/LEGIARTI000021940425/2010-02-26/)

[https://www.legifrance.gouv.fr/codes/article\\_lc/LEGIARTI000006909666#:~:text=Une%20eau%20min%C3%A9rale%20naturelle%20est,fix%C3%A9es%20par%20l'article%20R.&text=l'une%20et%20l'autre,de%20tout%20risque%20de%20pollution](https://www.legifrance.gouv.fr/codes/article_lc/LEGIARTI000006909666#:~:text=Une%20eau%20min%C3%A9rale%20naturelle%20est,fix%C3%A9es%20par%20l'article%20R.&text=l'une%20et%20l'autre,de%20tout%20risque%20de%20pollution)

Décret n° 2007-49 du 11 janvier 2007 relatif à la sécurité sanitaire des eaux destinées à la consommation humaine - Légifrance (<https://www.legifrance.gouv.fr>)

(<https://www.legifrance.gouv.fr/loda/id/LEGIARTI000006259300/2007-01-12/>)

National regulation on thermal waters. Article R. 1322-52 of the Public Health Code and the Decree 2007-49 11 January 2007 [https://www.legifrance.gouv.fr/codes/article\\_lc/LEGIARTI000006909777](https://www.legifrance.gouv.fr/codes/article_lc/LEGIARTI000006909777)

### **Hungary**

59/2006 (VIII. 14.) FVM-EüM-SZMM. Internet: <https://net.jogtar.hu/jogszabaly?docid=A0600059.FVM&txtreferer=A0400065.FVM> (12.10.2021)

65/2004 (IV. 27.) FVM-ESzCsM-GKM. Internet: <https://net.jogtar.hu/jogszabaly?docid=a0400065.fvm> (12.10.2021.)

Mineral water according to Hungarian law LVII from 1995. Internet: <https://net.jogtar.hu/jogszabaly?-docid=99500057.tv> (12.10.2021.)

Ministerial decree on natural mineral waters, 74/1999 (XII. 25.). Internet: <https://net.jogtar.hu/jogszabaly?docid=99900074.eum> (12.10.2021)

National law implementing 2003/40/EC. Internet: <https://eur-lex.europa.eu/legal-content/EN/>

[ALL/?uri=CELEX%3A32003L0040](#) (12.10.2021)

National law implementing 80/777/EEC. Internet: <https://eur-lex.europa.eu/legal-content/EN/ALL/?uri=CELEX%3A31980L0777> (12.10.2021.)

National law implementing 96/70/EC. Internet: <https://eur-lex.europa.eu/legal-content/EN/TXT/?uri=celex%3A31996L0070> (12.10.2021)

### Italy

Implementation of Directive 2009/54/EC on the use and marketing of natural mineral waters. Decree N.176 of 8 October 2011. Official Gazette of Italian Republic, General Serie n.258, 1-13 (05/11/2011)

Reorganization of the thermal water sector. Law N.323 of 24 October 2000. Official Gazette of Italian Republic, General Serie n.261, 4-14 (08/11/2000)

### Poland

Act of 25 August 2006 on Food and Nutrition Safety. Jour. of Law 2006 No 171 item 1563. Internet: <http://prawo.sejm.gov.pl/isap.nsf/DocDetails.xsp?id=WDU20061711225> (25.10.2021)

Regulation of 31 March 2011 on natural mineral water, spring water and table water. Jour. of Law 2011 No 85 item 466. Internet: <http://prawo.sejm.gov.pl/isap.nsf/DocDetails.xsp?id=WDU20110850466> (25.10.2021)

Jour. of Law 2018 item 1563

### Portugal

Geological Resources Law. Law no° 54/2015 of 22 June. Internet: <https://dre.pt/pesquisa/-/search/67552498/details/maximized> (25.10.2021)

Decree for natural mineral waters. Decree-Law no. 86/90 of 16 March. Internet: <https://dre.pt/web/guest/pesquisa/-/search/333159/details/normal?l=1> (25.10.2021)

Decree for spring waters. Decree-Law no. 84/90 of 16 March. Internet: <https://dre.pt/web/guest/pesquisa/-/search/333157/details/maximized?jp=true> (25.10.2021)

### Romania

Definition of natural mineral water. Government Decision 1020/2005.

Definition of thermal water. Governmental Decision no. 1154/2004.

### Serbia

Regulation on Quality and Other Requirements for Natural mineral water, Spring Water and Bottled Drinking Water. Official Gazette of Serbia and Montenegro, number 53/05.

Regulation on the Hygienic Acceptability of Potable Water. Official Gazette of FRY, number 42/98 and 44/99.

### Slovenia

Rules on natural mineral water, spring water and table water. Official Gazette of Rep. of Slovenia No. 50/04, 75/05 in 45/08 – ZKme-1. <http://www.pisrs.si/Pis.web/pregledPredpisa?id=PRAV5392> (11.11.2021)

Water Act. Official Gazette of Rep. of Slovenia No. 67/02, 2/04 – ZZdrI-A, 41/04 – ZVO-1, 57/08, 57/12, 100/13, 40/14, 56/15, 65/20. <http://pisrs.si/Pis.web/pregledPredpisa?id=ZAKO1244> (11.11.2021)

### Spain

Law of Mines 22/1973 (BOE number 189, de 24-07-1973). Internet: <https://www.boe.es/buscar/doc.php?id=BOE-A-1973-1018> (25.10.2021)

Royal Law 2857/1978 (BOE number 295, de 11-12-1978). Internet: <https://www.boe.es/buscar/doc.php?id=BOE-A-1978-29905> (25.10.2021)

Royal Law 1798/2010. Internet: <https://ec.europa.eu/growth/tools-databases/tris/en/search/?trisaction=search.detail&year=2018&num=67> (25.10.2021)





# Comparison of mapping efficiency for small datasets using inverse distance weighting vs. moving average, Northern Croatia Miocene hydrocarbon reservoir

## Primerjava učinkovitosti kartiranja za majhne podatkovne nize z uporabo metode inverzne utežene razdalje in metode drsečega povprečja v miocenskem rezervoarju ogljikovodikov, Severna Hrvaška

Josip IVŠINOVIĆ<sup>1</sup> & Tomislav MALVIĆ<sup>2</sup>

<sup>1</sup>Vodnikova 17, HR-10000 Zagreb, Croatia; e-mail: jivsinovic@gmail.com

<sup>2</sup>Faculty of Mining, Geology and Petroleum Engineering, University of Zagreb, Zagreb, Croatia; e-mail: tomlav.malvic@rgn.unizg.hr

Prejeto / Received 7. 1. 2022; Sprejeto / Accepted 15. 7. 2022; Objavljeno na spletu / Published online 22. 07. 2022

*Key words:* Sava depression, Croatia, interpolation, hydrocarbon reservoirs, mapping spatial comparison

### Abstract

Mapping of geological variables in the Croatian part of the Pannonian Basin System (CPBS) is mostly based on small input datasets. In the case of the analyzed hydrocarbon field "B", reservoir "K", due to the complex geological structure and pronounced tectonics, the interpretations are restricted on several blocks, where each has very limited dataset. The porosity (19 data) and permeability (18 data) variables were analyzed. The applied interpolation methods are the Inverse Distance Weighting (IDW) and the Moving Average (MA). They were compared and analyzed by visual inspection of the obtained maps, comparison of mathematical background and by calculation of cross-validation (CV). The cross-validation value for the porosity of the "K" reservoir in the case of IDW application is 0.0011, and in the case of MA 0.0010; while in the case of permeability the IDW is 480.84, and in the case of MA 1346.41. According to the visual review of maps, the values of descriptive statistics of estimated values and the results of cross-validation, the IDW method is recommended for mapping the porosity and permeability of reservoirs blocks in the Sava Depression.

### Izveček

Kartiranje geoloških spremenljivk v hrvaškem delu Panonskega bazena temelji večinoma na majhnih vhodnih podatkovnih nizih. V primeru preučevanega polja ogljikovodikov »B«, rezervoarja »K« je zaradi kompleksne geološke zgradbe in močno izražene tektonike, interpretacija omejena na nekaj blokov, od katerih ima vsak zelo omejen nabor podatkov. Analizirane spremenljivke so bile poroznost (19 podatkov) in prepustnost (18 podatkov). Kot interpolacijski metodi sta bili uporabljeni metoda inverzne utežene razdalje (IUR) in metoda drsečega povprečja (DP). Metodi smo primerjali in analizirali s pomočjo vizualnega pregleda dobljenih kart, primerjavo matematičnega ozadja in z izračunom navzkrižne validacije. Vrednost navzkrižne validacije za poroznost rezervoarja »K« pri uporabi IDW je 0,0011, v primeru uporabe DP pa 0,0010. Vrednost navzkrižne validacije v primeru prepustnosti pa je bila pri uporabi IDW 480,84 in pri uporabi DP 1346,41. Glede na vizualni pregled kart, vrednosti opisne statistike ocenjenih vrednosti in rezultate navzkrižne validacije, se je metoda IDW izkazala za priporočljivo metodo pri kartiranju poroznosti in prepustnosti rezervoarskih blokov v Savski depresiji.

### Introduction

Complex geological structures result in a relatively small volumes and consequently small datasets. The tectonics causes the fragmentation in several block, often separate hydrodynamic units, what negatively affected production. In such complex conditions, it is necessary to set up a reliable spatial model of selected variables. Any

successful application of the recommended interpolation method is always welcome because can be repeated in similar geological environments as the best approach. Here are analyzed the porosity and permeability of the Neogene reservoir "K" using Moving Average (MA) and Inverse Distance Weighting (IDW) methods.

The MA method was applied in different research areas: economics (Fan & Wang, 2020; Raudys & Pabarškaitė, 2018), food industry (Kolko-va, 2018), medicine (Mustapa et al., 2019), geology (Balić et al., 2008), environment protection (Kumar et al., 2020), agriculture (Hatchett et al., 2009), transportation (Adeniran et al., 2018; Lenkutis et al., 2021), energy (Alsharif et al., 2019; Xin et al., 2020) etc.

The IDW method is also widely used in various research areas (Achilleos, 2011; Al-Hassan & Adjei, 2015; Moeletsi et al., 2016; Tunçay et al., 2016; Ikechukwu et al., 2017; Maleika, 2020; Liu et al., 2021). In petroleum geology, IDW is used to map a small set of geological variables in the area of the Croatian Pannonian Basin System (CPBS), which has proven to be a reliable interpolation method (Ivšinović, 2018a; Malvić et al., 2019; Malvić et al., 2020; Ivšinović & Malvić, 2020). Also, this could be often applied method in mapping of hydrocarbon reservoirs worldwide (Wenli et al., 2021; Liu et al., 2020; Otchere et al., 2021) or subsurface resource in general (Busygin et al., 2019).

The paper analyzes the possibility of applying the MA on particular subsurface structure in the CPBS, the reservoir “K” of the field “B” located in the western part of the Sava Depression (Fig. 1). The analyzed input data set is less than 20 points, which according to the classification (Malvić et al., 2019) belongs to a small dataset. The mapping can be also done with different hybrid algorithms, not using pure interpolation, but connecting points from the very dense seismic, gravimetric or similar grids (*e.g.*, Vrdoljak et al., 2021; Lemenkova, 2021). As quality check the MA results are compared with the IDW method, which is previously proven as very reliable mapping method in the research area (Malvić et al., 2019; Ivšinović & Malvić, 2020).

This research is continuation of analyses of different mathematical interpolation algorithms application in the Miocene reservoirs of the CPBS. This task is important, not only for better knowing of the geological subsurface of this part of the PBS, but also because such algorithm is mostly applied in hydrocarbon reservoirs, still in production, and results have also economic value. The testing of different mathematical interpolation algorithms extensively started in this part more than decade ago (*e.g.*, Balić, et al., 2008; Malvić, 2008), where some of the knowing algorithms had been compared regarding their efficiency in mapping of geological variables collected in Miocene of the CPBS. So, Balić et al., (2008) compared also in the Sava Depression, in the Kloštar Field, four

interpolations, namely: Inverse Distance Weighting, Nearest Neighborhood, Moving Average and Kriging, using 20 porosity values from Upper Miocene reservoir. Interestingly, cross validation/mean square errors formula resulted in very similar values, orderly: Kriging 366.93, Moving Average 369.26, Inverse Distance Weighting 371.97, Nearest Neighborhood 389.00. It was concluded that limited dataset influenced variogram model as well as successfulness of exact interpolators like (Ordinary Kriging or IDW, especially because distribution could not be concluded. Authors pointed out that calculation of residual map can help in the interpretation of zones with higher uncertainty. Simultaneously, Malvić (2008) performed comparison between three geostatistical approaches – Kriging, CoKriging and stochastic simulation (*i.e.*, deterministic vs. stochastic) for datasets taken in the Drava Depression (also in the CPBS). The analysis was done with only 14 data points, so the application of geostatistics strongly depended on assumption of normal distribution (the 2<sup>nd</sup> order stationarity assumption for Kriging and related methods). The simulations are described as the most descriptive approach, where zones of errors are the easiest recognizable.

In analysis presented here, the input datasets are not characterized with normal distribution as well as the entire dataset can be set up in only three classes, so distribution cannot be examined with any statistical formal test for normality like Shapiro-Wilk, Kolmogorov-Smirnov, Lilliefors and Anderson-Darling (Razali & Wah, 2011). To bypass the normality condition, we selected two methods where such distribution is not strong condition, namely Inverse Distance Weighting and Moving Average, to improve conclusions obtained in earlier publications, especially in (*e.g.*, Balić et al., 2008).

### Geological settings of analyzed area

Analyzed oil reservoir is part of the typical hydrocarbon field in the CPBS. The geographical position of the analyzed field “B” is shown in Figure 1.

The reservoir is composed of medium to fine-grained sandstone, altered with marls. The age is Upper Miocene. A typical geological column of the western part of the Sava Depression is shown in Figure 2.

The reservoir had been formed by the deposition of turbidities originating from the eastern part of the Alps. A schematic representation of the sedimentary environment during the Upper Pannonian and Lower Pontian is shown in Figure 3.

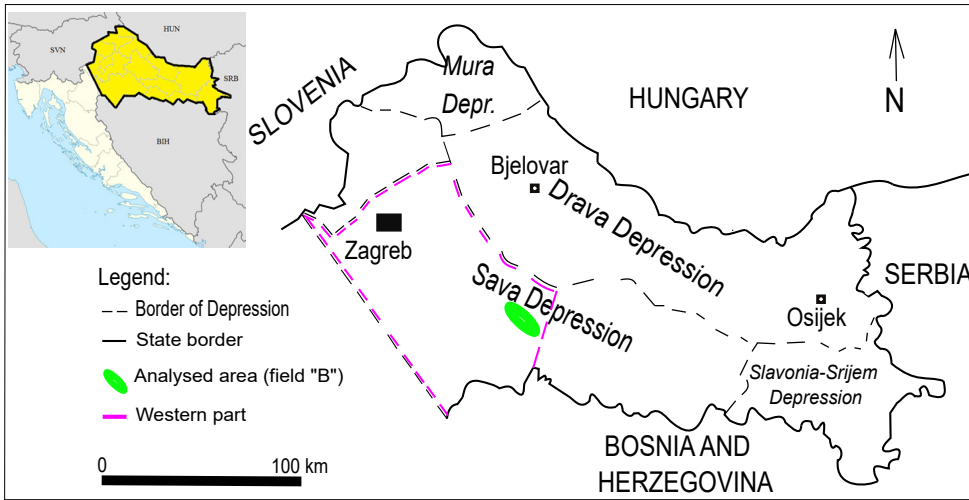


Fig. 1. Geographical position of the western part of the Sava Depression and field "B" (Ivšinović et al., 2020).

| Age in Ma                | Chronostratigraphy      | Lithostratigraphy  | Megacycle (Velić et al., 2002) | Tectonic (Malvić and Velić, 2011) | Depositional environment | Schematic dominant lithology and legend   |
|--------------------------|-------------------------|--------------------|--------------------------------|-----------------------------------|--------------------------|---|
| 5.6-0.0                  | QUATERNARY              |                    | 3rd megacycle                  | 2nd transpression                 | Alluvial-terrestrial     | clay<br>sandy clay<br>sandstone<br>marlitic sandstone<br>silty sandstone<br>alternation of sandstone and marlstone<br>marlstone<br>clayey marlstone<br>breccia-conglomerate<br>calcite marlstone<br>dolomitic breccia<br>gneiss |
|                          | PLIOCENE                | Lonja Formation    |                                |                                   |                          |   |
| 6.3-5.6                  | NEOGENE                 | UPPER PONTIAN      | 2nd megacycle                  | 2nd transtension                  | Brackish-freshwater      | clay<br>sandy clay<br>sandstone<br>marlitic sandstone<br>silty sandstone<br>alternation of sandstone and marlstone<br>marlstone<br>clayey marlstone<br>breccia-conglomerate<br>calcite marlstone<br>dolomitic breccia<br>gneiss |
|                          |                         | Lower Pontian      |                                |                                   |                          |   |
| 7.1-6.3                  | MIOCENE                 | LOWER PONTIAN      | 2nd megacycle                  | 2nd transtension                  | Brackish-freshwater      | clay<br>sandy clay<br>sandstone<br>marlitic sandstone<br>silty sandstone<br>alternation of sandstone and marlstone<br>marlstone<br>clayey marlstone<br>breccia-conglomerate<br>calcite marlstone<br>dolomitic breccia<br>gneiss |
| Klostar Ivanič Formation |                         |                    |                                |                                   |                          |   |
| 9.3-7.1                  | MIOCENE                 | UPPER PANNONIAN    | 2nd megacycle                  | 2nd transtension                  | Brackish-freshwater      | clay<br>sandy clay<br>sandstone<br>marlitic sandstone<br>silty sandstone<br>alternation of sandstone and marlstone<br>marlstone<br>clayey marlstone<br>breccia-conglomerate<br>calcite marlstone<br>dolomitic breccia<br>gneiss |
| Ivanič-Grad Formation    |                         |                    |                                |                                   |                          |   |
| 11.5-9.3                 | MIOCENE                 | LOWER PANNONIAN    | 2nd megacycle                  | 2nd transtension                  | Lacustrine               | clay<br>sandy clay<br>sandstone<br>marlitic sandstone<br>silty sandstone<br>alternation of sandstone and marlstone<br>marlstone<br>clayey marlstone<br>breccia-conglomerate<br>calcite marlstone<br>dolomitic breccia<br>gneiss |
| Prkos Formation          |                         |                    |                                |                                   |                          |   |
| 16.4-11.5                | MESOZOIC and PALAEOZOIC | BADENIAN SARMATIAN | 1st megacycle                  | 1st transpress., 1st transtens.   | Marine                   | clay<br>sandy clay<br>sandstone<br>marlitic sandstone<br>silty sandstone<br>alternation of sandstone and marlstone<br>marlstone<br>clayey marlstone<br>breccia-conglomerate<br>calcite marlstone<br>dolomitic breccia<br>gneiss |
| Precec Formation         |                         |                    |                                |                                   |                          |   |

Fig. 2. Typical geological column of the Sava Depression (e.g., Novak Zelenika, 2013; Novak Zelenika et al., 2018).

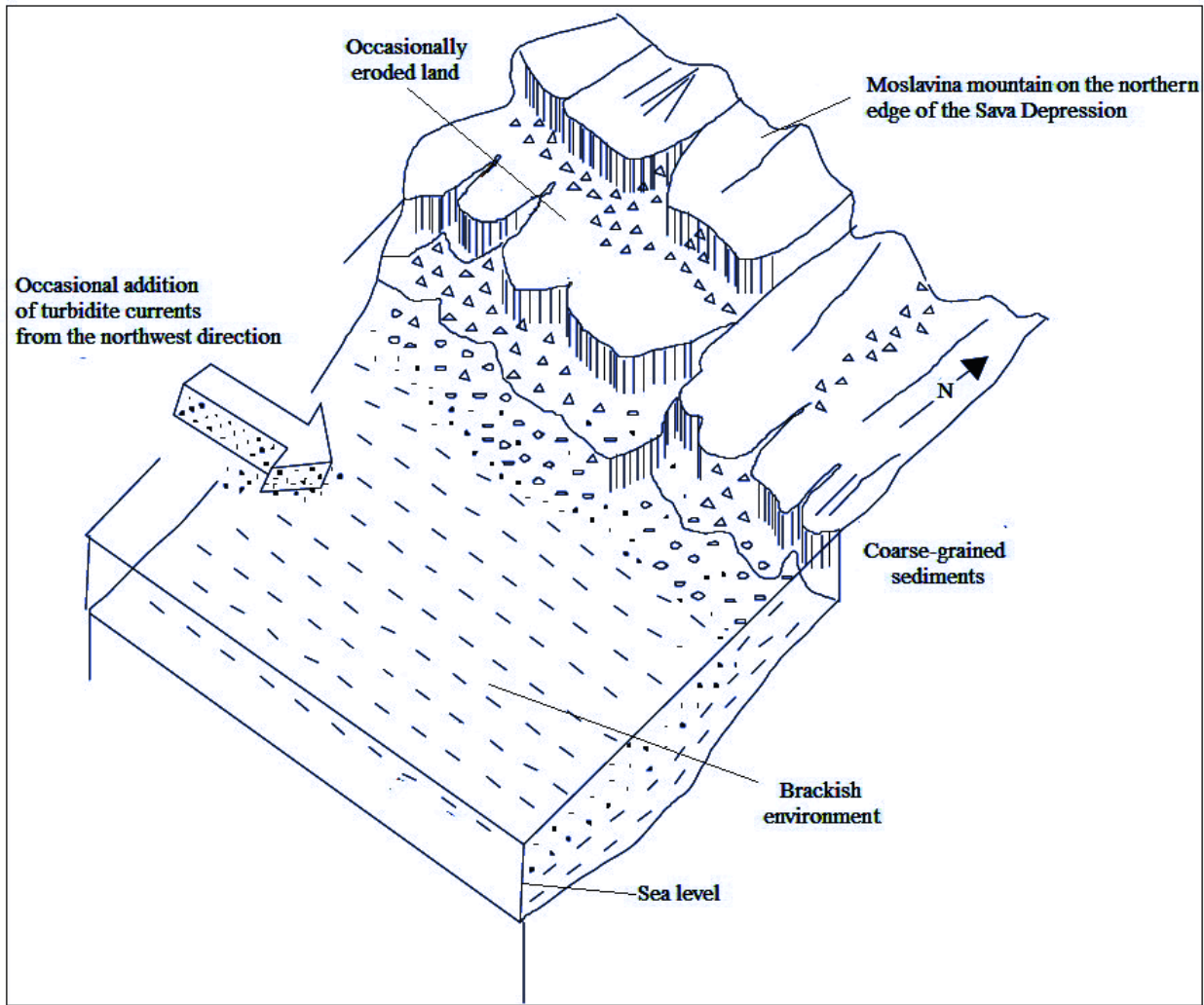


Fig. 3. Sedimentary environment during the Upper Pannonian and Lower Pontian western part of the Sava Depression (Ivšinović et al., 2021).

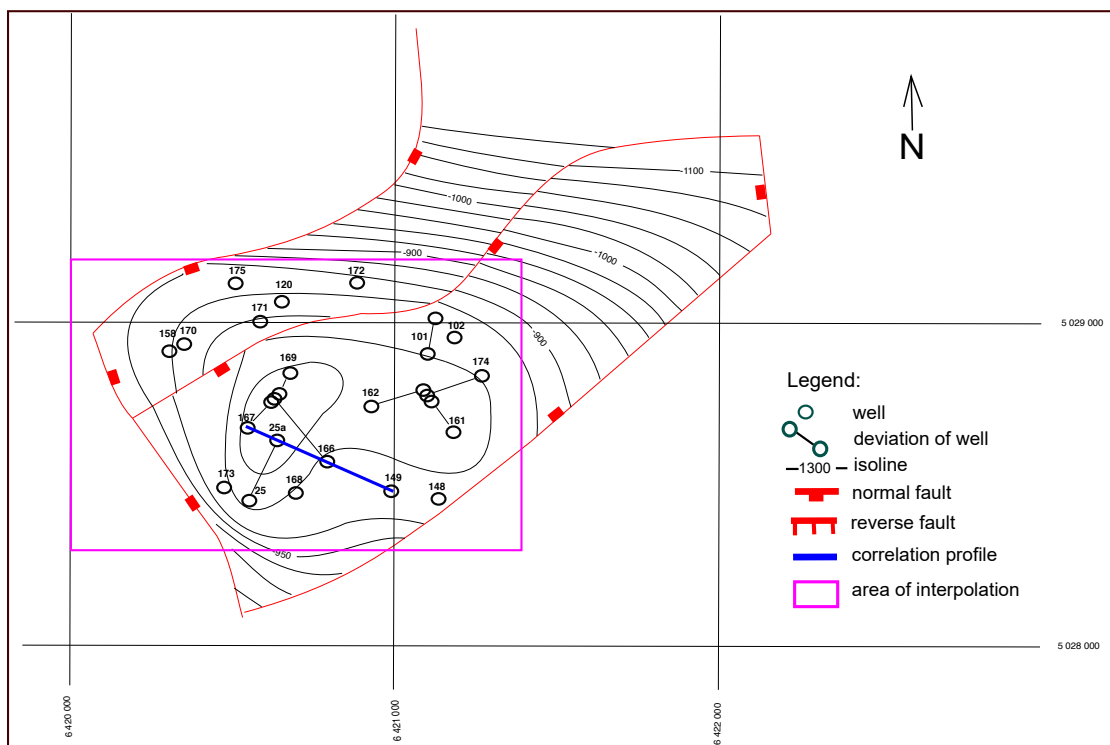


Fig. 4. Structural map of reservoir "K" (Malvić et al., 2020).

Reservoir hydrodynamics is defined by faults, which created several blocks with different permeabilities. In the beginning the contact oil-water was unique for entire reservoir, i.e., reservoir was single hydrodynamic unit. However, after some recovery period, parts are characterized with larger permeability caused that that fluids faster moving upward as well as contact, and consequently larger portion of water in produced fluid, until the production was not ceased. The structural map of the analyzed deposit “K” of the field “B” is shown in Figure 4. The reservoir is classified as layer type or with structural-stratigraphic trap.

Simultaneously, reservoir pressure was dropped, but also minor communication of fluids had happened through fault zones.

### Methodology

The applied interpolations were Moving Average (MA), and Inverse Distance Weighting (IDW). Their results had been compared visually, numerically and theoretically.

#### *Moving Average (MA)*

The MA method (Eq. 1) assigns values to spatial points by determining the mean value of measured data located within a particular area around the grid node (un-known value that is estimated by MA). The minimum (sometimes also maximum) amount of analyzed data should be defined. The value calculated in each grid node is equal to the arithmetic mean of the measured data located within the defined range of spatial dependence. The mathematical equation for calculating the moving average value is (e.g., Johnston et al., 1999; Ekhosuehi & Omorogbe Dickson, 2016; Rusdiana et al., 2020):

$$y_{i,j} = \frac{1}{n} \sum_{k=1}^n x_{i,j-k} \quad (1)$$

where:  $y_{i,j}$ -interpolated value of moving average method;  $n$ - number of data set;  $x_{i,j-k}$ - input data.

#### *Inverse Distance Weighting (IDW)*

The IDW method is based on the distance (ponder with exponent, mostly second power) between the measured data and the location where unknown value is estimated. Such values are in grid nodes. The measured data included in calculation are values inside the searching radius/radii, i.e. inside circle/ellipsoid of spatial dependence. The mathematical expression for inverse distance estimation (e.g., Setianto & Triandini, 2013; Ivšinović, 2018b) is:

$$z_{iu} = \frac{\frac{z_1}{d_1^p} + \frac{z_2}{d_2^p} + \dots + \frac{z_n}{d_n^p}}{\frac{1}{d_1^p} + \frac{1}{d_2^p} + \dots + \frac{1}{d_n^p}} \quad (2)$$

where:  $z_{iu}$ -estimated value;  $d_i$ -distance to “i-th” location;  $p$ -power of distance;  $z_i$ -measured values at “i-th” location.

The result of IDW interpolation depends on the value of the exponent  $p$ , which is obtained experimentally and has a different value in different fields of science. In subsurface mapping, for the CPBS, the proposed value exponent “ $p$ ” is 2.

#### *Cross-validation (CV)*

Cross-validation (CV) or out-of-sample testing is a method of assessing the quality of a map obtained by implemented an interpolation method. It is based on the re-placement of the any measured (original) data(s) from an entire measured dataset and is replaced by a new value(s) estimating from the existing data set. In geology the most often is applied “ $p=1$ ”, i.e., leaving-one-out CV. Differences between measured and estimated value on the same location is error. The very often such error are calculated using mean square error algorithm (MSE). The mathematical formula for calculating MSE is (e.g., Malvić & Novak Zelenika, 2013):

$$MSE = \frac{1}{n} \sum_{i=1}^n (\text{measured} - \text{estimated})^2 \quad (3)$$

where: MSE- mean square error; measured-known value at location “i”; estimated- unknown value (deleted) at location “i”;  $n$  - number of locations.

The quality of the map obtained by the interpolation method is based on the numerical value of the MSE, the lower the value of the MSE the better the applied interpolation method.

#### *Mathematical differences in MA and IDW and reflections of searching radius*

Basically, both methods are considered as mathematically simpler interpolation methods, that highly depend on number of input data. However, both use so called searching radius or radii. If anisotropy could be recognized and quantitatively described, two axes/ellipsoid of dependency are defined, if not – the circle outlined area with hard data included in calculation. The small datasets ( $n < 20$ ) hardly allow unambiguous recognition of anisotropy, even with lot of

qualitative geological data, so the most often MA or IDW works with searching radius or circle (of spatial dependance), without any further separation of circle in quadrants or octants, because most of them would be without single hard value, i.e., would be empty.

Definition of searching radius is much more important in MA than IDW, because MA does not honor distances among unknown value/location and known, measured, hard data. However, one of the geological axioms is that if what two measurements are more distant in space, the difference must be larger. It is valid for any geological variable, like thickness, granulometry, porosity, permeability, depths etc., simply because any geological value is result of particular geological environment, limited in space and time. Consequently, the equally weighting of each measured value (MA) inside searching radius surely does not honor such rule (Equation 1), especially because area of spatial dependance has to cover large part or entire analyzed area to include at least one measured value.

Oppositely, the IDW honor the distances among estimated and measured values, equally for any direction (Equation 2). Even for single reservoir this could be crucial advantage, because reservoir's lithofacies is not homogeneous and will gradually change from the center of structure, especially if depocenter remained in the current structure top, toward the reservoir

margins. This presumption has been tested in this work and elaborated with results, discussion and conclusions.

## Results and discussion

The analyzed variables were obtained from laboratory measurements of well cores and logging measurements. Data from reservoir "K" are shown in Figure 5.

The analyzed porosity (19 data) and permeability (18 data) belong to a small datasets. They are characterized by intervallic grouped data - in the case of permeability two, and in the case of porosity three groups, which is results of analytical approximation and reservoir heterogeneity. However, the problem is what the formal normality tests cannot be applied, and empirical Q-Q plot cannot be calculated. It is why those two interpolation algorithms, where normal distribution is not strong condition for their application, had been selected.

Based on selected area and structural axes, the searching radius was in both algorithms set on 628 m. It is done using the "rule of the thumb" that if data do not allow create reliable spatial model, omnidirectional or anisotropic, for searching radius is recommended to use structural or depositional axes and their ration (if exists). So, 628 m is about half of the quadrat used to border researched area and is used for omnidirectional/circle searching radius. The research area is

| Well  | Surface X | Surface Y | Porosity (part of units) |
|-------|-----------|-----------|--------------------------|
| J-101 | 6421096   | 5028877   | 0.217                    |
| J-120 | 6420658   | 5029068   | 0.272                    |
| J-161 | 6420957   | 5028870   | 0.217                    |
| J-162 | 6421034   | 5028593   | 0.217                    |
| J-167 | 6420529   | 5028674   | 0.217                    |
| J-168 | 6420699   | 5028475   | 0.315                    |
| J-169 | 6420724   | 5028825   | 0.217                    |
| J-170 | 6420349   | 5028926   | 0.223                    |
| J-174 | 6421298   | 5028863   | 0.217                    |
| J-175 | 6420475   | 5029136   | 0.223                    |
| J-158 | 6420303   | 5028910   | 0.223                    |
| J-171 | 6420576   | 5028970   | 0.223                    |
| J-172 | 6420928   | 5029147   | 0.223                    |
| J-102 | 6421208   | 5028926   | 0.217                    |
| J-148 | 6421126   | 5028437   | 0.217                    |
| J-149 | 6420959   | 5028501   | 0.217                    |
| J-166 | 6420771   | 5028650   | 0.217                    |
| J-25  | 6420546   | 5028460   | 0.315                    |
| J-173 | 6420539   | 5028382   | 0.217                    |

Fig. 5. Raw data set of porosity and permeability of reservoir "K" (Malvić et al., 2020).

Table 1. Cross-validation values and descriptive statistics of estimated values for IDW and MA methods for geological variables porosity and permeability of reservoir "K".

| Variable     | Method | Cross-validation (MSE) | Min   | Max    | Mean  | Standard deviation |
|--------------|--------|------------------------|-------|--------|-------|--------------------|
| Porosity     | IDW    | 0.0011                 | 0.219 | 0.293  | 0.232 | 0.016              |
| Porosity     | MA     | 0.0010                 | 0.217 | 0.243  | 0.231 | 0.006              |
| Permeability | IDW    | 480.84                 | 36.33 | 115.97 | 90.97 | 28.97              |
| Permeability | MA     | 1346.41                | 63.95 | 121.20 | 93.06 | 13.34              |

42.3 km<sup>2</sup>. Obtained permeability and porosity interpolations by IDW and MA methods are shown in Figure 6, while the results of cross-validation and descriptive statistics are shown in Table 1.

The results given on Figure 6 are influenced with, and reflected in, the complexity of the geological structure, and especially depositional environments that are responsible for clastic types and their petrophysics. Here is also included the problem of measurement errors and consequently fitting of measured values into classes. It is well known that laboratory and logging results can differ, even for an order of magnitude, so sometimes they are not directly comparable or have to be used jointly only with caution. The step of

caution had been selection of values in group, decreasing influence of measurement error, but also decreasing data spectrum, what made interpolation significantly less representative, especially on smaller scales of changes.

The IDW porosity map (Fig. 6, a) shown many outliers of individual points resulted in so-called bull-eyes and even on NW part butterfly effects. That was expected due to the distances of measured data, applied power exponent and values of minimum and maximum. According to Table 1 IDW porosity values have standard deviation of 0.016 and MSE 0.0011.

The MA porosity map (Fig. 6, b) is more uniformly shaped at first glance. No butterfly or bull-

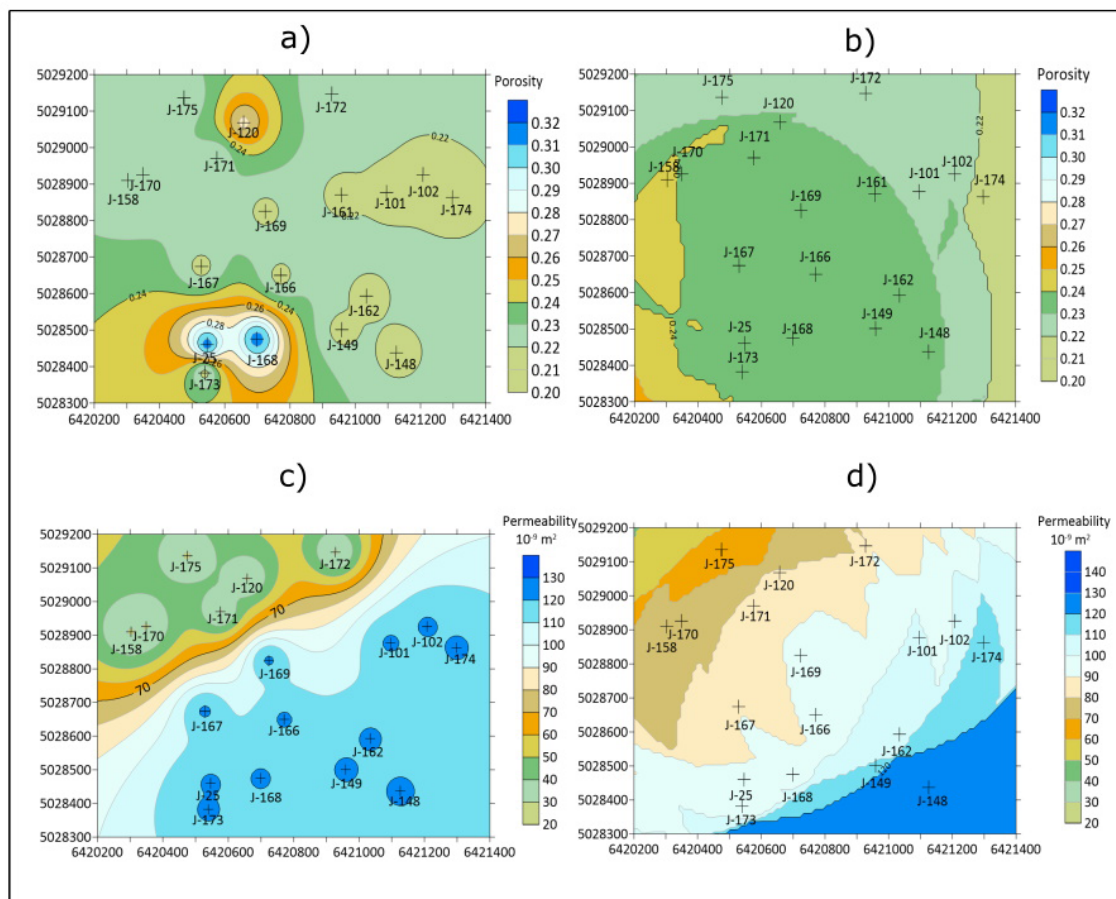


Fig. 6. Maps of reservoir "K" obtained by interpolation methods: (a) Porosity (IDW); (b) Porosity (MA); (c) Permeability (IDW); (d) Permeability (MA).

eyes are pronounced, which is understandable because it is a local calculation of the mean value around the estimated data, i.e., in the searching radius. So, if averaging is dominant, and total number of data is small, the consequence is that many estimations will be averaged with the same values. Furthermore, it means that complex shapes like butterfly or bull-eye effects will not be developed. Moreover, the transition area between the data is not emphasized, but island-like irregularities are formed in this area (between wells J-170 and J-175 or J-162 and J-174. Due to the data averaging, the usual butterfly or bull-eyes effects cannot occur, as in the IDW method. That is clearly seen by the circular appearance of the “green” surface in the center of Figures 6, b. Comparing the data of descriptive statistics (Table 1) the values of standard deviation (0.006) and MSE (0.0010) are slightly smaller than in the IDW.

The IDW permeability map (Fig. 6, c) emphasized the butterfly or bull-eyes effects. In the northwestern part of the reservoir, it is less pronounced, while in the southeastern more. Fig. 6, c clearly shows the zone of abrupt changes between wells J-169 and J-171 or J-167 and J-158. The transition zone between the zone of higher reservoir permeability and lower reservoir permeability can be follow along entire map and correspond to fault zone shown on structural map (Fig. 4). The data of the descriptive statistics from Table 1 showed relatively small standard deviation (28.97) and high MSE (480.84).

On the MA permeability map (Fig. 6, d) is clearly seen no uniform transition zone between the different permeability values. This can be seen in Figure 6, d through the peninsula-like shape between wells J-166 and J-167 or J-101 and J-102. The values are averaged as seen from the descriptive statistics in Table 1 and although standard deviation is smaller than by IDW (13.34) the MSE is extremely high (1346.41). The difference between the original and estimated data (MSE) is twice as large in the case of the min values of the set. This can be seen from the interpolated map (Fig. 6, d) that the permeability values of wells J-167 and J-169 differ significantly, and the measured values are the same ( $121.2 \cdot 10^{-9} \text{ m}^2$ ). Regarding large difference between MSE(IDW) and MSE(MA), here 480.84 vs. 1346.41, the range of permeability is much higher than of porosity, so consequently any estimation will varies significantly depending on applied mathematical algorithm, like it is shown in results.

As can be seen from Table 1, the cross-validation/MSE value has a lower value of MA than

IDW in the case of porosity, while in the case of throughput it is the reverse case. The difference in cross-validation in bandwidth between the MA and IDW methods is 0.0001. This difference can be ignored due to the other results of the descriptive statistics in Table 1. It can be observed that the coverage of the estimated values in the IDW method is much more realistic than in the case of the MA method. In such cases, the rule of accepting the interpolation method to the amount of the lower CV value can be deviated from. Most importantly, the estimated values obtained by interpolation methods must be an approximate reflection of the measured data.

## Conclusions

Here is solved one local problem of selection the appropriate interpolation algorithm for small datasets of petrophysics measured in the sub-surface Miocene hydrocarbon reservoirs in the Northern Croatia (CPBS). So, the results are of interest for researchers engaged in the studying of such reservoirs in the Sava Depression as well as in all other depressions in the CPBS. However, all researching that included interpolation of small geological datasets ( $n \leq 20$  points) could find those achievements and conclusions worth of testing in their own explorations, whatever the data are collected from surface or subsurface. The specific outcomes obtained with this analysis are:

- Visual inspection of the obtained interpolated maps revealed that the maps obtained by the IDW method are more acceptable for interpretation of reservoir petrophysics compared to the MA method.
- The permeability map of the “K” reservoir obtained by the MA method can be described with mosaic effect, with sharply wavy, peninsular, and island shapes, which is not an unusual case in mapping of small datasets, but cannot be interpreted with sense. This is characterized by a high value of cross-validation.
- Descriptive statistics, histograms and maps showed that the values obtained by the IDW method are closer to the ranges of original datasets. The differences between IDW and MA are about 25 % for porosity and more than 200 % for permeability.
- The calculated cross-validation/MSE for the MA method in the case of porosity is 0.0010, and permeability is 1346.41 for reservoir “K”. In the case of the IDW method the MSE for porosity is 0.0011, while for permeability 480.84. The difference between the MSE values for porosity can

be neglected with respect to the results of descriptive statistics and visual inspection of the obtained maps.

- This researching showed that mapping the porosity and permeability of Neogene reservoir in the CPBS highly depends on the experience of the interpreter in the application of different mathematical methods and geological understanding of spatial distribution of selected variables. The MA showed one large disadvantages – in the case of small datasets there is not enough measured values inside searching radius for reliable calculation of average. So, the “distance weighting” approach of the IDW is far better approach for mapping of reservoirs in such case.

### Acknowledgment

This work has been supported in part under the project “Mathematical researching in geology VII (led by T. Malvić), at the University of Zagreb, Faculty of Mining, Geology and Petroleum Engineering.

### References

- Achilleos, G.A. 2011: The Inverse Distance Weighted interpolation method and error propagation mechanism – creating a DEM from an analogue topographical map. *Journal of Spatial Science*, 56/2: 283–304. <https://doi.org/10.1080/14498596.2011.623348>
- Adeniran, A., Kanyio, O. & Adelanke Samuel, O. 2018: Forecasting Methods for Domestic Air Passenger Demand in Nigeria. *J. Appl. Res. Ind. Eng.*, 5: 146–155. <https://doi.org/10.22105/jarie.2018.133561.1038>
- Al-Hassan S. & Adjei, D. 2015: Competitiveness of Inverse Distance Weighting Method for the Evaluation of Gold Resources in Flu-vial Sedimentary Deposits: A Case Study. *Journal of Geosciences and Geomatics*, 3/5: 122-127. <https://doi.org/10.12691/jgg-3-5-2>
- Alsharif, M.H., Younes, M.K. & Kim, J. 2019: Time Series ARIMA Model for Prediction of Daily and Monthly Average Global Solar Radiation: The Case Study of Seoul, South Korea. *Symmetry*, 11/2: 240. <https://doi.org/10.3390/sym11020240>
- Balić, D., Velić, J. & Malvić, T. 2008: Selection of the most appropriate interpolation method for sandstone reservoirs in the Kloštar oil and gas field. *Geologia Croatica*, 61: 27-35.
- Busygina, B., S. Nikulin, S. & Sergieieva, K. 2019: Solving the tasks of subsurface resources management in gis rapid environment. *Mining of Mineral Deposits*, 13/3: 49-57. <https://doi.org/10.33271/mining13.03.049>
- Ekhosuehi, N. & Omorogbe Dickson, E. A. 2016: On Forecast Performance Using a Class of Weighted Moving Average Processes for Time Series. *Journal of Natural Sciences Research*, 6: 87-92.
- Fan, Q. & Wang, F. 2020: Detrending-moving-average-based bivariate regression estimator. *Phys. Rev. E* 102. <https://doi.org/10.1103/PhysRevE.102.012218>
- Hatchett, R. B., Brorsen, B. W., K. B. & Anderson, K. B. 2009: Optimal Length of Moving Average to Forecast Futures Basis. *Proceedings of the NCCC-134 Conference on Applied Commodity Price Analysis, Forecasting, and Market Risk Management*, St. Louis, U.S.A., 20-21 April 2009.
- Ikechukwu, M., Ebinne, E., Idorenyin, U. & Raphael, N. 2017: Accuracy Assessment and Comparative Analysis of IDW, Spline and Kriging in Spatial Interpolation of Landform (Topography): An Experimental Study. *Journal of Geographic Information System*, 9/3: 354-371. <https://doi.org/10.4236/jgis.2017.93022>
- Ivšinić, J. & Malvić, T. 2020: Application of the radial basis function interpolation method in selected reservoirs of the Croatian part of the Pannonian Basin System. *Mining of mineral deposits*, 14: 37-42. <https://doi.org/10.33271/mining14.03.037>
- Ivšinić, J. 2018a: The relationship between sandstone depositional environment and water injection system, a case study from the Upper Miocene hydrocarbon reservoir in northern Croatia. In *Proceedings of the 2nd Croatian scientific congress from geomathematics and terminology in geology*, Zagreb, Croatia, 6 October 2018.
- Ivšinić, J. 2018b: Deep mapping of hydrocarbon reservoirs in the case of a small number of data using the example of the Lower Pontian reservoirs of the western part of the Sava Depression. In *Proceedings of the 2nd Croatian scientific congress from geo-mathematics and terminology in geology*, Zagreb, Croatia, 6 October 2018.
- Ivšinić, J., Pimenta Dinis, M., Malvić, T. & Pleše, D. 2021: Application of the bootstrap method in low-sampled Upper Miocene sandstone hydrocarbon reservoirs: a case study. *Energy sources part A-recovery utilization and environmental effects*, 43. <https://doi.org/10.1080/15567036.2021.1883773>

- Ivšiniović, J., Malvić, T., Velić, J. & Sremac, J. 2020: Geological Probability of Success (POS), case study in the Late Miocene structures of the western part of the Sava Depression, Croatia. *Arabian Journal of Geosciences*, 13: 1-12. <https://doi.org/10.1007/s12517-020-05640-z>
- Johnston, F. R., Boyland, J. E., Meadows, M. & Shale, E. 1999: Some properties of a simple moving average when applied to forecasting a time series. *Journal of the Operational Research Society*, 50: 1267-1271.
- Liu, H., Chen, S., Hou, M. & He, L. 2020: Improved inverse distance weighting method application considering spatial autocorrelation in 3D geological modeling. *Earth Sci Inform* 13, 619-632. <https://doi.org/10.1007/s12145-019-00436-6>
- Kolkova, A. 2018: Indicators of Technical Analysis on the Basis of Moving Averages as Prognostic Methods in the Food Industry. *Journal of Competitiveness*, 10: 102-119. <https://doi.org/10.7441/joc.2018.04.07>
- Kumar, A. K., Lakshmi, A. S. & Nivas Rao, P. J. 2020: Moving average method based air pollution monitoring system using IoT plat-form. In *Proceedings of the First International Conference on Advances in Physical Sciences and Materials*, Coimbatore, India, 13-14 August 2020. <https://doi.org/10.1088/1742-6596/1706/1/012078>
- Lemenkova, P. 2021: Submarine tectonic geomorphology of the Pliny and Hellenic Trenches reflecting geologic evolution of the southern Greece. *Rudarsko-geološko-naftni Zbornik (The Mining-Geological-Petroleum Bulletin)*, 36/4: 33-48 <https://doi.org/10.17794/rgn.2021.4.4>
- Lenkutis, T., Čerškus, A., Šešok, N., Dzedzickis, A. & Bučinskis, V. 2021: Road Surface Profile Synthesis: Assessment of Suitability for Simulation. *Symmetry*, 13/1: 68. <https://doi.org/10.3390/sym13010068>
- Liu, Z., Zhang, Z., Zhou, C., Ming, W. & Du, Z. 2021: An Adaptive Inverse-Distance Weighting Interpolation Method Considering Spatial Differentiation in 3D Geological Modeling. *Geosciences*, 11: 51. <https://doi.org/10.3390/geosciences11020051>
- Maleika, W. 2020: Inverse distance weighting method optimization in the process of digital terrain model creation based on data collected from a multibeam echosounder. *Appl Geomat*, 12: 397-407. <https://doi.org/10.1007/s12518-020-00307-6>
- Malvić, T. & Novak Zelenika, K. 2013: Hrvatski rječnik odabranih geostatističkih pojmova. *Rudarsko-geološko-naftni zbornik*, 26: 1-9.
- Malvić, T. 2008: Kriging, cokriging or stochastic simulations, and the choice between deterministic or sequential approaches. *Geologia Croatica*, 61: 37-47.
- Malvić, T., Ivšiniović, J., Velić, J. & Rajić, R. 2019: Interpolation of Small Datasets in the Sandstone Hydrocarbon Reservoirs, Case Study of the Sava Depression, Croatia. *Geosciences*, 9: 201. <https://doi.org/10.3390/geosciences9050201>
- Malvić, T., Ivšiniović, J., Velić, J., Sremac, J. & Barudžija, U. 2020: Application of the Modified Shepard's Method (MSM): A Case Study with the Interpolation of Neogene Reservoir Variables in Northern Croatia. *Stats*, 3/1: 68-83. <https://doi.org/10.3390/stats3010007>
- Moeletsi, M., Shabalala, Z., Nysschen, G. & Walker, S. 2016: Evaluation of an inverse distance weighting method for patching daily and dekadal rainfall over the Free State Province, South Africa. *Water SA*, 42: 466-474. <https://doi.org/10.4314/wsa.v42i3.12>
- Mustapa, R., Latief, M. & Rohandi, M. 2019: Double moving average method for predicting the number of patients with dengue fever in Gorontalo City. *Global Conferences Series: Sciences and Technology (GCSST)*, 2: 332-337. <https://doi.org/10.32698/tech1315168>
- Novak Zelenika, K. 2013: Lithofacies definition based on cut-offs in Indicator Kriging mapping, case study Lower Pontian reservoir, Sava Depression. *Nafta*, 64: 39-44.
- Novak Zelenika, K., Novak Mavar, K. & Brnada, S. 2018: Comparison of the Sweetness Seismic Attribute and Porosity-Thickness Maps, Sava Depression, Croatia. *Geosciences*, 8/11: 426. <https://doi.org/10.3390/geosciences8110426>
- Otchere, D. A., Hodgetts, D., Ganat, T. A. O., Ullah, N. & Alidu R. 2021: Static Reservoir Modeling Comparing Inverse Distance Weighting to Kriging Interpolation Algorithm in Volumetric Estimation. Case Study: Gullfaks Field. In *Proceedings of the Offshore Technology Conference, Virtual and Houston, USA*, 16-19 August 2021. <https://doi.org/10.4043/30919-MS>
- Raudys, A. & Pabarškaitė, Ž. 2018: Optimising the smoothness and accuracy of moving average for stock price data. *Technological and Economic Development of Economy*, 24: 984-1003. <https://doi.org/10.3846/20294913.2016.1216906>

- Razali, N., M. & Wah, Y., B. 2011: Power comparisons of Shapiro-Wilk, Kolmogorov-Smirnov, Lilliefors and Anderson-Darling tests. *Journal of Statistical Modeling and Analytics*, 2: 21-33.
- Rusdiana, S., Yuni, S. M. & Khairunnisa, D. 2020: Comparison of Rainfall Forecasting in Simple Moving Average (SMA) and Weighted Moving Average (WMA) Methods (Case Study at Village of Gampong Blang Bintang, Big Aceh District-Sumatera-Indonesia). *Journal of Research in Mathematics Trends and Technology*, 2/1: 21-27. <https://doi.org/10.32734/jormtt.v2i1.3753>
- Setianto, A. & Triandini, T. J. 2013: Comparison of Kriging and Inverse Distance Weighted (IDW) interpolation methods in lineament extraction and analysis. *Journal of Applied Geology*, 5: 21–29. <https://doi.org/10.22146/jag.7204>
- Tunçay, T., Bayramin, İ., Atalay, F. & Ünver, İ. 2016: Assessment of Inverse Distance Weighting IDW Interpolation on Spatial Var-iability of Selected Soil Properties in the Cukurova Plain. *Journal of Agricultural Sciences*, 22/3: 377-384. [https://doi.org/10.1501/Tarimbil\\_0000001396](https://doi.org/10.1501/Tarimbil_0000001396)
- Vrdoljak, L., Režić, M. & Petričević, I. 2021: Bathymetric and Geological Properties of the Adriatic Sea. *Rudarsko-geološko-naftni Zbornik = The Mining-Geological-Petroleum Bulletin*, 36/2: 93–107. <https://doi.org/10.17794/rgn.2021.2.9>
- Xin, P., Liu, Y., Yang, N., Song, X. & Huang, Y. 2020: Probability distribution of wind power volatility based on the moving average method and improved nonparametric kernel density estimation. *Global Energy Interconnection*, 3/3: 247–258. <https://doi.org/10.1016/j.gloe.2020.07.006>
- Wenli H., Xiankang X., Xinbo Z., Li L., Shengli N., Qingquan L., Gaoming Y. & Li W. 2021: Application of production splitting method based on inverse distance weighted interpolation in X Oilfield. *Energy Reports*, 7/7: 850-855 <https://doi.org/10.1016/j.egy.2021.09.189>





# Carbon isotopic composition of methane and its origin in natural gas from the Petišovci-Dolina oil and gas field (Pannonian Basin System, NE Slovenia) – a preliminary study

## Izotopska sestava ogljika v metanu in njegov izvor v naravnem plinu na območju nafto-plinskega polja Petišovci-Dolina (Panonski bazenski sistem, SV Slovenija) – preliminarna raziskava

Miloš MARKIČ<sup>1</sup> & Tjaša KANDUČ<sup>2</sup>

<sup>1</sup>Geological Survey of Slovenia, Dimičeva ulica 14, SI-1000 Ljubljana, Slovenia; e-mail: milos.markic@geo-zs.si,

<sup>2</sup>Department of Environmental Sciences, Jožef Stefan Institute, Jamova cesta 39, SI-1000 Ljubljana, Slovenia; e-mail: tjasa.kanduc@ijs.si

Prejeto / Received 10. 2. 2022; Sprejeto / Accepted 15. 7. 2022; Objavljeno na spletu / Published online 22. 07. 2022

*Key words:* Petišovci-Dolina, gas, methane, isotopes, origin

*Ključne besede:* Petišovci-Dolina, plin, metan, izotopi, izvor

### Abstract

The carbon isotopic composition of methane ( $\delta^{13}\text{C}_{\text{CH}_4}$ ) in natural gas from the Petišovci-Dolina oil and gas field (NE Slovenia) was measured for the first time in August and September 2021. The gas samples from different depths were taken from three wells: Dolina-deep (Pg-6) from the depth interval 3102–3104 m, Petišovci-deep (Pg-5) from the depth interval 2772–2795 m, and Petišovci-shallow (D-5) from the depth interval 1212–1250 m. According to the available composition dataset of gas, available from the Petrol Geo d.o.o. documentation, the “deep” gases sampled from the Pg-6 and Pg-5 wells consist of 85 % methane (C1), 11 % hydrocarbons heavier than methane (C2–C6) and 4 %  $\text{CO}_2$ . The “shallow” gas from well D-5 contains more than 89 % methane, up to 11 % C2–C6 gases, while the  $\text{CO}_2$  content is negligible. The “deep” gas from the Pg-6 and Pg-5 wells has  $\delta^{13}\text{C}_{\text{CH}_4}$  of  $-36.7\text{‰}$  and  $-36.6\text{‰}$ , respectively, while the “shallow” gas from the D-5 well has the  $\delta^{13}\text{C}_{\text{CH}_4}$  of  $-38.6\text{‰}$ . The methane from the “shallow” gas is slightly enriched in the lighter  $^{12}\text{C}$  isotope.  $\delta^{13}\text{C}_{\text{CH}_4}$  in the range from  $-38.6$  to  $-36.6\text{‰}$  clearly indicates the thermogenic origin of methane formed during the catagenesis phase of gas formation.

### Izvleček

Izotopsko sestavo metana ( $\delta^{13}\text{C}_{\text{CH}_4}$ ) v naravnem (zemeljskem) plinu naftno-plinskega polja Petišovci-Dolina (Ormoško-selniška antiklinala, NE Slovenija) smo prvič merili v avgustu in septembru 2021. Plinske vzorce smo vzorčili iz različnih globin iz treh plinskih vrtin: iz Petišovci-globoka (Pg-6) iz globine 3102–3104 m, iz Petišovci-globoka (Pg-5) iz globine 2772–2795 m in iz Dolina-plitva (D-5) iz globine 1212–1250 m. Glede na dostopne podatke o sestavi plina iz dokumentacije Petrol Geo d.o.o., so “globoki” plini iz vrtin Pg-6 in Pg-5 sestavljeni iz 85 % metana (C1), iz 11 % ogljikovodikov, težjih od metana (C2–C6) in 4 %  $\text{CO}_2$ . “Plitvi” plin iz vrtine D-5 je sestavljen iz več kot 89 % metana in do 11 % C2–C6, medtem ko je koncentracija  $\text{CO}_2$  zanemarljiva. “Globoki” plin iz vrtin Pg-6 in Pg-5 ima  $\delta^{13}\text{C}_{\text{CH}_4}$  vrednost od  $-36.7$  do  $-36.6\text{‰}$ , medtem ko ima “plitvi” plin iz vrtine D-5  $\delta^{13}\text{C}_{\text{CH}_4}$   $-38.6\text{‰}$ . “Plitvi” plin iz vrtine D-5 je obogaten na lažjem  $^{12}\text{C}$  izotopu. Razpon  $\delta^{13}\text{C}_{\text{CH}_4}$  od  $-38.6$  do  $-36.6\text{‰}$  jasno kaže termogeni izvor metana, ki je nastal v fazi katageneze nastajanja plina.

### Introduction

Correlation of petroleum fluids (oil and gas) with their source rocks based on their molecular and/or isotopic characteristics is an important task in fundamental and applied petroleum

(and coal) studies (Milkov, 2021). Biomarkers and the carbon and hydrogen isotopic composition of compounds in petroleum fluids facilitate to clarify relations between reservoir hydrocarbons and their specific source rocks (Boreham et al., 2004;

Gratzer et al., 2011; Yang et al., 2017). Natural gases contain relatively few compounds – mostly methane to hexane ( $\text{CH}_4$ - $\text{C}_6\text{H}_{14}$ , i.e., C1-C6),  $\text{N}_2$  and  $\text{CO}_2$ . Such a low molecular diversification limits the ways for interpreting their sources (Whiticar, 1994). Milkov and Etiope (2018) considerably re-defined the boundaries for genetic fields of thermogenic gas, primary microbial gas from  $\text{CO}_2$  reduction, primary microbial gas from methyl-type fermentation, secondary microbial gas and abiotic gas. Their study bases on the study of isotopic composition of carbon and hydrogen in methane and  $\text{CO}_2$  fractions of more than 20,000 samples from different geological realms worldwide. The revised gas diagrams of Milkov and Etiope (2018) became therefore new standard tools for gas genesis interpretations (Buttitta et al., 2020; Wieclaw et al., 2020, Babadi et al., 2021). There are still ongoing debates about the definition of the exact burial depth and ultra-deep resources (Ni et al., 2021). Natural gas can form in deep parts of the sedimentary basin, migrate upwards and accumulate in the shallow layers. Studies have already shown that several factors contribute to the origin of deep gas e.g., type of organic matter, thermal maturity, oil stability (Dyman et al., 2003).

In the last 20 years, numerous theoretical and applied studies have been conducted and published on gases in the intermontane Pliocene lignite-bearing Velenje basin (Kanduč & Pezdič, 2005; Kanduč et al., 2011; Sedlar et al., 2014; Kanduč et al. 2021), about 100 km west of the PDOGF area. There, the situation is much more complicated. Reservoir “rock” in Velenje is lignite, in which the gases are very heterogeneous in composition, of different origins and a result of different processes. Especially the ratio between methane and  $\text{CO}_2$  varies greatly, and this fact is more a risk of mining than an advantage for example for coalbed gas exploitation (see e.g., Flores 2014).

The study presented in this paper on the isotopic composition of the carbon of the gases of the PDOGF is the first such study in the Petišovci-Dolina area. This preliminary study is based on very few measurements. The aim of this paper is to publish first analysed data on isotopic composition of carbon of natural gas of the studied PDOGF, which is predominantly methane – mostly above 85 % in the deep gasses (INA Zagreb, 2019) and above 89 % (Lisjak et al., 1988; Lisjak et al., 2011;) in the “shallow” gases, and to ascertain the question of its origin at different reservoir levels.

### Study area -

#### Petišovci-Dolina Oil and Gas Field (PDOGF)

Oil and gas in the Petišovci-Dolina area E-SE of Lendava (Figs. 1 and 2) were discovered in 1942 – as a continuation of an already known Lovászi field in neighbouring Hungary. Also in Croatia, there were operating oil and gas fields in the immediate vicinity, especially at Selnica and Peklenica, which were exploited since the mid-19<sup>th</sup> century (Pleničar, 1954). At some localities oil seeps were known, as well. The peak of oil production was reached in a very narrow time-period between 1950 and 1952, with an annual production of between 50 and 70 thousand tonnes of oil (Pleničar, 1954). In the following years, oil production decreased. On the other hand, gas production increased (Kerčmar, 2018; Internet 1).

From 1942 to 2011, a total of 145 oil and gas wells were drilled in the Petišovci-Dolina Oil and Gas Field (PDOGF) and its surroundings (Lendava, Murski Gozd, Kog) (Lisjak et al., 1988; Lisjak et al., 2011; Markič, 2014). The most numerous, 107, are the wells abbreviated as the “Pt” (Petišovci) wells, and 13 wells abbreviated as the “D” (Dolina) wells. The PDOGF is 7.5 km long and 2 km wide (Fig. 2), and the area is a flat land, between +155 and +160 m above sea level. Numerous deep seismic profiles were carried out prior to drilling (Djurasek, 1988; and confidential data).

The “Pt” and “D” wells were up to 1775 m deep and they drilled the “upper” sequence of oil- and gas-bearing horizons (Fig. 3). These horizons (from the bottom at 1750 m depth to the top at 1200 m depth) have been for a long time known as the Petišovci, Lovászi, Paka, and Ratka horizons of the Lendava Formation (Fig. 3). The later used to be “conventionally” classified as a formation of the Upper Pannonian/Pontian age (e.g., Lisjak et al., 1988). However, in the last decade, the Pontian interval - in Slovenia *sensu* Škerlj, 1985; Stevanović & Škerlj, 1985; Škerlj, 1987; Turk, 1993; Pavšič & Horvat, 2009) has been excluded from the regional stratigraphic nomenclature of the Pannonian Basin System (Pavelić & Kovačić, 2018; p. 464, and references therein). Thus, the Lendava Formation is now classified as a formation of the Upper Pannonian age (*sensu lato*). The Petišovci, Lovászi, Paka, and Ratka horizons are 50 to 90 m thick and consist of alternating impermeable marls and porous oil- and especially gas-bearing sandstones. Each horizon comprises several hydrocarbon-bearing sandstones, which are up to 3.5 m effectively thick. Their porosity is 14–16 %, saturation with water

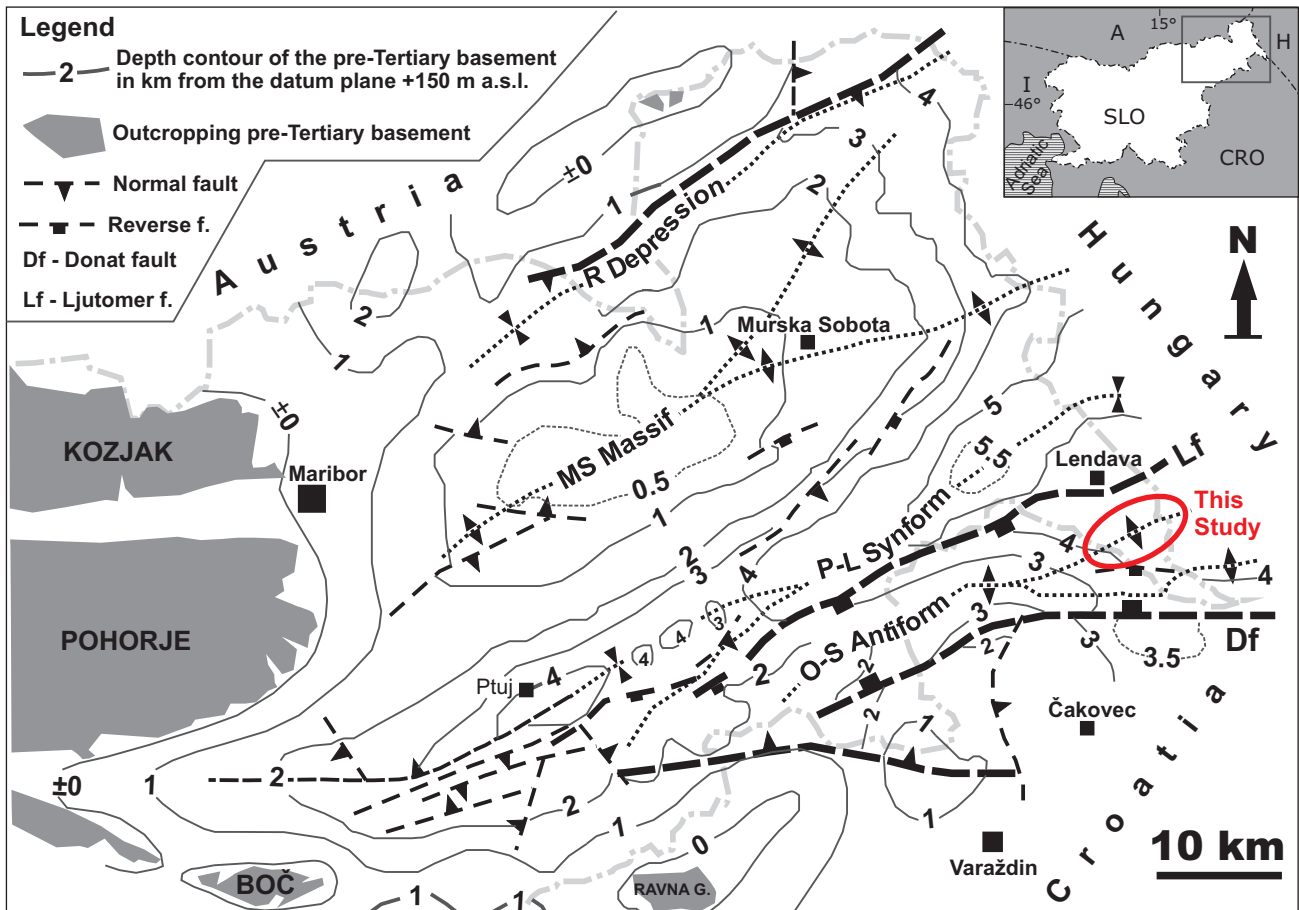


Fig. 1. Structural map of the Mura-Zala Basin. Isolines are depth contours (in km) of the pre-Tertiary basement (adopted after Djurasek, 1988; Gosar, 1994/95). Study area (PDOGF) is shown on the E of the map.

varies between 30 % and 40 % (Lisjak et al., 2011). Nowadays, the “upper” hydrocarbon-bearing reservoir sandstones are depleted – offering a possibility for storing imported gas, or for CO<sub>2</sub> sequestration.

In this paper, we call hydrocarbons in the “upper” sequence as the “shallow” hydrocarbons and gases, respectively.

In 1960, the Pg-1 well was drilled to a depth of 2977 m and encountered “deep” gas (Fig. 3). The “Pg” name means “Petišovci-globoka” (in English: “Petišovci-deep” well). Later, ten more Pg wells were drilled. The last and the deepest two were Pg-10 and Pg-11A wells from 2011, which reached a depth of 3492 m (length: 3535 m, but deviated) and 3500 m, respectively.

More than 15 gas-bearing early to middle Miocene (Karpatian to Badenian) sandstone reservoirs (“A-Q” reservoirs) were discovered by the “Pg” wells in a depth from 2200 m downwards to 3500 m (Toth & Tari, 2014; Kerčmar, 2018). Maybe there are even more reservoirs in a greater depth. The formation for “deep” gas used to be termed Murska Sobota Formation, while in the last ten years the Murska Sobota Formation is known as the Špilje Formation (e.g., Toth & Tari, 2014, Šram et al., 2015). The “deep” reservoirs are even thicker than the “shallow”, but porosity is lower, 7–11 %. The “deep” Petišovci gas is characterized as the “tight gas” (Markič et al., 2016).

In the frame of the study presented in this paper, we sampled gases from three wells, from the depth intervals: 1212–1250 m (D-5), 2772–2795 m (Pg-5), and from 3102–3104 m (Pg-6) (Table 1).

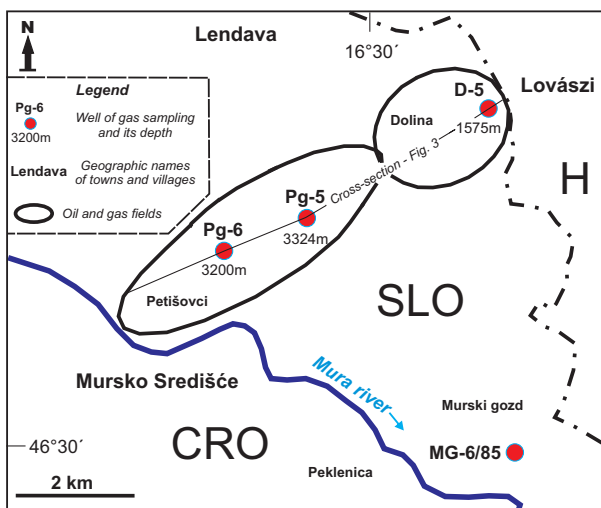


Fig. 2. Gas sampled wells Pg-6 and Pg-5 (“deep” gasses), and D-5 (“shallow” gas) within the Petišovci-Dolina oil and gas field (PDOGF). For the cross-section see Figure 3.

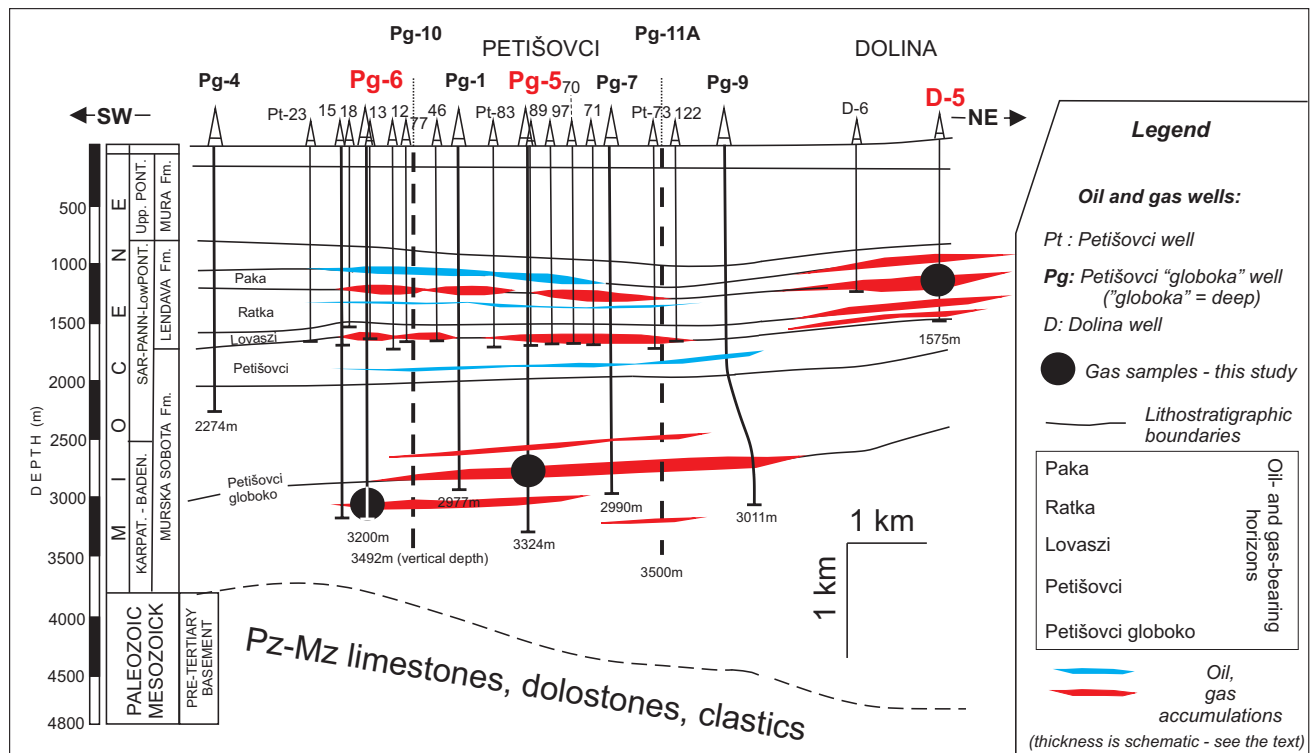


Fig. 3. A “classical” cross-section along the Petišovci-Dolina oil and gas field (PDOGF) adopted after Lisjak (1988). Thicknesses of oil and gas reservoirs are somewhat exaggerated.

According to geophysical data (Djurasek, 1988), the basement rocks in the study area occur at a depth greater than 4 km (Fig. 1). Based on available data from the MG-6 well (3858 m) located in Murski Gozd few kilometres E from the PDOGF the basement rocks (only reached by the mentioned well) are composed of cataclastic breccia and shale (3732–3858 m) of “? Mesozoic” age (Brodarić, 1985). In the Mura-1 and Mura-2 wells in the Mura Depression in Croatia, the basement rocks consist of Mesozoic carbonates (Barić et al., 1996).

The PDOGF is now the only active oil and gas field in Slovenia with a small but permanent production of hydrocarbons (oil, gas, and a little of condensate). In the last 15 years, oil production varied between 150 and 365 tonnes per year and that of gas between 1.8 and 5.4 million Sm<sup>3</sup>, with an extreme of 16 million Sm<sup>3</sup> in 2018 (Mineral resources in Slovenia, 2020). The highest gas production in the past was between 1988 and 1995 when it reached more than 30 million Sm<sup>3</sup> (1988) but dropped to 15 million Sm<sup>3</sup> (1995) (Kerčmar, 2018; Internet 1). This “high” production was achieved with “mechanical stimulation” of hydrocarbon-bearing strata (Fig. 9 in Kerčmar, 2018), and the same case was with a mentioned gas-peak in 2018. “Mechanical stimulation” is in general known today as “hydraulic fracturing”.

Concessionaire for the exploitation and exploration of hydrocarbons in the Petišovci-Dolina oil and gas field (PDOGF) is the company Petrol Geoenergo d.o.o.

Study of source rocks and of thermal history of the Mura-Zala Basin (then called the Mura Depression) started in the late 1990s (Barić et al., 1996). A group of Slovenian and Austrian geologists initiated further investigation in the early 2000s, and two fundamental studies were published by Hasenhüttl et al. (2001) and by Sachsenhofer et al. (2001).

### Geological setting

It is well known that the PDOGF is related to the Ormož-Selnica Anticline, more precisely to its northern segment, which is in Hungary named Lovászi Anticline, while the southern segment is called the Újfalu-Budafa Anticline (Toth & Tari, 2014). The northern anticline segment could be termed as the Petišovci-Lóvaszi anticline, which “bears” both oil and gas. The Újfalu Budafa anticline is hydrocarbon-bearing only in Hungary. The Ormož-Selnica Anticline, and the divided Petišovci-Lóvaszi and Újfalu Budafa anticlines are both a consequence of tectonic inversion (“up-lifting”) between two regional reverse faults, the Ljutomer Fault, and the Donat Fault (Fig.1); (Djurasek, 1988; Hasenhüttl et al., 2001, Sachsenhofer et al., 2001, Toth & Tari, 2014).

The Ormož-Selnica Anticline with the PDOGF is composed of numerous alternating hydrocarbon-bearing sandstones and isolating marls (in detail Lisjak et al. 1988, Lisjak et al., 2011; and confidential data). It is a typical anticlinal hydrocarbon trap as are broadly known worldwide (e.g., Tissot & Welte, 1984; North, 1985; Ercegovic, 2002; Flores, 2014, Internet 2, and many others).

The host basin of the PDOGF is the Mura-Zala Basin (Fig. 1) situated in the SW part of the Pannonian Basin System – Central Paratethis (Placer, 1998; Fodor et al., 2002; Márton et al., 2002; Jelen et al., 2006; Pavšič & Horvat, 2009; Markič et al., 2011; Nadór et al., 2012; Šram et al., 2015; Sachsenhofer et al., 2018). Slovenian part of the Mura-Zala Basin was earlier known as the Mura Depression (Grandić & Ogorelec, 1986; Djurasek, 1988; Royden & Horváth, 1988; Gosar, 1994/1995; Mioč & Marković, 1998; Hasenhüttl et al., 2001, Sachsenhofer et al., 2001), while the Hungarian part was termed as the Zala Basin. This integration of the Mura Depression and the Zala Basin in the last twenty years was based on the above cited regional geologic, stratigraphic, tectonic, geophysical and paleomagnetic studies, and well confirmed by studying transboundary geothermal resources and management (e.g., Nadór et al., 2012). However, Mura Depression extends also to Croatia in a territory between the Mura and the Drava rivers where it is still termed as the Mura Depression (Barić et al., 1996; Saftić et al., 2003; Velić et al., 2012) and the Hrvatsko Zagorje Basin (Pavelić & Kovačić, 2018), respectively.

Tectonic structures of the Mura-Zala Basin in Slovenia characteristically consist of “antiforms” and “synforms” termed from NNW to SSE (Fig. 1): The South Burgenland Swell, Radgona Depression (or Sub-basin), Murska Sobota Massif (or High), Ptuj-Ljutomer Synform (or Ljutomer Depression), Ormož-Selnica Antiform (or Anticline) (Vončina, 1965; Djurasek, 1988; Mioč & Marković, 1998; Hasenhüttl et al., 2001, Sachsenhofer et al., 2001; Fodor et al., 2002). All these structures extend in a typical WSW-ESE direction. In the deepest “synform” structures, the thickness of Neogene sediments reaches 4 to extremely more than 5 km. A neighbouring basin to the Mura-Zala Basin is the WNW-ESE trending Drava Depression in N Slavonia in Croatia, also hosting numerous oil and gas fields (Saftić et al., 2003; Velić et al., 2012; and references therein). Along its depocenter, thickness of the Neogene sediments also reaches more than 5 km, extremely 6 km at Virovitica.

### Source rocks - based on previous studies

Barić et al. (1996) studied source rocks and hydrocarbon accumulations in the Croatian part of the Mura Depression. Based on studying sediments in two wells (Mura-1 and Mura-2, about 3.8 and 4 km deep) they concluded that in the Mura Depression of Croatia source rocks for natural wet gas and condensate are Lower Miocene – Eggenburgian silty marls and limy pelites. Hydrocarbons derived from thermally altered kerogen III organic facies with hydrogen index  $HI < 70 \text{ mgHC/gTOC}$ , having TOC contents mostly in a range of 0.5–1 wt % and maturity by vitrinite reflectance between 1 and 2 %  $R_0$ . The Eggenburgian source rocks being encountered at depths usually more than 3 km are up to 200 to 500 m thick. Next younger source rocks are Middle Miocene – mainly Sarmatian fine grained sediments (marlstones), but they are less spread than the Eggenburgian sediments, and up to 120 m thick. Their TOC content is 1–2 wt % and organic facies is characterized as the kerogen type II, therefore potentially gas and oil-prone. Sarmatian source rocks are in an oil window, not reaching the gas window, generating only oil.

Hasenhüttl et al. (2001) studied source rocks and generation of hydrocarbons of the whole Mura Depression in Slovenia using source rock analysis (organic carbon, Rock-Eval, gas chromatography, vitrinite reflectance) and numeric modelling techniques. They stated that most silty and marly Tertiary sediments of the Mura Depression in Slovenia ranging from Egerian/Eggenburgian to Upper Miocene host kerogen type III and are therefore gas prone. Oil-prone marly and silty sediments characterized by the kerogen type II organic matter occur in Lower Miocene (Egerian/Eggenburgian) strata in the Boč Anticline (Rogatec-1 well), in Karpatian sediments of the Radgona Depression (Šomat-1 well), and in Sarmatian sediments of the Ljutomer Depression (Ljutomer-1 well). TOC values in different hydrocarbons prone strata vary mostly in a range of < 0.5–1.5 wt %. In some strata they are somewhat greater. “Extreme” TOC contents of up to 4.1 wt % were measured in the Upper Miocene (?) brackish strata (marls, shales, sandstones, coals, coaly sediments). But these sediments are generally immature.

Hasenhüttl et al. (2001) finally concluded that the generation of hydrocarbons in different parts of the Mura Depression occurred during different time intervals. On the W (Maribor – Šomat – Benedikt – Radgona/Radkersburg – Pichla) and

on the SW (Boč), Karpatian sediments are over-mature, and hydrocarbons are interpreted to be most probably lost. Over-maturation was caused by the so-called “Karpatian heating event” in the mentioned areas with an estimated heat flow density of  $375 \text{ mW/m}^2$  (Sachsenhofer et al., 1998) and could be a consequence of a shallow hidden pluton (Sachsenhofer et al., 2001). Also, the present heat flow density is the highest and spatially the widest in the Maribor – Šomat – Benedikt – Radgona/Radkersburg – Murska Sobota area, reaching  $110\text{--}130 \text{ mW/m}^2$  (Rajver, 2018).

For the Ormož-Selnica Anticline, Hasenhüttl et al. (2001) measured hydrogen index (HI) to be below  $130 \text{ gHC/gTOC}$  for Lower Miocene sediments, and thus clearly showing the kerogen III type of organic matter and the gas prone-ness, respectively. In this area of the (present) Ormož-Selnica Anticline an early generation of hydrocarbons “probably” (Hasenhüttl et al., 2001) occurred in the Lower/Middle Miocene i.e., Karpatian/Badenian times as well, while the second hydrocarbon generation phase lasted from Middle/Late Miocene times to Early Pliocene (Hasenhüttl et al., 2001). According to the mentioned authors, the first phase of generation of hydrocarbons was probably caused by the heating event in Karpatian/Badenian (heat flow density about  $150 \text{ mW/m}^2$ ), while the second one due to deep burial in Late Miocene. The heating event was the most outstanding in the previously mentioned W area, while it ceased towards the E and the Ormož-Selnica Anticline, respectively. The present heat flow density in the Petišovci area is similarly  $110\text{--}130 \text{ mW/m}^2$  (Rajver, 2018a). From the maps of expected temperatures at different depths, it is evident that temperatures at a depth of 4 km exceed  $180 \text{ }^\circ\text{C}$  (Rajver, 2018 b) and at 2 km depth, they exceed  $100 \text{ }^\circ\text{C}$  (Rajver et al., 2016). Lisjak et al. (2011) cite temperature data for the upper hydrocarbon-bearing strata of the PDOGF in depths of 1240 to 1730 m in a range of  $62\text{--}80 \text{ }^\circ\text{C}$ .

As concluded by Hasenhüttl et al. (2001), the second phase terminated in the Pliocene times because of the basin inversion between the Donat and the Ljutomer Faults (Djurasek, 1988). Inversion of the basin, giving a rise of the Ormož-Selnica Anticline, is also evident by a typically slight convex structure of the Uppermost Panonian (“Pontian”) brown coal measures in the Lendava–Benica/Petišovci–Mursko Središće area (Markič et al., 2011).



Fig. 4. Left – steel cylinder for sampling natural gas (volume  $0.475 \text{ l}$ ; maximal pressure  $150 \text{ bar}$ ); Right – sampling of natural gas from the Pg-5 well (gas field Petišovci, photo: Tjaša Kanduč, August 2021).

### Sampling and methods – this study

Sampling of natural gas was performed in August and September 2021 at the gas station in Petišovci from wells Pg-5 and Pg-6 (deep gas) and in Dolina for well D-5 (shallow gas). Gas was collected with the use of steel cylinders (manufacturer: Swagelok, USA) as shown in Figure 4. Natural gas was sampled from the pipeline before entering the process of “cleaning” (removal of the other than methane components) under the (reduced) pressure of  $5 \text{ bar}$ . In fact (see Results and Discussion – last paragraph), also sampled with gas was condensate. Samples were then transferred to a  $12 \text{ ml}$  glass Labco ampoules fitted with a gas-tight septum using a vacuum line.

The isotopic composition of methane ( $\delta^{13}\text{C}_{\text{CH}_4}$ ) was determined using a Europa 20-20 mass spectrometer in continuous flow isotope ratio mass spectrometer with ANCA-trace gas (TG) preparation module. For  $\text{CH}_4$  measurements,  $\text{CO}_2$  was first removed and then the  $\text{CH}_4$  was combusted over hot  $10 \text{ } \%$  platinum  $\text{CuO}$  ( $1000 \text{ }^\circ\text{C}$ ). The  $\text{CH}_4$  completely converted to  $\text{CO}_2$  was then analysed directly for the isotopic composition of carbon ( $\delta^{13}\text{C}$ ). Working standard with  $\delta^{13}\text{C}_{\text{CH}_4}$  value of  $-53.4 \text{ } \text{‰} \pm 0.1 \text{ } \text{‰}$  calibrated to International Atomic Agency (IAEA) reference material was used with known  $\delta^{13}\text{C}_{\text{CH}_4}$  values. The analytical precision for carbon isotope composition is estimated to be  $\pm 0.6 \text{ } \text{‰}$  for  $\text{CH}_4$ .

The relative difference of isotope ratios (also called relative isotope-ratio or delta values) has been reported using the short-hand notation  $\delta^{i/j}\text{E}$ . The isotope – delta value is obtained from isotope number ratios  $R(^i\text{E}, ^j\text{E})_p$  as follows (Brand et al., 2014):

$$\delta^{(i/j)E} = \delta^{i/j}E = \frac{{}^{i/j}R_p - {}^{i/j}R_{Ref}}{{}^{i/j}R_{Ref}} \quad (1)$$

Where  ${}^iE$  denotes the higher (superscript i) and  ${}^jE$  the lower (superscript j) atomic mass number of element E. The subscript P denotes the substance used to determine the respective values,  $R({}^iE, {}^jE)_p$  is isotope number – ratios.

A free web-based machine learning tool (Snodgrass & Milkov, 2020) was used to determine the origin of natural gases. The input geochemical parameters are:  $CH_4/(C_2H_6+C_3H_8)$ ,  $\delta^{13}C_{CH_4}$ ,  $\delta^2H_{CH_4}$ ,  $\delta^{13}C_{CO_2}$ , and  $\delta^2H_{CH_4}$ , and the output parameters are gas origin, confidence scores, model accuracy. In our study, the following input parameters were considered: for D-5 well  $C_1/C_{2+}$  ratio of 9.0 (90/10) and  $\delta^{13}C_{CH_4} = -38.6$  ‰, for Pg-5 well  $C_1/C_{2+}$  ratio of 7.72 (85/11) and  $\delta^{13}C_{CH_4} = -36.6$  ‰ and for Pg-6 well  $C_1/C_{2+}$  ratio of 7.72 (85/11) and  $\delta^{13}C_{CH_4} = -36.7$  ‰. The coding also works with reduced number of parameters.

At this stage of our investigation, we did not perform gas composition analyses. However, we included in our study some existing gas composition data as summarized in Lisjak et al. (1988) and Lisjak et al. (2011). A more recent chromatographic analysis using HRN EN ISO 6974-5: 2014 standardization was done by Žuvela (2019) from INA Zagreb. The data were kindly provided by the Petrol Geo company in Lendava.

## Results and discussion

Our results of analysed  $\delta^{13}C_{CH_4}$  values together with existing major gas components are summarized in Table 1. All samples are methane dominant up to 92 % ( $CH_4$ ). The “deep” natural gases from the Pg wells (Pg-1, Pg-3, Pg-5–Pg-9), which provide with gas the “CPP Lek pipeline” consist of about 85 % methane (C1), 11 % hydrocarbons heavier than methane (C2–C6) and of 4 %  $CO_2$  (Žuvela, 2019). The “shallow” gas contains more than 89 % methane, and up to 11 % C2–C6 gases, while the  $CO_2$  content is negligible (Lisjak et al., 1988; Lisjak et al., 2011). Also, according to personal communication with engineers of the Petrol Geo company,  $CO_2$  content is often detected (in few %) in the “deep” gases, while it is insignificant in the “shallow” gases. According to existing data, composition of gases in close hydrocarbon-bearing strata is stable. It varies within a range of around  $\pm 1.5$  % for the methane concentration. In this paper we attribute the concentrations as approximations for the isotopically studied “shallow” and “deep” gases in the wells D-5, Pg-5, and Pg-6 (Table 1).

If supposing in general a unique source rock and gas formation realm, isotope fractionation can be explained in a way that  $CO_2$  is heavier than  $CH_4$  which is more mobile and migrates easier upwards than  $CO_2$ . This effect quite often occurs in e. g. thick coal beds as for example in the Velenje lignite seam (Kanduč & Pezdič, 2005; Kanduč et al., 2021).

Table 1. Results of carbon isotopic composition of methane ( $\delta^{13}C_{CH_4}$ ) in D-5, Pg-5, and Pg-6 wells as measured for this study in 2021, approximate gas concentrations of methane (C1), C2–C6 gases, and carbon dioxide ( $CO_2$ ) after Lisjak et al. (1988) as average for “shallow” gas-bearing layers (Petišovci, Ratka, Paka), and one available datum considered in this preliminary study for deep gas-bearing layers (the Lek pipeline) (INA Zagreb; Žuvela, 2019 - for Petrol Geo, d.o.o.), and classification into genetic typology after Snodgrass & Milkov (2020).

| Well | Well-depth (m) | Gas-sampling depth (m) | Gas layer        | CH <sub>4</sub> (C1)           | C2-C6 | CO <sub>2</sub> | $\delta^{13}C_{CH_4}$ (‰) | Genetic type of gas in classification after Snodgrass & Milkov (2020)   |
|------|----------------|------------------------|------------------|--------------------------------|-------|-----------------|---------------------------|---|
|      |                |                        |                  | Approximate concentrations (%) |       |                 |                           |   |
| D-5  | 1575           | 1212–1250              | “Shallow” (Paka) | 89–92                          | < 11  | < 0.1           | -38.6±0.4                 | <b>Thermogenic</b> , confidence score: thermogenic = 84 %, secondary microbial: 14 %, abiotic: 2 %, <i>model accuracy: 91 %</i> |
| Pg-5 | 3324           | 2772–2795              | “Deep”           | 85                             | 11    | 4               | -36.6±0.2                 | <b>Thermogenic</b> , confidence scores: thermogenic: 84 %, abiotic 16 %, <i>model accuracy: 90 %</i>                            |
| Pg-6 | 3200           | 3102–3104              |                  |                                |       |                 | -36.7±0.6                 | <b>Thermogenic</b> , confidence scores: thermogenic: 98 %, second. microb.: 2 %, <i>model accuracy: 90 %</i>                    |

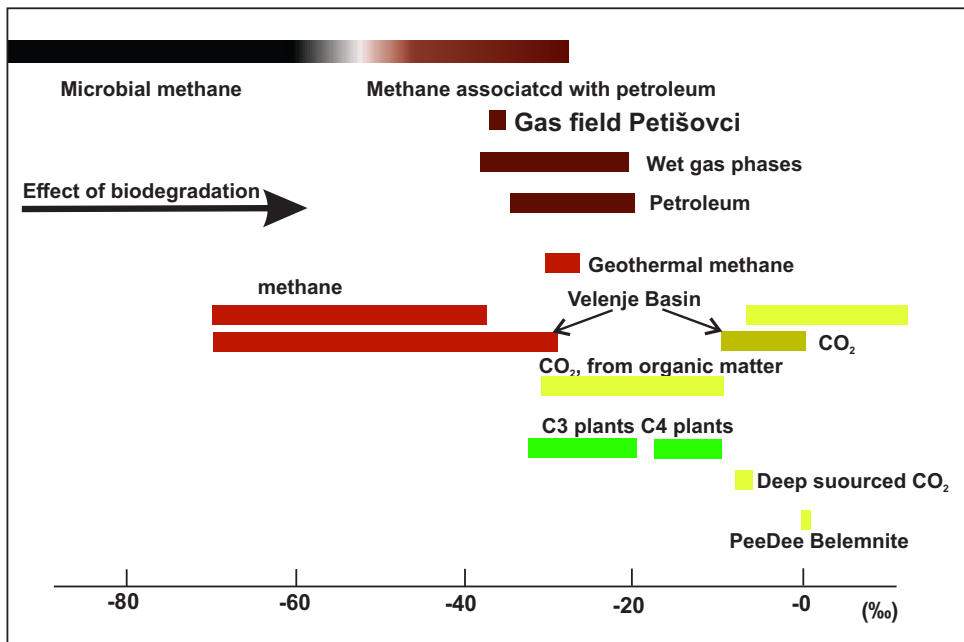


Fig. 5. Origin of methane from the Petišovci-Dolina oil and gas field (PDOGF) based on ranges of  $\delta^{13}C_{CH_4}$  values (‰) in diagram after Petroleum Geochemistry group CSIRO (2000).

The gas composition in terms of the methane (C1) versus all alkanes ( $\Sigma C_n$ ) ratio (from Tissot & Welte, 1984) around 0.89 (<0.98) is characteristic for both the shallow and deep wet gases generated during main stage of the catagenesis evolution.

The isotope signature of methane ( $\delta^{13}C_{CH_4}$ ) shows that the  $\delta^{13}C_{CH_4}$  values in the D-5, Pg-5 and Pg-6 wells range from -38.6 to -36.7 ‰. The “deep” gases from the wells Pg-5 and Pg-6 show very similar  $\delta^{13}C_{CH_4}$  values, -36.6 ‰ and -36.7 ‰, respectively, while the “shallow” gas around -38.6 ‰. In the diagram done by the Petroleum Geochemistry Group CSIRO (2000), the whole range of our isotopic values indicates the “methane associated with petroleum” (i.e., predominantly thermogenic origin) (Fig. 5).

Gas concentration from Table 1 and measured  $\delta^{13}C_{CH_4}$  were put in the “web-based machine learning tool” developed after Snodgrass and Milkov (2020) to decipher genetic type of gas (Fig. 6). The output data in Table 1 (the right-most column) are genetic type-origin of gases, confidence score and model accuracy in correspondence to revised genetic diagrams for natural gases (Milkov & Etiope, 2018). Methane to ethane plus propane ratio versus carbon isotopic composition of methane ( $\delta^{13}C_{CH_4}$ ) in the diagram after Milkov et al. (2020) (Fig. 6) shows clear thermogenic origin of investigated gas samples. Black dots refer to characterization of more than 20.000 natural gas samples all around the world from different geological habitats (Milkov & Etiope, 2018). Abbreviations CR, F, SM, LMT, EMT, and OA refer to different genesis processes of gas formation – see Milkov et al. (2020). Petišovci-Dolina (PDOGH) gas fall close

to the “oil-associated (mid-mature) thermogenic gas”, thus confirming their thermogenic origin.

The results show that the investigated natural gases are predominantly thermogenic in origin (Table 1). Almost entirely thermogenic is the “deep gas” from the Pg-6 well (98 % thermogenic, secondary microbial 2 %), while the deep gas from the Pg-5 is 84 % thermogenic, and 16 % abiotic. The “shallow” gas from the D-5 well is by confidence 84 % thermogenic, 14 % secondary microbial, and 2 % abiotic.

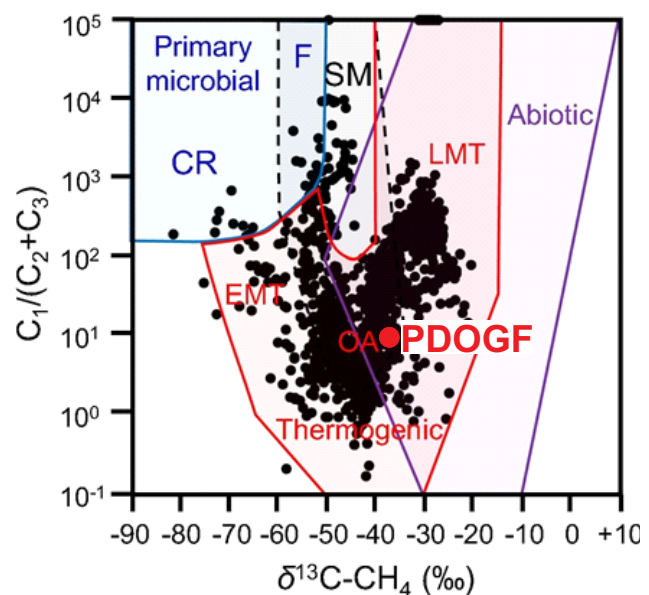


Fig. 6. Methane to ethane-plus-propane ratio ( $C_1/(C_2+C_3)$ ) versus carbon isotopic composition of methane ( $\delta^{13}C_{CH_4}$ ) plot after Milkov et al. (2020). Red circle (PDOGF) represents the Petišovci-Dolina gas samples. CR, F, SM, LMT, EMT, and OA refer to different genesis processes of gas formation – CR – CO<sub>2</sub> reduction (hydrogenotrophy), F – methyl-type (acetate) fermentation, SM – secondary microbial, EMT – early mature thermogenic gas, OA – oil-associated (mid-mature) thermogenic gas, LMT – late mature thermogenic gas.

At the present preliminary level of our knowledge, a question about the role and processes giving the shares of abiotic and secondary microbial gases, respectively, remains unanswered. Some artificial, un-natural effects of drilling are not excluded.

Methane from the “shallow” gas (D-5 well) has slightly more negative  $\delta^{13}\text{C}_{\text{CH}_4}$  value. This difference may be due to isotope fractionation due to migration from the primary reservoir, or possible mixing.

In Slovenia, based on research of natural gases and their dynamics in the last decades, it is interesting to compare results from different realms, e.g., from the Velenje lignite-bearing basin and the here studied from the PDOGF.

If we compare gas composition and  $\delta^{13}\text{C}_{\text{CH}_4}$  and  $\text{CO}_2$  from the PDOGF with free coalbed gas sampled from excavation fields from the Velenje lignite-bearing basin (Kanduč et al., 2021) we can conclude that they are completely different in origin. We found out in the Velenje basin that the major coalbed gas constituents were  $\text{CO}_2$ , methane, and nitrogen, while in the PDOGF natural

gas is by far predominantly composed of methane. Coalbed gas samples from excavation fields from the Velenje basin have gas concentration and isotopic values that reveal methane of biogenic origin and rarely thermogenic origin with  $\delta^{13}\text{C}_{\text{CH}_4}$  values of  $-69.4$  to  $-29.5$  ‰,  $\delta^2\text{H}_{\text{CH}_4}$  values of  $301.4$  to  $-221.9$  ‰, and a fractionation factor ( $\alpha_{\text{CO}_2-\text{CH}_4}$ ) of  $0.998$  to  $1.073$ , suggesting that methane derives from microbial acetate fermentation and  $\text{CO}_2$  reduction (Fig. 5). High  $\delta^{13}\text{C}_{\text{CH}_4}$  values (from  $-40$  ‰ to  $-29.5$  ‰) indicate thermogenic methane, which could be originated in shales forming pre-Pliocene basement of the Velenje Basin (Kanduč et al., 2021). The Carbon Dioxide Methane Index (CDMI) values ranged from  $50$  to  $98.3$  % and  $\delta^{13}\text{C}_{\text{CO}_2}$  values from  $-11.8$  to  $0.54$  ‰, indicating that  $\text{CO}_2$  is biogenic and endogenic in origin. In the PDOGF, the major gas component is methane with very low concentrations of  $\text{CO}_2$  and higher hydrocarbons (Table 1), and  $\delta^{13}\text{C}_{\text{CH}_4}$  reveals methane associated with petroleum – i.e., thermogenic gas (Figs. 5 and 6).

Our study clearly revealed that the gases in the PDOGF are prevailingly thermogenic in origin.

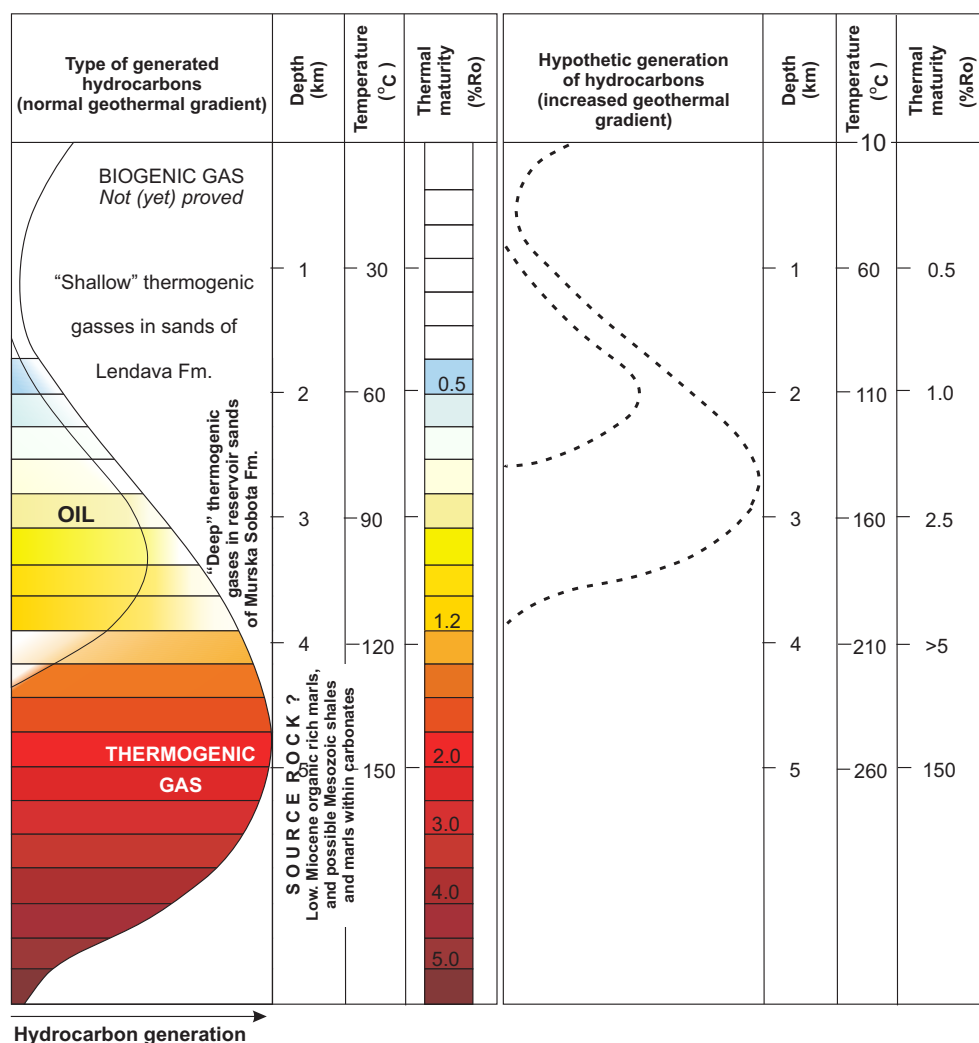


Fig. 7. Left – Generation of biogenic gas, oil, and thermogenic gas at a “normal” geothermal gradient of ca  $30$  °C/1km (Bjørlykke, K., 1989). Present occurrence of “shallow” thermogenic gases of the Lendava Formation (Upper Miocene) at the depth interval from  $1200$  to  $1750$  m, the “deep” thermogenic gases of the Murska Sobota Formation (Lower Miocene/Karpatian) from a depth of  $2.2$  km downwards to  $3.5$  km (and maybe more), and source of hydrocarbons are shown. Right – hypothetic generation of gases at a gradient of  $50$  °C/1km.

Due to increased geothermal gradient, between the normal 33 °C/km to nowadays ca. 50 °C/km (Rajver et al., 2018a, b), generation of hydrocarbons occurred at shallower depths than at normal gradients (Fig. 7). The Karpatian heat event did not most probably reach the Ormož-Selnica Anticline, and this effect of not too high maturity, and the alternation of porous and non-porous (impermeable) sediments as a trap was the reason that hydrocarbons were trapped and not lost.

According to Hasenhüttl et al. (2001), and Sachsenhofer et al. (2001) the gas was formed in the source rocks of the Lower Miocene Karpatian organic matter rich marls and shales. However, considering the source rocks studies in the Mura depression – Croatian part of Barić et al. (1996) and the Troškot-Čorbić's study from INA Zagreb (personal communication 2022), source rocks within the PDOGF could also be older than Karpatian, i.e., of the Eggenburgian age. Further stratigraphic investigations and correlations would be welcome to clarify this question. We suppose that the generated gas did not overcome a considerable migration from deeper to younger strata. Vitrinite reflectance measurements of organic clasts in the deepest shales and marls (Karpatian) (Sachsenhofer et al., 2001) showed maturity by vitrinite reflectance of up to 1.5 %Rr (Pt-5 well), extremely to 2.0 %Rr (Mg-6) (Sachsenhofer et al. (2001), while by Barić et al. (1996) in a range of 1.3–1.5 %Rr for the Eggenburgian shales and 2 %Rr for Mesozoic shales within carbonates. At a normal geothermal gradient of 33 °C/km this indicates a depth of about 4.5–5 km (Fig. 7 - left). Nowadays accumulations in Petišovci of hydrocarbons are at a depth of 1200 to 3500 m. If an increased geothermal gradient is considered, e.g., about 50 °C/km (Rajver, 2018 b) the depths of hydrocarbons generation would be considerably shallower (Fig. 7 – right). The vitrinite reflectance of source rock indicates transition to late catagenesis and thermogenic gases associated with condensates (LMT in Milkov et al, 2020). The gases are associated with condensates according to Schoell (1980, 1983, 1988), as well.

### Conclusion

Both the “deep” methane from wells Pg-5 and Pg-6 and shallow methane from the well D-5 have  $\delta^{13}\text{C}_{\text{CH}_4}$  values which clearly indicate thermogenic in origin. According to the Milkov's et al. (2020) diagram, the investigated gases are classified as “oil-associated (mid-mature) thermogenic gas”. Because the Petišovci area was gradually lifted into antiformal (Djurasek, 1988; Mioč and Mark-

ović, 1998) the initially formed gas might migrate via fractures upwards into reservoir sands termed as the “deeper” reservoirs (or “deeper” gases), and the “shallower” reservoirs (or “shallower” gases). Lower  $\delta^{13}\text{C}_{\text{CH}_4}$  value observed in D-5 is maybe due to migration from deeper to shallower gas reservoirs. We presume that migration paths were not very long.

Furthermore, based on available literature data, thermogenic gas in Petišovci was formed in source rocks within Lower Miocene (Karpatian or even older?) sediments composed mainly of marls and shales rich in organic matter. Measurements of the vitrinite reflectance of organic clasts in the deepest shales and marls (Sachsenhofer et al., 2001) showed maturity of up to about 1.5 %Rr, extremely to 2.0 %Rr.

If we consider a normal geothermal gradient a depth of about 4.5–5 km is inferred. The depths of hydrocarbons generation would be considerably shallower if the geothermal gradient is about 50 °C/km (Rajver, 2018 b).

During the reverse uplifting between the Donat and Ljutomer faults a system of fractures was formed enabling migration of hydrocarbons upwards from source rocks into numerous reservoir sandstones. Further study with taking more samples for isotopic (with deuterium in addition to carbon) and accompanying gas chromatographic analyses is continuing in 2022 to get better insight and more representative results of gas characterization and typology of gases generated and occurring within the Petišovci-Dolina oil and gas field.

### Acknowledgements

We thank for financial support from the state budget by the Slovenian Research Agency - Research programmes P1- 0025: Mineral resources, and P1-0143: Cycling of substances in the environment, mass balances, modelling of environmental processes and risk assessment.

Our great thanks go to the Petrol Geo d.o.o. company in Lendava, to engineers Štefan Hozjan and Daniel Pücko, who successfully enabled us and carried out the sampling. Without their professional approach and help this study could not be carried out.

Petrol Geoenergo d.o.o. company is highly appreciated for its final agreement to publish this study.

We sincerely thank two anonymous reviewers whose comments, suggestions and indications greatly improved the firstly submitted version of this article. For the final editing of this paper we are honestly grateful to Bernarda Bole and Vida Pavlica.

## References

- Babadi, M.F., Mehrabi B., Tassi F., Cabassi J., Pecchioni, E., Shakeri A. & Vaselli O. 2021: Geochemistry of fluids discharged from mud volcanos in SE Caspian Sea (Gorgan Plain, Iran). *International Geology Review*, 63/4: 437-452. <https://doi.org/10.1080/00206814.2020.1716400>
- Barić, G., Britvić, V. & Dragaš, M. 1996: Source rocks and hydrocarbon accumulations in the Mura Depression, Republic of Croatia. *Nafta*, 47/1: 25-34.
- Bjørlykke, K. 1989: *Sedimentology and Petroleum Geology*. Springer-Verlag, xii + 363 pp.
- Boreham C.J., Hope, J.M., Jackson, P., Davenport, R., Earl, K.L., Edwards, D.S., Logan G.A. & Krassay, A.A. 2004: Gas – oil source correlations in the Otway Basin, Southern Australia. In: Boulton, P. J., Johns, D.R. & Lag, S.C. (eds.): *Eastern Australian Basins Symposium II. Special Publication*, Petroleum Exploration Society of Australia: 603-627.
- Brand WA, Coplen TB, Vogl J., et al., 2014. Assessment of international reference materials for isotope-ratio analysis (IUPAC Technical Report)1. *Pure Appl. Chem.*, 86/3: 425-467.
- Brodarić, A. 1985: Biostratigrafska i kronostratigrafska interpretacija istražne bušotine Murski gozd-6 (Biostratigraphic and chronostratigraphic interpretation of the exploration well Murski Gozd-6; in Croatian, p.37 In: Čabrac, S. 1985: Bušotina Murski gozd-6; Konačni izvještaj (petrografske, biostratigrafske, petrofizičke i geokemijske karakteristike stijena) (Well Murski gozd-6; Final report (petrographic, biostratigraphic, petrophysical and granulometric characteristics of the rocks – in Croatian). INA-Naftaplin OOUR GIR, Služba za laboratorijska istraživanja. Arhiv INA, Zagreb in arhiv Geološkoga zavoda Slovenije, Ljubljana: 63 p.
- Buttitta, D., Caracausi, A., Chiaraluce, L., Favara, R., Morticelli, M.G. & Sulli, A. 2020: Continental degassing of helium in an active tectonic setting (northern Italy): the role of seismicity. *Scientific Reports*, 10: 162. <https://doi.org/10.1038/s411598-019-55678-7>
- Djurasek, S. 1988: Rezultati suvremenih geofizičkih istraživanja u SR Sloveniji (1985-1987) = Results of geophysical exploration in Slovenia (1985-1987) (in Croatian, Engl. abstract. *Nafta*, 39: 311-326.
- Dyman, T., S., Wyman, R- E., Kuuskraa, V. A., Lewan, M.D. & Cook, T.A. 2003: Deep natural gas resources. *Natural Resources*, 12: 41-56.
- Ercegovac, D.M. 2002: *Geologija nafte*. Rudarsko-geološki fakultet Univerziteta u Beogradu, DIT NIS Naftagas: 463 p.
- Flores, R.M. 2014: *Coal and Coalbed Gas*. Elsevier: 697 p.
- Fodor, L., Jelen, B., Márton, M., Rifelj, H., Kraljić, M., Kevrić, R., Márton, P., Koroknai, B. & Báldi-Beke, M. 2002: Miocene to Quaternary deformation, stratigraphy and paleogeography in Northeastern Slovenia and Southwestern Hungary. *Geologija*, 45/1: 103-114.
- Gosar, A. 1995: Modeliranje refleksijskih seizmičnih podataka za podzemno skladištenje plina v strukturah Pečarovci in Dankovci – Murska depresija = Modelling of seismic reflection data for underground gas storage in the Pečarovci and Dankovci structures – Mura depression; in Slovene with English abstract and summary. *Geologija*, 37/38(1994/95): 483-549.
- Grandić, S. & Ogorelec, B. (Coordinators) 1986: Plan in program raziskav ležišč nafte in plina v S.R.Sloveniji za obdobje 1986-1990. Knjige 1-6 (Plan and programme for geological exploration of natural oil and gas deposits in Slovenia for the period 1986-1990). Books 1-6 (in Slovene). Ljubljana, Zagreb, INA Projekt Zagreb, GZL-TOZD GGG, Archive GeoZS.
- Gratzer, R., Bechtel, A., Sachsenhofer, R.F., Linzer H.-G., Reischenbacher, D. & Schulz, H. M. 2011: Oil and oil-source rock correlations in the Alpine Foreland Basin of Austria: insights from biomarker and stable carbon isotope studies. *Marine and Petroleum Geology* 28, 1171-1186.
- Hasenhüttl, C., Kraljić, M., Sachsenhofer, R.F., Jelen, B. & Rieger, R. 2001: Source rocks and hydrocarbon generation in Slovenia = Mura Depression, Pannonian Basin. *Marine and Petroleum Geology*, 18: 115-132. [https://doi.org/10.1016/S0264-8172\(00\)00046-5](https://doi.org/10.1016/S0264-8172(00)00046-5)
- Jelen, B., Rifelj, H., Bavec, M. & Rajver, D. 2006: Opredelitev dosedanjega konceptualnega geološkega modela "Murske depresije". *Geološki zavod Slovenije*: 28 p.
- Kanduč, T. & Pezdič, J. 2005: Origin and distribution of coalbed gases from the Velenje basin, Slovenia. *Geochemical Journal*, 39: 397-409.
- Kanduč, T., Žula, J. & Zavšek, S. 2011: Tracing coalbed gas dynamics and origin of gases in advancement of the working faces at mining areas Preloge and Pesje, Velenje Basin. *RMZ – Materials and geoenvironment: periodical for mining, metallurgy, and geology*, 3: 273-288.

- Kanduč T., Sedlar, J., Novak, R., Zadnik, I., Jamnikar, S., Verbovšek, T., Grassa F. & Rošer J. 2021: Exploring the 2013-2018 degassing mechanism from the Pesje and Preloge excavation fields from the Velenje Coal Basin, Slovenia: insight from molecular composition and stable isotopes. *Isotopes in Environmental and Health Studies*, 57/6: 585-609. <https://doi.org/10.1080/10256016.2021.1981309>
- Kerčmar, J. 2018: Nahajališča zemeljskega plina na naftno-plinskem polju Petišovci = Natural gas reservoirs on the oil-gas field Petišovci.
- Lisjak, L., Sovilj-Legčević, J. Bokor, N. 1988: Naftno plinsko polje Petišovci – Elaborat o rezervama nafte i plina. = Oil and gas field Petišovci - Elaboration on reserves of oil and gas in Croatian. INA-Nafta Lendava.
- Lisjak, L., Horn, B. & Kraljič, M. 2011: Možnosti za geološko skladiščenje CO<sub>2</sub> v Sloveniji in izven Slovenije – Popis možnih lokacij za geološko skladiščenje v osiromašenih/opuščenih nahajališčih nafte/plina v Sloveniji z oceno skladiščne kapacitete (Professional report by Nafta Geoterm, ERICO, GeoZS, HGEM, NTF-OGR. Holding Slovenske elektrarne, TE Šoštanj, TE Trbovlje, Premogovnik Velenje.
- Markič, M., Turk, V., Kruk, B. & Šolar, S.V. 2011: Premog v Murski formaciji (pontij) med Lendavo in Murskim Središčem ter v širšem prostoru SV Slovenije = Coal in the Mura Formation (Pontian) between Lendava and Mursko Središče, and in the wider area of NE Slovenia (in Slovene; with Eng. abstract). *Geologija*, 54/1: 97-120. <https://doi.org/10.5474/geologija.2011.008>
- Markič, M. 2014: Zakaj nastopata zemeljski plin in nafta ravno na območju Lendave = Why natural gas and oil occur in the Lendava area – in Slovene. *Geološki zavod Slovenije - Bilten Mineralne surovine v letu 2013*: 122-138.
- Markič, M., Lapanje, A., Rajver, D., Rman, N., Šram, D. & Kumelj, Š. 2016: Geological evaluation of potential unconventional oil and gas resources in Europe – Evaluation of the potential in Slovenia: H2020 call, B.2.9. Energy policy support on unconventional gas and oil. *Geološki zavod Slovenije / Geological Survey of Slovenia*, 35 p.
- Márton, E., Fodor, L., Jelen, B., Márton, P., Rifelj, H. & Kevrić, R. 2002: Miocene to Quaternary deformation in NE Slovenia: complex paleomagnetic and structural study. *Journal of Geodynamics*, 34: 627-651.
- Milkov, A.V., Faiz, M. & Etiope, G. 2020: Geochemistry of shale gases from around the world: Composition, origins, isotope reversals and rollovers, and implications for the exploration of shale plays. *Organic Geochemistry*, 143. <https://doi.org/10.1016/j.orggeochem.2020.103997>
- Milkov, A. V. 2021: New approaches to distinguish shale-sourced and coal-sourced gases in petroleum systems. *Organic geochemistry*, 158: 104271.
- Milkov, A. V. & Etiope, G. 2018. Revised genetic diagrams for natural gases based on a global dataset of >20,000 samples. *Organic geochemistry*, 125: 109-120.
- Mineral Resources in Slovenia, 2020: Production of mineral commodities in Slovenia (2005 – 2019). *Bulletin, Geological Survey of Slovenia*, 16 p.
- Mioč, P. & Marković, S. 1998: Tolmač za list Čakovec. Osnovna geološka karta R Slovenije in R. Hrvaške. Inštitut za geologijo, geotehniko in geofiziko, Ljubljana in Inštitut za geološka istraživanja, Zagreb: 84 p.
- Nádor, A., Lapanje, A., Tóth, G., Rman, N., Szocs, T., Prestor, J., Uhrin, A., Rajver, D., Fodor, L., Murati, J. & Szekely, E. 2012: Transboundary geothermal resources of the Mura-Zala basin: a need for joint thermal aquifer management. *Geologija*, 55/2: 209-224. <https://doi:10.5474/geologija.2012.013>
- Ni, Y., Yao, L., Liao, F., Chen, J., Yu, C. & Zhu, G. 2021: Geochemical comparison of the deep gases from the Sichuan and Tarim basins, China. *Frontiers in Earth Science*, 1-22/9. <https://doi.org/10.3389/feart.2021.634921>
- North, F.K. 1985: *Petroleum Geology*. Allen & Unwin: 607 p.
- Pavelić, D. & Kovačić, M. 2018: Sedimentology and stratigraphy of the Neogene rift-type North Croatian Basin = Pannonian Basin System, Croatia: A review. *Marine and Petroleum Geology*, 91: 455-469. <https://doi.org/10.1016/j.marpetgeo.2018.01.026>
- Pavšič, J. & Horvat, A. 2009: Eocen, oligocen in miocen v osrednji in vzhodni Sloveniji = The Eocene, Oligocene and Miocene in Central and Eastern Slovenia. In: Pleničar, M., Ogorelec, B. & Novak, M. (eds.): *Geologija Slovenije = The Geology of Slovenia*. Geološki zavod Slovenije: 373 – 426.
- Petroleum geochemistry group, CSIRO. Internet: <http://www.dpr.csiro.au/rearesearch/erp/gcig.html>. Gas composition and isotope geochemistry. (cited 6/12/2000).

- Pleničar, M. 1954: Obmurska naftna nahajališča. *Geologija*, 2: 36-93.
- Rajver, D. 2018a: Surface heat-flow density. In: Novak, M. & Rman, N. (eds.): *Geological Atlas of Slovenia*. Geological Survey of Slovenia, 32-33.
- Rajver, D. 2018b: Expected temperatures at depths of 100 m and 4000 m. In: Novak, M. & Rman, N. (eds.): *Geological Atlas of Slovenia*. Geological Survey of Slovenia, 34-35.
- Rajver, D., Rman, N., Lapanje, A. & Prestor, J. 2016: Geotermalni viri Slovenije = Geothermal Sources of Slovenia – in Slovene. *Mineralne surovine v letu 2015*. Geološki zavod Slovenije, 137-147.
- Royden, L.H. & Horváth, F. 1988: The Pannonian Basin, a study in basin evolution. *Tulsa, Budapest, AAPG Memoir*, 45: 394.
- Sachsenhofer, R.F., Dunkl, I., Hasenhüttl, Ch. & Jelen, B. 1998: Miocene thermal history of the southwestern margin of the Styrian Basin: coalification and fission track data from the Pohorje/Kozjak area (Slovenia). *Tectonophysics*, 297: 11-29.
- Sachsenhofer, R.F., Jelen, B., Hasenhüttl, C., Dunkl, I., Rainer T. 2001: Thermal history of Tertiary basins in Slovenia (Alpine-Dinaride-Pannonian junction). *Tectonophysics*, 334: 77-99.
- Sachsenhofer, R.F., Popov, S.V., Čorić, S., Mayer, J., Misch, D., Morton, M.T., Pupp, M., Rauball, J. & Tari, G. 2018: Paratethian Petroleum Source Rocks - An Overview. *Journal of Petroleum Geology*, 41/3: 219-246.
- Saftić, B., Velić, J., Sztanó, O., Juhász, G. & Ivković, Ž. 2003: Tertiary Subsurface Facies, Source Rocks and Hydrocarbon Reservoirs in the SW Part of the Pannonian Basin (Northern Croatia and South-Western Hungary). *Geologia Croatica*, 56/1: 101-122.
- Schoell, M. 1980: The hydrogen and carbon isotopic composition of methane from natural gases of various origins. *Geochim. Cosmochim. Acta*, 44: 649-661.
- Schoell, M. 1983: Genetic characterization of natural gases. *Am. Assoc. Geol. Bull.*, 67: 2225-2238.
- Schoell, M. 1988: Multiple origins of methane in the earth. *Chem Geol.*, 71: 1-10.
- Sedlar, J., Kanduč, T., Jamnikar, S., Grassa, F. & Zavšek, S. 2014: Distribution, composition and origin of coalbed gases in excavation fields from the Preloge and Pesje mining areas, Velenje Basin, Slovenia. *International journal of coal geology*, 131: 363-377.
- Kerčmar, J. 2018: Natural gas reservoirs on the oil-gas field Petišovci (in Slovene, Engl. abstract). *Geologija*, 61/2: 163-176. <https://doi.org/10.5474/geologija.2018.011>
- Snodgrass, J.E. & Milkov, A.V. 2020: Web-based machine learning tool that determines the origin of natural gases. *Comput Geosci.*, 145: 104595.
- Šram, D., Rman, N., Rižnar, I. & Lapanje, A. 2015: The three-dimensional regional geological model of the Mura-Zala Basin, northeastern Slovenia. *Geologija*, 58/2: 139-154. <https://doi.org/10.5474/geologija.2015.011>
- Tissot, B.P. & Welte, D.H. 1984: *Petroleum Formation and Occurrence*. Springer-Verlag: 699 p.
- Toth, T. & Tari, G. 2014: Structural Inversion in Western Hungary and Eastern Slovenia: Their Impact on Hydrocarbon Trapping and Reservoir Quality. Internet: [https://www.searchanddiscovery.com/documents/2014/30387toth/ndx\\_toth.pdf](https://www.searchanddiscovery.com/documents/2014/30387toth/ndx_toth.pdf)
- Toth, T. & Tari, G. 2014: Structural Inversion in Western Hungary and Eastern Slovenia: Their Impact on Hydrocarbon Trapping and Reservoir Quality. *Geomega – from Ideas to Implementation – Ötletektől a Megvalósításig*. Internet: *Structural Inversions in Western Hungary and Eastern Slovenia: Their Impact on Hydrocarbon Trapping and Reservoir Quality*; #30387 (2014) (searchanddiscovery.com).
- Turk, V. 1993: Reinterpretacija kronostratigrafskih in litostratigrafskih odnosov v Murski udorini = Reinterpretation of chronostratigraphic and litostratigraphic relations in the Mura Depression (in Slovene). *Rudarsko-metalurški zbornik*, 40/1-2: 145-148.
- Velić, J., Malvić, T., Cvetković, M. & Vrbanac, B. 2012: Reservoir geology, hydrocarbon reserves and production in the Croatian part of the Pannonian Basin System. *Geologia Croatica*, 65/1. <https://doi.org/10.4154/GC.2012.07>
- Vončina, Z. 1965: Prikaz geotektonske rajonizacije Murske potoline. *Nafta*, 1: 1-3.
- Whiticar, M.J. 1994: Correlation of natural gases with their sources. In: Magoon, I. & Dow, W. (eds.): *The Petroleum System- From Source to Trap*. AAPG Memoir 60, 261-284.
- Whiticar, M.J. 1994: Correlation of natural gases with their sources. In: Magoon, I.B. & Dow, W.G. (eds.): *The Petroleum System – from Source to Trap*. AAPG Memoir, 60: 261-283.
- Więclaw, D., Bilkiewicz, E., Kotarba, M.J., Lillis, P.G., Dziadzio, P.S., Kowalski A., Kmiecik, N., Romanowski, T. & Jurek, K. 2020: Origin and secondary processes in petroleum in the

- eastern part of the Polish Outer Carpathians. *International Journal of Earth Sciences (Geol Rundsch)*, 109: 63-99. <https://doi.org/10.1007/s00531-019-01790-y>
- Žuvela, D. 2019: CPP Lek pipeline - Gas Chromatography Analyses and Hydrogen Sulfide and Mercaptans fluid Characterization. INA Zagreb (a report for Petrol Geo, Lendava): 4 p.
- Yang, S., Schulz, H.M., Schovsbo, N.H. & Bojesen-Koefoed, J. A. 2017: Oil – source rock correlation of the Lower Paleozoic petroleum system in the Baltic Basin (northern Europe). *AAPG Bulletin* 101, 1971-1993.
- Internet sources:
- Internet 1: <https://www.energetika-portal.si/> - Statistika – proizvodnja zemeljskega plina 1948-2019. R Slovenija – Ministrstvo za infrastrukturo – Portal energetika.
- Internet 2: <https://www.britannica.com/science/gas-reservoir>



# Rare earth elements and yttrium in cold mineral and thermal (~30–60 °C) waters from Tertiary aquifers in the Mura Basin, north-eastern Slovenia: A review

## Elementi redkih zemelj in itrij v hladnih mineralnih in termalnih (~30–60 °C) vodah iz terciarnih vodonosnikov Murskega bazena v severovzhodni Sloveniji: pregled dosedanjih raziskav

Polona KRALJ

Geological Survey of Slovenia, Dimičeva ulica 14, SI-1000 Ljubljana, Slovenia; e-mail: polona.kralj@geo-zs.si.

Prejeto / Received 3. 2. 2022; Sprejeto / Accepted 15. 7. 2022; Objavljeno na spletu / Published online 22. 07. 2022

*Key words:* Rare earth elements, Yttrium, Mineral waters, Thermal waters, Well cycling, Mura Basin

*Ključne besede:* elementi redkih zemelj, itrij, mineralne vode, termalne vode, prekomerno izkoriščanje vrtin, Murski bazen

### Abstract

Cold mineral and thermal waters from Tertiary aquifers in the Mura Basin mainly belong to the Ca-(Mg)-(Na)-HCO<sub>3</sub> and Na-HCO<sub>3</sub> hydrogeochemical facies, respectively, and the concentrations of yttrium (Y) and lanthanides or rare earth elements (REEs) are far below (10<sup>-2</sup> – 10<sup>-4</sup>) the abundances in the aquifer sediments. Mineral waters are high pCO<sub>2</sub>, and the plots of concentrations of YREEs normalised to Post Archean Australian Shale (PAAS) show fractionation of Y and heavy REEs (HREEs) over light REEs (LREEs), and a significant positive europium (Eu) anomaly. Thermal water from regionally developed aquifer Thermal I (recently also termed the Mura/Ujfalú Formation aquifer) shows a similar PAAS-normalised pattern with an obvious positive Eu anomaly and the tendency of enrichment with middle REEs (MREEs). The plots of PAAS-normalised YREE concentrations in thermal waters from the underlying low-permeability aquifers with poorly developed fracture porosity and abundant CO<sub>2</sub> are flat with insignificant positive Eu anomaly. The abundance and fractionation of YREEs in mineral and thermal waters seems to be mainly controlled by the presence of carbonate complexing ligands, permeability of the aquifers and the related time of water-rock interaction.

YREEs have been used for geochemical recognition of overexploitation of the Sob-1 well that yields mixed waters from Thermal I and the underlying low-permeability aquifers. The well overexploitation has resulted in continuous 30-to-80-minute changes in hydrodynamic pressure in Thermal I, and the related change in temperature and chemical composition of abstracted water. Leakage from clayey-silty layers rich in coal and organic matter has been recognised over a several-year time scale by increased abundances of total organic carbon (TOC), YREEs, gallium (Ga), thallium (Tl) and selenium (Se). PAAS-normalised plots of YREE concentrations have shown significant positive anomalies of samarium (Sm), terbium (Tb) and holmium (Ho) and indicate the YHREE complexing ligands could be, beside carbonate species, humic and/or fulvic acids.

### Izvleček

Hladne mineralne vode iz terciarnih vodonosnikov Murskega bazena večinoma pripadajo Ca-(Mg)-(Na)-HCO<sub>3</sub> ali Na-HCO<sub>3</sub> hidrogeokemičnemu faciesu, koncentracije itrija (Y) in lantanoidov oziroma elementov redkih zemelj (REE) pa so za faktor 10<sup>-2</sup> do 10<sup>-4</sup> nižje od vsebnosti v prikamnini vodonosnika. Za mineralne vode je značilen visok pCO<sub>2</sub>, grafi koncentracij YREE, normaliziranih na vsebnosti Po arhajskega avstralskega skrilavca (PAAS) pa kažejo na frakcionacijo, ki se odraža v sorazmerno višji vsebnosti Y in težkih REE (HREE) glede na lahke REE (LREE), ter na značilno visoko pozitivno evropijevo (Eu) anomalijo. Termalne vode iz vodonosnika Termal I, ki je razvit v globinah Murskega bazena, kažejo podobno grafično razporeditev na PAAS normaliziranih koncentracij YREE z jasno izraženo pozitivno Eu anomalijo in težnjo po obogatitvi s srednjimi REE (MREE). Grafi na PAAS normaliziranih koncentracij YREE v termalnih vodah iz vodonosnikov, ki leže pod Termalom I in ki imajo nizko prepustnost in slabo razvito razpoklinsko poroznost ter so bogati s plinom CO<sub>2</sub>, pa so bolj ravni s komaj zaznavno pozitivno Eu anomalijo. Vsebnosti in frakcionacija YREE v mineralnih in termalnih vodah je najverjetneje odvisna od prisotnosti karbonatnih ligandov, prepustnosti vodonosnika in časa interakcije vode in prikamnine.

YREE so se izkazale kot dober pokazatelj prekomernega izkoriščanja vrtine Sob-1, kjer so bile zajete vode iz Termala I in slabo prepustnih vodonosnikov pod njim. Prekomerno izkoriščanje vrtine je imelo za posledico zvezno ciklično spreminjanje hidrodinamičnega tlaka v Termalu I, s hkratnim spreminjanjem temperature in kemijske sestave vode v časovnih intervalih 30-80 minut. Izcejanje iz glinasto-meljastih plasti bogatih z lečami premoga in organske snovi smo zaznali v časovnem obdobju več let kot povečanje vsebnosti celokupnega organskega ogljika (TOC), YREE, galijs (Ga), talijs (Tl) in selena (Se). Grafi na PAAS normaliziranih koncentracij YREE so pokazali visoke pozitivne anomalije samarijs (Sm), terbijs (Tb) in holmij (Ho) in kažejo, da so bile poleg karbonatnih ligandov v kompleksnih spojinah YHREE najverjetneje pomembne tudi huminske in/ali fulvične kisline.

## Introduction

The series of lanthanides or rare earth elements (REEs) and yttrium (Y) - here abbreviated as YREEs, have been recognised exceptionally important in various aspects of hydrogeochemical research. The early studies refer to marine waters and hydrothermal vents associated with mid-ocean spreading centres (Elderfield & Greaves, 1982; DeBaar et al., 1985; 1988; Klinkhammer et al., 1994; Bau & Dulski, 1999; Douville et al., 1999; 2002) while in continental areas, the abundances of REEs were first investigated in thermal waters in France and the Himalayas (Michard & Albarède, 1986; Michard et al., 1987; Michard, 1989). REEs have been used as geochemical tracers in several studies of groundwater regional flow and mixing (e.g., Johannesson et al., 1996; 1997; 2000; 2005; Dia et al., 2000; Tweed et al., 2006; Möller et al., 2007; Biddau et al., 2009; Yuan et al., 2014; Liu et al., 2017), exploration of power-producing geothermal systems and identification of potential high-level nuclear waste repositories (Möller, 2000; Shannon et al., 2001; van Middlesworth & Wood, 1998; Möller et al., 2003; Wood, 2006). During the past four decades the potential of REEs as environmental pollutants exponentially increased as they have become indispensable in several sectors of modern industry such as clean-energy, electronics or military, and have been utilised in a number of medical, agricultural and zootechnical applications (e.g., Möller et al., 2000; Kulaksiz & Bau, 2011; Hissler et al., 2014; Gonzales et al., 2014; Hatje et al., 2016; Nigro et al., 2018; Aide, 2018; Ladonin, 2019).

The utility of REEs as geochemical tracers is based on their conservative behaviour in many natural systems although several processes related to the REE aqueous chemistry can cause their fractionation. The most important are solubility and precipitation of REE hosting minerals, REE chemical speciation and complexation in solution and on mineral surfaces, ion distribution in the electric double layer attached to mineral surfaces, the changes in pH, redox conditions and

temperature of the aqueous medium, and hydrogeological factors such as flow pathways or residence time (Brookins, 1989; Wood, 1990; Drever, 1997; Möller, 2000). Furthermore, while REEs exist mostly in trivalent state, europium  $\text{Eu}^{3+}$  and cerium  $\text{Ce}^{3+}$  can be reduced or oxidised to  $\text{Eu}^{2+}$  and  $\text{Ce}^{4+}$ , respectively (Sverjensky, 1984; Smedley, 1991; Bilal, 1991; Bau, 1991; 1999; Johannesson et al., 1996; Liu & Byrne 1998). REEs, especially heavy rare earth elements (HREEs), are known for their affinity to form strong solution complexes with carbonate ions and are commonly relatively enriched in  $\text{CO}_2$ -rich cold mineral or thermal waters although surface complexation can reduce their abundance in solution (Cantrell & Byrne, 1987; Lee & Byrne, 1993; Michard et al., 1987; Guo et al., 2005; Shand et al., 2005).

Absolute concentrations of REEs are highly variable in natural waters and they are customary displayed as plots of normalised values on a logarithmic scale versus atomic number or ionic radius on a linear scale (Coryell et al., 1963). Yttrium is plotted at about the position of holmium (Ho). Commonly used datasets for normalisation are C1-chondrite (Anders & Grevesse 1989) and Post Archean Australian Shale (PAAS, McLennan, 1989) as the use of such reference materials enables easy comparison of large number of analyses worldwide. Recently, an improved data set for the European Shale has been proposed for environmental studies in Europe (Bau et al., 2018). Sometimes reservoir rocks are used in order to obtain more specific information on water-rock interaction, pathways of flow or mixing of waters.

In Slovenia, the first study on REE abundances in natural waters has been related to thermal and mineral waters in the Mura Basin, north-eastern Slovenia (Kralj & Kralj, 2000a), and up to the present, an upgraded and extended research of this topic has been the only available source of data (Kralj & Kralj, 2000b; 2009; 2012; Kralj, 2001; 2004a). In the end of the year 2021, a common Slovenian-Austrian project on geochemistry of water and stream sediment of the river Mur started (<https://www.geo-zs.si/index.php/projekti/drugi-projekti>;

[unileoben.ac.at/en/news](http://unileoben.ac.at/en/news)). The project has been termed MURmap, and the research is focused on classical heavy metal (HM) pollutants and technology-critical elements (TCEs), including YREEs. Therefore, a need for critical review of state-of-the-art of research of YREEs in natural waters and sediments in north-eastern Slovenia occurred, and that is the primary aim of the present contribution.

North-eastern Slovenia forms a part of the Pannonian Mura Basin (Fig. 1) which has been known for centuries for sources of mineral and thermal water. During the past five decades, thermal water from a particular intergranular

aquifer named Thermal I (and recently also the Mura/Ujfalú Formation aquifer) has become a basis of economically important spa tourism in the area (Žlebnič et al., 1988a; b; Ravnik et al., 1992; Kralj, 1993; 1994; 1995; 2001; Rman, 2014; Szócs et al., 2018). Mineral waters are high  $p\text{CO}_2$  and belong to the  $\text{Na-Ca-HCO}_3$ ,  $\text{Ca-Na-HCO}_3$ ,  $\text{Ca-Mg-Na-HCO}_3$  or  $\text{Ca-Mg-(Na)-HCO}_3$  hydro-geochemical facies. The plots of PAAS-normalised concentrations of YREE in mineral waters are characterised by high positive Eu anomalies and the enrichment of heavy REEs (HREEs) over light REEs (LREEs), (Kralj & Kralj, 2000a).

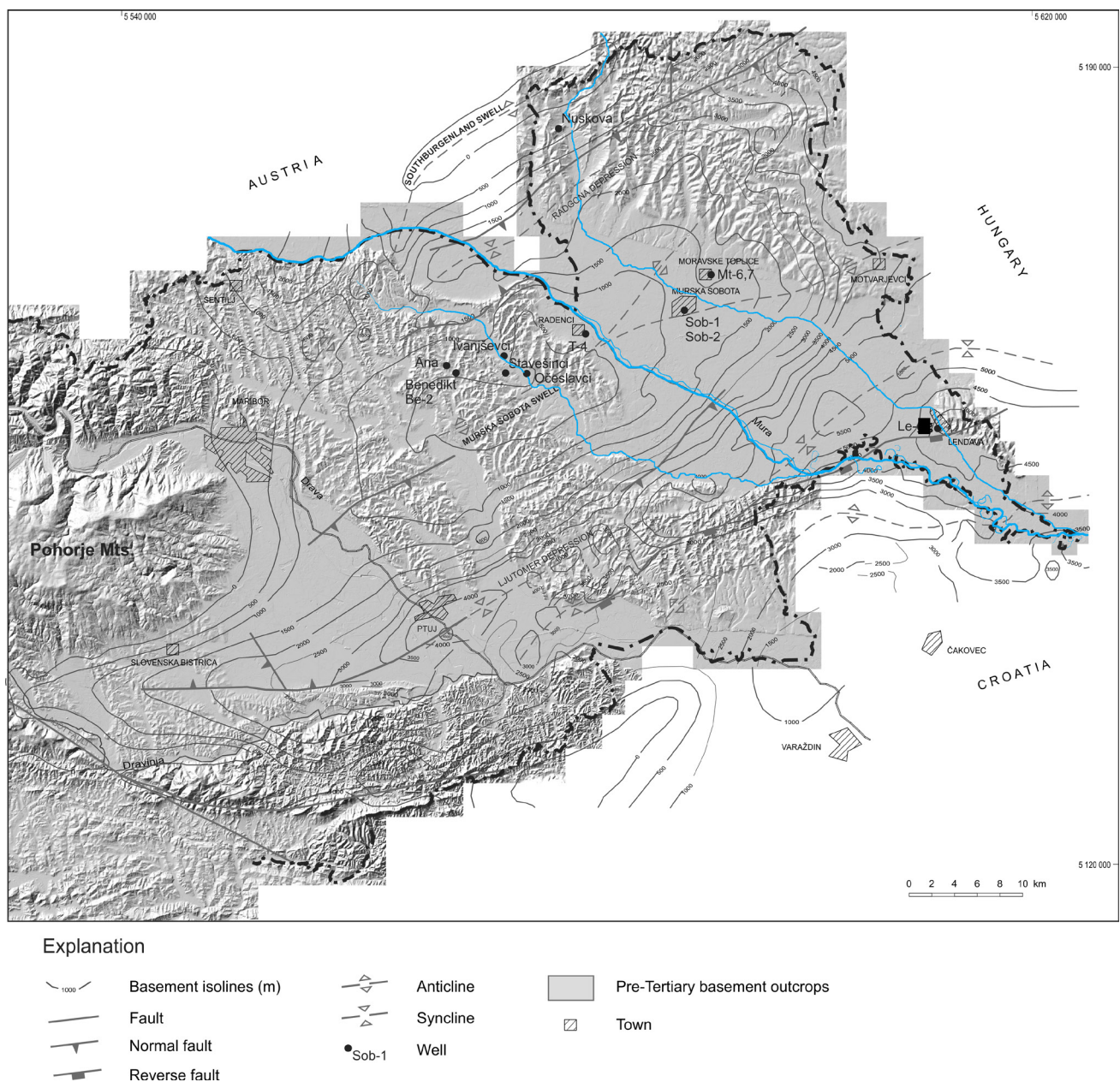


Fig. 1. Structural map of the Mura Basin and geographic position of the discussed geothermal wells, and springs and shallow drill-holes capturing mineral waters (modified after Rajver et al., 1994; Kralj & Kralj, 2000a; 2012). Recent geological models (e.g., Šram et al., 2015) use modified naming of geological structures in comparison to those listed in the present contribution.

Thermal waters are low- to medium-temperature (~30–60 °C) and essentially belong to the Na-HCO<sub>3</sub> hydrogeochemical facies. The abundances of YREEs and their PAAS-normalised patterns are not uniform, and for the water from Thermal I they resemble those of mineral waters. Thermal waters from poorly fractured aquifers in the Lendava, Haloze and Špilje Formations have higher concentrations of YREEs and their PAAS-normalised plots are flatter. From the wells Sob-1 and Sob-2, a mixture of thermal waters from Thermal I and several underlying low-yield aquifers in the Lendava Formation has been produced, and the plots of PAAS-normalised YREE concentrations are specific owing to temporal variations of chemical composition of abstracted mixture of thermal waters (Kralj, 2004a; b; Kralj & Kralj, 2009; 2012).

In the present contribution the significance of YREEs in recognition of water-rock interaction, well overexploitation and mixing of waters from various aquifers in the Tertiary sedimentary succession of the Mura Basin is discussed. Abundant analytical data, normalisation technique using various materials and its interpretation have been included in the article in order to serve as a basis for future studies of YREEs in natural waters and sediments in the Mura Basin and also broader, the catchment area of the river Mur.

### Analytical techniques

The measurements of pressure and temperature in the aquifer Thermal I were performed in the Sob-1 well simultaneously with, i) Amerada-type survey clock with mechanical temperature and pressure recorder, and ii) Leutert pressure-temperature gauge having a resolution of 0.007 bar and 0.01 °C, with measurements taken every 10 seconds and computer-managed data output. In the Sob-1 well, the measurements have been performed in the years from 1990 to 1999, at a depth of 600 m, four times a year in a period of one week. Since September 1995, the well-head water temperature ( $\pm 0.3$  °C), electrical conductivity ( $\pm 0.5$  % of the measured value), pH ( $\pm 0.1$  unit), redox potential Eh ( $\pm 0.3$  mV) and dissolved oxygen DO ( $\pm 0.5$  % of the measured value) were measured at the well-head using WTW MultiLine P3 pH/LF/Oxymeter portable instrument.

In the same week, water samples were collected from the well-head outflow using pre-cleaned polyethylene bottles of one-liter and two-decilitr volumes for the analysis of major ions and minor ions/elements, and trace elements, respectively. The bottles were rinsed three times with

the sampled water, and for the analysis of trace elements the samples were acidified by ultrapure HNO<sub>3</sub> (Merck) to pH<2 without prior filtration. After collection, the samples were sent immediately in the laboratories.

The major ions (Na<sup>+</sup>, K<sup>+</sup>, Ca<sup>2+</sup>, Mg<sup>2+</sup>, HCO<sub>3</sub><sup>-</sup>, Cl<sup>-</sup>, SO<sub>4</sub><sup>2-</sup>), minor ions/elements (F<sup>-</sup>, J<sup>-</sup>, Br<sup>-</sup>, NH<sub>4</sub><sup>+</sup>, Fe, Mn), the dissolved CO<sub>2</sub>-gas and total organic carbon (TOC) were determined in 95 samples. The concentrations of major cations were analysed by ion chromatography (IC). The concentration of bicarbonate was determined by potentiometric titration using 0.1 N HCl. The chloride and fluoride ions were analysed by IC and ion-selective electrode (ISE), respectively, and the bromide and iodide ions by Inductively Coupled Plasma Source Emission Spectroscopy combined with Mass Spectroscopy (ICP-MS). The charge balance between the sum of milliequivalent concentrations (meq/L) of major anions and cations

$$\left(\frac{\sum[\text{Anions}] - \sum[\text{Cations}]}{\sum[\text{Anions}] + \sum[\text{Cations}]}\right)$$

was assessed and the analyses with deviations of <5 % accepted.

Trace elements Li, Be, B, Al, Sc, Ga, As, Se, Rb, Sr, Tl, Y and REEs (along with V, Cr, Co, Ni, Cu, Zn, Zr, Nb, Mo, Ag, Cd, In, Sn, Sb, Te, Cs, Ba, Hf, Ta, W, Hg, Pb, Bi, Th and U that are not discussed in this paper) have been determined in 36 samples of thermal water from the Sob-1 well that were collected from May 1997 to June 1999. Trace elements were analysed in X-RAL Activation Services Inc., Ann Arbor, Michigan, the United States of America. The abundances of Y and REE were determined by ICP/MS (inductively coupled plasma source emission spectroscopy combined with mass spectroscopy) techniques without using any preconcentration method such as solid phase extraction, solvent extraction (e.g., Shannon & Wood, 2005) or coprecipitation with iron hydroxide (Zhu et al., 2010).

From June 1988 till December 1996, the samples of thermal water from the Sob-2 well have been collected in the same time period, and the sampling and analytical procedure performed in the same manner as for thermal water from the Sob-1 well. Major ions (Na<sup>+</sup>, K<sup>+</sup>, Ca<sup>2+</sup>, Mg<sup>2+</sup>, HCO<sub>3</sub><sup>-</sup>, Cl<sup>-</sup>, SO<sub>4</sub><sup>2-</sup>), minor ions/elements (F<sup>-</sup>, J<sup>-</sup>, Br<sup>-</sup>, Fe, Mn), the CO<sub>2</sub>-gas and total organic carbon (TOC) were determined in 53 samples. In October 1998 and June 1999, altogether 8 samples were collected for the analysis of major ions, minor ions/elements, the CO<sub>2</sub>-gas, TOC and trace elements including Y and REEs.

The same well-head measurements of water temperature, pH, Eh, conductivity and DO, and sampling procedure and analytical technique for determination of major ions, minor ions/elements, the gases CO<sub>2</sub> and H<sub>2</sub>S, TOC and trace elements as carried out for thermal water from the Sob-1 well were applied for thermal waters from the wells Le-2g and T-4, and mineral waters from shallow drill-holes/walled springs at Benedikt, Nuskova, Ivanjševci, Očeslavci, and Stavešinci. In each thermal well and drill-hole/walled spring 3 and 1 samples, respectively, were collected.

The abundances of major oxides and trace elements in Tertiary sediments including Y and REE were determined in ACME analytical Laboratories, Vancouver, Canada. The analysis of trace elements was performed using ICP/MS and XRF (X-ray fluorescence) techniques. Mineral composition of aquifer sediments was determined by X-ray diffraction analysis of powdered samples using Philips diffractometer PW 3719 and goniometer PW 1820 owned by the Department of Geology, Faculty of Natural Sciences and Technology, University of Ljubljana. Digital data were processed with peak-fitting program X'Pert HighScore Plus 4.0.

### Geological setting

The most important tectonic structure in north-eastern Slovenia is the Mura Basin (INA-Projekt Zagreb & Geološki zavod Ljubljana, 1991) which has been also considered as a part of much larger structural complexes of the southern Pannonian Basin System, namely, of the Mura-Zala Basin (sensu Fodor et al., 2002; Jelen et al., 2006) and the Zala-Drava Basin (e.g., Royden, 1988; Malvić & Velić, 2011), respectively. In the west, the Mura Basin terminates along the Pohorje Mountains that belong to the Eastern Alps (Fig. 1) and deepens toward the east where it reaches maximum depths of over 4 km in some isolated compartments near the Slovenian-Hungarian border. The formation of the Mura Basin begun in Late Oligocene as a result of continental rifting and the following extension and subsidence along two fault zones, more specifically, the Raba Fault in the north and the Ljutomer Fault in the south. The faults have regional extent and they evolved into the Radgona-Vas and Haloze-Ljutomer-Budafa sub-basins (Fodor et al., 2002; Márton et al., 2002; Jelen & Rifelj 2011). The sub-basins have been separated by the Murska Sobota Swell (INA-Projekt Zagreb & Geološki zavod Ljubljana, 1991).

Pre-Tertiary basement of the Mura Basin consists of Paleozoic metamorphic rocks, Upper Carboniferous and Lower Permian sedimentary deposits, and rare erosional remnants of Triassic dolomite and limestone (Koščec & Jovanović, 1968). The oldest Neogene deposits are Oligocene fluvial-limnic and Lower Badenian marine deposits, and the successions are united in the Haloze Formation. Sarmatian to Early Pannonian depositional environment was brackish. Sarmatian deposits are developed as well compacted and partially lithified sand, silt, clayey silt and marl, and Lower Pannonian sediments are dominated by silt, siltstone, fine-grained sand and marl. The successions are united in the Špilje Formation (Rijavec et al., 1985; Jelen et al., 2006). During Late Miocene, the Mura Basin became a part of extensive Lake Pannon. The environment gradually changed from brackish to freshwater owing to its isolation from Western Paratethys and advance of fluvial systems draining the Eastern Alps (Rijavec et al., 1985; Piler et al., 2007; Kováč et al., 2017). Deltaic systems developed and fine-grained turbidites fed from delta slopes form the Middle Pannonian to Lower Pontian Lendava Formation. Delta front and delta plain deposits are united in the Upper Pannonian to Upper Pontian Mura Formation. The overlying Dacian and Romanian deposits are related to the systems of alluvial fans and braided rivers (Kralj, 2010), and the successions are united in the Ptuj-Grad Formation (Jelen & Rifelj 2011; Nádor et al., 2012; Šram et al., 2015). Some 3 My ago, alkali basaltic volcanism occurred in the vicinity of the South Burgenland Swell and produced a variety of volcanic and mixed volcanoclastic-fluvial deposits (Pleničar, 1968; Kralj, 2010).

Cold mineral waters spring out along the margins of the Radgona Depression at the place of Benedikt and the village of Nuskova (Fig. 1), and in the Ščavnica valley (Stavešinci, Ivanjševci, Očeslavci) just above the westernmost extending of the Murska Sobota Swell (e.g., Kralj & Kralj, 2000; Gabor & Rman, 2016). In the area Badenian and Sarmatian deposits of the Haloze and Špilje Formations outcrop, and deep-seated faults enable uplift of the CO<sub>2</sub>-gas from pre-Tertiary basement.

In the Mura Basin, thermal aquifers occur in pre-Tertiary basement, and in Haloze, Špilje, Lendava, Mura and Ptuj-Grad Formations (Fig. 2), (Kralj, 2001; Nádor et al., 2012; Šram et al., 2015). Pre-Tertiary aquifers are commonly fractured or cavernous. In the deepest confined and semi-confined compartments brines of essentially Na-Cl composition prevail, and in some

shallower carbonate aquifers thermal waters of the Na-HCO<sub>3</sub>, Na-HCO<sub>3</sub>-Cl or Na-SO<sub>4</sub>-HCO<sub>3</sub> hydrogeochemical facies have been encountered (Kralj, 1993; 1994; Kralj & Kralj, 2000a). In the Haloze and Špilje Formations low-permeability thermal aquifers occur and chemical composition of waters depends on their depth and paleoenvironmental conditions that locally enabled infiltration of younger fresh-waters. The amount of total dissolved solids commonly exceeds 10 g/L (Szocs et al., 2013) and the CO<sub>2</sub>-gas is common (INA-Projekt Zagreb & Geološki zavod Ljubljana,

1991; Kralj, 2001). In the Lendava Formation isolated aquifers occur (Szocs et al., 2013), the yield of thermal water is low, and the CO<sub>2</sub>-gas originating from lithospheric mantle (Bräuer et al., 2016) is abundant. The waters have high amount of total dissolved ions (TDI) that commonly exceeds 10 g/L, and they essentially belong to the Na-HCO<sub>3</sub> hydrogeochemical facies (Table 1, T-4). The concentrations of the Ca<sup>2+</sup>, K<sup>+</sup> and Mg<sup>2+</sup> may be much higher than in the waters from pre-Tertiary basement (Kralj & Kralj, 2000a; Szocs et al., 2013).

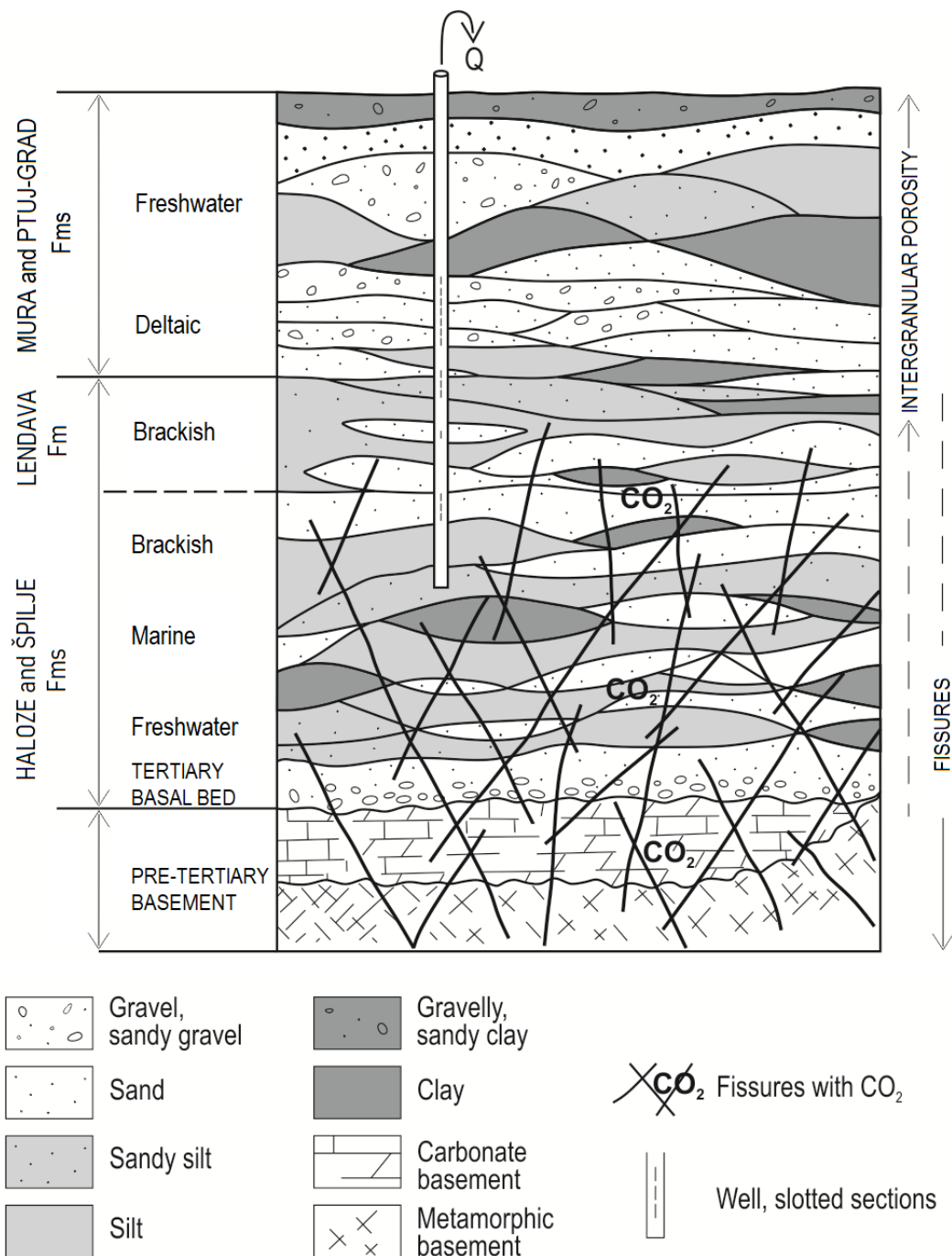


Fig. 2. Idealised model of sedimentary formations with thermal aquifers in the Mura Basin and a typical productive well capturing waters from several thermal aquifers (modified from Kralj, 2001). The names of formations are adopted from Jelen et al., 2006.

Table 1. Average chemical composition of thermal waters; major ions, minor ions/elements, dissolved CO<sub>2</sub>-gas, dissolved silica (SiO<sub>2</sub>), total organic carbon (TOC), total dissolved ions (TDI), pH, temperature of water at well-head (T<sub>wh</sub>) and yttrium and rare earth elements (YREEs). The wells T-4 (Radenci), Sob-1 and Sob-2 (Murska Sobota) and Le-2g (Lendava) tapped thermal aquifers in the Haloze, Špilje and Lendava Formations, Lendava and Mura Formations, and Mura Formation, respectively. For the Sob-1 and Sob-2, low-TDI and high-TDI indicate 30-to-80-minute variations of chemical composition (also referred as well cycling), and low and high pumping rate, respectively.

| Well                          |      | Le-2g* | Sob-1* | Sob-1<br>(low-TDI) | Sob-1<br>(high-TDI) | Sob-2* | Sob-2<br>(low-TDI) | Sob-2<br>(high-TDI) | T-4*   |
|-------------------------------|------|--------|--------|--------------------|---------------------|--------|--------------------|---------------------|--------|
| Average                       |      | 3      | 71     | 1                  | 1                   | 46     | 1                  | 1                   | 3      |
| Ion/Oxide/<br>Parameter       | Unit |        |        |                    |                     |        |                    |                     |        |
| Na <sup>+</sup>               | mg/L | 280    | 731    | 450                | 970                 | 653    | 300                | 1,100               | 2,087  |
| K <sup>+</sup>                | mg/L | 7.8    | 92     | 70                 | 105                 | 39     | 31                 | 52                  | 440    |
| Ca <sup>2+</sup>              | mg/L | 5.3    | 37.0   | 15                 | 71                  | 12.2   | 7                  | 18                  | 233    |
| Mg <sup>2+</sup>              | mg/L | 7.7    | 8      | 5                  | 7                   | 3.7    | 4.0                | 2                   | 147    |
| Fe                            | mg/L | 0.28   | 0.15   | 0.06               | 0.21                | 1.12   | 0.15               | 0.12                | 0.047  |
| Mn                            | µg/L | 9      | 13     | 6                  | 21                  | 8      | 7                  | 69                  | 72     |
| Br <sup>-</sup>               | mg/L | 0.11   | 0.61   | 0.45               | 0.92                | 0.9    | 0.41               | 1.52                | 0.80   |
| J <sup>-</sup>                | mg/L | <0.01  | 0.16   | 0.10               | 0.09                | 0.34   | 0.08               | 0.67                | 0.17   |
| F <sup>-</sup>                | mg/L | 0.53   | 0.78   | 0.45               | 0.75                | 1.40   | 0.20               | 0.55                | 0.84   |
| Cl <sup>-</sup>               | mg/L | 3.3    | 141    | 95                 | 175                 | 117    | 85                 | 180                 | 133    |
| HCO <sub>3</sub> <sup>-</sup> | mg/L | 856    | 2,214  | 1,500              | 2,900               | 1,645  | 960                | 2,600               | 7,633  |
| SO <sub>4</sub> <sup>2-</sup> | mg/L | 2      | 30     | 12                 | 48                  | 7      | 13                 | 2                   | 233    |
| CO <sub>2</sub>               | mg/L | 1      | 677    | 440                | 869                 | 303    | 88                 | 713                 | 1,476  |
| SiO <sub>2</sub>              | µg/L | 14     | 18     | 14                 | 19                  | 15     | 3                  | 26                  | 32     |
| TOC                           | mg/L | 2.4    | 2.5    | 2.5                | 2.0                 | 5.1    | 2.5                | 5.5                 | 2.3    |
| TDI                           | mg/L | 1,173  | 3,263  | 2,165              | 4,300               | 2,491  | 1,407              | 3,989               | 10,939 |
| pH                            |      | 7.30   | 7.0    | 6.81               | 6.85                | 7.9    | 7.02               | 6.78                | 6.85   |
| T <sub>wh</sub>               | °C   | 58.3   | 49.0   | 48.7               | 49.1                | 46.6   | 45.8               | 47.4                | 29.8   |
| La                            | µg/L | 0.03   | 0.19   | 0.04               | 1.09                | 0.06   | 0.02               | 0.14                | 0.39   |
| Ce                            | µg/L | 0.02   | 0.27   | 0.06               | 2.21                | 0.08   | 0.03               | 0.23                | 0.82   |
| Pr                            | µg/L | <0.01  | 0.04   | 0.01               | 0.27                | 0.02   | 0.01               | 0.05                | 0.11   |
| Nd                            | µg/L | 0.02   | 0.17   | 0.06               | 1.08                | 0.07   | 0.02               | 0.17                | 0.42   |
| Sm                            | µg/L | 0.03   | 0.11   | 0.05               | 0.21                | 0.10   | 0.04               | 0.21                | 0.18   |
| Eu                            | µg/L | 0.04   | 0.99   | 0.07               | 0.08                | 0.12   | 0.06               | 0.20                | 0.08   |
| Gd                            | µg/L | 0.03   | 0.08   | 0.03               | 0.24                | 0.08   | 0.02               | 0.16                | 0.19   |
| Tb                            | µg/L | 0.01   | 0.13   | 0.06               | 0.03                | 0.02   | 0.01               | 0.04                | 0.01   |
| Dy                            | µg/L | 0.03   | 0.05   | 0.04               | 0.13                | 0.06   | 0.02               | 0.09                | 0.16   |
| Y                             | µg/L | 0.03   | 0.29   | 0.10               | 0.75                | 0.10   | 0.03               | 0.19                | 0.79   |
| Ho                            | µg/L | <0.01  | 0.08   | 0.01               | 0.03                | 0.02   | 0.01               | 0.03                | 0.01   |
| Er                            | µg/L | 0.02   | 0.04   | 0.03               | 0.06                | 0.04   | 0.01               | 0.10                | 0.09   |
| Tm                            | µg/L | 0.01   | 0.01   | 0.01               | 0.01                | 0.02   | <0.01              | 0.03                | <0.01  |
| Yb                            | µg/L | 0.02   | 0.03   | 0.03               | 0.04                | 0.05   | <0.01              | 0.11                | 0.07   |
| ΣYREEs                        | µg/L | <0.30  | 2.48   | 0.60               | 6.23                | 0.84   | <0.28              | 1.75                | 3.32   |

\*data from Kralj, 2004a and Kralj & Kralj, 2009

The Mura Formation comprises a subsurface interconnected delta-front sand body that developed into thermal aquifer (Nádor et al., 2012; Šram et al., 2015; Tóth et al., 2016) locally termed Thermal I (INA-Projekt Zagreb & Geološki zavod Ljubljana, 1991; Ravnik et al., 1992; Kralj, 2001; Kralj & Kralj, 2012). In the Mura Basin Thermal I encompasses a subsurface area of about 1,372 km<sup>2</sup> (Kralj, 1995; Kralj & Kralj, 2000a, b;

2012; Kralj, 2001; Rajver et al., 1994) although it extends on the territory of Hungary, Austria, Slovakia and Croatia as a large transboundary thermal groundwater body (TTGWB) occupying a subsurface area of over 22,128 km<sup>2</sup> (Nádor et al., 2012; Szocs et al., 2013; Rman, 2014; Šram et al., 2015; Tóth et al., 2016; Rotár-Szalkai et al., 2017; Szöcs et al., 2018).

Thermal I outcrops in the west of the Mura Basin near the town of Radenci and deepens toward the east reaching a depth of over 1000 m at the Slovenian-Hungarian border. In general, the waters belong to the Na-HCO<sub>3</sub> hydrogeochemical facies, TDI commonly ranges from 1,000 – 1,500 mg/L, and free CO<sub>2</sub> is practically absent. Isotopic studies indicate the Pleistocene age of waters from the Mura Formation and the replacement of formation waters by infiltration has been assumed (Szocs et al., 2013). At greater basin's depths where Thermal I is underlain by thick deposits that still belong to the Mura Formation, the concentrations of the chloride ions are low

(Table 1, Le-2g). In places where the underlying deposits are thin and/or tectonically displaced, some thermal waters seem to have naturally admixed minor quantities of waters from the Lendava Formation, and as a result, the concentrations of the chloride ions are higher (Table 1, Sob-1 and Sob-2). In the Sob-1 and Sob-2 wells chemical composition of abstracted water has varied in time owing to the well overexploitation (Kralj & Kralj, 2000b; 2012). Recently, hydrogeochemistry, mixing of waters and well cycling and overexploitation during several-year period have been recognised by changes in the abundance of halide ions (Kralj & Kralj, 2020).

| Ion/Oxide/<br>Parameter       | Unit | Benedikt<br>Ana | Ivanjševci | Očeslavci | Stavešinci | Nuskova |
|-------------------------------|------|-----------------|------------|-----------|------------|---------|
| Na <sup>+</sup>               | mg/L | 51              | 104        | 685       | 162        | 276     |
| K <sup>+</sup>                | mg/L | 21              | 15         | 65        | 13         | 3       |
| Ca <sup>2+</sup>              | mg/L | 800             | 487        | 417       | 375        | 328     |
| Mg <sup>2+</sup>              | mg/L | 180             | 203        | 69        | 32         | 47      |
| Fe                            | mg/L | 7.2             | 6.7        | 1.2       | 2.7        | 0.9     |
| Mn                            | mg/L | 0.170           | 0.143      | 0.178     | 0.359      | 0.428   |
| J <sup>-</sup>                | mg/L | <0.01           | 0.02       | 0.21      | 0.05       | 0.02    |
| F <sup>-</sup>                | mg/L | 0.04            | <0.01      | 0.78      | 0.22       | 0.40    |
| Cl <sup>-</sup>               | mg/L | 3               | 7          | 170       | 25         | 32      |
| HCO <sub>3</sub> <sup>-</sup> | mg/L | 3,400           | 2,590      | 2,970     | 1,690      | 1,790   |
| SO <sub>4</sub> <sup>2-</sup> | mg/L | 23              | 2          | 118       | 19         | 68      |
| CO <sub>2</sub>               | mg/L | 1,830           | 2,500      | 3,800     | 3,300      | 3,300   |
| SiO <sub>2</sub>              | µg/L | 43              | 18         | 15        | 17         | 11      |
| TOC                           | mg/L | 1.3             | 0.9        | 0.8       | 0.6        | 0.9     |
| TDI                           | mg/L | 4,536           | 3,420      | 4,499     | 2,321      | 2,547   |
| pH                            |      | 6.37            | 6.22       | 6.22      | 6.02       | 6.00    |
| La                            | µg/L | 0.07            | 0.02       | 0.06      | 0.10       | 0.11    |
| Ce                            | µg/L | 0.14            | 0.01       | 0.01      | 0.15       | 0.19    |
| Pr                            | µg/L | 0.02            | <0.01      | <0.01     | 0.02       | 0.02    |
| Nd                            | µg/L | 0.08            | <0.01      | 0.09      | 0.12       | 0.10    |
| Sm                            | µg/L | 0.06            | <0.01      | 0.02      | 0.02       | 0.02    |
| Eu                            | µg/L | 0.17            | 0.21       | 0.04      | 0.08       | 0.03    |
| Gd                            | µg/L | 0.01            | 0.01       | <0.01     | 0.05       | 0.02    |
| Tb                            | µg/L | 0.01            | <0.01      | <0.01     | 0.01       | 0.01    |
| Dy                            | µg/L | 0.02            | <0.01      | 0.01      | 0.08       | 0.02    |
| Y                             | µg/L | 0.24            | 0.70       | 0.03      | 1.00       | 0.28    |
| Ho                            | µg/L | 0.01            | <0.01      | <0.01     | 0.02       | 0.01    |
| Er                            | µg/L | 0.03            | 0.01       | 0.01      | 0.07       | 0.04    |
| Yb                            | µg/L | 0.02            | <0.01      | <0.01     | 0.05       | 0.02    |
| ΣYREEs                        | µg/L | 0.87            | <1.03      | <0.32     | 1.84       | 0.86    |

Table 2. Chemical composition of mineral waters; major ions, dissolved CO<sub>2</sub>-gas, dissolved silica (SiO<sub>2</sub>), total organic carbon (TOC), total dissolved ions (TDI), pH and yttrium and rare earth elements (YREEs). Data from Kralj & Kralj, 2000.

## Rare earth elements and yttrium in cold mineral and thermal waters

### Cold mineral waters

Cold mineral waters belong to the Na-Ca-HCO<sub>3</sub>, Ca-Na-HCO<sub>3</sub>, Ca-Mg-Na-HCO<sub>3</sub> or Ca-Mg-(Na)-HCO<sub>3</sub> hydrogeochemical facies. The amount of total dissolved ions (TDI) is variable and ranges from about 2,300 mg/L to over 4,500 mg/L (Table 2). The waters are high pCO<sub>2</sub> and in the analysed samples, the amount of dissolved carbon dioxide ranges from 1,800 to 3,800 mg/L. The concentrations of the chloride and sulphate ions are generally low and the highest recorded were in the spring Očeslavci where they amounted to 170 mg/L and 118 mg/L, respectively. The content of YREE ranges from <0.32 µg/L to 1.84 µg/L and is not proportional to TDI or the amount of dissolved CO<sub>2</sub>-gas.

To compare YREE concentrations in cold mineral waters normalised to PAAS and aquifer sediment, Sarmatian calcareous siltstones, the Špilje Formation, from the well Be-2/03, Benedikt at a depth of 122–124 m, have been used (Kralj et al., 2009). The abundances of YREEs in the aquifer sediment show a proportional depletion with the increase in calcite present either as cement, microfossils or limestone lithic fragments (Table 3).

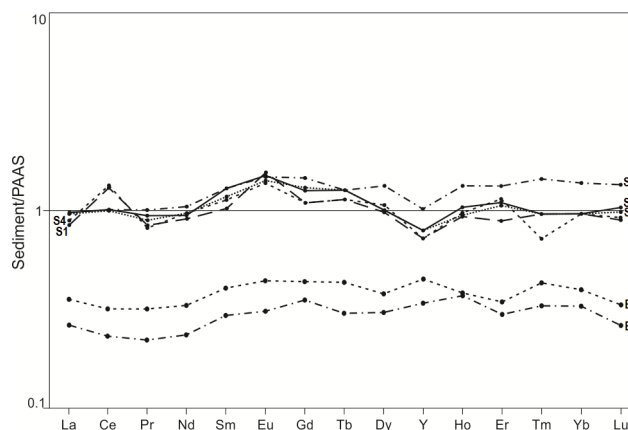


Fig. 3. The plots of PAAS-normalised YREE abundances in aquifer sediments from the wells Be-2/03, Benedikt (B1, B3) and Sob-1, Murska Sobota (S1–S5). For detailed information see Table 3.

The PAAS-normalised plots are alike (Fig. 3) but well below the shale abundance, and MREEs and HREEs are slightly fractionated over LREEs. The plots of YREE concentrations in mineral waters normalised to PAAS and to the average of 3 aquifer sediments do not differ significantly in the shape but only in the magnitude of about  $<10^{-1}$  (Fig. 4). They are characterised by fractionation of YHREEs over LREEs and a significant positive Eu anomaly, while Ce anomaly is absent or slightly negative.

Table 3. YREEs in aquifer sediments and PAAS (after McLennan 1989). B1–B3, Špilje Formation, the well Be-2/03, Benedikt; S1–S5, Mura and Lendava Formations, well Sob-1, Murska Sobota.

| Sample/<br>Well<br>Depth       | Sediment<br>Type                             | La   | Ce    | Pr   | Nd   | Sm   | Eu   | Gd   | Tb    | Dy   | Y    | Ho    | Er   | Tm    | Yb   | Lu    |
|--------------------------------|--|------|-------|------|------|------|------|------|-------|------|------|-------|------|-------|------|-------|
| <b>B1 Be-2/03</b><br>122–124 m | Siltstone<br>(30 wt.%<br>CaCO <sub>3</sub> ) | 10.0 | 18.3  | 1.94 | 7.9  | 1.6  | 0.33 | 1.62 | 0.23  | 1.40 | 9.0  | 0.36  | 0.83 | 0.13  | 0.90 | 0.11  |
| <b>B2 Be-2/03</b><br>122–124 m | Siltstone<br>(25 wt.%<br>CaCO <sub>3</sub> ) | 13.5 | 25.1  | 2.78 | 11.1 | 2.2  | 0.47 | 2.01 | 0.33  | 1.74 | 11.9 | 0.37  | 0.96 | 0.17  | 1.09 | 0.14  |
| <b>B3 Be-2/03</b><br>122–124 m | Siltstone<br>(8 wt.%<br>CaCO <sub>3</sub> )  | 31.8 | 63.1  | 7.05 | 27.9 | 5.6  | 1.10 | 4.73 | 0.64  | 4.16 | 20.8 | 0.81  | 1.95 | 0.25  | 2.10 | 0.33  |
| <b>S1 Sob-1</b><br>633 m       | Sand   | 32.9 | 106.0 | 7.6  | 31.6 | 5.8  | 1.72 | 5.2  | 0.9   | 4.7  | 20   | 0.95  | 2.6  | 0.4   | 2.8  | 0.40  |
| <b>S2 Sob-1</b><br>802 m       | Sand   | 38.4 | 81.0  | 9.1  | 36.1 | 7.4  | 1.93 | 6.9  | 1.0   | 6.4  | 28   | 1.35  | 3.9  | 0.6   | 4.0  | 0.60  |
| <b>S3 Sob-1</b><br>802 m       | Silt   | 37.6 | 80.9  | 8.6  | 33.7 | 6.7  | 1.56 | 6.2  | 1.0   | 4.8  | 22   | 0.96  | 3.1  | 0.4   | 2.8  | 0.44  |
| <b>S4 Sob-1</b><br>853 m       | Silty sand                                   | 34.4 | 109.0 | 7.4  | 33.8 | 6.4  | 1.52 | 5.2  | 0.9   | 5.1  | 20   | 0.99  | 3.0  | 0.3   | 2.8  | 0.41  |
| <b>S5 Sob-1</b><br>853 m       | Silt   | 38.2 | 82.3  | 8.5  | 32.8 | 7.3  | 1.67 | 6.0  | 1.0   | 4.8  | 22   | 1.05  | 3.2  | 0.4   | 2.8  | 0.46  |
| <b>PAAS</b>                    | Shale  | 38.2 | 79.6  | 8.83 | 33.9 | 5.55 | 1.08 | 4.66 | 0.774 | 4.68 | 27   | 0.991 | 2.85 | 0.405 | 2.82 | 0.443 |

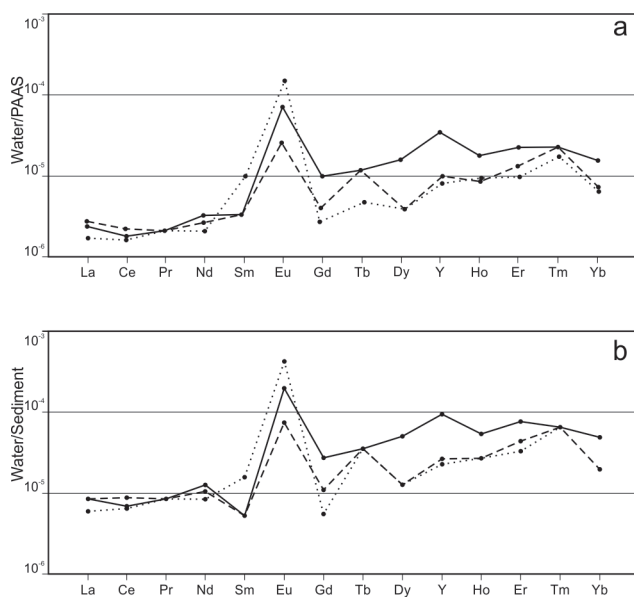


Fig. 4. a, The plots of PAAS-normalised YREE concentrations in mineral waters; b, The plots of concentrations of YREEs in mineral waters normalised to the average of 3 aquifer sediments from the well Be-2/03, Benedikt (122-124 m). Solid line – Stavešinci, dotted line – Ana (Benedikt), dashed line – Nuskova.

#### Thermal waters from the T-4, Le-2g, Sob-1 and Sob-2 wells

Thermal water from the T-4 well in the town of Radenci belongs to the Na-HCO<sub>3</sub> hydrogeochemical facies and is abstracted from a depth of 400–540 m in the Haloze and Špilje Formations. TDI and the dissolved CO<sub>2</sub>-gas amount to nearly 11 g/L and 1.5 g/L, respectively (Table 1), and the sum of YREE concentrations averages to 3.32 µg/L. The plots of PAAS-normalised YREE abundances in the water have shown that MREEs and YHREEs are slightly fractionated over LREEs, and there are very small negative Ce and moderate positive Eu anomalies (Fig. 5).

The well Le-2g in the town of Lendava penetrated Thermal I at a depth of 825–950 m and captures some underlying aquifers in the Mura Formation at a depth interval of 970–1,500 m as well. The water belongs to the Na-HCO<sub>3</sub> hy-

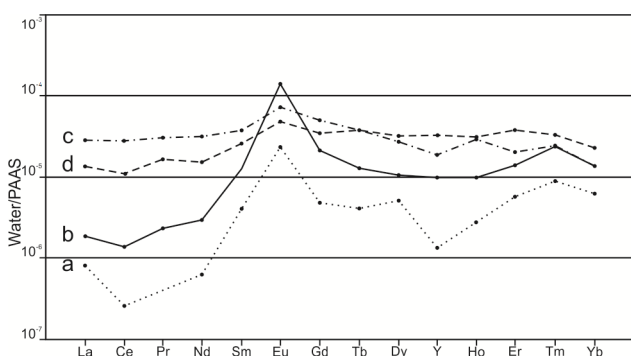


Fig. 5. The plots of PAAS-normalised YREE concentrations in thermal waters from the Mura Basin; a, Le-2g; b, Sob-1, low TDI; c, Sob-1, high TDI; d, T-4 (modified after Kralj, 2004a).

drogeochemical facies, TDI amounts to about 1.2 g/L and the dissolved CO<sub>2</sub>-gas is practically absent (Table 1). The sum of YREEs averages to < 0.28 µg/L, and the plots of PAAS-normalised values show small negative Ce and moderate positive Eu anomalies, and fractionation of MREEs and HREEs over LREEs (Fig. 5).

The wells Sob-1 and Sob-2 reached depths of 870.0 m and 855.8 m and tapped Thermal I at 600–646 m and 605–660 m, respectively, as well as some underlying aquifers in the Mura and Lendava Formations. The water belongs to the Na-HCO<sub>3</sub> hydrogeochemical facies, TDI ranges from <1.4 g/L to over 4.3 g/L and averages to 3.2 g/L and 2.5 g/L for the Sob-1 and Sob-2 well, respectively (Table 3). The amount of dissolved CO<sub>2</sub>-gas is variable and ranges from some 10 mg/L to over 1,500 mg/L (Kralj, 2001).

Chemical composition of thermal water from the Sob-1 and Sob-2 wells has been varying in time and often considerably deviated from the average (Table 1). In the Sob-1 well, hydrodynamic pressure and temperature in Thermal I have been commonly changing within the time interval of about 70–80 minutes, although during severe over-exploitation conditions, the intervals have been as short as 30–40 minutes. When the pressure in Thermal I increased, the temperature decreased, and vice versa. The maximum recorded difference in pressure and temperature is 0.8 bar and 2.5 °C, respectively. The changes are continuously reoccurring during the well operation, and for that reason, they have been arbitrarily termed well cycling and the time interval of 30–40 and 70–80 minutes a cycle (Kralj, 2004a; Kralj & Kralj 2009; 2012).

Chemical composition of abstracted thermal water varied with the changing temperature and hydrodynamic pressure as well. With the increase in temperature TDI, the amount of dissolved CO<sub>2</sub> and the concentrations of almost all major ions, minor ions/elements and trace elements including YREEs increased in nearly the same manner (Figs. 6, 7), (Kralj & Kralj, 2000a; 2012; Kralj, 2001). When hydrodynamic pressure in Thermal I increased and the temperature decreased, the composition of abstracted thermal water began to change toward lower TDI, lower amount of dissolved CO<sub>2</sub>, and lower concentrations of nearly all major ions, minor ions/elements and trace elements. As the abstracted water is a mixture supplied from Thermal I and the underlying aquifers in the Mura and Lendava Formations, the change in hydrodynamic pressure in the aquifers and the change in temperature and chemical composition of water indicates the changing supply from the aquifers.

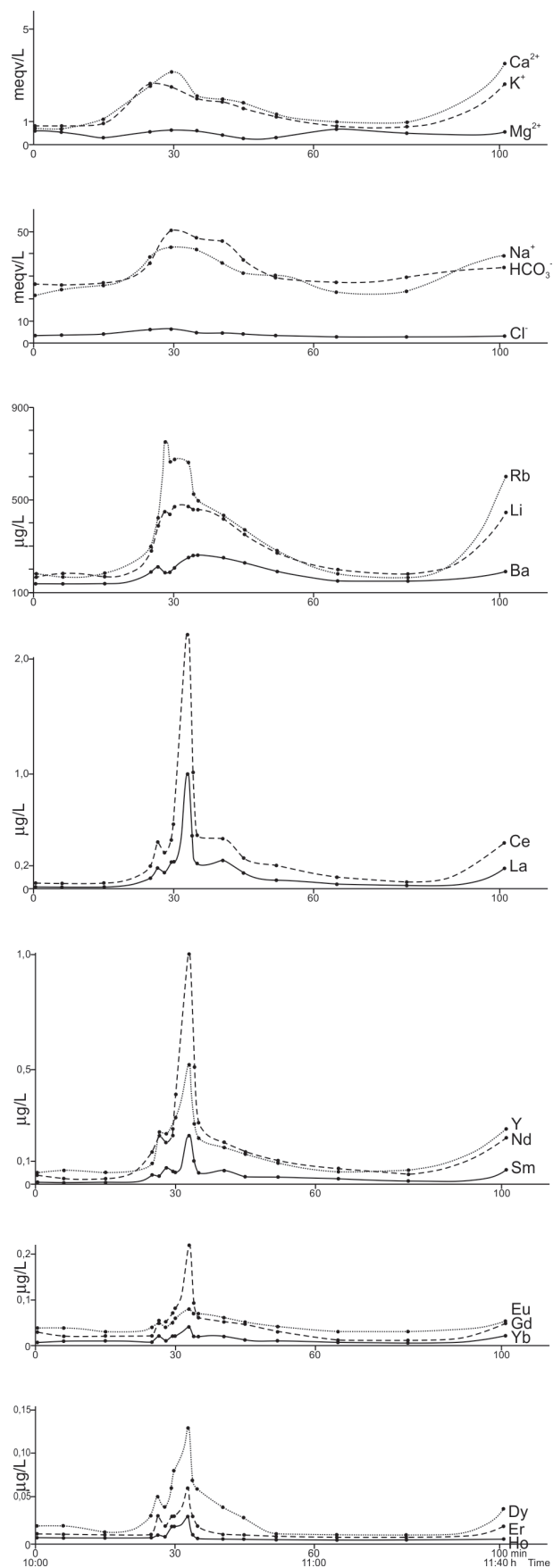


Fig. 6. Temporal variation of concentrations of some major ions, minor ions/elements, trace elements and YREEs in thermal water abstracted from the Sob-1 well on November 11, 1997, from 10:00 h to 11:43 h. The peak of concentrations correlates with the decrease in hydrodynamic pressure in Thermal I (data from Kralj & Kralj, 2000a; 2012).

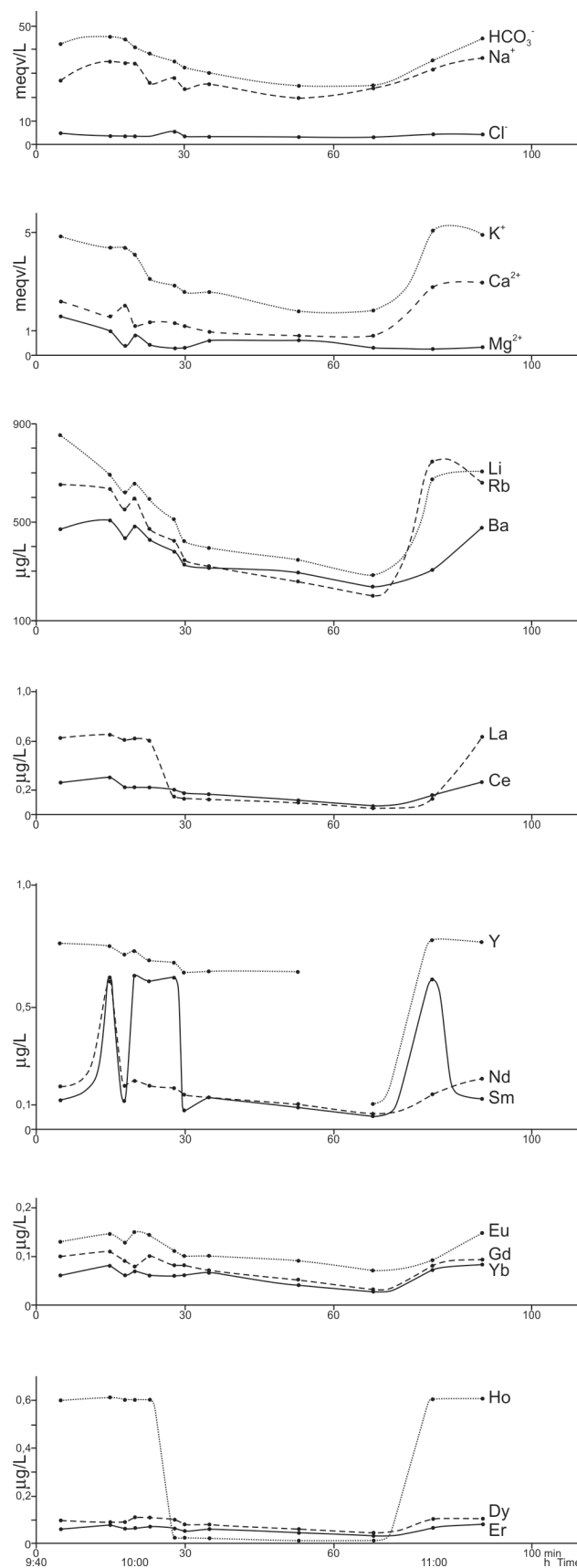


Fig. 7. Temporal variation of concentrations of some major ions, trace elements and YREEs in thermal water abstracted from the Sob-1 well on April 7, 1999, from 09:45 h to 11:10 h (data from Kralj & Kralj, 2000a; 2012).

In thermal water abstracted from the wells Sob-1 and Sob-2, the sum of concentrations of YREEs is, in general, relatively low. For water from Thermal I it amounts to  $<0.30 \mu\text{g/L}$  (Table 1; Le-2g and Sob-2, low TDI). The highest sum of  $6.23 \mu\text{g/L}$  has been recorded in water from the Sob-1 well, and the average for the Sob-1 and Sob-2 wells is  $2.48 \mu\text{g/L}$  and  $0.84 \mu\text{g/L}$ , respectively.

The concentrations of YREEs in thermal waters have been normalised to PAAS rather than the aquifer sediment (Table 3). YREE abundances in silty and sandy aquifer sediments from the Sob-1 well-core show some variations (Fig. 3) related to the grain-size and the amount of heavy minerals such as monazite, allanite and xenotime (Ce, Sm, Gd, Dy, Tb), or light minerals, in particular plagioclases (Eu). For that reason, the YREE abundances in the aquifer sediments normalised to PAAS commonly show positive Ce anomaly and positive fractionation of MREEs over HREEs. Yet, the abovementioned heavy minerals have very low solubility in water and therefore unlikely contribute significant amounts of YREEs in thermal water.

The PAAS-normalised YREE concentrations in thermal water from the Le-2g well (Fig. 5) and mixtures of waters from the Sob-1 and Sob-2 wells sourced from or dominated by Thermal I are characterised by fractionation of HREEs and to a lesser extent MREEs over LREEs, with slightly negative Ce and pronounced positive Eu anomalies. In mixed waters from the Sob-1 and Sob-2 wells having higher TDI (Fig. 5), MREEs are positively fractionated over LREEs and HREEs, and the Eu anomaly is moderately positive.

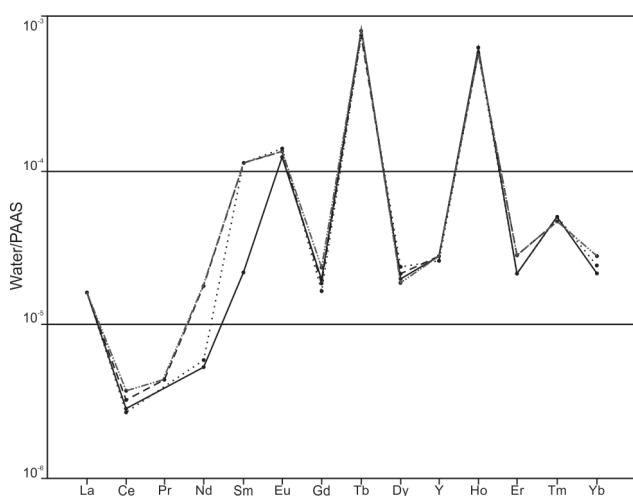


Fig. 8. The plots of PAAS-normalised YREE concentrations in low-TDI thermal water from the Sob-1 well sampled on October 28, 1998 (modified from Kralj & Kralj, 2009). Dotted line – sample taken at 13h 00 min; solid line – sample taken at 13h 35 min; dashed line – sample taken at 13h 45 min.

Similar trends can be seen for temporal variations in chemical composition of abstracted thermal water from the Sob-1 well sampled on October 28, 1998 (Fig. 8) and November 11, 1997 (Fig. 9). On April 7, 1999, the concentrations of YREEs were substantially increased and their PAAS-normalised plots show more pronounced negative Ce anomaly, very high positive Sm and Tb anomalies and very high and moderate positive Ho and Tm anomaly, respectively (Fig. 10).

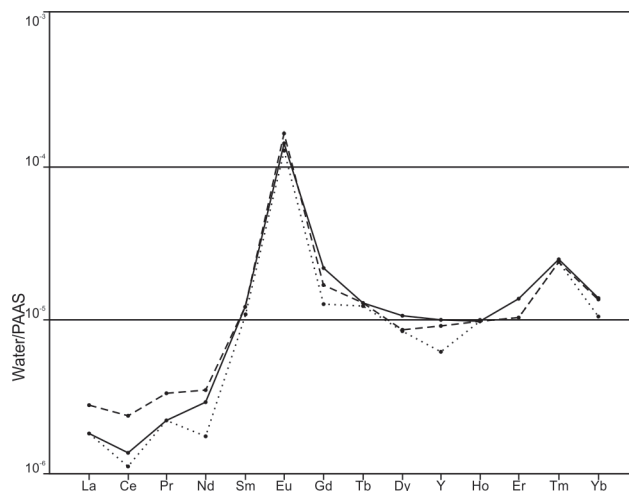


Fig. 9. The plots of PAAS-normalised YREE concentrations in high- (H) and low-TDI (L) thermal water from the Sob-1 well sampled November 11, 1997, from 12:57 h to 13:43 h (data from Kralj & Kralj, 2009). Dotted line – sample taken at 10h 26 min 30 sec; solid line – sample taken at 10h 28 min 45 sec; dashed line – sample taken at 10h 30 min 15 sec; dash-dotted line – sample taken at 10h 32 min 00 sec.

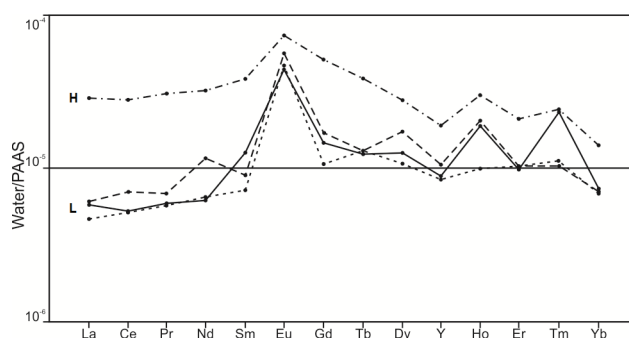


Fig. 10. The plots of PAAS-normalised YREE concentrations in high-TDI thermal water for the Sob-1 well sampled on April 7, 1999 (modified from Kralj & Kralj, 2009). Dashed line – sample taken at 9h 45 min; dash-dotted line – sample taken at 9h 55 min; solid line – sample taken at 9h 58 min; dotted line – sample taken at 10h 00 min.

## Discussion

Rare earth elements and yttrium analysed in mineral and thermal waters from Tertiary aquifers in the Mura Basin occur in concentrations far below ( $10^{-2}$  to  $10^{-4}$ ) the abundances in the aquifer sediments. The original idea of the present study was to identify similarities of the YREE

distribution patterns in water and aquifer sediment as they have been reported from various hydrological environments worldwide (e.g., Smedely, 1991; Gosselin et al., 1992; Johannesson & Lyons, 1996; Fee et al., 1992; Möller, 2000; Zhou et al., 2005; Möller et al., 2007). Yet, the normalisation to PAAS seems more convenient. The first reason is mineralogical and geochemical diversity of Tertiary sedimentary successions cold mineral and particularly thermal waters migrated through during their geochemical and thermal evolution. The second reason is carbonate type of waters that influences the solubility and complexation reactions of YREEs and is an important control of their fractionation (Lee & Byrne, 1993; Luo & Byrne, 2004; Guo et al., 2005).

In the areas of cold mineral water springs, Badenian and Sarmatian sediments of the Haloze and Špilje Formations outcrop. Their deeper compartments comprise low-permeability aquifers with waters of diverse hydrogeochemical facies varying inside the composition range of Na-Ca-K-Cl-HCO<sub>3</sub>-SO<sub>4</sub> (Kralj & Kralj, 2000a; 2012; Bräuer et al., 2016; Nádor et al., 2012). Deep waters and carbon dioxide ascend toward the surface through fault systems and mix with shallower groundwaters. Owing to the presence of carbon dioxide, the mixed waters undergo further geochemical change related to water-rock interaction. The resulting diverse major ion composition of mineral waters (Table 2) indicates rather individual evolution patterns.

The plots of YREE concentrations in cold mineral waters normalised to PAAS show fractionation of Y and HREEs (YHREEs) over LREEs, and positive Eu anomaly. The observed YHREE/LREE fractionation can be explained by the solubility and complexation of Y and REEs in carbonate waters as they increase with the increasing atomic number or smaller ionic radius (Lee & Byrne, 1993; Luo & Byrne, 2004; Guo et al., 2005). Positive Eu anomalies have been typically encountered in anoxic thermal waters (Michard & Albarède, 1986; Michard et al., 1987; Michard, 1989; Klinkhammer et al., 1994; Douville et al., 1999; 2002) as europium tends to be reduced to more soluble Eu<sup>2+</sup> state (Sverjensky, 1984; Bilal, 1991), and when in solution, the large Eu<sup>2+</sup> ion is not easily incorporated in precipitating minerals but commonly remains in solution and/or adsorbed onto mineral surfaces (Möller, 2000).

Low-temperature thermal water (30 °C) from the Haloze and Špilje Formations captured in the well T-4 at Radenci has relatively flat PAAS-normalised YREE pattern with insignificant posi-

tive Eu anomaly, although MREEs, Y and HREEs are fractionated over LREEs (Fig. 5). Thermal aquifers in the Haloze and Špilje Formations are characterised by very low permeability, the flow of fluids is slow, and the water-rock interaction times are much longer than in fractured aquifers of mineral waters.

Similar relationship can be recognised for thermal waters captured in the wells Le-2g, Sob-1 and Sob-2. The aquifer Thermal I has relatively well-developed intergranular porosity and good permeability. The plots of PAAS-normalised YREE concentrations in thermal waters captured or sourced from or mainly from Thermal I resemble, in general, those of cold mineral waters showing a distinct positive Eu anomaly and fractionation of MREEs and HREEs over LREEs (Fig. 5). For mixed waters with a higher proportion of waters from the Lendava Formation the YREE PAAS-normalised plots become flatter with a weak positive Eu anomaly and slightly acquired other MREEs, whilst the fractionation of HREEs over LREEs disappears. In the Lendava Formation the aquifers have similar characteristics as in the Haloze and Špilje Formations, carbon dioxide is abundant, the aquifer sediment and water are more equilibrated, and longer times of water-rock interaction enable LREEs to undergo complexation with carbonate ligands and enter the solution the last, after more soluble HREEs and MREEs.

The plots of PAAS-normalised YREE concentrations obtained for thermal waters produced from the Sob-1 well on April 7, 1999 (Fig. 10) differ from those typical for Thermal I or various mixtures with waters from the Lendava Formation. Beside moderate negative Ce anomaly, a pronounced positive Sm, Eu, Tb and Ho anomalies have been recognised. In Table 4, six selected analyses of major ions and trace elements from the cycles sampled on November 11, 1997 and April 7, 1999 are shown. The cycle of April 7, 1999, shows a general increase in the concentration of the potassium ions (K<sup>+</sup>), total organic carbon (TOC) and several trace elements, in particular, lithium (Li), boron (B), scandium (Sc), gallium (Ga), selenium (Se), rubidium (Rb), strontium (Sr), caesium (Cs), barium (Ba), thallium (Tl) and YREEs. Chemical composition of thermal water from this cycle and PAAS-normalised YREE concentrations could only be explained by activation of an additional source of thermal water with specific chemical composition and possibly low permeability as it has been recognised as late as during severe overexploitation conditions in the well.

Table 4. Chemical composition of selected samples of thermal water from the Sob-1 well collected on November 11, 1997 (10:00 – 11:43 h) and April 7, 1999, (09:45 – 11:10 h); major ions, dissolved CO<sub>2</sub>-gas, dissolved silica (SiO<sub>2</sub>), total organic carbon (TOC), total dissolved ions (TDI), pH, temperature of water at well-head (T<sub>wh</sub>) and trace elements with yttrium and rare earth elements (YREEs).

| Sample                        | 180*              | 184*                 | 190               | 210              | 218               | 221               |
|-------------------------------|-------------------|----------------------|-------------------|------------------|-------------------|-------------------|
| Date                          | 11.11. 97         | 11.11.97             | 11.11.97          | 7.4.99           | 7.4.99            | 7.4.99            |
| Time                          | 10 <sup>00'</sup> | 10 <sup>28'45"</sup> | 11 <sup>20'</sup> | 9 <sup>45'</sup> | 10 <sup>33'</sup> | 11 <sup>10'</sup> |
| Ions (mg/L)                   |                   |                      |                   |                  |                   |                   |
| Na <sup>+</sup>               | 490               | 990                  | 530               | 620              | 450               | 820               |
| K <sup>+</sup>                | 32                | 98                   | 33                | 190              | 70                | 190               |
| Ca <sup>2+</sup>              | 14                | 63                   | 21                | 43               | 15                | 57                |
| Mg <sup>2+</sup>              | 8                 | 6                    | 5                 | 19               | 5                 | 3                 |
| HCO <sub>3</sub> <sup>-</sup> | 1600              | 3100                 | 1830              | 2600             | 1500              | 2700              |
| Cl <sup>-</sup>               | 120               | 220                  | 91                | 159              | 95                | 124               |
| F <sup>-</sup>                | 0.45              | 0.92                 | 0.73              | 0.47             | 0.45              | 0.62              |
| J <sup>-</sup>                | 0.05              | 0.07                 | 0.04              | 0.15             | 0.10              | 0.19              |
| Br <sup>-</sup>               | 0.41              | 0.64                 | 0.36              | 0.60             | 0.45              | 0.77              |
| SO <sub>4</sub> <sup>2-</sup> | 8                 | 51                   | 8                 | 75               | 12                | 48                |
| TDI                           | 2,273             | 4,530                | 2,519             | 3,708            | 2,148             | 3,944             |
| Oxides/Dissolved gas          |                   |                      |                   |                  |                   |                   |
| SiO <sub>2</sub> (µg/L)       | 18                | 17                   | 18                | 13               | 14                | 24                |
| CO <sub>2</sub> (mg/L)        | 546               | 744                  | 637               | 575              | 440               | 712               |
| Parameters                    |                   |                      |                   |                  |                   |                   |
| TOC (mg/L)                    | 1.2               | 1.9                  | 1.4               | 2.3              | 2.5               | 12.1              |
| T <sub>wh</sub> (°C)          | 48.4              | 48.7                 | 48.7              | 48.8             | 48.6              | 48.9              |
| pH                            | 6.44              | 6.67                 | 6.49              | 6.69             | 6.81              | 6.86              |
| Trace elements (µg/L)         |                   |                      |                   |                  |                   |                   |
| Li                            | 170               | 440                  | 180               | 854              | 343               | 700               |
| Be                            | 0.2               | 1.1                  | 0.3               | 1.5              | 0.7               | 1.3               |
| B                             | 559               | 1480                 | 678               | 4000             | 1100              | 2800              |
| Al                            | 31                | 22                   | 17                | 28               | 19                | 75                |
| Sc                            | 1.8               | 2.2                  | 1.9               | 7.1              | 7.6               | 7.1               |
| Ga                            | 0.09              | 0.12                 | 0.10              | 0.62             | 0.64              | 0.62              |
| As                            | 2.7               | 2.9                  | 2.3               | 3.0              | 3.8               | 3.1               |
| Se                            | 2.1               | 4.8                  | 1.3               | 6.5              | 4.4               | 7.1               |
| Rb                            | 181               | 668                  | 166               | 654              | 258               | 656               |
| Sr                            | 775               | 969                  | 827               | 1470             | 982               | 1530              |
| Y                             | 0.05              | 0.24                 | 0.06              | 0.76             | 0.64              | 0.76              |
| Zr                            | 0.1               | 0.3                  | 0.1               | 1.3              | 0.4               | 1.0               |
| Cs                            | 6.1               | 26.8                 | 6.3               | 34.4             | 13.2              | 32.3              |
| Ba                            | 140               | 190                  | 150               | 477              | 292               | 477               |
| La                            | 0.02              | 0.24                 | 0.03              | 0.63             | 0.09              | 0.63              |
| Ce                            | 0.05              | 0.42                 | 0.06              | 0.26             | 0.11              | 0.25              |
| Pr                            | <0.01             | 0.05                 | <0.01             | 0.04             | 0.02              | 0.04              |
| Nd                            | 0.04              | 0.21                 | 0.04              | 0.18             | 0.10              | 0.20              |
| Sm                            | <0.01             | 0.07                 | 0.01              | 0.12             | 0.09              | 0.12              |
| Eu                            | 0.04              | 0.05                 | 0.03              | 0.13             | 0.09              | 0.14              |
| Gd                            | 0.03              | 0.07                 | 0.01              | 0.10             | 0.05              | 0.09              |
| Tb                            | <0.01             | 0.01                 | 0.01              | 0.61             | 0.60              | 0.61              |
| Dy                            | 0.02              | 0.06                 | 0.01              | 0.10             | 0.06              | 0.10              |
| Ho                            | <0.01             | 0.02                 | <0.01             | 0.60             | 0.01              | 0.60              |
| Er                            | <0.01             | 0.03                 | <0.01             | 0.06             | 0.04              | 0.08              |
| Tm                            | <0.01             | 0.01                 | <0.01             | 0.02             | 0.02              | 0.02              |
| Yb                            | <0.01             | 0.02                 | <0.01             | 0.06             | 0.04              | 0.08              |
| Tl                            | 0.17              | 0.37                 | 0.11              | 0.86             | 0.62              | 0.79              |

\*data from Kralj & Kralj, 2009

The increased concentrations of the K<sup>+</sup> ions and Li, B, Rb, Ba and Cs in the water from the assumed additional source indicate a possible origin in dissolution of illite and muscovite, which are the principal phyllosilicate minerals of the aquifer sediments in the Sob-1 well (Žlebnik et al., 1988a; Kralj, 2001). Illite contains trace amounts of YREEs and its decomposition could also be the source of YREEs and their fractionation. Many studies carried out worldwide have shown that during water-rock interaction LREEs are retained at the site of reaction by adsorption to residual phases while YHREEs are preferentially mobilized by solution complexation reactions (e.g., Duddy, 1980; Braun et al., 1993; Johannesson and Zhou, 1999; Zhou et al., 2005). Guo et al. (2005) have shown for carbonate waters that there is a steady increasing trend of REE solubility according to atomic number or decreasing ionic radii for (+3) ions, except for Sm and Ho, and to a lesser extent Tb that show relatively higher solubilities. The observed PAAS-normalised pattern in the waters from the cycle of April 7, 1999, could be explained by the process of decomposition of illite and muscovite, and preferential mobilisation of HREEs into solution.

On the other hand, the increased concentrations of TOC, gallium, selenium, thallium and the iodide ions I<sup>-</sup> also indicate the assumed additional (or another additional) source. This group of elements could have an origin in waters leaked from silty and clayey layers rich in organic matter and coal, that have been activated only during severe overexploitation conditions. In that case the ligands complexing YHREEs could be, beside carbonate species, humic and/or fulvic acids.

### Conclusions

Rare earth elements and yttrium analysed in mineral and thermal waters from Tertiary aquifers in the Mura Basin occur in concentrations that are far below ( $10^{-2}$  to  $10^{-4}$ ) the abundances in the aquifer sediments. Mineral and thermal waters are carbonate waters, and the concentrations of YREEs and their PAAS-normalised patterns strongly depend on the YREE solubility, complexation reactions and the duration of water-rock interaction. In aquifers with moderate to high permeability and high flow rates YREE concentrations in water indicate lower degree of equilibration with the aquifer sediment. The plots of YREE concentrations normalised to PAAS show fractionation of YHREEs over LREEs which could be attributed to the higher solubility of YHREEs and their preferential mobilisation into solution

by complexation reactions. In low-permeability aquifers the retention times and water-sediment interactions are longer and equilibration reactions more advanced as the fractionation of YHREEs over LREEs disappears. The same trend has been recognised for the positive Eu anomaly which is outstanding in cold mineral waters and thermal waters from Thermal I, and weak in the waters from low-permeability aquifers in the Haloze, Špilje and Lendava Formations.

In the Sob-1, uncommonly high concentrations of YREEs and their specific PAAS-normalised plots indicate the well overexploitation and the consequent leakage from low-permeability clayey and silty lenses rich in organic matter and coal. Here, the YHREE complexing ligands could be, beside carbonate species, humic and/or fulvic acids.

### Acknowledgements

The Slovenian Research Agency ARRS is greatly acknowledged for granting the research (Geotermalna energija - Geothermal Energy L2-7062 and Programme Mineral Resources P-0025). Ms. Staška Čertalič, Geological Survey of Slovenia, is kindly appreciated for technical support.

### References

- Aide, M. 2018: Lanthanide soil chemistry and its importance in understanding soil pathways: mobility, plant uptake, and soil health. In: Awwad, N.S. & Mubarak, A.T. (eds.): Lanthanides, IntechOpen. <https://doi.org/10.5772/intechopen.79238>
- Anders, E. & Gravenese, N. 1989: Abundance of elements: meteoritic and solar. *Geochim. Cosmochim. Acta* 53:197-21.
- Bau, M. 1991: Rare-earth element mobility during hydrothermal and metamorphic fluid-rock interaction and the significance of the oxidation state of europium. *Chem. Geol.*, 93: 219-230.
- Bau, M. 1999: Scavenging of dissolved yttrium and rare earths by precipitating iron hydroxides: Experimental evidence for Ce oxidation, Y-Ho fractionation, and lanthanide tetrad effect. *Geochim. Cosmochim. Acta*, 63: 67-77.
- Bau, M. & Dulski, P. 1999: Comparing yttrium and rare earths in hydrothermal fluids from Mid-Atlantic Ridge: implications for Y and REE behaviour during near-vent mixing and for Y/Ho ratio of Proterozoic seawater. *Chem. Geol.*, 155: 77-90.

- Bau, M., Schmidt, K., Pack, A., Bendel, V. & Kraemer, D. 2018: The European Shale: an improved data set for normalisation of rare earth element and yttrium concentrations in environmental and biological samples from Europe. *Appl. Geochem.*, 90: 142-149.
- Biddau, R., Bensimon, M., Cidu, R. & Parriaux, A. 2009: Rare earth elements in groundwater from different Alpine aquifers. *Chem. Erde*, 69: 327-339.
- Bilal, B.A. 1991: Thermodynamic study of  $\text{Eu}^{3+}/\text{Eu}^{2+}$  redox reaction in aqueous solutions at elevated temperatures and pressures by means of cyclic voltammetry. *Z. Naturforschung*, 46a:1108-1116.
- Bräuer, K., Geissler, W.H., Kämpf, H., Niedermann, S. & Rman, N. 2016: Helium and carbon isotope signatures of gas exhalations in the westernmost part of the Pannonian Basin (SE Austria/NE Slovenia): Evidence for active mantle degassing. *Chem. Geol.*, 422: 60-70.
- Braun, J.J., Viers, J., Dupré, B., Polve, M., Ndam, J. & Muller, J.P. 1998: Solid/liquid REE fractionation in the lateritic system of Goyum, East Cameroon: the implications for the present dynamics of the soil covers of the humid tropical regions. *Geochim. Cosmochim. Acta*, 62: 273-299.
- Brookins, D.G. 1989: Aqueous chemistry of rare earth elements. In: Lipin, B.R. & McKay, G.A. (eds.): *Geochemistry and mineralogy of rare earth elements*. *Rev. Mineral.*, 21: 201-223.
- Cantrell, K.J. & Byrne, R.H. 1987: Rare earth element complexation by carbonate and oxalate ions. *Geochim. Cosmochim. Acta*, 51: 597-605.
- Coryell, C.D., Chase, J.W. & Winchester, J.W. 1963: A procedure for geochemical interpretation of terrestrial rare earth abundance patterns. *J. Geophys. Res.*, 68: 559-566.
- DeBaar, H.J.W., Bacon, M.P., Brewer, P.G. & Bruland, K.W. 1985: Rare earth elements in the Pacific and Atlantic oceans. *Geochim. Cosmochim. Acta*, 49: 1943-1954.
- DeBaar, H.J.W., German, C.R., Elderfield, H. & Van Gaans, P. 1988: Rare earth element distribution in anoxic waters of the Cariaco Trench. *Geochim. Cosmochim. Acta*, 52: 1203-1219.
- Dia, A., Gruau, G., Olivié-Lauquet, G., Riou, C., Molénat, J. & Curmi, P. 2000: The distribution of rare earth elements in groundwaters: Assessing the role of source-rock composition, redox changes and colloidal particles. *Geochim. Cosmochim. Acta*, 64/24: 4131-4151. [https://doi.org/10.1016/S0016-7037\(00\)00494-4](https://doi.org/10.1016/S0016-7037(00)00494-4)
- Douville, E., Bienvenu, P., Charlou, J.L., Donval, J.P., Fouquet, Y., Appriou, P. & Gamo, T. 1999: Yttrium and rare earth elements in fluids from various deep-sea hydrothermal systems. *Geochim. Cosmochim. Acta*, 63/5: 627-634.
- Douville, E., Charlou, J.L., Oelkers, E.H., Bienvenu, P., Jove Colon, C.F., Donval, J.P., Fouquet, Y., Prieur, D. & Appriou, P. 2002: The rainbow vent fluid (36° 14' N, MAR): the influence of ultramafic rocks and phase separation on trace metal content in Mid-Atlantic Ridge hydrothermal fluids. *Chem. Geol.*, 184: 37-48. [https://doi.org/10.1016/s0009-2541\(01\)00351-5](https://doi.org/10.1016/s0009-2541(01)00351-5)
- Drever, J.I. 1997: *The geochemistry of natural waters: surface and groundwater environments*. 3<sup>rd</sup> edn., Prentice-Hall Inc., Upper Saddle River, NJ.
- Duddy, I.R. 1980: Redistribution and fractionation of the rare-earth and other elements in a weathering profile. *Chem. Geol.*, 30: 363-381.
- Elderfield, H. & Greaves, M.J. 1982: The rare earth elements in sea water. *Nature*, 296: 214-219.
- Fee, J.A., Gaudette, H.E., Lyons, W.B. & Long, D.T. 1992: Rare earth element distribution in Lake Tyrell groundwaters, Victoria, Australia. *Chem. Geol.*, 96: 67-93.
- Fodor, L., Jelen, B., Márton, E., Rifelj, H., Kraljić, M., Kevrić, R., Márton, P., Koroknai, B. & Báldi-Beke, M. 2002: Miocene to Quaternary deformation, stratigraphy and paleogeography in Northeastern Slovenia and Southwestern Hungary. *Geologija*, 45/1: 103-114. <https://doi.org/10.5474/geologija.2002.009>
- Gabor, L. & Rman, N. 2016: Mofettes in Slovenske gorice, Slovenia. *Geologija*, 59/2: 155-177. <https://doi.org/10.5474/geologija.2016.009>
- Gonzalez, V., Vignati, D.A.L., Leyval, C. & Giamberini, L. 2014: Environmental fate and ecotoxicity of lanthanides: are they uniform group beyond chemistry? *Environ. Int.*, 71: 148-157. <https://doi.org/10.1016/j.envint.2014.06.019>
- Gosselin, D.G., Smith, M.R., Lepel, E.A. & Laul, J.C. 1992: Rare earth elements in chloride-rich groundwater, Palo Duro Basin, Texas, USA. *Geochim. Cosmochim. Acta*, 56: 1495-1505.
- Guo, C., Stetzenbach, K.J. & Hodge, V. 2005: Determination of 56 trace elements in three aquifer-type rocks by ICP-MS and approximation of the relative solubilities for these elements in a carbonate system by water-rock concentration ratios. In: Johannesson, K.H. (ed.): *Rare Earth Elements in Groundwater*

- Flow Systems. Water Science and Technology Library, 51: 39–65.
- Hatje, V., Bruland, K.W. & Flegal, A.R. 2016: Increases in anthropogenic gadolinium anomalies and rare earth element concentrations in San Francisco Bay over a 20 year record. *Environ. Sci. Technol.*, 50/8: 4159–4168. <https://doi.org/10.1021/acs.est.5b04322>
- Hissler, C., Stille, P., Guignard, C., Iffly, J.F. & Pfister, L. 2014: Rare earth elements as hydrological tracers of anthropogenic and critical zone contributions: a case study at the Alzette river basin scale. *Procedia Earth Planet. Sci.*, 10: 349–352
- INA-Projekt Zagreb OOUR KGI & Geološki zavod Ljubljana TOZD GGG 1991: Raziskave nafte in plina v Sloveniji, Vol 1: Murska Depresija (Exploration of oil and gas in Slovenia, Vol. 1: The Mura Depression). Geološki zavod Ljubljana, Ljubljana: 406 p.
- Jelen, B. & Rifelj, H. 2011: Površinska litostratigrafska in tektonska strukturna karta območja T-JAM projekta, severovzhodna Slovenija 1:100,000 = Surface lithostratigraphic and tectonic map of T-JAM project area, northeastern Slovenia 1:100,000. Geological Survey of Slovenia, Ljubljana. [https://www.geo-zs.si/PDF/LitostratigrafskaTektonskaKarta/Karta\\_T\\_Jam\\_slv.pdf](https://www.geo-zs.si/PDF/LitostratigrafskaTektonskaKarta/Karta_T_Jam_slv.pdf)
- Jelen, B. & Rifelj, H., Bavec, M. & Rajver, D. 2006: Opredelitev dosedanjega konceptualnega geološkega modela Murske depresije = Definition of current conceptual geological model of the Mura depression in Slovenian. Archive of Geological Survey of Slovenia, Ljubljana.
- Johannesson, K.H. & Lyons, W.B. 1996: The rare earth element geochemistry of Mono Lake water and the importance of carbonate complexing. *Limnol. Oceanogr.*, 39: 1141–1154.
- Johannesson, K.H. & Zhou, X. 1999: Origin of middle rare earth element enrichments in acid waters of a Canadian High Arctic Lake. *Geochim. Cosmochim. Acta*, 63/1: 153–165.
- Johannesson, K.H., Stetzenbach, K.J., Hodge, V.F. & Lyons, W.B. 1996: Rare earth element complexation behaviour in circumneutral pH groundwaters: Assessing the role of carbonate and phosphate ions. *Earth Planet. Sci. Lett.*, 139: 305–319.
- Johannesson, K.H., Stetzenbach, K.J. & Hodge, V.F. 1997: Rare earth elements as geochemical tracers of regional groundwater mixing. *Geochim. Cosmochim. Acta*, 61/17: 3605–3618.
- Johannesson, K.H., Zhou, X., Guo, C., Stetzenbach, K.J. & Hodge, V.F. 2000: Origin of rare earth element signatures in groundwaters of circumneutral pH from southern Nevada and eastern California. *Chem. Geology*, 164: 239–257.
- Johannesson, K.H., Cortes, A., Ramos Leal, J.A., Ramirez, A.G. & Durazco, J. 2005: Geochemistry of rare earth elements in groundwaters from a rhyolite aquifer, central Mexico. In: Johannesson, K.H. (ed.): Rare Earth Elements in Groundwater Flow Systems. Water Science and Technology Library, 51: 188–222.
- Klinkhammer, G.P., Elderfield, H., Edmond, J.M. & Mitra, A. 1994: Geochemical implications of rare earth element patterns in hydrothermal fluids from mid-ocean ridges. *Geochim. Cosmochim. Acta.*, 58/23: 5105–5113.
- Košćec, J. & Jovanović, M. 1968: Litostratigrafski profili terciarnog kompleksa u dubokim bušotinama Murske potoline = Lithostratigraphic sections of the Tertiary complex in deep wells of the Mura Basin. (in Croatian). Fond Geol. Dok. INA-Projekt Zagreb, INA-Naftaplin, Zagreb.
- Kováč, M., Hudáčková, N., Halásová, E., Kováčová, M., Holcová, K., Oszczyk-Clowes, M., Báldi, K., Less, G., Nagymarosy, A., Ruman, A., Klučiar, T. & Jamrich, M. 2017: The Central Paratethys palaeoceanography: a water circulation model based on microfossil proxies, climate, and changes of depositional environment. *AGEOS*, 9/2: 75–114.
- Kralj, P. 1993: Optimizacija predterciarnega visokotemperaturnega geotermalnega sistema Termal II v severovzhodni in vzhodni Sloveniji = Optimization of pre-Tertiary high-temperature geothermal system Thermal II in Northeastern and Eastern Slovenia. Geološki zavod Ljubljana, Ljubljana: 56 p.
- Kralj, P. 1994: Prostorska in ekonomska ocen izdatnosti predterciarnih vodonosnikov na območju severovzhodne Slovenije, I. faza = Spatial and economic evaluation of capacity of pre-Tertiary aquifers in the area of Northeastern Slovenia, Phase I. SP Geološki zavod Ljubljana, Ljubljana: 13 p.
- Kralj, P. 1995: Hidrodinamične in hidrokemijske lastnosti termalne vode v geotermalnem sistemu Termal I v Prekmurju, II. faza = Hydrodynamical and hydrogeochemical characteristics of thermal water in the geothermal system Thermal I in Prekmurje, Phase II. Geološki zavod Ljubljana, Ljubljana: 26.

- Kralj, P. 2001: Das Thermalwasser-System des Mur-Beckens in Nordost-Slovenien. *Mitteil. Ingenieur Hydrogeol.*, 81: 1-82.
- Kralj, P. 2004a: Trace elements in medium-temperature (40-80°C) thermal waters from the Mura basin (North-Eastern Slovenia). *Environ. Geol.*, 46: 622-629.
- Kralj, P. 2004b: Chemical composition of low-temperature (<20-40°C) thermal waters in Slovenia. *Environ. Geol.*, 46: 635-642.
- Kralj, P. 2010: Eruptive and sedimentary evolution of the Pliocene Grad Volcanic Field, North-east Slovenia. *J. Volcanol. Geoth. Res.*, 201: 272-284.
- Kralj, P. & Kralj, P. 2000a: Thermal and mineral waters in north-eastern Slovenia. *Environ. Geol.*, 39: 488-500.
- Kralj, P. & Kralj, P. 2000b: Overexploitation of geothermal wells in Murska Sobota, Northeastern Slovenia. In: *Proceedings World Geothermal Congress 2000*, 837-842.
- Kralj, P. & Kralj, P. 2009: Rare earth elements in thermal water from the Sob-1 well, Murska Sobota, NE Slovenia. *Environ. Earth. Sci.*, 59: 5-13. <https://doi.org/10.1007/s12665-009-0006-8>
- Kralj, P. & Kralj, P. 2012: Geothermal waters from composite clastic sedimentary reservoirs: geology, production, overexploitation, well cycling and leakage – a case study of the Mura Basin (SW Pannonian Basin). In: Yang, J. (ed.): *Geothermal energy, technology and geology*. Nova Science Publishers Inc., New York: 47-91.
- Kralj, P. & Kralj, P. 2020: Temporal variation of the halide ions (F<sup>-</sup>, Cl<sup>-</sup>, Br<sup>-</sup>, I<sup>-</sup>) in medium-temperature (46–52 °C) thermal waters from the Sob-1 and Sob-2 wells, the Mura Basin, north-eastern Slovenia. *Environ. Earth Sci.* 79, 283. <https://doi.org/10.1007/s12665-020-09034-y>
- Kralj, P., Eichinger, L. & Kralj, P. 2009: The Benedikt hydrothermal system (north-eastern Slovenia). *Environ. Geol.*, 58/8: 1653-1661. <https://doi.org/10.1007/s00254-008-1631-3>
- Kulaksiz, S. & Bau, M. 2011: Rare earth elements in the Rhine river, Germany: first case of anthropogenic lanthanum a dissolved microcontaminant in the hydrosphere. *Environ. Int.*, 37/5: 973-979.
- Ladonin, D.V. 2019: Lantanides in soils of the Cherepovets steel mill. In: Awwad, N.S. & Mubarak, A.T. (eds.): *Lanthanides*. IntechOpen. <https://doi.org/10.5772/intechopen.80294>
- Lee, J.H. & Byrne, R.H. 1993: Complexation of trivalent rare earth elements (Ce, Eu, Gd, Tb, Yb) by carbonate ions. *Geochim. Cosmochim. Acta*, 57: 295-302.
- Liu, H., Guo, H. & Wu, L. 2017: Rare earth elements as indicators of groundwater mixing in the North China Plain: A case study in the area of Hengshui city, China. *Procedia Earth Planet. Sci.*, 17: 396-399.
- Liu, X. & Byrne, R.H. 1998: Comprehensive investigation of yttrium and rare earth element complexation by carbonate ions using ICP-Mass spectrometry. *J. Sol. Chem.*, 27: 803-815.
- Luo, Y.R. & Byrne, R.H. 2004: Carbonate complexation of yttrium and the rare earth elements in natural waters. *Geochim. Cosmochim. Acta*, 68: 691-699.
- Malvić, T. & Velić, J. 2011: Neogene tectonics in Croatian part of the Pannonian Basin and reflectance in hydrocarbon accumulations. In: Schattner, U. (ed.): *New frontier in tectonic research – at the midst of plate convergence*, 215-238. InTech, Rijeka, Croatia. <https://doi.org/10.5772/21270>
- Márton, E., Fodor, L., Jelen, B., Márton, P., Rifelj, H. & Kevrić, R. 2002: Miocene to Quaternary deformation in NE Slovenia: complex paleomagnetic and structural study. *J. Geodyn.*, 34/5: 627-651. [https://doi.org/10.1016/S0264-3707\(02\)00036-4](https://doi.org/10.1016/S0264-3707(02)00036-4)
- McLennan, S.M. 1989: Rare earth elements in sedimentary rocks: influence of provenance and sedimentary processes. In: Lipin, B.R. & McKay, G.A. (eds.): *Geochemistry and mineralogy of rare earth elements*. *Rev. Mineral.*, 21: 169-196.
- Michard, A. 1989: Rare earth element systematics in hydrothermal fluids. *Geochim. Cosmochim. Acta*, 53: 745-750.
- Michard, A. & Albarede, F. 1986: The REE content in some hydrothermal fluids. *Chem. Geology*, 55: 51-60.
- Michard, A., Beaucaire, C. & Michard, G. 1987: Uranium and rare earth elements in CO<sub>2</sub>-rich waters from Vals-les-bains (France). *Geochim. Cosmochim. Acta*, 51: 901-909.
- van Middlesworth, P.E. & Wood, S.A. 1998: The aqueous geochemistry of the rare earth elements and yttrium. Part 7. REE, Th and U contents in thermal springs associated with the Idaho batholith. *Appl. Geochem.*, 13/7: 861-884. [https://doi.org/10.1016/S0883-2927\(98\)00019-5](https://doi.org/10.1016/S0883-2927(98)00019-5)
- Möller, P. 2000: Rare earth elements and yttrium as geochemical indicators of the source of

- mineral and thermal waters. In: Stober, I., Bucher, K. (eds): *Hydrology of crystalline rocks*, Kluwer Academic Press, 227–246.
- Möller, P., Dulski, P., Bau, M., Knappe, A., Pekdeger, A. & Sommer-von Jarmersted, C. 2000: Anthropogenic gadolinium as a conservative tracer in hydrology. *J. Geochem. Explor.*, 69–70: 409–414.
- Möller, P., Dulski, P. & Morteani, G. 2003: Partitioning of rare earth elements, yttrium and selected major elements among source rocks, liquid and steam of the Larderello-Travale Geothermal Field (Tuscany, Central Italy). *Geochim. Cosmochim. Acta*, 67: 171–183.
- Möller, P., Rosenthal, E., Geyer, S., Guttman, J., Dulski, P., Rybakov, M., Zilberbrand, M., Jahnke, C. & Flexer, A. 2007: Hydrochemical processes in the Lower Jordan valley and in the Dead Sea area. *Chem. Geology*, 239: 27–49.
- MURmap (2022–2024) Hollistic geochemical tracking of inorganic pollutants in the Mur/Mura River catchment <https://www.geo-zs.si/index.php/projekti/drugi-projekti>; <https://aach.unileoben.ac.at/en/news>
- Nádor, A., Lapanje, A., Tóth, G., Rman, N., Szócs, T., Prestor, J., Uhrin, A., Rajver, D., Fodor, L., Muráti, J. & Székely, E. 2012: Transboundary geothermal resources of the Mura-Zala basin: a need for joint thermal aquifer management of Slovenia and Hungary. *Geologija*, 55/2: 209–224. <https://doi.org/10.5474/geologija.2012.013>
- Nigro, A., Sappa, G. & Barbieri, M. 2018: Boron isotopes and rare earth elements in the groundwater of a landfill site. *J. Geochem. Explor.*, 190: 200–206. <https://doi.org/10.1016/j.gexplo.2018.02.019>
- Piller, W.E., Harzhauser, M. & Mandic, O. 2007: Miocene Central Paratethys stratigraphy – current status and future directions. *Stratigraphy*, 4/2: 151–168.
- Pleničar, M. 1968: Basic geological map SFR Yugoslavia, scale 1:100,000, Sheet Goričko and Leibnitz. Federal geological survey, Belgrade.
- Rajver, D., Kralj, P., Žlebničnik, L., Drobne, F. & Kranjc, S. 1994: Program za učinkovito rabo energije in obnovljivih virov energije, Pridobivanje energije iz obnovljivih virov, Prostorska in ekonomska ocena izdatnosti predterciarnih vodonosnikov na območju severovzhodne Slovenije = Programme for efficient utilization of energy and renewable resources, Extraction of energy from renewable resources, Spatial and economical evaluation of capacity of pre-Tertiary aquifers in north-eastern Slovenia. Internal report. Archive of Geological Survey of Slovenia, Ljubljana.
- Ravnik, D., Rajver, D., Žlebničnik, L. & Kralj, P. 1992: Geološke strukture: viri termalnih in mineralnih vod v Sloveniji = Geological structures: the resources of thermal and mineral waters in Slovenia. In: Kralj, P. (ed.): *Mineralne in termalne vode v gospodarstvu in znanosti Slovenije = Mineral and thermal waters in economy and science of Slovenia*. Geološki zavod Ljubljana, Ljubljana: 9–32.
- Rijavec, L., Bistričič, A. & Jenko, M. 1985: Mura Basin. In: Steininger, F.F., Senes, J., Kleemann, K. & Rogl, F. (eds.): *Neogene of the Mediterranean Tethys and Paratethys*, Vol 1, 2, Institute of Paleontology, University of Vienna, Vienna.
- Rman, N. 2014: Analysis of long-term thermal water abstraction and its impact on low-temperature intergranular geothermal aquifers in the Mura-Zala basin, NE Slovenia. *Geothermics*, 55: 214–227. <https://doi.org/10.1016/j.geothermics.2014.01.011>
- Rotár-Szalkai, A., Nádor, A., Szócs, T., Maros, G., Goetzl, G. & Zekiri, F. 2017: Outline and joint characterization of Transboundary geothermal reservoirs in the western part of the Pannonian basin. *Geothermics* 70: 1–16. <https://doi.org/10.1016/j.geothermics.2017.05.005>
- Royden, L.H. 1988: Late Cenozoic tectonics of the Pannonian basin system. In: Royden, L.H. & Horvath, F. (eds.): *The Pannonian Basin, a study in basin evolution*. Am. Assoc. Pet. Geol. Mem., 45: 1–16.
- Shand, P., Johannesson, K.H., Chudaev, O., Chudaeva, V. & Edmunds, W.M. 2005: Rare earth element contents of high pCO<sub>2</sub> groundwaters of Primorye, Russia: Mineral stability and complexation controls. In: Johannesson, K.H. (ed.): *Rare earth elements in groundwater flow systems*. Water Science and Technology Library, 51: 161–186.
- Shannon, W.M. & Wood, S.A. 2005: The analysis of picogram quantities of rare earth elements in natural waters. In: Johannesson, K.H. (ed.): *Rare Earth Elements in Groundwater Flow Systems*. Water Science and Technology Library, 51: 1–37.
- Shannon, W.M., Wood, S.A., Brown, K. et al. 2001: Behavior of rare earth elements in geothermal systems: A new exploration/exploitation tool? *Exploration Technology, Geothermal Energy R&D Program*, 2–31.

- Smedley, P. 1991: The geochemistry of rare earth elements in groundwater from the Carnmenellis area, southwest England. *Geochim. Cosmochim. Acta*, 55: 2767-2779.
- Sverjensky, D.M. 1984: Europium redox equilibrium in aqueous solutions. *Earth Planet. Sci. Lett.*, 67: 70-78.
- Szocs, T., Rman, N., Süveges, M., Palcsu, L., Tóth, G. & Lapanje, A. 2013: The application of isotope and chemical analyses in managing transboundary groundwater resources. *Appl. Geochem.*, 32: 95-107. <https://doi.org/10.1016/j.apgeochem.2012.10.006>
- Szocs, T., Rman, N., Rotár-Szalkai, Á., Tóth, G., Lapanje, A., Černák, R. & Nádor, A. 2018: The Upper Pannonian thermal aquifer: cross-border cooperation as an essential step to transboundary groundwater management. *J. Hydrol.*, 20: 128-144. <https://doi.org/10.1016/j.ejrh.2018.02.004>
- Šram, D., Rman, N., Rižnar, I. & Lapanje, A. 2015: The three-dimensional regional geological model of the Mura-Zala Basin, northeastern Slovenia. *Geologija*, 58/2: 139-154. <https://doi.org/10.5474/geologija.2015.011>
- Tóth, G., Rman, N., Rotár-Szalkai, Á., Kerégyártó, T., Szócs, T., Lapanje, A., Černák, R., Remsík, A., Schubert, G. & Nádor, A. 2016: Transboundary fresh and thermal groundwater flows in the west part of the Pannonian Basin. *Renew. Sustain. Energy Rev.* 57: 439-454. <https://doi.org/10.1016/j.rser.2015.12.021>
- Tweed, S.O., Weaver, T.R., Cartwright, I. & Schaefer, B. 2006: Behaviour of rare earth elements in groundwater during flow and mixing in fractured rock aquifers: an example from the Dandenong ranges, southeast Australia. *Chem. Geol.*, 234: 291-307.
- Wood, S. 1990: The aqueous geochemistry of rare-earth elements and yttrium. Theoretical prediction of speciation in hydrothermal solutions to 350 °C at saturation water vapor pressure. *Chem. Geol.*, 88: 99-125.
- Wood, S.A. 2006: Rare earth element systematics of acidic geothermal waters from the Taupo Volcanic Zone, New Zealand. *J. Geochem. Explor.*, 89: 424-427.
- Yuan, J., Mao, X., Wang, Y., Deng, Z. & Huang, L. 2014: Geochemistry of rare-earth elements in shallow groundwater, northeastern Guangdong Province, China. *Chin. J. Geochem.*, 33: 53-64. <https://doi.org/10.1007/s11631-014-0659-1>
- Zhou, X., Stetzenbach, K.J., Yu, Z. & Johannesson, K.H. 2005: Origin of rare earth element signatures in groundwaters of South Nevada, USA: Implications from preliminary batch leach tests using aquifer rocks. In: Johannesson, K.H. (ed): *Rare Earth Elements in Groundwater Flow Systems*. Water Science and Technology Library, 51: 141-160.
- Zhu, Y., Inagaki, K., Haraguchi, H. & Chiba, K. 2010: On-line elution of iron hydroxide coprecipitate carrier for determination of REEs in natural water by mix-gas ICP-MS. *J. Anal. At. Spectrom.*, 25: 364-369.
- Žlebnik, L., Kralj, P. & Kokol, L. 1988a: Termalne vode na območju Murske Sobote, vrtina Sob-1 = Thermal waters in the Murska Sobota area, The Sob-1 well. Geološki zavod Ljubljana, Ljubljana: 1-24.
- Žlebnik, L., Žižek, D., Kralj, P. & Kokol, L. 1988b: Termalne vode na območju Murske Sobote = Thermal waters in the Murska Sobota area. Geološki zavod Ljubljana, Ljubljana: 1-42.



# Addendum to Diercks et al., 2021: A model for the formation of the Pradol (Pradolino) dry valley in W Slovenia and NE Italy

Manuel DIERCKS<sup>1,2</sup>, Christoph GRÜTZNER<sup>3</sup>, Marko VRABEC<sup>4</sup> & Kamil USTASZEWSKI<sup>3</sup>

<sup>1</sup>Institute for Geology, TU Bergakademie Freiberg, 09599 Freiberg, Germany

<sup>2</sup>Now at: School of Geography, Earth and Environmental Sciences, University of Plymouth, Plymouth PL4 8AA, United Kingdom

<sup>3</sup>Institute of Geological Sciences, Friedrich Schiller University Jena, 07749 Jena, Germany; e-mail: christoph.gruetzner@uni-jena.de

<sup>4</sup>University of Ljubljana, Faculty of Natural Sciences and Engineering, Department of Geology, SI- 1000 Ljubljana, Slovenia

Prejeto / Received 18. 3. 2022; Sprejeto / Accepted 15. 7. 2022; Objavljeno na spletu / Published online 22. 07. 2022

## Abstract

In our paper Diercks et al. (2021) we presented geomorphological data and field observations from W Slovenia and NE Italy to develop a model for the formation of the Pradolino (slov. Pradol) dry valley. After publication we were kindly pointed to existing studies on the area that we were unaware of. To fill that gap and to properly credit previous work, in this addendum we summarise the research history on the study area and briefly compare earlier views with our model.

## Introduction

In our paper Diercks et al. (2021) we developed a model for the formation of the Pradolino (slov. *Pradol*) dry valley using geomorphological analyses and field observations. After publication, we were made aware of previous studies that investigated the geomorphological evolution of the area. These papers were mainly published in the 1980s and 1990s in Italian geoscience journals. In order to give proper credit to earlier work, we summarise these studies here. For the sake of completeness, we also include older studies from the Italian and German literature that date back to the 19<sup>th</sup> and early 20<sup>th</sup> centuries. In the following we will use Italian names for locations that are on Italian territory today, and Slovenian names for locations that are on Slovenian territory. For clarity, such toponyms in the respective other language are put in parentheses and in italics. For the same reason, original quotes from earlier papers are also put in italics.

## Research history

The Pradolino dry valley is located in NE Italy and interpreted as a former course of the Nadiža river (ital. *Natisone*), when the valleys now oc-

cupied by the river were blocked by glaciers. Its entrance lies about 200 m above the course of the Nadiža and it is deeply incised between Monte Mia and Monte Vogu. The Nadiža takes a highly curved course around Monte Mia (Fig. 1) at present. Notably, it does not enter the wide valley between Robič (ital. *Robis*) and Kobarid (ital. *Caporetto*), where it could join the Soča (ital. *Isonzo*) river, but it turns sharply south towards Stupizza (slov. *Šupca*). This conspicuous geomorphology has caught the attention of various scholars.

The general geology of the study area was studied in a modern sense since the 19<sup>th</sup> century, for example by Štúr (1858). He already described the low drainage divide between the present-day Nadiža and the Soča east of Robič. The divide is only a few meters higher than the floor of the wide and U-shaped valley and mainly consists of a landslide deposit that originates from the northern flanks of the Matajur mountain (Fig. 1.). Štúr, however, classified all moraines as of Tertiary age. This notation made it even into the map of Stache (1889), although Taramelli (1870) pointed out this erroneous age assignment.

The evolution of the fluvial system and the geomorphology in the area has, however, already

been a matter of debate much earlier. This debate rested on field observations and the interpretation of historical texts, especially on the change of geographical names. It would lead too far to summarize the discussion, which started as early as in the 16<sup>th</sup> century, and the interested reader is referred to the extensive work of Tellini (1898), who provided a broad overview. The debate about the Nadiža and Soča rivers, together with the birth of modern geology, can be seen as the driver of an intensification of research on the area. Especially the work of Kandler was used as a starting point for a long-lasting discussion.

Pietro Kandler, a historian from Trieste, argued that the Soča had flown from Kobarid towards the west in Roman times, occupying the Staro Selo (ital. *Starasella*) valley. It had then joined the Nadiža near Robič, from which it reached south towards Stupizza (Kandler, 1864, 1867). He claimed that the landslide near Robič occurred in 586 or 587 AD due to a flood event. With the valley being blocked, the Soča would have been dammed and finally occupied its present-day course towards Tolmin (ital. *Tolmino*) and Most na Soči (ital. *Santa Lucia d'Isonzo*). Kandler's theory faced harsh criticism based on archaeological and geological arguments.

Taramelli (1871) argued against Kandler's theories. He considered it impossible that the Soča once had flown to the west. Instead, he held the view that the western branch of the Soča glacier blocked the Staro Selo valley and forced the Nadiža to flow south, instead of continuing to the east and joining the Soča. He also already stated that the Nadiža might have occupied the Pradolino valley. In later publications, Taramelli described glacial deposits in the Nadiža valley and reaffirmed the view that the glacier advanced via the Staro Selo valley from Kobarid as a branch of the Soča glacier (Taramelli, 1875). Taramelli (1882) summarized the debate about a possible connection of the Nadiža/Natisone and the Soča/Isonzo system based on archaeological and historical arguments by Kandler and others (Kandler, 1864, 1867). Again, he strongly opposed Kandler's views and argued that the course of the Nadiža towards Stupizza was established following the abandonment of the moraine of Staro Selo, which blocked the connection between the Nadiža and the Soča. Taramelli was the first one to have established a more or less correct view on the Soča glacier according to Penck and Brückner (1909).

Von Czoernig (1873) was fond of Kandler's interpretation and suspected that the Soča once

flowed from Kobarid to the west in the Staro Selo valley, where it joined with the Nadiža at Robič. He argued based on the wide valley floor, the almost flat morphology between Kobarid and Robič, and fluvial gravels. He detailed historical arguments based on ancient texts, going back even to Plinius and Strabo, from which he concluded that the Nadiža once must have had more erosive power. However, even with von Czoernig's assertive support, Kandler's ideas could not prevail for long.

In his dissertation, Gumprecht (1886) worked on the relation between the Soča and Nadiža rivers. He outrightly rejected Kandler's hypotheses and argued that the Nadiža once (after the Tertiary) followed the valley of Staro Selo to Kobarid, where it joined the Soča river. Only later, he argued, did the Nadiža turn south at Robič to occupy its present-day course. Gumprecht reported that the drainage divide near Staro Selo is made up of moraine material, and that the landslide masses only form the very top of the divide. He detailed on the distribution of glacial deposits in the area and on the slope of the Staro Selo valley, which he reported to be clearly inclined towards the east with a vertical drop of ca. 20 m along a 5 km stretch between Robič and the Soča bridge near Kobarid. He concluded that there were four stages of drainage development: First, after the Tertiary, the Nadiža used the Staro Selo valley to join the Soča. Second, during the pre-glacial period, backward erosion in the Pulfero-Stupizza valley caused the Nadiža to flow to the south, at least partly. Third, during the glacial period, the Soča glacier blocked the Staro Selo valley up to Sedlo and Logje; the Nadiža had to turn south at Robič and perhaps even used the Pradolino gorge. Fourth, in post-glacial times the Nadiža continued to use the course it has today. A small tributary to the Soča originating in the Staro Selo valley, the Idrija, got repeatedly dammed by material from the Šjak stream, causing temporary lakes and leaving lacustrine deposits in the Staro Selo valley.

Gumprecht's arguments against Kandler were partly confirmed by the archaeologist Gregorutti (1890) based on the interpretation of historical and archaeological data. However, Gregorutti claimed that there never was a communication between the Nadiža and the Soča systems at all – a claim that should never find wide support.

Marchesetti's (1890) work did not add any more observations to the distribution of glacial deposits other than Gumprecht's, although Marchesetti dealt in detail with the age of the Staro Selo

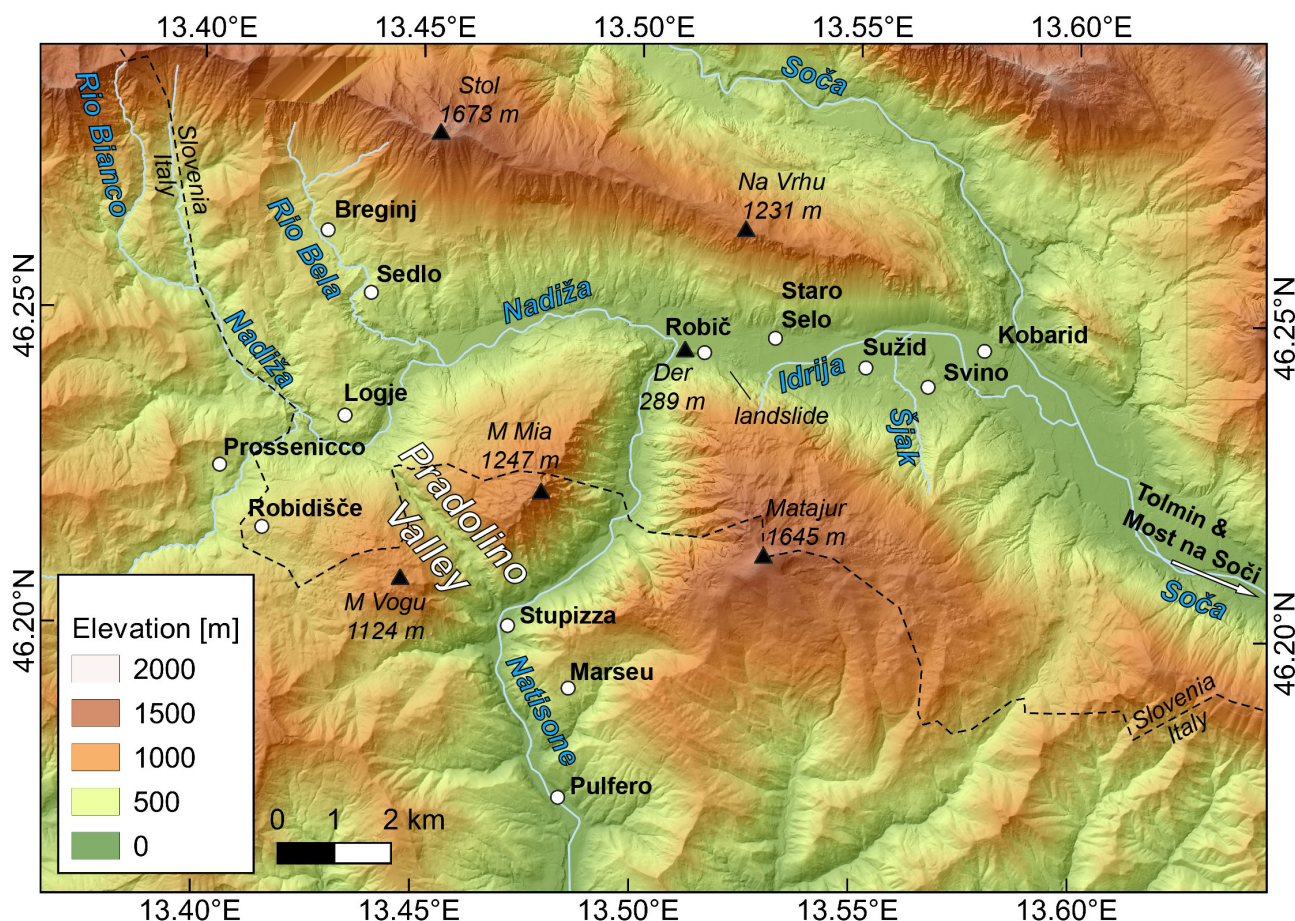


Fig. 1. Map of the study area in NE Italy and W Slovenia. Digital elevation data are from ARSO (2020) and Tarquini et al. (2007).

valley. For example, he assumed that the rockfall near Robič might have occurred in 586 AD based on local oral tradition and the limited amount of erosion that can be seen in the rockfall boulders. He argued that the Nadiža could not enter the Stupizza valley in pre-glacial times, such that it had to flow towards the Soča, where large lakes had formed between Kobarid and Most na Soči. A later glacial phase would then have left moraines near Staro Selo, forcing the Nadiža to flow towards Stupizza. It is argued that the finding of Roman roads and necropolises in the Kobarid area exclude Kandler's hypotheses. In general, Marchesetti followed Gumprecht's ideas, but differed in the timing of the change of the hydrological system. According to him the Soča started to flow towards Stupizza at Robič as soon as the Soča glacier advanced into the Staro Selo valley.

Brückner (1891) also rejected Kandler's hypothesis. He praised Gumprecht for his insightful work and agreed with him that archaeological data prove Kandler wrong – a Roman floor was found in Robič and a Roman graveyard was unearthed near Kobarid, both showing that the palaeolandscape in Roman times was similar to today's. Brückner, however, also noted that the

drainage divide near Staro Selo is almost exclusively formed by mass movement deposits from the Robič landslide, thereby disagreeing with Gumprecht.

Marinelli (1894) interpreted the Pradolino valley as a former course of the Nadiža/Natisone mainly based on observations on the morphology and the elevations of the past and present river courses. He stated that the abandonment of the Pradolino gorge must significantly pre-date the formation of the moraine that can be found in the Staro Selo valley (here he was citing Marchesetti, 1890, because he himself was not able to verify a moraine near Staro Selo). Due to backward incision, the Nadiža then occupied its present-day course. Marinelli also reported that the Pradolino valley exhibits W-dipping Triassic to Eocene strata and claimed that knowledge on the Friulian hydrography is still incomplete.

Tellini (1898) reported in detail on the glacial remains and lake deposits around Logje and Prossenicco, which testify to the Pleistocene glaciers having reached this area and to the fact that the present course of the Nadiža was once blocked by a glacier that created a glacial lake. According to him, sedimentological observations

indicate repeated glacial advances and retreats. Interestingly, Tellini remarked that this observation demonstrates the considerable length of the interglacial period, and he regretted that the lack of quarries does not allow a detailed paleontological study to prove his hypothesis. He regarded conglomerates found near Robič, Robidišče (ital. *Robedischis*), and Svino (ital. *Svina*) as preglacial and concluded that the Nadiža/Natisone occupied the Pradolino valley in preglacial times. Tellini stated that he follows the earlier ideas of Gumprecht (1886) and Marinelli (1894) that the Pradolino valley is a former course of the Nadiža/Natisone, which was occupied by the river when the Soča glacier blocked the main valley near Robič. The deep incision of the gorge led him to assume that it must have been occupied by the Nadiža/Natisone for longer times. The ideas of a long-lasting lake system between Most na Soči and Kobarid lacks geological evidence according to his observations. He mentioned that no moraines can be found in the Nadiža/Natisone valley south of Robič, which led him to assume that the incision of this valley is mainly post-glacial. Tellini also mentioned earlier observations by Taramelli (1870) that the Soča glacier reached at least until Robič and discussed the field observations of Gumprecht (1886). In Tellini's opinion, Gregorutti (1890) was too strict when stating there was never a connection between Nadiža and Soča. He also mentioned that glacial deposits in that area were depicted on the geological map of von Hauer (1868) and in the one that accompanied the publication of Gumprecht (1886).

Penck and Brückner (1909) rejected Tellini's (1898) hypothesis that conglomerates of the lower Natisone valley are of Villafranchian age and would, thus, testify to a ~Pliocene occupation of the Pradolino valley by the river. Instead, Penck and Brückner (1909) interpreted these deposits as typical "*Niederterrassenschotter*", i.e., from the Würm stage. Based on Kossmat's report of such terrace deposits near Logje (Kossmat, 1907, and private communication between Penck and Brückner and Kossmat) they argued that a glacier may well have blocked the present-day course of the Nadiža and led to drainage through the Pradolino valley. The limited amount of incision of the Pradolino valley near Stupizza allows drawing conclusions on the thickness of the glacier according to Penck and Brückner (1909) – the sediments would have been deposited on top of this glacier. Despite this, Penck and Brückner supported most of Tellini's ideas and applauded him for thoroughly referencing the available lit-

erature, but also stated that Tellini apparently missed Brückner (1891).

Feruglio (1929) briefly described the glacial system of the Soča glacier and its deposits around Prossenico and Breginj (ital. *Bergogna*). He stated that the glacier blocked the valley and caused a glacial lake, and that the melt waters temporarily flowed through the Pradolino gorge.

The study area gained new attention several decades after these early works. For example, Tunis and Venturini (1987) detailed on the stratigraphy of the region and reported a section through the Pradolino valley, in which they mapped dip-slip faults striking  $\sim 70^\circ$ , more or less perpendicular to the gorge. Later, Tunis and Venturini (1997) provided further details on the stratigraphy and the paleogeographic evolution, building upon their earlier works (e.g., Tunis and Venturini, 1984, 1986, 1987, 1992; Venturini and Tunis 1988, 1991, 1992, 1996).

Muscio & Zucchini (1997) briefly discussed the origin of the Pradolino valley and followed the interpretation of Marinelli (1894, 1912) and Cavallin & Martinis (1980), who regarded it as a paleo-course of the Nadiža/Natisone, which was later abandoned due to incision of the river into its current bed. They stated that the depressions at the base of the Pradolino valley are not only the results of karst phenomena (dolines) but that their formation was also related to the presence of faults that run  $\sim$ perpendicular to the gorge, forming vertical steps in the strata.

In the same publication, Vaia (1997) dealt in detail with the geomorphology of the Pradolino valley. Although the text does not provide too much detail and individual observations, Vaia presented a six-step model for the evolution of the Nadiža/Natisone since the Pliocene, modified from Tellini (1898). First, in the Pliocene, a drainage divide existed between the Rio Bela and the upper course of the Nadiža; this ridge was connected to M. Mia and caused the Nadiža/Natisone to flow through the Pradolino valley towards Stupizza. The Rio Bela occupied what is now the Nadiža valley downstream of Logje but continued east towards Kobarid through the Staro Selo valley. Between M. Mia and Matajur another drainage divide existed in the valley south of Robič. Second, backward erosion led to drainage capture of the Nadiža by the Rio Bela system south of Logje. The Nadiža/Natisone abandoned the Pradolino valley (probably aided by normal faulting that caused NW-facing steps in the gorge) and flowed towards Robič, from where it continued towards Kobarid. Third, in a phase of glacial advance, the

Soča glacier blocked the Staro Selo valley all the way up to Podbela (ital. *Podbiela*) and caused a lake upstream. The Nadiža/Natisone re-occupied the Pradolino valley. The glacier's meltwater spilled over the drainage divide between M. Mia and Matajur, paving the way for the future Nadiža/Natisone. However, Vaia's figure includes a lake upstream of this drainage divide, indicating that he assumes it was only partially eroded. Fourth, when the glacier retreated beyond Robič, the Nadiža/Natisone again abandoned the Pradolino valley and had to flow south from Robič towards Stupizza and Pulfero. A lake was supposed to still have existed behind the former drainage divide between M. Mia and Matajur. Fifth, in the post-glacial phase, moraines remaining in the Staro Selo valley continued to block the old path of the Nadiža. Vaia assumed a lake persisted as the Nadiža was still partially dammed between Robič and Stupizza. Sixth, apparently showing the present-day configuration, the moraines in the Staro Selo valley now act as the watershed between the Nadiža/Natisone and the Soča systems. No lake exists south of Robič anymore.

Zendron (2018) summarized the research history of the Šušterjova Jama, a cave ca. 3 km south of the Pradolino valley. She mentioned that the formation of the cave might have been aided by the erosive power of the Natisone. Citing Muscio et al. (1980), the author stated that the mouth of the Pradolino valley is ten metres above the location of the cave, and that the gorge is a former course of the Natisone.

### Previous works compared with our model

The model that we developed in Diercks et al. (2021) is in line with the proposed six-stage evolution by Vaia (1997) based on Tellini (1898). We did neither include the location and extent of glacial lakes, nor did we work on the Pliocene course of the Nadiža/Natisone. The idea of a Pliocene paleo- Nadiža/Natisone that ran through the Pradolino gorge (Vaia, 1997, after Tellini, 1898) is attractive since it would remove the need for exceptionally high incision during the glacials as we have assumed in Diercks et al. (2021). In Vaia's view, the Pradolino valley was already established before the glaciations. However, this model would require significant erosion of the watershed near Logje to establish the present-day fluvial system. None of our own field observations is suitable to solve this question. We also concluded that the only possibility to form the wide valley of Staro Selo is that it was the pre-glacial course of the Nadiža.

### Location of the Predjama Fault

The fact that we were kindly pointed to literature that we had not been aware of when writing Diercks et al. (2021) also raises the question if the north-western segment of the Predjama Fault runs through the Pradolino valley. The models of Vaia (1997) and earlier authors do not assume that the formation of the Pradolino valley was aided by tectonically weakened rocks in a fault zone underlying the gorge. We speculated that the Predjama Fault could probably run through the Pradolino valley, (i) because the valley is parallel to the general active fault trend in the area (Atanackov et al., 2021), (ii) because a morphological lineament can be seen on LiDAR data (similar to the trace of the fault as depicted by Moulin et al., 2014), and (iii) because the fault is drawn on several published maps. We did not map the fault in the field ourselves.

Kossmat's (1908) map shows a fault along the Pradolino valley, without further detailing its source. Fabiani et al. (1937) did not show a fault in their 1:100,000 geological map sheet Tolmino. Pirini Radrizzani et al. (1986, Fig. 19) drew a dashed line along the Pradolino valley in their map, indicating a potential or probably buried fault (*presunte o coperte*). These authors also showed a couple of short faults perpendicular to the Pradolino valley. The maps of Tunis & Venturini (1997) and Mocchiutti (1997) do not show a fault along the Pradolino valley, but the previously mentioned faults perpendicular to the gorge. Their studies relied on very detailed mapping of the area, during which a fault that manifested in sheared limestones likely would have been noticed. Carulli's (2006) 1:150,000 geological map of Friuli Venezia Giulia shows the Predjama Fault to run SW of the Pradolino valley and in a more westerly direction. The 1:250,000 geological map of Slovenia (Buser, 2009) shows a fault that enters the Pradolino valley from the northwest, parallel to the general strike of active faults in the region. Kokošin & Gosar (2013) did not mention the Predjama Fault in the area of Logje in their microzonation study. Moulin et al. (2014) suggested the Predjama Fault to run through the Pradolino valley. In Moulin et al. (2016), the north-western tip of the Predjama Fault lies at the entrance of the Pradolino valley near Stupizza.

If the Predjama Fault does not run beneath the Pradolino valley as indicated by most of the Italian studies, there is no reason to assume that the gorge developed due to an inherited weakness of the rocks. Instead, the erosive power of

the melt waters – and perhaps the paleo-Nadiža/Natisone – alone would be responsible for the spectacular incision.

### Conclusions

Numerous studies published in Italian and German have dealt with the evolution of the Nadiža/Natisone and the Pradolino valley. After an intense debate in the late 19<sup>th</sup> and early 20<sup>th</sup> centuries, the model by Vaia (1997) after Tellini (1898) seems to be widely accepted. Our own conclusions drawn from field observations and geomorphological data are fully compatible with this model. If the Predjama Fault does not run through the Pradolino valley (see for example the detailed mapping of Tunis and Venturini, 1997), the idea that a former course of the Nadiža/Natisone created the proto-gorge (Vaia, 1997) seems plausible.

### Acknowledgements

We are indebted to our colleagues who have pointed us towards the literature that we had overlooked and who helped us to get access to the Italian literature.

### References

- ARSO – Environmental Agency of the Republic Slovenia, 2019: 1-meter LiDAR DEM Slovenia, open-access download <http://gis.arso.gov.si/> (accessed 5/2019).
- Atanackov, J., Jamšek Rupnik, P., Jež, J., Celarc, B., Novak, M., Milanič, B., Markelj, A., Bavec, M. & Kastelic, V. 2021: Database of active faults in Slovenia: compiling a new active fault database at the junction between the Alps, the Dinarides and the Pannonian Basin tectonic domains. *Frontiers in Earth Science*, 9: 151. <https://doi.org/10.3389/feart.2021.604388>
- Brückner, E. 1891: Eiszeit-Studien in den südöstlichen Alpen. *Jahresbericht der Geographischen Gesellschaft von Bern*.
- Buser, S. 2009: Geološka karta Slovenije 1: 250.000. Geološki zavod Slovenije, Ljubljana.
- Carulli, G.B. 2006: Carta Geologica del Friuli Venezia Giulia 1: 150.000. Regione Autonoma Friuli Venezia Giulia, Direzione Regionale Ambiente e Lavori Pubblici, Servizio Geologico Regionale, SELCA Firenze.
- Cavallin, A. & Martinis, B. 1980: I movimenti recenti ed attuali della regione Friulana. In *Alto*, 58, Udine.
- Diercks, M., Grützner, C., Vrabec, M. & Ustaszewski, K. 2021: A model for the formation of the Pradol (Pradolino) dry valley in W Slovenia and NE Italy. *Geologija*, 64/1: 21–33. <https://doi.org/10.5474/geologija.2021.002>
- Fabiani, R., Kossmat, F. & Winkler, A. 1937: Carta geologica delle tre Venezie, Foglio 26 Tolmino. Firenze.
- Feruglio, E. 1929: Note illustrative della carta geologica delle Tre Venezie foglio „Udine“. Società Cooperativa Tipografica, Padova.
- Gregorutti, C. 1890: L'antico Timavo e le vie Gemina e Postumia. *L'Archeografo triestino: raccolta di opuscoli e notizie per Trieste e per l'Istria*. Serie 2, XVI (XX), Trieste.
- Gumprecht, O. 1886: Der mittlere Isonzo und sein Verhältnis zum Natisone: ein Beitrag zur Lösung der Frage nach dem Alter des Isonzosystems. Dissertation Universität Leipzig.
- Kandler, P. 1864: Discorso sul Timavo. Lloyd Austriaco, Trieste.
- Kandler, P. 1867: Discorso sulla Giulia e sulle strade antiche che l'attraversarono. Lloyd Austriaco, Trieste.
- Kokošin, J. & Gosar, A. 2013: Seismic microzonation of Breginjski kot (NW Slovenia) based on detailed engineering geological mapping. *The Scientific World Journal*, 2013. <https://doi.org/10.1155/2013/626854>
- Kossmat, F. 1907: Geologie des Wocheinertunnels und der südlichen Anschlusslinie. *Denkschriften der. math.-nat. Kl. der k. Akademie der Wiss., LXXXII, 4<sup>o</sup>*, Wien.
- Kossmat, F. 1908: Beobachtungen über den Gebirgsbau des mittleren Isonzgebietes. *Verhandlungen der Geologischen Bundesanstalt*, Wien, p. 69–84.
- Marchesetti, C. 1890: Sull'antico corso del fiume Isonzo. *Tip. del Lloyd Austro-Ungarico*. Trieste.
- Marinelli O. 1894: La chiusa di Pradolino (Valle del Natisone). In *Alto*, 5/5: 73–74.
- Marinelli, O. 1912: Guida delle Prealpi Giulie. *Soc. Alpina Friul.*, pp. 804.
- Mocchiutti, A. 1997: I depositi chimici secondari delle grotte delle Valli del Natisone. Il fenomeno carsico delle Valli del Natisone. *Mem. Ist. It. Spel.* s. II. vol. IX., 49–56.
- Moulin, A., Benedetti, L., Gosar, A., Jamšek Rupnik, P., Rizza, M., Bourlès, D. & Ritz, J. F. 2014: Determining the present-day kinematics of the Idrija fault (Slovenia) from airborne LiDAR topography. *Tectonophysics*, 628: 188–205. <https://doi.org/10.1016/j.tecto.2014.04.043>
- Moulin, A., Benedetti, L., Rizza, M., Jamšek Rupnik, P., Gosar, A., Bourlès, D.,

- Keddadouche, K., Aumaître, G., Arnold, M., Guillou, V. & Ritz, J. F. 2016: The Dinaric fault system: Large-scale structure, rates of slip, and Plio-Pleistocene evolution of the transpressive northeastern boundary of the Adria microplate. *Tectonics*, 35/10: 2258-2292. <https://doi.org/10.1002/2016TC004188>
- Muscio, G., Vaia, F. & Zucchini, R. 1980: Suosteriova Jama. (Fr. 300, Val Natisone): note geomorfologiche. *Mondo sotterraneo n.s.*, 4/1: 33-40.
- Muscio, G. & Zucchini, R. 1997: La Valle di Pradolino ed il Monte Mia ed i loro fenomeni carsici. Il fenomeno carsico delle Valli del Natisone. *Mem. Ist. It. Spel. s. II. vol. IX.*, 127-130.
- Penck, A. & Brückner, E. 1909: Bd. Die Eiszeiten in den Südalpen und im Bereich der Ostabdachung der Alpen. 3. Chr. Herm. Tauchnitz.
- Pirini Radrizzani, C., Tunis, G. & Venturini, S. 1986: Biostratigrafia e paleogeografia dell'area sud-occidentale dell'anticlinale M. Mia-M. Matajur (Prealpi Giulie). *Rivista Italiana di Paleontologia e Stratigrafia*, 92/3.
- Stache, G. 1889: Übersicht der geologischen Verhältnisse der Küstenländer von Österreich- Ungarn. *Abh. d. k. k. geol. Reichsanstalt, Wien.*
- Štúr, D. 1858: Das Isonzo-Thal von Flitsch abwärts bis Görz, die Umgebungen von Wippach, Adelsberg, Planina und die Wochein. *K. k. geologische Reichsanstalt, 9. Jahrgang. III.*
- Taramelli, T. 1870: Sugli antichi ghiacciai della Drava, della Sava e dell'Isonzo. *Atti Soc. It. Sc. Nat. Milano*, XIII, 1-16.
- Taramelli, T. 1871: Escursioni geologiche fatte nell'anno 1871. *Ann. Ist. Tecnico di Udine, Anno V.*
- Taramelli, T. 1875: Dei terreni morenici ed alluvionali del Friuli. *Udine.*
- Taramelli, T. 1882: *Geologia delle Provincie Venete.* Reale Accademia Dei Lincei, Roma.
- Tarquini S., Isola I., Favalli M. & Battistini A. 2007: TINITALY, a digital elevation model of Italy with a 10 meters cell size (Version 1.0) [Data set]. Istituto Nazionale di Geofisica e Vulcanologia (INGV). <https://doi.org/10.13127/TINITALY/1.0>
- Tellini, A. 1898: Intorno alle tracce abbandonate da un ramo dell'antico ghiacciaio del Fiume Isonzo nell'alta valle del Fiume Natisone e sull'antica connessione tra il corso superiore dei due fiumi. *Tipografia Seitz, Udine.*
- Tunis, G. & Venturini, S. 1984: Stratigrafia e sedimentologia del flysch maastrichtiano-paleocenico del Friuli Orientale. *Gortania, Atti Mus. Friul. Storia Nat.*, 6: 5-58.
- Tunis, G. & Venturini, S. 1986: Nuove osservazioni stratigrafiche sul Mesozoico delle Valli del Natisone (Friuli orientale). *Gortania, Atti Mus. Friul. Storia Nat.*, 8: 17-68.
- Tunis, G. & Venturini, S. 1987: New data and interpretation on the geology of the Southern Julian Prealps (Eastern Friuli). *Mem. Soc. Geol. It.*, 40: 219-222.
- Tunis, G. & Venturini, S. 1992: Evolution of the southern margin of the Julian Basin with emphasis on the megabeds and turbiditic sequence of the Southern Julian Prealps (NE Italy). *Geol. Croatica*, 45: 127-150. <https://doi.org/10.4154/GC.1992.10>
- Tunis, G. & Venturini, S. 1997: La geologia delle Valli del Natisone. Il fenomeno carsico delle Valli del Natisone. *Mem. Ist. It. Spel. s. II. vol. IX.*: 35-48.
- Vaia, F. 1997: Caratteri morfologici delle Valli del Natisone. *Mem. Ist. It. Spel. s. II. vol. IX.*: 27-34.
- Venturini, S. & Tunis, G. 1988: Nuovi dati ed interpretazioni sulla tettonica del settore meridionale delle Prealpi Giulie e della regione al confine tra Italia e Jugoslavia. *Gortania - Atti Mus. Friul. Storia Nat.*, 10: 5-34.
- Venturini, S. & Tunis, G. 1991: Nuovi dati stratigrafici, paleoambientali e tettonici sui Flysch di Cormons (Friuli Orientale). *Gortania - Atti Mus. Friul. Storia Nat.*, 13: 5-30.
- Venturini, S. & Tunis, G. 1992: La composizione dei conglomerati cenozoici del Friuli: dati preliminari. *St. Geol. Camerti, CROP I*: 285-296.
- Venturini, S. & Tunis, G. 1996: Riflessioni sulla fase tettonica mesoalpina nel Sudalpino orientale. *Natura nascosta*, 12: 22-31.
- von Czoernig, C. 1873: *Das Land Görz und Gradisca (mit Einschluss von Aquileja).* Wien.
- von Hauer, F. R. 1868: *Geologische Uebersichtskarte der Oesterreichischen Monarchie (Blatt VI).* K. k. geologische Reichsanstalt.
- Zendron, F. 2018: Šuošterjova Jama (Pulfero, Udine). *Storia delle ricerche. Gortania - Geologia, Paleontologia, Paleontologia*, 40: 105-119.





# Multi-method study of the Roman quarry at Podpeč sedimentary succession and stone products

## Večmetodne raziskave sedimentarnega zaporedja in kamnitih izdelkov rimskodobnega kamnoloma v Podpeči

Rok BRAJKOVIČ<sup>1</sup>, Luka GALE<sup>1,2</sup> & Bojan DJURIČ<sup>3</sup>

<sup>1</sup>Geological Survey of Slovenia, Dimičeva ul. 14, SI-1000 Ljubljana, Slovenia; e-mail: rok.brajkovic@geo-zs.si; luka.gale@geo-zs.si

<sup>2</sup>Faculty of Natural Sciences and Engineering, Department of Geology, Aškerčeva 12, SI- 1000 Ljubljana, Slovenia; e-mail: luka.gale@ntf.uni-lj.si

<sup>3</sup>Faculty of Arts, Department of Archaeology, Aškerčeva 2, SI-1000 Ljubljana, Slovenia; e-mail: bojan.djuric@gmail.com

Prejeto / Received 7. 3. 2022; Sprejeto / Accepted 15. 7. 2022; Objavljeno na spletu / Published online 22. 07. 2022

*Key words:* Lower Jurassic, Podbukovje Formation, provenance, facies, foraminifera, geochemistry, Emona, geoarchaeology

*Ključne besede:* spodnja jura, Podbukovška formacija, provenienca, facies, foraminifere, geokemija, Emona, geoarheologija

### Abstract

The paper presents a multi-method characterisation of the Roman quarry of the middle Lower Jurassic (Pliensbachian) limestone situated in the village of Podpeč, south of Ljubljana, and examples of the placement of stone products made from micritic, fine-grained, and oolitic facies into the known extent of the quarry. 23 m of the rock succession from the ancient quarry was exposed at the northern tip of the St. Ana Hill by archaeological trenching. Petrological, micropaleontological, mineralogical, geochemical, and isotopic analyses of carbon, oxygen, and strontium were performed in order to characterise the rocks exploited in the quarry. Additionally, a new detailed geological map of the wider Podpeč area was prepared, which defines in detail the lithostratigraphic units in the area.

The recorded succession contains facies that also occur in the modern part of the quarry. Interpretation of the sedimentation environment is consistent with previous interpretations and occurred in an internally differentiated lagoon. The studied succession is characterised by  $\delta^{13}\text{C}$  isotope values ranging from -2.44 to +2.5 ‰;  $\delta^{18}\text{O}$  values ranging from -4.0 to -1.2 ‰; and  $^{87}\text{Sr}/^{86}\text{Sr}$  values ranging from 0.707414 ‰ (SD 0.000003) to 0.707329 ‰ (SD 0.000012). The Sr isotope values can prove a decisive factor when studying the provenance of stone products, while  $\delta^{13}\text{C}$  and  $\delta^{18}\text{O}$  values can help narrow the place of extraction within the known extent of the Roman quarry at Podpeč. The high positive correlation of  $\text{SiO}_2$  with  $\text{Al}_2\text{O}_3$ ,  $\text{K}_2\text{O}$  and  $\text{TiO}_2$  recognised both in the logged succession and in the studied stone products indicates a low terrigenous input into the depositional area and further confirms the provenance determination.

By applying a multi-method approach to the characterisation of the known extent of the ancient part of the Podpeč quarry, we have reliably determined the provenance of stone products that have their origin in the quarry and have successfully applied this approach to several stone products made of micritic, fine-grained and oolitic limestones.

### Izvešček

Članek predstavlja večmetodno karakterizacijo rimskega kamnoloma v vasi Podpeč južno od Ljubljane in primere umeščanja apnenca kamnitih izdelkov iz spodnjeljurskih (pliensbachijskih) mikritnih, drobnozrnatih in oolitnih faciesov v znan obseg kamnoloma. Na severnem robu hriba sv. Ane je bilo z arheološkimi izkopi razkrito 23 m debelo kamninsko zaporedje antičnega kamnoloma. Za karakterizacijo kamnin, ki so jih izkoriščali v kamnolomu, so bile opravljene petrološke, mineraloške, mikropaleontološke in geokemične analize ter izotopske analize ogljika, kisika in stroncija. Poleg tega je bila izdelana nova podrobna geološka karta širšega območja Podpeči, na kateri so natančno opredeljene litostratigrafske enote na tem območju.

Preučeno zaporedje vsebuje faciese, ki se pojavljajo tudi v sodobnem delu kamnoloma. Potrjena je bila interpretacija sedimentacije v notranje diferencirani laguni. Za preučeno zaporedje so značilne vrednosti izotopov  $\delta^{13}\text{C}$  od -2,44 do +2,5 ‰, vrednosti  $\delta^{18}\text{O}$  od -4,0 do -1,2 ‰ in vrednosti  $^{87}\text{Sr}/^{86}\text{Sr}$  od 0,707414 ‰

(SD 0,000003) do 0,707329 ‰ (SD 0,000012). Izotopske vrednosti Sr lahko uporabimo kot najzanesljivejši podatek pri določitvi izvora kamnitih izdelkov, vrednosti  $\delta^{13}\text{C}$ ,  $\delta^{18}\text{O}$  pa lahko pomagajo pri zožitvi opredelitve mesta pridobivanja znotraj znanega zaporedja plasti rimskega kamnoloma v Podpeči. Visoka pozitivna korelacija  $\text{SiO}_2$  z  $\text{Al}_2\text{O}_3$ ,  $\text{K}_2\text{O}$  in  $\text{TiO}_2$ , ugotovljena v preučnem zaporedju in kamnitih izdelkih, kaže na majhen vnos terigene komponente v primarno sedimentacijsko okolje ter dodatno potrjuje določitev provenience.

Z uporabo večmetodnega pristopa h karakterizaciji znanega obsega antičnega dela Podpeškega kamnoloma smo omogočili zanesljivo določitev izvora kamnitih izdelkov iz kamnoloma in ta pristop uspešno uporabili na več kamnitih izdelkih izdelanih iz mikritnih, drobnozrnatih in oolitnih apnencev.

## Introduction

The present article follows the publication by Djurić et al. (2022), in which the authors defined the location of the ancient quarry at Podpeč and investigated the stone products with presumed origin from the quarry. Since the provenance of micritic, fine-grained, as well as partially oolithic limestones used to produce stone products could not be reliably determined using the macro- and microscopic studies presented in previous studies, further analyses were carried out and are presented in this article. This study was prepared using a multi-method approach widely used in geoarchaeology (Galan et al., 1999; Maritan et al., 2003; Brilli et al., 2010; Brilli et al., 2011; Šmuc et al., 2016; Miletić et al., 2021).

The middle Lower Jurassic (Pliensbachian) limestone from quarries at Podpeč, south of Ljubljana, is amongst the well-known dimension stones in Slovenia (Mirtič et al., 1999; Ramovš, 2000). Among the beds of different colours and textures we also find dark grey to almost black limestone with white shells of lithotid bivalves, which was particularly valued for its decorative properties throughout the 20<sup>th</sup> century (Ramovš, 2000). The history of quarrying in Podpeč,

however, goes as far back as Antiquity (Müllner, 1879; Brodar et al., 1955; Šašel Kos, 1997; Ramovš, 2000; Kramar et al., 2015; Djurić & Rižnar, 2017; Djurić et al., 2017; Djurić et al., 2022). According to Djurić et al. (2022), a well-organised and continuous production of dimension stone can be confirmed – at least for the period between the 1<sup>st</sup> and 3<sup>rd</sup> centuries AD when the area belonged to Regio X (Italia) of the Roman state. The production of stone from this area, however, may go even further back in time to the earliest beginnings of the Roman colony (Djurić & Rižnar, 2017). Most of these stone products ended up in Emona, a colony located 15 km to the north of present-day Ljubljana, which was connected to the quarry via the Ljubljanica River (Djurić & Rižnar, 2017; Djurić et al. 2018b; Djurić et al., 2022). Based on the lithological characteristics of the limestone beds, the historical topography of the village of Podpeč, and the archaeological remains, the exact location of the Roman quarry was very likely the northern tip of the St. Ana hill (Fig. 1) (Djurić et al., 2022). The entire succession exposed in both the ancient and modern Podpeč quarry, from the base of the archaeological trenches (probes) in the north, to the base of the

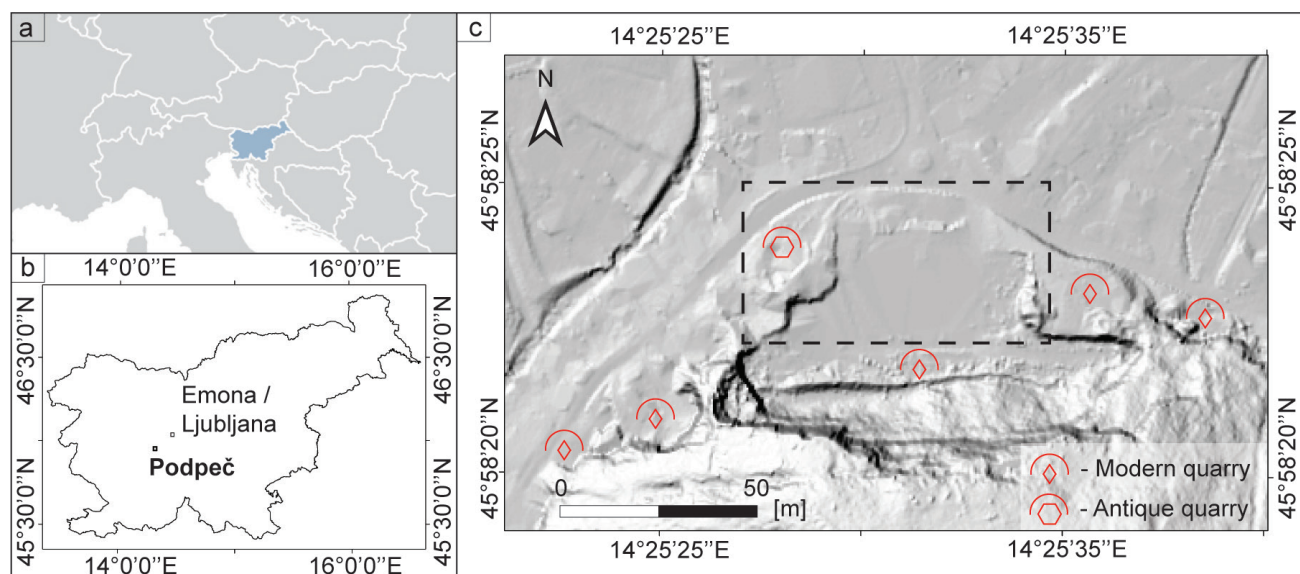


Fig. 1. Position of the main quarries at Podpeč. a: Marked position of Slovenia. b: Position of the modern village of Podpeč. c: Narrow study area at the village of Podpeč with marked position of Figure 3. The source of the topography is a 1 m × 1 m resolution digital relief model (The Surveying and Mapping Authority of the Republic of Slovenia, 2011).

Laze Formation in the south, measures 114 stratigraphic meters in thickness, and approximately 30 m of this succession is known to be quarried during the Antiquity (Djurić et al., 2022).

Covered by rubble and built upon, the surface of the antique quarry is no longer visible today. Parts of it were, however, accessible during archaeological excavations in 2016 and 2017 (Djurić et al., 2017, Djurić et al., 2022). Methodological approaches used to determine provenance can vary depending on the lithology in question, while a common denominator in the study of limestone provenance in recent decades is the multi-method approach proposed by Galan et al. (1999). This approach was recognized as the most effective and has since successfully been replicated and further developed by numerous authors (e.g. Maritan et al., 2003; Brilli et al., 2010, 2011).

Whereas the facies of the limestone beds uncovered in archaeological probes is briefly described in Djurić et al. (2022), the purpose of this paper is to provide a detailed multi-method characterisation of the beds excavated in the antique quarry and to use this data to help determine the provenance of the stone products. The hypothesis set-out held that by applying the same multi-method characterization approach to the ancient quarry and stone products samples, reliable provenance determinations of Roman stone products could also be made for micritic, fine-grained, and oolitic facies in stone products. These facies

can also be found in other possible source-areas located near Emona, e.g. Podutik (Ramovš, 1990; Vodnik, 2017) or Staje (Rožič et al., 2018). Therefore, it is important for any further studies on the provenance of stone products to define their characteristics in the ancient Podpeč quarry. In addition to the detailed multi-method characterisation of the antique Podpeč quarry and stone products, a geological map of the wider research area was prepared in order to define the stratigraphic units available for quarrying and their spatial relationships in the wider Podpeč area.

### Geological setting

The Podpeč quarry is situated in central Slovenia at the base of the St. Ana hill, which represents the northern tip of the mountain range overlooking the Barje basin. The range itself and the rocky base of the Quaternary Barje basin (Vrabec & Fodor, 2006) are structurally part of the External Dinarides thrust system (more precisely, of the Hrušica Nappe), mainly formed during the Oligocene-early Miocene (Placer, 1999; Vrabec & Fodor, 2006). The SW-verging Dinaric thrust units are largely composed of carbonate rocks, which deposited during the Mesozoic on the Adriatic Carbonate Platform (Vlahović et al., 2005). The rocky southern surroundings of the Podpeč quarry (Fig. 2a) are thus mostly formed of the Upper Triassic peritidal dolomite of the Main Dolomite Formation, the Lower Jurassic

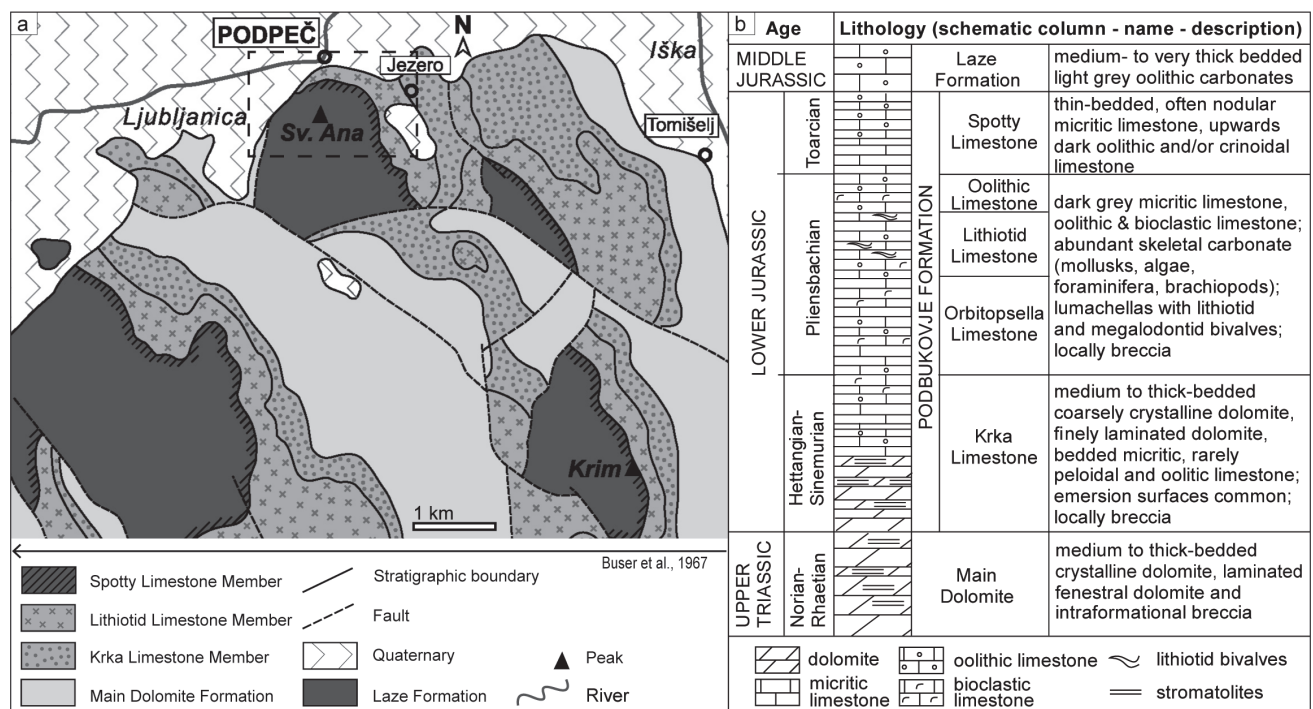


Fig. 2. Geological map of the quarry at Podpeč (modified after Buser, 1967) with stratigraphic column modified after Dozet & Strohenger (2000) with marked area (dashed rectangle) of the broader research area.

dolomites and predominant limestones of the Podbukovje Formation, and the Middle Jurassic oolitic limestones of the Laze Formation (Fig. 2b) (Buser et al., 1967; Buser, 1968; Ogorelec & Rothe, 1993; Miler & Pavšič, 2008; Ogorelec, 2009; Gale & Kelemen, 2017). The Podbukovje Formation is further divided into five members. The lowest is the Hettangian to Sinemurian Krka Limestone Member, characterised by micritic limestone successions with signs of subaerial exposure (Dozet, 2009). The Orbitopsela Limestone Member (Orbitopsella beds) is the second member, for which Pliensbachian age was determined owing to the occurrence of large *Orbitopsella foraminifera*. The stratigraphic range of this genus, however, continues to the third member, known as the Lithiotid Limestone Member (Gale, 2015), characterised by Lithiotid bivalves (Buser & Debeljak, 1995; Debeljak & Buser, 1997). The fourth member is the Oolitic limestone (Dozet, 2009), still Pliensbachian in age. The Podbukovje Formation ends with the dark micritic Toarcian Spotty Limestone Member. This in turn gradually passes into the Middle Jurassic oolitic limestone of the Laze Formation (sensu Dozet & Strohmenger 2000).

### Material and methods

The broader research area was geologically mapped at a scale of 1: 5000.

The lithological succession in the antique quarry in Podpeč was logged in three probes (archaeological trenches) dug in the years 2016–2017 immediately north and northwest of the modern quarry, at the northernmost base of the St. Ana hill. An additional section was logged in the basement of House Podpeč 44 (Fig. 3). Based on these partial sections, a composite section 23 m thick was reconstructed, which is stratigraphically older than the Lithiotid Limestone Member from the exposed part of the modern quarry. During logging, samples of rock were taken from each bed. Thin sections (47 × 28 mm in size) were made from representative samples of each lithofacies. Finely ground surfaces of hand-specimens, as well as thin sections, were scanned with a high-resolution optical scanner. Thin sections were further investigated using a polarizing optical microscope. Limestone varieties were named according to classification by Dunham (1962), with modifications by Embry and Klovan (1971). In adding the components to the names of the samples we have followed the recommendations by Wright (1992) and express the predominant component first.

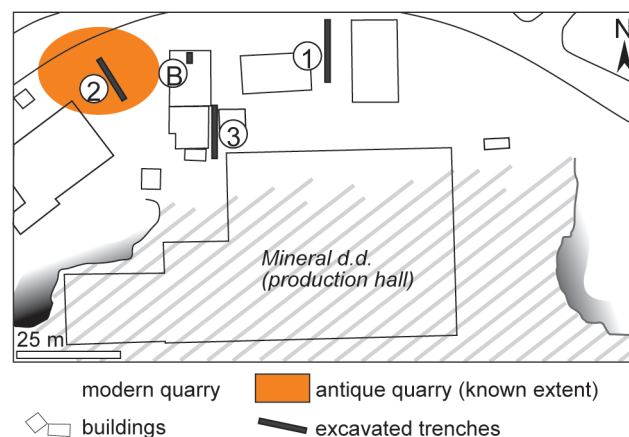


Fig. 3. Position of the excavated probes (archaeological trenches) that re-exposed the Roman quarry. The numbers 1–3 of the probes refer to sedimentary section logs presented in Fig. 5. Letter B denotes the outcrop in the basement of the house Podpeč 44.

The colour of the dry, broken surface of the stone was determined using the standardised Rock Color Chart (Munsell Color, 2010).

Mineralogical composition, concentrations of major, minor, and trace elements, and the isotopic composition of strontium, oxygen, and carbon isotopes of the samples from the ancient part of the quarry were measured. The analysis was performed on bulk rock samples. All secondary features (calcite veins, void fillings) were removed from the samples to obtain the geochemical values of the rock matrix.

Mineralogical composition was determined for seven samples. From each sample, 5 g of the rock was powdered and analysed with an X-ray diffractometer (XRD) Philips PW3710 under the following conditions: power 1.2 kW, voltage 40 kV, current 30 mA, wavelength of X-ray light with copper tube and  $K\alpha$ -rays 1.5460 Å. A secondary graphite monochromator and a proportional counter were used. The continuous recording range was 2° – 70° 2 $\theta$ , at a rate of 3°/min. The mineralogical composition of the samples was determined using the X'Pert Highscore Plus computer programme. The measurements and analysis were carried out at the University of Ljubljana, Faculty of Natural Sciences and Engineering, Department of Geology.

Concentrations of major, minor, and trace elements were measured in Actlabs (Canada) from 16 samples (each weighing 5 g) using Fusion-ICP-MS. The accuracy of the measurements was ensured by certified lab standards, while precision was ensured by duplicating measurements. All values reported deviate from replicate samples by less than 2.15 %.

Samples for stable isotope values of  $\delta^{18}\text{O}$  and  $\delta^{13}\text{C}$  were taken in 90 cm intervals or less. Isotope values were measured for 37 samples (1 g in size) at the GeoZentrum Nordbayern laboratory at the University of Erlangen, Germany, using a Gasbench II connected to a ThermoFisher Delta V Plus mass spectrometer (Rosenbaum & Sheppard, 1986; Kim & Taylor, 2007). Results are given in the notation  $\delta\text{‰}$  (per mil) with respect to the international PDB scale. Reported reproducibility of the calibration standards was 0.05 SD for  $\delta^{13}\text{C}$  and 0.04 SD for  $\delta^{18}\text{O}$  isotope measurements. The effects of diagenesis were checked by cross-plotting the oxygen ( $\delta^{18}\text{O}$ ) and carbon ( $\delta^{13}\text{C}$ ) values.

Strontium ( $^{87}\text{Sr}/^{86}\text{Sr}$ ) isotope values from seven samples were prepared and measured according to the laboratory procedure (Romaniello et al., 2015) at the Department of Earth Sciences, University of Oxford, and measured by a multi-collector inductively-coupled plasma mass spectrometer (MC-ICP-MS) using a standard bracketing method and the NIST SRM 987 standard (Weis, et al., 2006). Each sample was measured three times. The instrument mass fractionation was internally corrected to  $^{86}\text{Sr}/^{88}\text{Sr} = 0.1194$ . All reported  $^{87}\text{Sr}/^{86}\text{Sr}$  ratios were normalised to SRM 987  $^{87}\text{Sr}/^{86}\text{Sr} = 0.710248$  (McArthur et al., 2012a). The external reproducibility of  $^{87}\text{Sr}/^{86}\text{Sr}$  using the NIST SRM 987 standard (Weis, et al., 2006) yielded a value of  $0.710251 \pm 0.000025$  (2SD,  $n=30$ ). The measured ratios were correlated with the Locally Weighted Regression Scatterplot Smoother (LOWESS) fit curve constructed by McArthur et al. (2012b).

In addition, stone products kept by the National Museum of Slovenia (samples marked as NMS), and the Museum in Ljubljana (samples marked as MGML) were analysed following the multi-method approach ( $n=4$ ) by using the same methods as described above. In addition, the minimum bed thickness required to produce the stone products studied was determined based on the unworked back-side of the product, which corresponds to the bedding plane.

## Results

### Geological map of Podpeč – St. Ana area

The mapped area is characterised by the presence of Mesozoic carbonates and various faults and folds (Fig. 4a). Upper Triassic Main Dolomite Formation outcrops only in the westernmost part of the mapped area, while the lowermost Jurassic

Krka Limestone Member occurs in the northeast-ernmost part. Both are in fault contact with the rest of the Lower and Middle Jurassic succession. The Lithiotid Limestone Member was mapped as a single unit consisting of an abundance of medium grey biogenic limestones. Where possible, this unit was further subdivided into the Orbitopsella Limestone Member (recognised by dark grey micritic, peloidal, and biogenic limestones without lithiotid bivalves), the Lithiotid Limestone Member, and the Oolithic Limestone Member. To the south, the Lithiotid Limestone Member or Oolithic Limestone Member passes into the Spotty Limestone Member. The Spotty Limestone Member is characterised by dark grey, thin-bedded, nodular oolithic and/or crinoidal limestones with rare micritic parts. It gradually passes into the Middle Jurassic Laze Formation. This unit consists of medium- to thick-bedded, sometimes even massive oolithic carbonates. Limestone varieties predominate at Podpeč, while mainly dolomitized oolithic limestone outcrops on the slopes of the St. Ana Hill and in the westernmost parts. The succession is dissected by strike slip and normal faults, and a SW plunging syncline was inferred from changes in the strike and dip direction of the beds. The shape of the surface is strongly modified by human activities (Fig. 4b). Numerous abandoned quarries can be found along the entire northeastern, northern, and northwestern slopes of the St. Ana hill, extending up to 100 m above the Barje basin.

### Description of sedimentological sections

The archaeological trenches exposed almost 32 m of the limestone succession. Since some trenches were positioned lateral to each other, the stratigraphic thickness of the exposed outcrops totals 23 m. Bedding planes dip at  $70^{\circ}$ – $80^{\circ}$  towards the south. Some minor fissures are present, but we could not detect any off-sets of the beds.

Two facies assemblages can be defined – the first for the lower part of the succession (probes 1 and 2, and short section Basement Podpeč 44), and a second for the upper part of the logged succession (probe 3).

Facies assemblage 1 can be defined on the prevailing occurrence of dark varieties of micritic limestone (Fig. 5). A lower energy environment can be defined for this part, interrupted occasionally by high energy events. Although probes 1 and 2 are nearly parallel to each other and perpendicular to the bedding, the logged sections differ in the thickness of the beds and to some

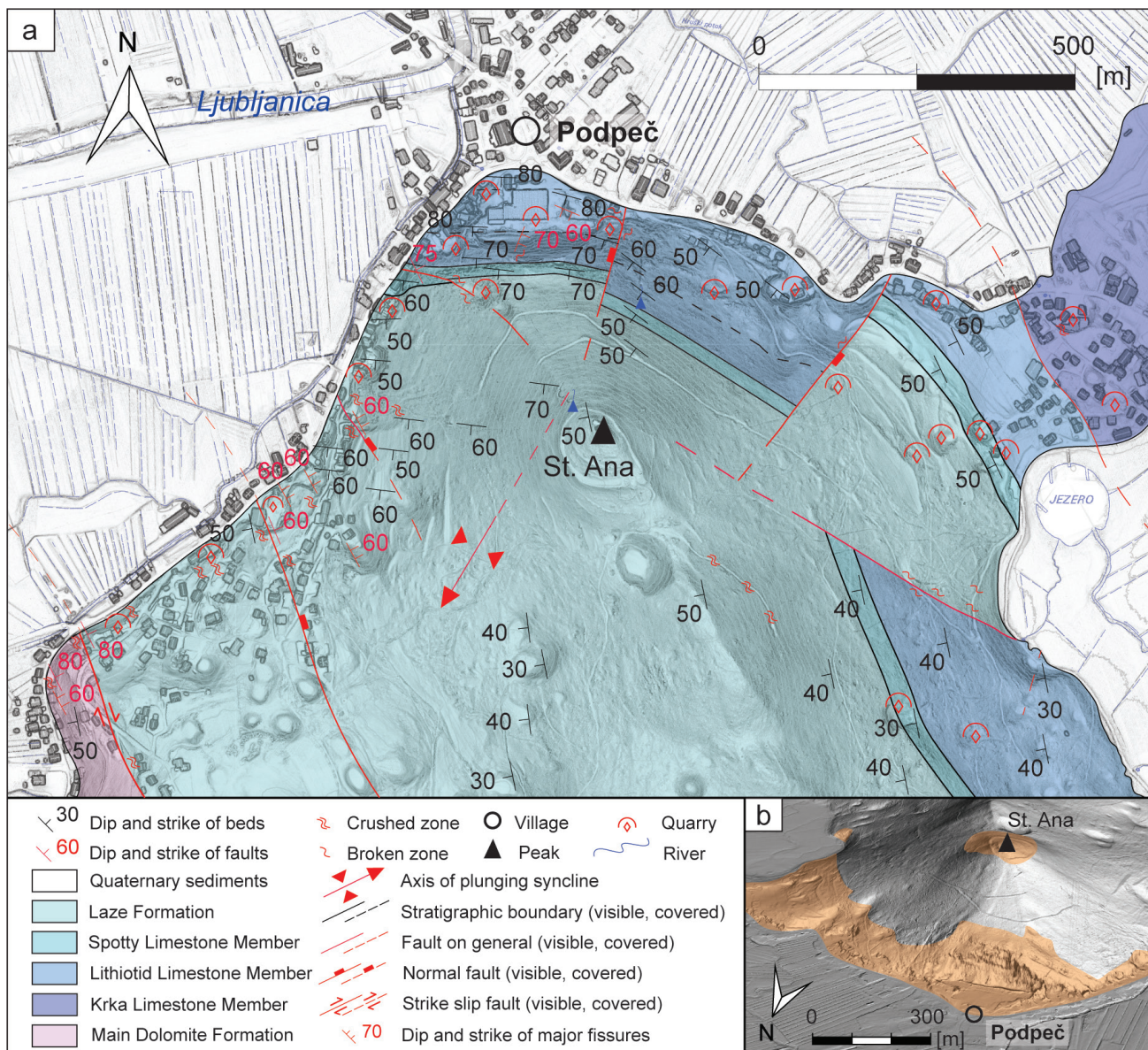
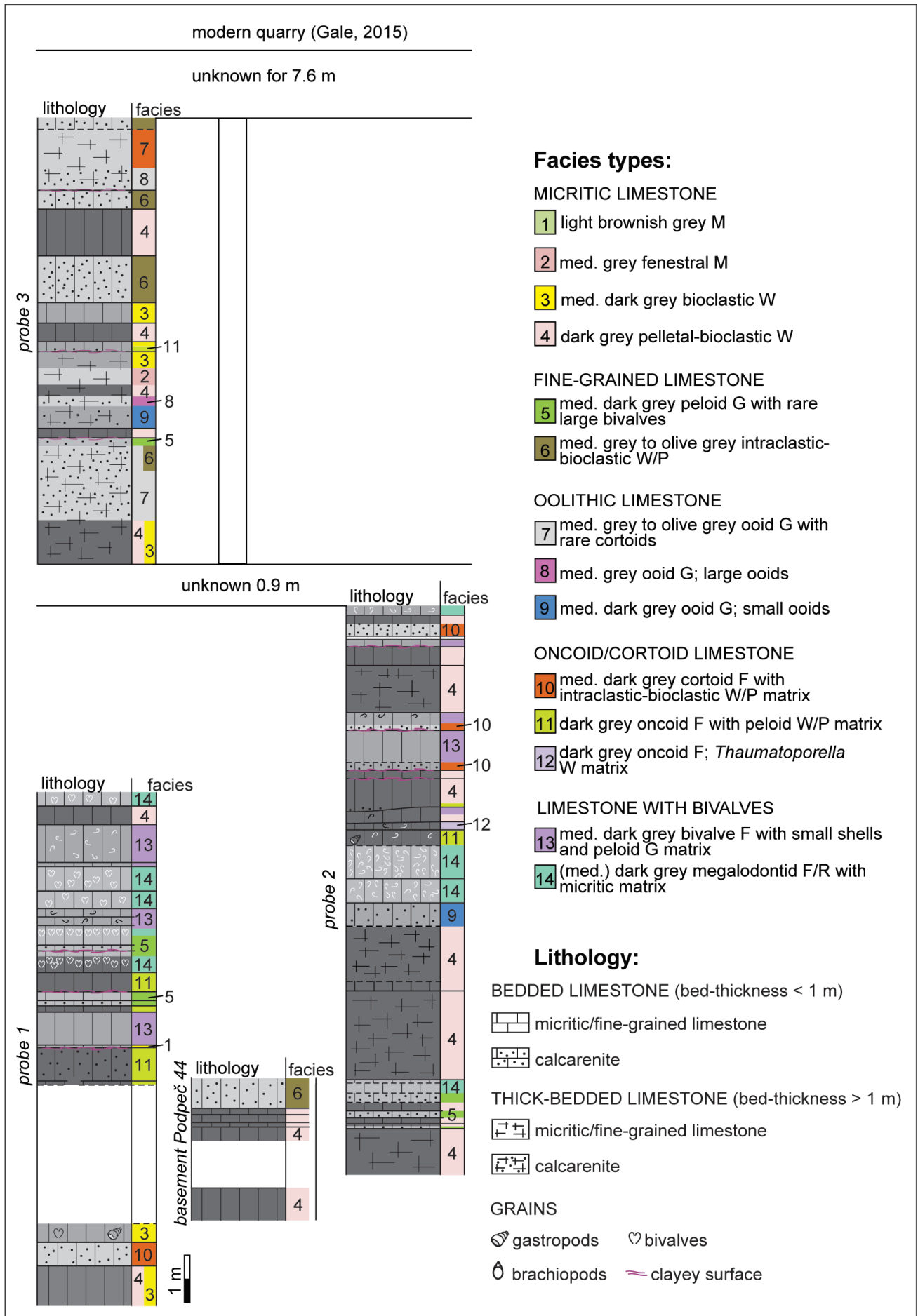


Fig. 4. a – Geological map on the scale 1: 5000 of Podpeč – St. Ana area; b – digital elevation model of Podpeč – St. Ana with marked anthropogenically altered areas. The source of the topography is a 1 m × 1 m resolution digital relief model (The Surveying and Mapping Authority of the Republic of Slovenia, 2011).

extent also in their microfacies, so the correlation between the beds is not entirely straightforward. The reason for the differences among the sections is most likely due to lateral changes in microfacies (e.g. the microfacies with megalodontid bivalves likely represents storm deposits, which may laterally pinch out), the limited availability of the outcrop (trenches were only a few decimetres wide, so some fissures could be

mistaken for bedding planes, and vice-versa), or (less likely) due to some minor fault. Despite this, the microfacies association in probes 1 and 2, as well as from the section logged in the basement of House Podpeč 44, is the same: dark micritic and fine-grained facies (microfacies 4 and 5) and limestone with bivalves predominates (microfacies 13 and 14) over microfacies with oncoids or ooids (microfacies 9–11).

Fig. 5. Sedimentological section in the scale 1: 50 of the antique quarry. Abbreviations for the textures: M- mudstone, W- wackestone, P- packstone, G- grainstone, F- floatstone, R- rudstone. Note that the facies are numbered somewhat differently than in Djurić et al. (2022) and that more varieties are distinguished here.



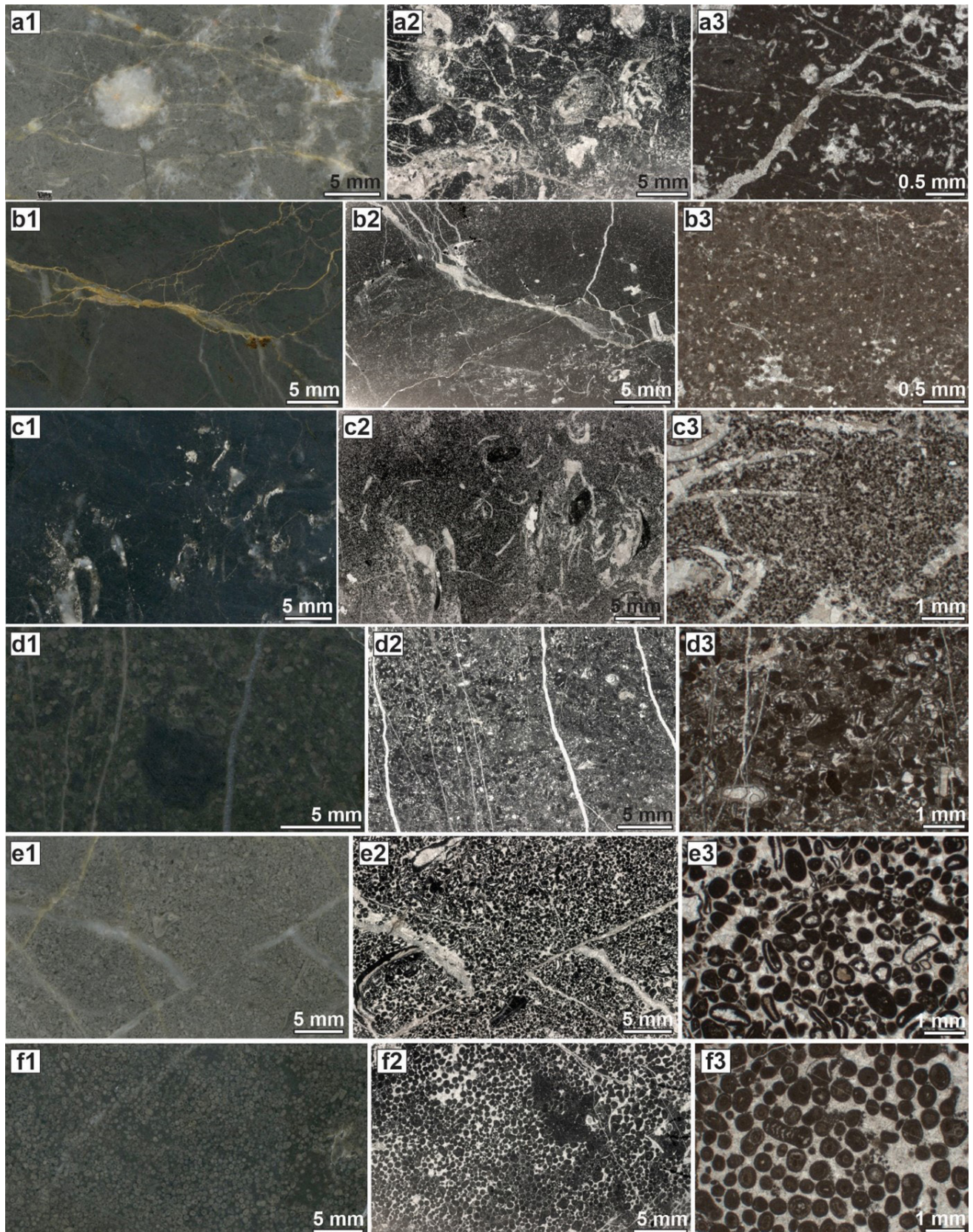


Fig. 6. Microfacies (MF) of limestone from the antique quarry at Podpeč. Numbers indicate polished surface of the stone in reflected light (1), thin section scan (2), and microphotograph of the same sample (3). a: Medium grey bioclastic wackestone (MF 3). Thin section 1689. b: Dark grey pelletal- bioclastic wackestone (MF 4). Thin section 1677. c: Medium dark grey peloid grainstone with rare larger bivalves (MF 5). Thin section 1683. d: Medium grey to olive grey intraclastic-bioclastic wackestone and packstone (MF 6). Thin section 1684. e: Medium dark grey ooid grainstone; with rare cortoids (MF 7). Thin section 1686. f: Medium dark grey ooid grainstone; large ooids (MF 8). Thin section 1691.

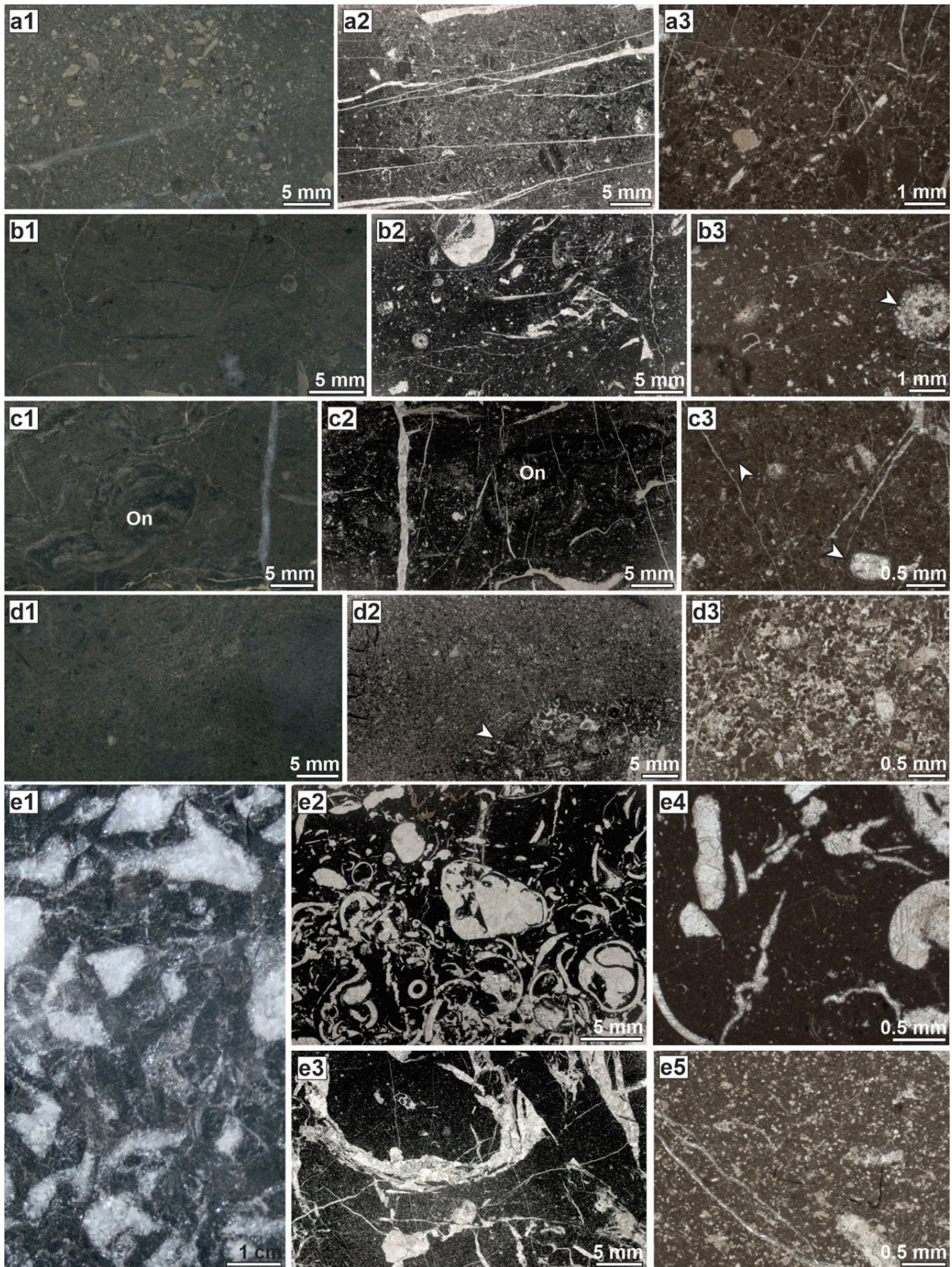


Fig. 7. Microfacies of limestone from the antique quarry at Podpeč (*continued*). a: Medium dark grey cortoid floatstone with intraclastic-bioclastic wackestone and packstone matrix (MF 10). Thin section 1690. b: Dark grey oncooid floatstone with peloid wackestone to packstone matrix (MF 11). Arrow in *b3* is pointing at the dasycladacean algae. Thin section 1681. c: Dark grey oncooid floatstone with *Thaumatoporella* wackestone matrix (MF 12). *On* indicates an oncooid. Arrows point at *Thaumatoporella*. Thin section 1688. d: Medium dark grey bivalve floatstone with small shells and peloid grainstone matrix (MF 13). Arrow points at an irregular contact with bivalve floatstone. Thin section 1680. e: (Medium) dark grey megalodontid floatstone to rudstone with micritic matrix (MF 14). Photos *e2* and *e4* are from a variety with mudstone matrix (thin section 1687), while *e3* and *e5* contain small particles of shells within the matrix (thin section 1682).

The upper part of the logged succession is attributed to facies assemblage 2. Lighter varieties of oolitic limestone (microfacies 7–9) become common along with micritic limestone. No shell deposits were found in the stratigraphically highest probe 3. A higher energy environment of sedimentation was interpreted for facies assem-

blage 2, based on the larger presence of oolitic limestones. Due to the higher energy setting, foraminifera assemblages within the oolitic microfacies cannot be considered autochthonous but are rather parautochthonous.

The microfacies are documented in Figures 6–7 and described in detail in Table 1.

Table 1. Description of microfacies from the antique quarry at Podpeč. The most abundant and diagnostic fossil taxa are underlined.

| Microfacies  | Description   | Bed thickness (min-max; in cm) | Figure |
|--|---|--------------------------------|--------|
| 1 light brownish grey mudstone   | Micritic limestone with almost complete predominance of micritic matrix and less than 10 % of clasts.   | 4 - 18                         | /      |
| 2 medium grey fenestral mudstone   | Mudstone with irregular fenestrae.  | 40 - 100                       | /      |
| 3 medium grey bioclastic wackestone  | The amount of small bivalve shells within this heterogenous bioclastic wackestone varies from 10 to 50 %. Most are 0.3 mm in length. The original mineral was dissolved and replaced by calcite spar. Gastropods, echinoderms, ostracods, and foraminifera are subordinatedly present. The intergranular space is filled with dense micritic matrix. Small corrosion vugs and putative small neptunian dykes/desiccation cracks, filled with crystal silt, intraclasts and fragments of spar are also present. The foraminiferal assemblage comprises <i>Siphovalvulina</i> sp. and Textulariidae.  | 40 - 85                        | 5a     |
| 4 dark grey pelletal-bioclastic wackestone                                   | Sample is heterogeneous. Two microfacies types can be distinguished, but with intermediate transitions. Most of the rock is represented by bioclastic-pelletal wackestone with a few (0.5 %) clasts of larger size (gastropod and bivalve shells). Wackestone consists of 15 % of grains: small angular sparitic fragments, ostracods, and small (0.08 mm) rounded pellets. Ostracod valves are separated or still closed. The other end member is also a pelletal-bioclastic wackestone, but with pellets representing 30-40 % of the rock, and bioclasts (echinoderms, bivalve fragments, small <i>Siphovalvulina</i> foraminifera) amounting to 5-10 %. Wackestones contain some irregular vugs and cracks filled with pellets, microspar and cement. Some of these might be desiccation cracks and vugs, while some might be caused by bioturbation. Larger gastropod and bivalve shells are filled with crystal silt and drusy mosaic cement.  | 10 - 120                       | 5b     |
| 5 medium dark grey peloid grainstone with rare larger bivalves               | Large (1 cm or longer) bivalve shells and very rare intraclasts within the peloid cortoid grainstone matrix represent less than 10 % of the rock. Shells are altered to drusy mosaic spar and exhibit micritic outer rim (cortoids). The grainstone consists of peloids, which measure 0.08 - 0.12 mm in size and are very well sorted. They represent 90-95 % of the grains, disregarding the mentioned larger bivalve shells. Ostracods, foraminifera (?Valvulinidae), <i>Thaumatoporella</i> , echinoderm fragments, and undeterminable sparitic particles are subordinate.  | 10 - 25                        | 5c     |
| 6 medium grey to olive grey intraclastic-bioclastic wackestone and packstone | Heterogeneous texture is wackestone to packstone in nature. Grains are very poorly sorted and matrix-supported or in point contacts. Intraclasts (20-40 % of grains) are micritic, rounded, circular to semi-elongated. Some micritised ooids are also present, but difficult to distinguish from intraclasts. Approximately 10 % of the volume is occupied by bivalve shells. These are fragmented, abraded and have micritised margins (cortoids). <i>Thaumatoporella</i> is present in up to 5 % of the volume. Foraminifera represent 1-2.5 % of the rock. Gastropods, echinoderms, brachiopods, ostracods, and fragments of dasycladacean algae are sporadically present. Micritic matrix is locally partly washed away, and the intergranular space is locally filled with drusy mosaic cement.<br><br>Foraminifera are represented by <u>Valvulinidae</u> , <u><i>Meandrovoluta asiagoensis</i></u> Fugagnoli & Rettori, <u><i>Siphovalvulina</i></u> spp., <u><i>Duotaxis metula</i></u> Kristan, and <u><i>Gaudryina</i></u> sp.   | 25 - 100                       | 5d     |
| 7 medium dark grey ooid grainstone with rare cortoids                        | Moderately well sorted mature ooids and superficial ooids form almost 50 % of the rock volume and are the predominating grain type. They are in point contacts with each other and grains of other types. The mature ooids are concentric, with tangential structure. Their cores are mostly micritised. Foraminifera and sparitic particles rarely served as basis for the ooids' formation. Their average size is 0.5 mm. Less numerous are superficial ooids with 6-7 laminae, mostly formed around elongated mollusc shell fragments up to 0.7 mm in length. Both types of ooids form lumps and mature lumps up to 1 mm in size. Fragments of echinoderms, benthic foraminifera and micritised bivalves (cortoids) are subordinate. The intergranular space is filled with drusy mosaic calcite cement.<br><br>The foraminiferal assemblage consists of <u><i>Siphovalvulina</i></u> spp., Valvulinidae, Taxulariidae, <u><i>Reophax</i></u> sp., ? <u><i>Haurania deserta</i></u> Henson, unidentified large benthic foraminifera with coarsely agglutinated wall, <u><i>Involutina farinaciae</i></u> Brönnimann & Koehn-Zaninetti. | 13 - 85                        | 5e     |

|   |   |         |    |
|---|---|---------|----|
| 8 medium dark grey ooid grainstone; large ooids   | <p>Well sorted, 1 mm large ooids occupy approximately 50 % of the rock volume. Ooids were originally concentric but got slightly compacted during diagenesis and are now more ellipsoidal in shape. Although their tangential structure is clearly recognisable, their inner regions show some recrystallization. Some were formed around sparitic fragments or foraminifera but have micritic cores. The laminar part is thick, representing approximately 45 % of the ooids' radius. Nine to twelve laminae are visible on the outer part of the cortices. Spiny ooids are very few. Some of the ooids are glued together into aggregate grains (lump and mature lump stage) up to 2.5 mm in diameter.</p> <p>Peloids are irregularly distributed among ooids and represent a little less than 10 % of the rock. They measure approximately 0.15 mm in size. Neomorphically altered bivalve fragments, foraminifera, gastropods, and echinoderm plates are very rare. The intergranular space is filled with drusy mosaic calcite cement.</p> <p>The foraminiferal assemblage consists of <i>Lituosepta</i> sp., <i>Haurania deserta</i> Henson, <i>Meandrovoluta asiagoensis</i> Fugagnoli &amp; Rettori, <i>Lituolipora</i> sp., Textulariidae and Valvulinidae, <i>Pseudopfenderina butterlini</i> (Brun), small <i>Ophthalmidium</i> sp., and <i>Involutina farinacciae</i> Brönnimann &amp; Koehn-Zaninetti.</p>   | 32 - 40 | 5f |
| 9 medium dark grey ooid grainstone; small ooids   | <p>The composition and texture are as in microfacies 8. The difference is in the size of the ooids: average diameter of ooids in this microfacies is 0.55 mm, and peloids measure 0.07 mm. Foraminiferal assemblage is identical.</p>   | 28 - 50 | /  |
| 10 medium dark grey cortoid floatstone with intraclastic-bioclastic wackestone and packstone matrix | <p>The matrix is virtually indistinguishable from microfacies 6. The difference between the microfacies is in the greater abundance of larger clasts seen at the macroscopic level.</p> <p>Foraminifera are represented by Valvulinidae, <i>Meandrovoluta asiagoensis</i> Fugagnoli &amp; Rettori, <i>Siphovalvulina</i> spp., <i>Haurania deserta</i> Henson, <i>Duotaxis metula</i> Kristan, <i>Pseudopfenderina butterlini</i> (Brun), Textulariidae, Valvulinidae, <i>Mesoendothyra</i> or <i>Everticyclamina</i> sp., and <i>Planivoluta</i> sp.</p>   | 16 - 55 | 6a |
| 11 dark grey oncoid floatstone with peloid wackestone to packstone matrix                           | <p>Grains represent approximately 40 % of the rock volume. The rock is microscopically heterogeneous, probably bioturbated (one cm-size burrow is clearly distinguishable, at the bottom filled with pelletal packstone and in the upper part by blocky spar). Peloids are of variable sizes, ranging from 0.08–0.12 mm to 1 mm. The largest may be recognised as intraclasts. Most peloids are spherical to half-spherical, rounded to well rounded. They represent 20–30 % of the volume. Some of the sphaerical peloids are likely micritised ooids. Their size ranges from 0.2 to 0.4 mm. Other grains are subordinate: foraminifera and thalli of <i>Thaumatoporella</i> each form 1–2.5 % of the rock. Up to 2 mm long fragments of dasycladacean algae are irregularly distributed, on the edges micritised and partly overgrown by microbialites. Only one, at the edges heavily micritised and partly overgrown by <i>Thaumatoporella</i>, bivalve shell was recognised. Ostracods, echinoderm plates and gastropods are also very rare (1 %). Part of the micritic matrix has been washed away, but some of the vugs could also represent desiccation pores. Vugs are filled with drusy mosaic calcite cement.</p> <p>The foraminiferal assemblage consists of <i>Meandrovoluta asiagoensis</i> Fugagnoli &amp; Rettori, <i>Siphovalvulina</i> spp., Valvulinidae, and <i>Earlandia</i> sp.</p> <p>Remarks: Compared to the matrix in microfacies 12, and microfacies 13, these microfacies contains less <i>Thaumatoporella</i> grains and the greater presence of <i>Meandrovoluta</i>.</p> | 13 - 33 | 6b |
| 12 dark grey oncoid floatstone with <i>Thaumatoporella</i> wackestone matrix                        | <p>Oncoids are 2 cm in size, constructed of homogenous micrite, <i>Thaumatoporella</i> and calcimicrobes. Locally present are bivalve shells, which are heavily bioeroded and overgrown by microbialite. Large grains float in partly washed peloid-bioclastic wackestone (grains represent 10–30 % of surface) matrix with common thalli of <i>Thaumatoporella</i>. The latter may represent up to 10 % of the volume. Other bioclasts are large benthic foraminifera (5 %) and rare gastropods. Peloids and intraclasts are also abundant. Peloids range from 0.05 to 0.1 mm in size and are rounded, while intraclasts are sub-rounded and have an average size of 0.2 mm. Micritic matrix is in some places clotted.</p> <p>The foraminiferal assemblage consists of Valvulinidae, <i>Siphovalvulina</i> spp., <i>Meandrovoluta asiagoensis</i> Fugagnoli &amp; Rettori, and <i>Duotaxis metula</i> Kristan.</p>  | 13 - 70 | 6c |
| 13 medium dark grey bivalve floatstone with small shells and peloid grainstone matrix               | <p>The matrix is identical to facies 5. The distinction is at the macroscopic level, as the microfacies 13 contains bivalve shells representing more than 10 % of the rock volume. Within the thin section made and shown in Figure 6d, the grainstone is in irregular contact with bivalve floatstone (shells 2.5 mm in size) with bioclastic wackestone matrix. Besides bivalve shells and fragments of dasycladacean algae, gastropods, echinoderms, foraminifera (<i>Siphovalvulina</i> and a dubious <i>Ammobaculites</i>), and calcimicrobes are less commonly present.</p>   | 16 - 80 | 6d |
| 14 (medium) dark grey megalodontid floatstone to rudstone with micritic matrix                      | <p>Large (0.5–3 cm large) shells of bivalves and gastropods form 15–50 % of the rock volume. They are replaced by clear drusy mosaic spar. Micritic matrix contains rare ostracods, fragments of dasycladacean algae, some <i>Thaumatoporella</i> thalli, and calcimicrobes. Foraminifera are small and very rare. Very small fragments of bivalve shells may be locally more common, filling between 20 and 30 % of space.</p>   | 24 - 72 | 6e |

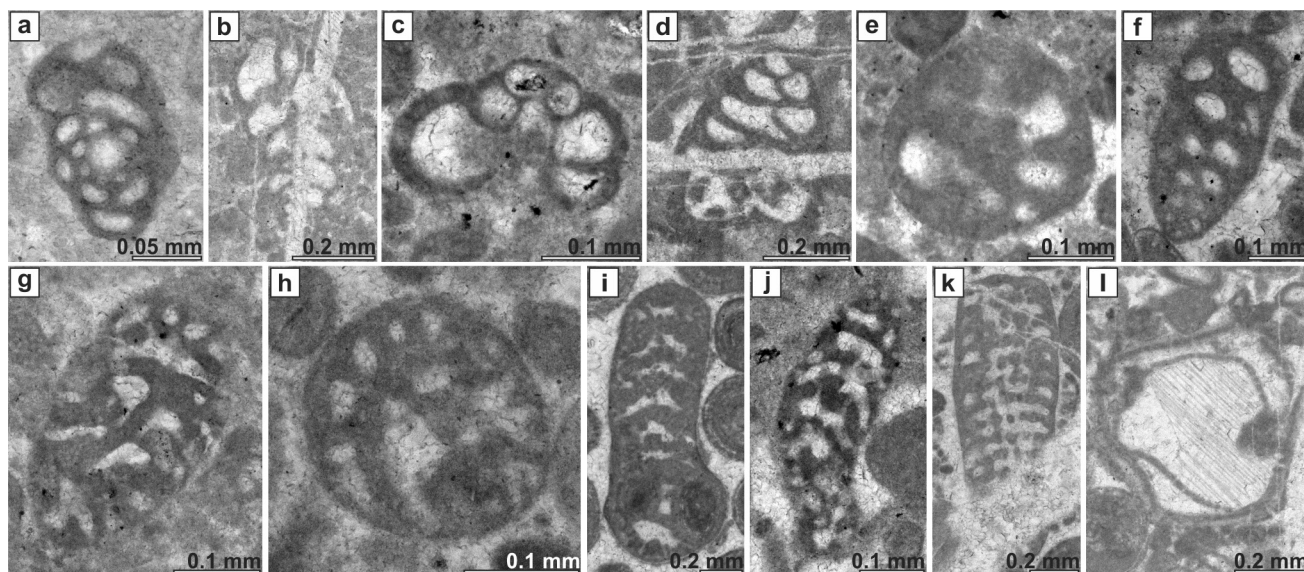


Fig. 8. Foraminifera from the Pliensbachian limestone in the antique quarry at Podpeč. a: *Meandrovoluta asiagoensis* Fugagnoli & Rettori. Thin section 1679. b: *Siphovalvulina* cf. *variabilis* Septfontaine. Thin section 1684. c: *Siphovalvulina gibraltarensis* BouDagher-Fadel, Rose, Bosence & Lord. Thin section 1679. d: *Duotaxis metula* Kristan. Thin section 1684. e: *Pseudopfenderina butterlini* (Brun). Transverse section. Thin section 1679. f: *Pseudopfenderina butterlini* (Brun). Oblique longitudinal section. Thin section 1679. g: *Amijiella amiji* (Henson). Oblique longitudinal section. Thin section 1679. h: *Amijiella amiji* (Henson). Oblique transverse section. Thin section 1679. i: *Lituosepta* sp. Longitudinal section. Thin section 1679. j: *Lituosepta* sp. Longitudinal section. Thin section 1679. k: ?*Lituosepta* sp. Longitudinal section. Thin section 1678. l: *Thaumatoporella* sp. Thin section 1684.

### Foraminiferal assemblages

The most abundant foraminiferal taxa in each microfacies are underlined in Table 1 and presented in Figure 8. Only *Siphovalvulina* and small Textulariidae are present in bioclastic wackestone and in pelletal-bioclastic wackestone. Peloid grainstone with rare bivalve shells, where only Valvulinidae are present, alongside with problematic algae *Thaumatoporella*. Intraclastic-bioclastic wackestone and packstone is characterised by the abundance of Valvulinidae and *Meandrovoluta asiagoensis*. Cortoid floatstone with intraclastic-bioclastic wackestone and packstone matrix contains an abundance of Valvulinidae, *Meandrovoluta asiagoensis*, *Siphovalvulina* spp., and *Haurania deserta*. Oncoid floatstone with peloid wackestone to packstone matrix commonly contains *Meandrovoluta asiagoensis* and *Siphovalvulina* spp., but, unlike the dark grey oncooid floatstone with *Thaumatoporella* wackestone matrix, it has much less of the *Thaumatoporella*. Foraminifera in bivalve and megalodontid floatstone are too few to be considered diagnostic for these facies. Based on the presence of *Lituosepta* and the absence of *Orbitopsella*, we tentatively place the logged succession in the late Sinemurian *Lituosepta recoarensis* lineage zone (Kabal & Tasli, 2003; Velić, 2007). However, *Orbitopsella* might also be absent due to environmental factors.

### Mineralogical, geochemical, and isotopic characterisation of the ancient Podpeč quarry

XRD analysis of the limestone revealed only the presence of calcite (Fig. 9a) due to mineralogical purity of the studied samples and method detection limits. Table 2 lists concentrations of major oxides, minor elements, trace elements above detection limits, and isotope values of  $\delta^{13}\text{C}$ ,  $\delta^{18}\text{O}$ ,  $^{87}\text{Sr}/^{86}\text{Sr}$ . The limestone is characterised by a high CaO content and a low MgO content, as is expected for pure limestones.  $\text{SiO}_2$  is positively correlated with  $\text{Al}_2\text{O}_3$ ,  $\text{K}_2\text{O}$  and TiO (linear correlation coefficients  $r = 0.87$ ,  $r = 0.76$ , and  $r = 0.54$  respectively; number of samples  $n = 15$ ). By cross-plotting the  $\delta^{18}\text{O}$  and  $\delta^{13}\text{C}$  isotope ratios it was found that only two samples indicate the influence of early meteoric diagenesis (Fig. 9b). These samples were eliminated from any further analysis. Strontium isotope data from the Lithitoid Limestone Member measured at the ancient Podpeč quarry were plotted on a box and whiskers diagram and correlated with a global strontium curve (Fig. 9c).

The local isotope curves of  $\delta^{18}\text{O}$  and  $\delta^{13}\text{C}$  are shown on a composite log in Figure 10. The carbon isotope compositions range from -2.44 ‰ to 2.5 ‰ ( $n=37$ ) for micritic limestone, 0.28 ‰ to 1.84 ‰ ( $n=6$ ) for fine-grained limestone, -0.21 ‰ to 0.93 ‰ ( $n=6$ ) for oolitic limestone, -0.07 ‰ to 1.12 ‰ ( $n=2$ ) for oncooid/cortoid limestone, and 0.02 ‰ to 1.95 ‰ ( $n=8$ ) for limestone with bi-

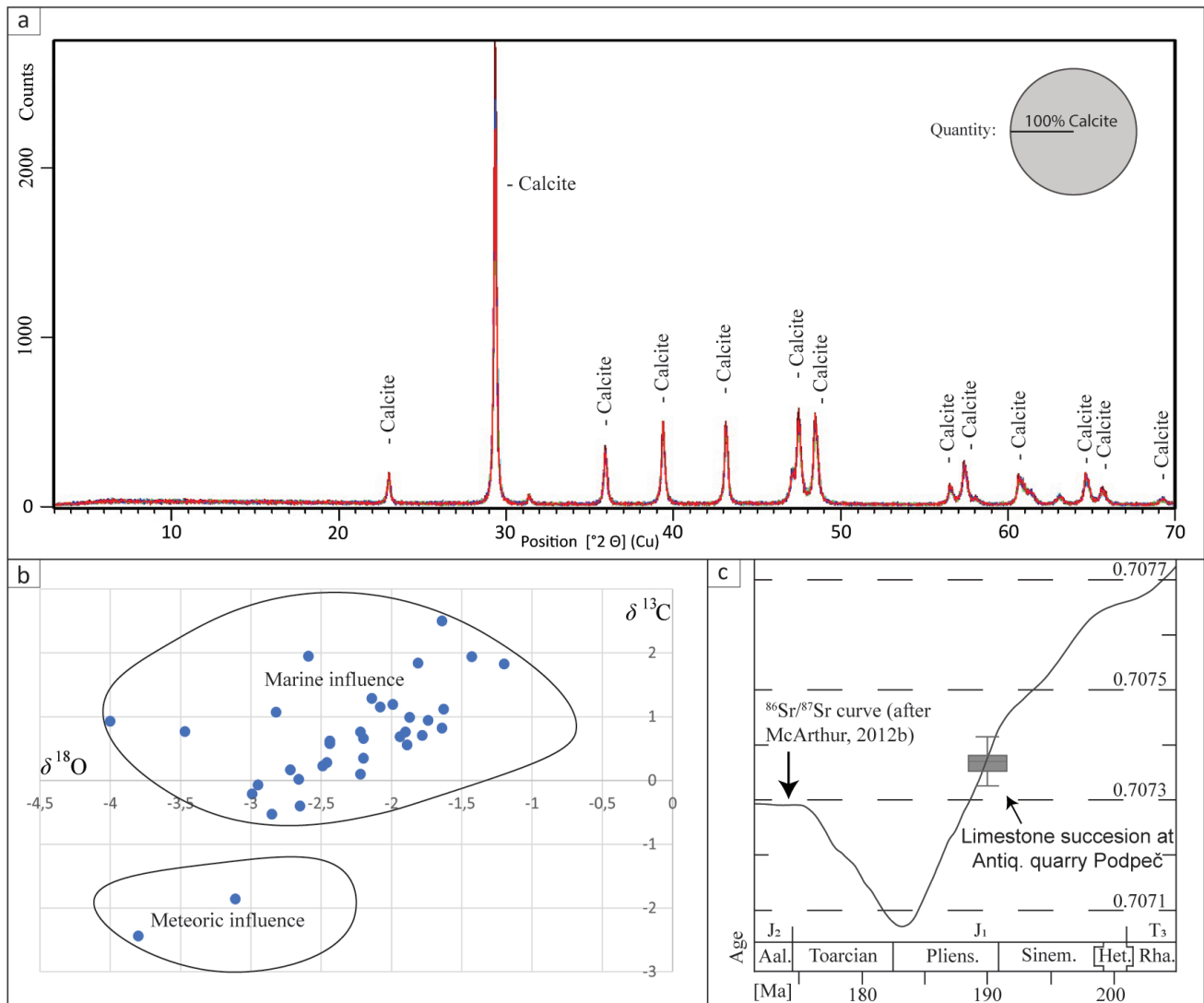


Fig. 9. Mineralogical, geochemical and isotope characterisation of antique part of Podpeč quarry. a: XDR mineralogical composition of the studied samples. Only calcite shows on all of the roentgenograms ( $n=7$ ). b:  $\delta^{13}\text{C}$  and  $\delta^{18}\text{O}$  cross scatter plot of diagenesis in the studied samples. Blue circles represent the individual measurements plots. c: Box and whiskers graph of  $^{87}\text{Sr}/^{86}\text{Sr}$  values of samples from antique part of Podpeč quarry correlated with the global Sr curve from McArthur et al. (2012b).

valves. Unique values can be reported only for micritic limestones in the range from  $-2.44\text{‰}$  to  $-0.21\text{‰}$  and  $1.95\text{‰}$  to  $2.5\text{‰}$ . The oxygen isotope compositions range from  $-3.8\text{‰}$  to  $-1.2\text{‰}$  ( $n=37$ ) for micritic limestone, from  $-2.82\text{‰}$  to  $-1.81\text{‰}$  ( $n=6$ ) for fine-grained limestone, from  $-4\text{‰}$  to  $-1.78\text{‰}$  ( $n=6$ ) for oolitic limestone, from  $-2.95\text{‰}$  to  $-1.63\text{‰}$  ( $n=2$ ) for oncoïd/cortoid limestone, and from  $-2.72\text{‰}$  to  $-1.87\text{‰}$  ( $n=8$ ) for limestone with bivalves. Values recorded in only one facies in oolitic limestone range from  $-4\text{‰}$  to  $-3.8\text{‰}$  and for micritic limestone facies from  $-1.63\text{‰}$  to  $-1.2\text{‰}$ .

The  $^{87}\text{Sr}/^{86}\text{Sr}$  isotope values within the succession in the antique quarry decrease from 0.707414 to 0.707329 (Table 2).

### Geological characterisation of stone products and its provenance determinations

The stone products MGML 48572, MGML 51180, NMS L209 and NMS 210 belong to microfacies 2 (micritic limestone), 6 (fine-grained limestone), 7 and 9 (oolitic limestone) respectively (for facies descriptions see Table 1). Multi-method data acquired from the analysis of the stone products are listed in Table 3. As in primary samples also the studied stone products are characterised by the high CaO and low MgO content. Linear correlation ( $n=4$ ) was analysed only between  $\text{SiO}_2$  with  $\text{Al}_2\text{O}_3$ ,  $\text{K}_2\text{O}$  and  $\text{TiO}_2$  to check the previously determined correlation from primary samples also in stone products. Linear correlation coefficients between  $\text{SiO}_2$  with  $\text{Al}_2\text{O}_3$

Table 2. Geochemical values of major (oxides), minor, and trace elements with measured concentration above detection limit and  $\delta^{13}\text{C}$ ,  $\delta^{18}\text{O}$ ,  $^{87}\text{Sr}/^{86}\text{Sr}$  isotope values for the Lower Jurassic limestone in the antique quarry at Podpeč.

| Position of the sample in the succession (m from the base) | Microfacies (see Fig. 4) | $\text{SiO}_2$ [wt%] | $\text{Al}_2\text{O}_3$ [wt%] | $\text{Fe}_2\text{O}_3$ [wt%] | $\text{MnO}$ [wt%] | $\text{MgO}$ [wt%] | $\text{CaO}$ [wt%] | $\text{Na}_2\text{O}$ [wt%] | $\text{K}_2\text{O}$ [wt%] | $\text{TiO}_2$ [wt%] | LOI [wt%] | Sr [ppm] | Zr [ppm] | U [ppm] | $\delta^{13}\text{C}$ | $\delta^{18}\text{O}$ | $^{87}\text{Sr}/^{86}\text{Sr}$ (2SD) |
|--|--------------------------|----------------------|-------------------------------|-------------------------------|--------------------|--------------------|--------------------|-----------------------------|----------------------------|----------------------|-----------|----------|----------|---------|-----------------------|-----------------------|---------------------------------------|
| 0.5  | 3                        | 0.31                 | 0.14                          | 0.05                          | 0.004              | 0.69               | 55.79              | 0.05                        | 0.03                       | 0.002                | 43.43     | 280      | 3        | 2.1     | 2.50                  | -1.64                 | 0.707414 (0.000003)                   |
| 1.1  | 10                       | /                    | /                             | /                             | /                  | /                  | /                  | /                           | /                          | /                    | /         | /        | /        | /       | 0.76                  | -2.22                 | /                                     |
| 1.6  | 2                        | 0.33                 | 0.16                          | 0.05                          | 0.005              | 0.44               | 56.32              | 0.06                        | 0.03                       | 0.002                | 43.36     | 120      | 2        | 2.6     | -0.53                 | -2.85                 | /                                     |
| 2.7  | 4                        | 0.37                 | 0.18                          | 0.07                          | 0.006              | 0.57               | 55.99              | 0.05                        | 0.05                       | 0.005                | 43.23     | 149      | 3        | 3.5     | 0.10                  | -2.22                 | /                                     |
| 3.3  | 14                       | /                    | /                             | /                             | /                  | /                  | /                  | /                           | /                          | /                    | /         | /        | /        | /       | 0.69                  | -1.94                 | /                                     |
| 3.8  | 4                        | /                    | /                             | /                             | /                  | /                  | /                  | /                           | /                          | /                    | /         | /        | /        | /       | 0.94                  | -1.74                 | /                                     |
| 4.0  | 3                        | 0.37                 | 0.18                          | 0.09                          | 0.005              | 0.73               | 54.73              | 0.05                        | 0.04                       | 0.005                | 43.41     | 270      | 3        | 2.9     | 1.94                  | -1.43                 | 0.707377 (0.000006)                   |
| 4.5  | 3                        | 0.34                 | 0.16                          | 0.08                          | 0.004              | 0.67               | 55.25              | 0.06                        | 0.04                       | 0.003                | 43.5      | 248      | 3        | 4.9     | 1.83                  | -1.20                 | /                                     |
| 5.4  | 1                        | /                    | /                             | /                             | /                  | /                  | /                  | /                           | /                          | /                    | /         | /        | /        | /       | -1.86                 | -3.11                 | /                                     |
| 5.6  | 4                        | 0.44                 | 0.23                          | 0.05                          | 0.007              | 0.67               | 53.33              | 0.06                        | 0.03                       | 0.002                | 43.53     | 178      | 7        | 3.7     | 0.82                  | -1.64                 | /                                     |
| 5.9  | 12                       | /                    | /                             | /                             | /                  | /                  | /                  | /                           | /                          | /                    | /         | /        | /        | /       | -0.07                 | -2.95                 | /                                     |
| 6.3  | 4                        | /                    | /                             | /                             | /                  | /                  | /                  | /                           | /                          | /                    | /         | /        | /        | /       | 0.35                  | -2.20                 | /                                     |
| 6.4  | 5                        | /                    | /                             | /                             | /                  | /                  | /                  | /                           | /                          | /                    | /         | /        | /        | /       | 1.84                  | -1.81                 | /                                     |
| 6.6  | 14                       | /                    | /                             | /                             | /                  | /                  | /                  | /                           | /                          | /                    | /         | /        | /        | /       | 1.19                  | -1.99                 | /                                     |
| 6.9  | 11                       | 0.43                 | 0.2                           | 0.12                          | 0.005              | 0.54               | 54.42              | 0.06                        | 0.04                       | 0.003                | 43.44     | 140      | 3        | 2.8     | /                     | /                     | /                                     |
| 7.3  | 14                       | 0.39                 | 0.19                          | 0.08                          | 0.005              | 0.6                | 55.63              | 0.05                        | 0.04                       | 0.004                | 42.56     | 193      | 3        | 2.7     | 1.95                  | -2.59                 | /                                     |
| 7.8  | 8                        | /                    | /                             | /                             | /                  | /                  | /                  | /                           | /                          | /                    | /         | /        | /        | /       | 0.58                  | -2.44                 | /                                     |
| 8.0  | 14                       | /                    | /                             | /                             | /                  | /                  | /                  | /                           | /                          | /                    | /         | /        | /        | /       | 0.99                  | -1.87                 | /                                     |
| 8.3  | 12                       | /                    | /                             | /                             | /                  | /                  | /                  | /                           | /                          | /                    | /         | /        | /        | /       | 1.12                  | -1.63                 | /                                     |
| 8.7  | 13                       | /                    | /                             | /                             | /                  | /                  | /                  | /                           | /                          | /                    | /         | /        | /        | /       | 0.02                  | -2.66                 | /                                     |
| 9.1  | 14                       | /                    | /                             | /                             | /                  | /                  | /                  | /                           | /                          | /                    | /         | /        | /        | /       | 1.29                  | -2.14                 | /                                     |
| 9.4  | 13                       | /                    | /                             | /                             | /                  | /                  | /                  | /                           | /                          | /                    | /         | /        | /        | /       | 0.23                  | -2.49                 | /                                     |
| 9.7  | 13                       | /                    | /                             | /                             | /                  | /                  | /                  | /                           | /                          | /                    | /         | /        | /        | /       | 0.17                  | -2.72                 | /                                     |
| 10.4   | 3                        | 0.55                 | 0.37                          | 0.07                          | 0.005              | 0.57               | 54.22              | 0.08                        | 0.09                       | 0.005                | 43.38     | 174      | 4        | 2.8     | 0.76                  | -1.90                 | 0.707375 (0.00004)                    |
| 10.9   | 4                        | 0.38                 | 0.19                          | 0.1                           | 0.005              | 0.6                | 55.25              | 0.05                        | 0.05                       | 0.005                | 43.24     | 177      | 3        | 4.3     | 0.62                  | -2.44                 | /                                     |
| 12.3   | 6                        | /                    | /                             | /                             | /                  | /                  | /                  | /                           | /                          | /                    | /         | /        | /        | /       | 0.66                  | -2.20                 | /                                     |
| 14.9   | 10                       | 0.41                 | 0.19                          | 0.07                          | 0.005              | 0.64               | 54.7               | 0.06                        | 0.04                       | 0.003                | 43.54     | 207      | 3        | 3       | 0.93                  | -4.00                 | /                                     |
| 15.8   | 5                        | /                    | /                             | /                             | /                  | /                  | /                  | /                           | /                          | /                    | /         | /        | /        | /       | 1.07                  | -2.82                 | /                                     |
| 16.7   | 9                        | /                    | /                             | /                             | /                  | /                  | /                  | /                           | /                          | /                    | /         | /        | /        | /       | 0.77                  | -3.47                 | /                                     |
| 17.6   | 2                        | /                    | /                             | /                             | /                  | /                  | /                  | /                           | /                          | /                    | /         | /        | /        | /       | -2.44                 | -3.80                 | /                                     |
| 18.2   | 3                        | /                    | /                             | /                             | /                  | /                  | /                  | /                           | /                          | /                    | /         | /        | /        | /       | -0.40                 | -2.65                 | /                                     |
| 18.9   | 6                        | 0.39                 | 0.19                          | 0.06                          | 0.005              | 0.53               | 55.31              | 0.05                        | 0.05                       | 0.004                | 43.42     | 138      | 3        | 3       | 0.28                  | -2.46                 | 0.707332 (0.000011)                   |
| 19.4   | 6                        | /                    | /                             | /                             | /                  | /                  | /                  | /                           | /                          | /                    | /         | /        | /        | /       | 0.56                  | -1.89                 | /                                     |
| 20.6   | 8                        | 0.55                 | 0.24                          | 0.06                          | 0.005              | 0.5                | 54.47              | 0.09                        | 0.05                       | 0.003                | 43.45     | 165      | 3        | 2.8     | -0.21                 | -2.99                 | /                                     |
| 21.7   | 7                        | 0.44                 | 0.21                          | 0.06                          | 0.006              | 0.63               | 54.6               | 0.06                        | 0.05                       | 0.004                | 43.23     | 172      | 3        | 1.4     | 0.71                  | -1.78                 | 0.707329 (0.000012)                   |
| 22.9   | 6                        | 0.59                 | 0.28                          | 0.08                          | 0.005              | 0.68               | 55.35              | 0.07                        | 0.08                       | 0.008                | 43.33     | 208      | 3        | 5.2     | 1.15                  | -2.08                 | /                                     |

Table 3. Geochemical values of major (oxides), minor, and trace elements with measured concentration above detection limit and  $\delta^{13}\text{C}$ ,  $\delta^{18}\text{O}$ ,  $^{87}\text{Sr}/^{86}\text{Sr}$  isotope values for the studied stone products (see Djurić et al, 2022 for complete set of the studied stone products).

| Inventory number (use)          | Micro-facies (see Fig. 5) | Minimal bed thickness [cm] | $\text{SiO}_2$ [wt%] | $\text{Al}_2\text{O}_3$ [wt%] | $\text{Fe}_2\text{O}_3$ [wt%] | $\text{MnO}$ [wt%] | $\text{MgO}$ [wt%] | $\text{CaO}$ [wt%] | $\text{Na}_2\text{O}$ [wt%] | $\text{K}_2\text{O}$ [wt%] | $\text{TiO}_2$ [wt%] | LOI [wt%] | Sr [ppm] | Zr [ppm] | U [ppm] | $\delta^{13}\text{C}$ | $\delta^{18}\text{O}$ | $^{87}\text{Sr}/^{86}\text{Sr}$ (2SD) |
|---------------------------------|---------------------------|----------------------------|----------------------|-------------------------------|-------------------------------|--------------------|--------------------|--------------------|-----------------------------|----------------------------|----------------------|-----------|----------|----------|---------|-----------------------|-----------------------|---------------------------------------|
| MGML 48572 (Inscripti-on stone) | 3                         | 10 cm                      | 1,19                 | 0,61                          | 0,23                          | 0,005              | 0,61               | 54,47              | 0,04                        | 0,17                       | 0,029                | 42,53     | 134      | 7        | 2,4     | 0,44                  | -2,94                 | 0,707352 (0,000077)                   |
| MGML 51180 (Inscripti-on stone) | 6                         | 43 cm                      | 0,34                 | 0,15                          | 0,07                          | 0,004              | 0,63               | 54,46              | 0,05                        | 0,03                       | 0,005                | 43,34     | 178      | 2        | 2,7     | 1,33                  | -1,12                 | 0,707351 (0,000026)                   |
| NMS L209 (lorica)               | 7                         | 30 cm                      | 0,27                 | 0,13                          | 0,11                          | 0,005              | 0,54               | 54,81              | 0,03                        | 0,02                       | 0,003                | 43,36     | 151      | 3        | 0,4     | 2,29                  | -3,17                 | 0,707331 (0,000047)                   |
| NMS L210 (lorica)               | 9                         | 30 cm                      | 1                    | 0,47                          | 0,24                          | 0,008              | 0,57               | 54,91              | 0,05                        | 0,11                       | 0,021                | 42,7      | 140      | 5        | 0,6     | 2,78                  | -2,24                 | 0,707406 (0,000024)                   |

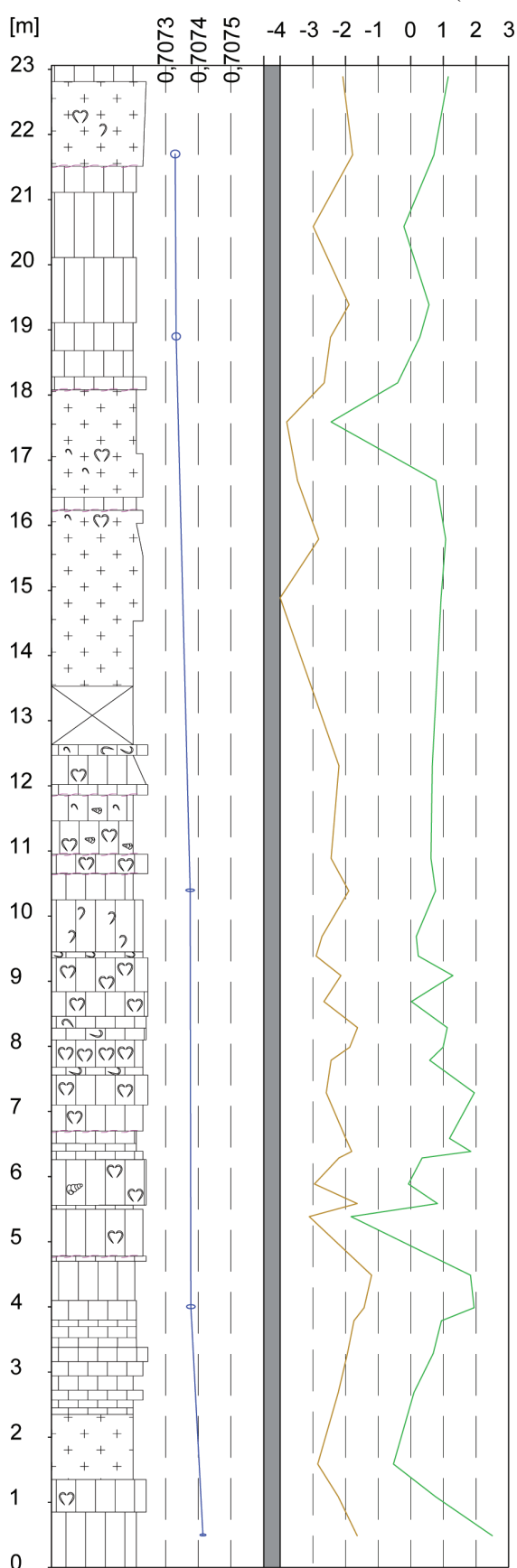
LITHOLOGY  $^{87}\text{Sr}/^{86}\text{Sr}$  ‰  $\delta^{18}\text{O}$  ‰ and  $\delta^{13}\text{C}$  ‰ (V-PDB)

Fig. 10.  $^{87}\text{Sr}/^{86}\text{Sr}$ ,  $\delta^{13}\text{C}$  and  $\delta^{18}\text{O}$  curves on a composite log with marked grains (see legend on Figure 4). Diameters of blue ellipse represent the standard deviation of measurement (y axis) and the calculated local uncertainty (x axis) for the  $^{87}\text{Sr}/^{86}\text{Sr}$  isotope values.

( $r = 0.99$ ),  $\text{SiO}_2$  with  $\text{K}_2\text{O}$  ( $r = 0.98$ ), and  $\text{SiO}_2$  with  $\text{TiO}_2$  ( $r = 0.99$ ) are high. This is consistent with the data from the primary sedimentological section, with slightly higher correlations for the stone products due to the relatively small number of samples. The multi-method data obtained shows a direct match with the values obtained in the characterisation of the sedimentological sections in the antient Podpeč quarry; thus, the stone products can be assigned to their specific place of extraction. Based on Strontium isotopic values, the appropriate bed thickness and microfacies type, and the alignment with geochemical measurements the provenance of lorica NMS L210 can be placed in the lower part of the antient quarry (see Fig. 5 – probe 2), the studied inscriptions stones MGML 48572 and MGML 51180 in the upper part of the succession (see Fig. 5 – probe 3) and lorica NMS L209 to the upper most part of probe 3.

### Discussion

Comparing the detailed geological map with the previous Basic Geological Map (Buser et al., 1967), new lithostratigraphic and structural relations could be interpreted from the detailed field data. On the western part of the St. Ana hill in the village of Podpeč, where lithostratigraphic division was in part recently presented (Djurić et al., 2018a), the new geological map shows good agreement with the geological boundaries and lithostratigraphic units presented therein. The new geological map defines the lithostratigraphic units available for quarrying on the wider Podpeč area (see Fig. 4a), and as seen from the digital elevation model (see Fig. 4b) all Members of the Lower Jurassic Podbukovje Formation have been quarried, either for the extraction of dimension stone (Djurić et al., 2018a; Djurić et al., 2022) and/or the production of lime (Bras, 1977).

None of the described facies is exclusive to the antique quarry, as all occur also within the younger part of the succession exposed in the modern quarry. The logged sedimentological sections record the lateral and vertical variability of microfacies typical for internally differentiated lagoonal sedimentation environments (Gale, 2015). The succession was previously placed in the Lithiotid Limestone Member (Djurić et al., 2022). However, based on the present sedimentological and paleontological data and the lack of lithiotid bivalves in the logged sections, this part could, alternatively, stratigraphically belong to the Orbitopsella Limestone Member. Knowing the detailed sedimentological composition of

the beds within the antique quarry, however, it is much easier to locate the products back to the original place of extraction. Telling examples are the bivalve (mainly megalodontid bivalve) microfacies found only in the lower part of the antique quarry.

As no age-characteristic foraminifera for Pliensbachian could be found for the succession logged at the antient Podpeč quarry, foraminiferal assemblages can be used to suggest the stratigraphic position of this quarry. To some extent, the *Lituosepta recoarensis* lineage zone (Kabal & Tasli, 2003; Velić, 2007) can be considered as characteristic for the studied part of the succession. Additionally, individual microfacies show enough consistency to be considered one of the features that help to distinguish between different microfacies. The facies dependence of Early Jurassic benthic foraminifera has been hypothesised previously by Fugagnoli (2004) and attributed to gradients in trophic resources, oxygen levels, and stability in nutrient supply. As shown by Gale and Kelemen (2017), such differences among the assemblages can be recognized from the Sinemurian onwards. Most of the taxa from the investigated assemblages are considered to be benthic opportunists (see Fugagnoli, 2004). Most notably, these include *Meandrovoluta asiagoensis* and *Siphovalvulina*. On the other hand, *Haurania* represents a lituolid with a complex wall structure. The trophic levels would thus shift between eutrophic and mesotrophic conditions (Fugagnoli, 2004). Foraminifera assemblages of the beds within the antique quarry can help in provenance determinations of ancient stone products with the typical assemblages for microfacies described. Acquired geochemical data, both in primary samples and stone products, can be assigned to the carbonate and non-carbonate components. CaO, MgO, Sr, LOI, and partially also NaO were grouped to the carbonate component. The low MgO values indicate that the carbonate component belongs to low-Mg calcite, which was likely formed by early diagenetic processes from the high-Mg calcite and aragonite. Sr and  $\text{Na}_2\text{O}$  values are consistent with those measured in Lower Jurassic marine carbonates (Veizer et al., 1999; Hamon & Merzeraud, 2007; Ogorelec, 2009). The non-carbonate component includes  $\text{Al}_2\text{O}_3$ ,  $\text{K}_2\text{O}$ ,  $\text{TiO}_2$ , Zr, and most of the  $\text{Na}_2\text{O}$ , while  $\text{SiO}_2$  can belong to the biogenic or terrigenous source. The high positive correlation of  $\text{SiO}_2$  with  $\text{Al}_2\text{O}_3$ ,  $\text{K}_2\text{O}$  and  $\text{TiO}_2$  indicates that  $\text{SiO}_2$  is also associated with a terrigenous influx. The low concentrations of non-carbonate components, specifically

the low values of  $K_2O$ ,  $TiO_2$ ,  $Al_2O_3$ , and Zr, show little terrigenous input, which is in accordance with sedimentation in a restricted lagoon of a carbonate platform (Buser & Debeljak, 1995; Debeljak & Buser, 1997; Gale, 2015). Some higher values of  $SiO_2$  implies that the studied succession (and stone products originating from it) was occasionally under the influence of subaerial exposure (Martinuš, et al., 2012), which is again in accordance with previous studies (Gale, 2015). Non-carbonate components  $Fe_2O_3$ , MnO, and U are all interpreted as partially terrigenous and partially diagenetic. The very low values of MnO and  $Fe_2O_3$  also indicate very low terrigenous and diagenetic influence, and the fact that the limestones were not enriched with minor and trace elements during the diagenetic processes and did not interact with circulating water of continental origin (Veizer, 1983). U values are higher in micritic and fine-grained limestones than they are in oolitic limestone, both in primary samples and in the studied stone products. We attribute this to a higher proportion of organic material in micritic samples (Goswami et al., 2017). Reported geochemical values herein can be considered, to some extent, typical for determinations of provenance in the ancient Podpeč quarry.

It must be kept in mind that in shallow marine environments terrigenous inputs can have a large influence on the isotopic record (Eystein, 1989), which means that local variations in isotope curves are possible. Previously defined low terrigenous input serves to strengthen the trust limit in the acquired data for the ancient Podpeč quarry.

All studied samples show little to no effect of diagenetic changes, both in terms of the ratio of  $\delta^{18}O$  and  $\delta^{13}C$  isotopes (Table 2), as data points fall within values documented for Jurassic marine limestones (Veizer et al., 1999; Jenkyns et al. 2002; Hamon & Merzeraud, 2007). The widest range of carbon and oxygen values in micrite facies might be also due to the fact that they represent the largest data set in these microfacies. The measured ranges of isotopic ratios of carbon and oxygen overlap in most cases; thus, in the case of the ancient Podpeč quarry this method can be used for the determination of provenance only as one of the factors that strengthen the determination but cannot be considered decisive. Carbon and oxygen isotope measurements show alignment with ranges of values for each facies defined above, except for stone products made from oolitic facies, which in both stone products shows higher values. This is likely due to the

small number of primary samples in these facies; thus, the full range of values was probably not detected.

The  $^{87}Sr/^{86}Sr$  values of marine carbonates can be used for geochronological and correlative purposes by comparing them with global curves for a time-period of interest (McArthur et al., 2012a). If, based on microfacies and biostratigraphic analysis, the provenance of a specific stone product cannot be reliably determined, strontium isotope values can be used to derive a more exact provenance (Galan et al., 1999; Maritan et al., 2003; Brilli et al., 2010; Brilli et al., 2011). The measured range of strontium values can be considered characteristic for this part of the succession (Brajkovič et al., 2021) and thus used to define the provenance of ancient stone products (see Fig. 9c) and place the studied succession in the early Pliensbachian Orbitopsela Limestone Member (Orbitopsela Beds sensu Dozet & Strohmenger 2000).

The same stone products were studied in the publication by Djurić et al. (2022), where their origin could not be reliably determined based solely on petrological data. This is due to the frequent occurrence of micritic and fine-grained limestones in other putative quarry areas (Ramovš, 1990; Šašel Kos, 1997; Rožič et al., 2018). The presumed quarry areas of Podutik (Ramovš, 1990) and Staje (Šašel Kos, 1997) belong to the Krka Limestone Member (Novak, 2003; Rožič et al., 2018), where micritic and fine-grained facies are most abundant and oolitic facies are also present. The multi-method approach used enabled us to determine the exact provenance of these facies in studied stone products to the exact place of extraction in the antique Podpeč quarry.

## Conclusions

Following the previous archaeological research, which located the Roman quarry at Podpeč (Djurić et al., 2022), the known extent of the antique quarry was studied in detail according to the multi-method approach.

A detailed lithological analysis of the beds quarried in the antique quarry revealed two facies assemblages that vary in the predominant facies component. From this, one of the transitions from a restricted to a more open marine lagoon was interpreted. The microfacies and expected foraminifera assemblages (see Tab. 1) provide a record of the antique quarry microfacies, which in turn lends more definitive credence to provenance determinations of the stone products to the Podpeč quarry. The low terrigenous influx and

the occasional sub-aerial exposure of the studied succession confirmed previous interpretations of the environment of sedimentation, and additionally provide values and correlations useful for provenance studies of the stone extracted from the ancient Podpeč quarry. The linear correlation of  $\text{SiO}_2$  with  $\text{Al}_2\text{O}_3$ ,  $\text{K}_2\text{O}$ , and  $\text{TiO}_2$  is thus expected. This can serve as one of the factors when determining the origin of the stone; however, it cannot serve as the sole determining factor. Isotope values  $\delta^{13}\text{C}$ ,  $\delta^{18}\text{O}$ , and  $^{87}\text{Sr}/^{86}\text{Sr}$  can be considered typical for the antique quarry at Podpeč. Based on the lack of Lithiotid bivalves and the correlation of Sr isotopic values with the global record, the succession was lithostratigraphically correlated to the Orbitopsela Limestone Member (Orbitopsela beds sensu Dozet & Strohmenger, 2000). The  $\delta^{13}\text{C}$  and  $\delta^{18}\text{O}$  values cannot be considered decisive in determining origin from the Podpeč quarry; however, it can help in limiting the part of the succession from which the limestone was extracted. The Sr isotope measurements allow us to place the individual measurements of the stone products into the range typical for the ancient Podpeč quarry. Where the standard deviation of single measurements of stone product values is low, the Sr values compared with the logged facies (see Fig. 5) can enable us to place the stone product in the appropriate part of the succession.

For determination of the provenance of the stone used in Antiquity, it is recommended that a thin section be made for a detailed examination of the facies. For those microfacies that are distributed over the larger part of the Podbukovje Formation (micritic, fine-grained, and oolitic limestone), the reliable means of determining the provenance is the multi-method approach. Determining the provenance of stone products made from micritic, fine-grained, and oolitic microfacies, and the foraminifera assemblages described herein, combined with the geochemical and isotopic values provided in this paper, serve to provide a suitable reference for the stone material derived from the Podpeč quarry. This study additionally enables further detailed archaeological studies of the antique production and trade related to the Podpeč quarry.

#### Acknowledgements

This study was financially supported by the Slovenian Research Agency (Programme No. P1-0011 and No. P1-0025). We thank the reviewers for their valuable comments and suggestions that helped improve the manuscript. Additionally, we thank Mineral Ltd. and the Vehar family (Podpeč 44)

for access to the premises; Dr. Ana Novak and Blaž Milanič for the preparation of digital elevation models and topographical data; Petra Škrap for help with the fieldwork; and Mladen Štumergar for the preparation of thin sections. For access to the museum collections and permissions for the sampling of stone products we thank Dr. Janka Istenič (National Museum of Slovenia) and Dr. Bernarda Županek (Museum of Ljubljana).

#### References

- Brajkovič, R., Žvab Rožič, P. & Gale, L. 2021: Methodological approach to provenance determination of stone products made from micritic and fine-grained limestones. In: Rožič (ed.): *Razprave, poročila = Treatises, reports: 25. posvetovanje slovenskih geologov = 25th Meeting of Slovenian Geologists*. Univerza v Ljubljani, Naravoslovnotehniška fakulteta, Oddelek za geologijo, Ljubljana.
- Bras, L. 1977: Apnenice v Podpeči pod Krimom. *Slovenski etnograf*, 30: 75–91.
- Brilli, M., Antonelli, F., Giustini, F., Lazzarini, L. & Pensabene, P. 2010: Black limestones used in antiquity: the petrographic, isotopic and EPR database for provenance determination. *Journal of Archaeological Science*, 37/5: 994–1005. <https://doi.org/10.1016/j.jas.2009.11.032>
- Brilli, M., Conti, L., Giustini, F., Occhiuzzi, M., Pensabene, P. & De Nuccio, M. 2011: Determining the provenance of black limestone artifacts using petrography, isotopes and EPR techniques: the case of the monument of Bocco. *Journal of Archaeological Science*, 38/6: 1377–1384. <https://doi.org/10.1016/j.jas.2011.02.005>
- Brodar, S., Grafenauer, B., Klemenc, J., Korošec, J. & Rakovec, I. 1955: *Zgodovina Ljubljane*. Geologija in arheologija. DZS, Ljubljana: 458 p.
- Buser, S., Grad, K. & Pleničar, M. 1967: *Osnovna geološka karta SFRJ, list Postojna*. Zvezni geološki zavod Jugoslavije, Beograd.
- Buser, S. 1968: *Osnovna geološka karta SFRJ, list Ribnica*. Zvezni geološki zavod Jugoslavije, Beograd.
- Buser, S. & Debeljak, I. 1995: Lower Jurassic beds with bivalves in South Slovenia. *Geologija*, 37/38: 23–62. <https://doi.org/10.5474/geologija.1995.001>
- Debeljak, I. & Buser, S. 1997: Lithiotid Bivalves in Slovenia and Their Mode of Life. *Geologija*, 40/1, 11–64. <https://doi.org/10.5474/geologija.1997.001>
- Dozet, S. & Strohmenger, C. 2000: Podbukovje Formation, Central Slovenia. *Geologija*, 43/2: 197–212. <https://doi.org/10.5474/geologija.2000.014>

- Dozet, S. 2009: Lower Jurassic carbonate succession between Predole and Mlačevo, Central Slovenia. *RMZ-materials and geoenvironment*, 56: 164-193.
- Dunham, R.J. 1962: Classification of carbonate rocks according to depositional texture. In: Han, W.E. (eds.): *Classification of carbonate rocks*, A symposium Amer. Ass. Petrol. Geol Mem., 108-121. <https://doi.org/10.1306/M1357>
- Djurić, B. & Rižnar, I. 2017: Kamen Emona / The rocks for Emona. In: Vičič, B. & Županek, B. (eds.): *Emona MM: [urbanizacija prostora - nastanek mesta = urbanisation of space - beginning of a town]*. Zavod za varstvo kulturne dediščine Slovenije: Mestni muzej, Muzej in galerije mesta Ljubljane: 121-144.
- Djurić, B., Gale, L., Lozić, E., Kovačič, N. & Okršlar, Š. 2017: Podpeč pri Ljubljani - kamnolom, EŠD 12509; sondiranje. In: Stipančič, & Djurić, B. (eds.): *Arheologija v letu 2017: dediščina za javnost: zbornik povzetkov: 14-15*.
- Djurić, B., Gale, L., Lozić, E. & Rižnar, I. 2018a: On the edge of the known. The quarry landscape at Podpeč. In: Janežič, M., Mulh, T., Nadbath, B. & Žižek, I. (eds.): *Nova odkritja med Alpami in Črnim morjem. Rezultati raziskav rimskodobnih najdišč v obdobju med leti 2005 in 2015 = New Discoveries between the Alps and the Black Sea. Results from the roman sites in the period between 2005 and 2015*, Zbornik 1. mednarodnega arheološkega simpozija / Proceedings of the 1st International Archaeological Conference, Ptuj, 8. in 9. oktober 2015 / Proceedings of the 1st International Archaeological Conference, Ptuj, 8th and 9th October 2015, Monografije CPA 6, 77-87.
- Djurić, B., Gale, L. & Miletić, S. 2018b: Podpeč limestone for colonia Iulia Emona (Regio X. Venetia et Histria). In: Coquelet, C. et al. (eds.): *Roman ornamental stones in Northwestern Europe: natural resources, manufacturing, supply, life & after-life: 107-112*.
- Djurić, B., Gale, L., Brajkovič, R., Bekljanov Zidanšek, I., Horn, B., Lozić, E., Mušič, B. & Vrabc, M. 2022: Kamnolom apnenca v Podpeči pri Ljubljani in njegovi izdelki. *Arheološki Vestnik*, 73: 155-198. <https://doi.org/10.3986/AV.73.06>
- Embry, A. F. & Klovan, J.E. 1971: A Late Devonian Reef Tract on Northeastern Banks Island. *Canadian Petroleum Geology*, 19/4: 730-781.
- Eystein, J. 1989: The use of stable oxygen and carbon isotope stratigraphy as a dating tool. *Quaternary International*, 1/1: 151-166. [https://doi.org/10.1016/1040-6182\(89\)90013-X](https://doi.org/10.1016/1040-6182(89)90013-X)
- Fugagnoli, A. 2004: Trophic regimes of benthic foraminiferal assemblages in Lower Jurassic shallow water carbonates from northeastern Italy (Calcarei Grigi, Trento Platform, Venetia Prealps). *Palaeogeogr., palaeoclimatol., palaeoecol.*, 205: 111-130. <https://doi.org/10.1016/j.palaeo.2003.12.004>
- Galan, E., Carretero, M. I. & Mayoral, E. 1999: A methodology for locating the original quarries used for constructing historical buildings: application to Malaga Cathedral, Spain. *Engineering Geology*, 54/3-4: 287-298. [https://doi.org/10.1016/S0013-7952\(99\)00042-3](https://doi.org/10.1016/S0013-7952(99)00042-3)
- Gale, L. 2015: Microfacies characteristics of the Lower Jurassic lithiotid limestone from Northern Adriatic Carbonate Platform Central Slovenia. *Geologija*, 58/2: 121-138. <https://doi.org/10.5474/geologija.2015.010>
- Gale, L. & Kelemen, M. 2017: Early Jurassic foraminiferal assemblage in platform carbonates of Mt. Krim, central Slovenia. *Geologija*, 60/1: 99-115. <https://doi.org/10.5474/geologija.2017.008>
- Goswami, S., Bhagat, S., Zakauilla, S., Kumar, S. & Rai, A. K. 2017: Role of organic matter in uranium mineralisation in Vempalle dolostone; Cuddapah basin, India. *Journal of the Geological Society of India*, 89/2: 145-154. <https://doi.org/10.1007/s12594-017-0578-y>
- Hamon, Y. & Merzeraud, G. 2007: C and O isotope stratigraphy in shallow-marine carbonate: a tool for sequence stratigraphy (example from the Lodève region, peritethian domain). *Swiss Journal of Geosciences*, 100/1: 71-84. <https://doi.org/10.1007/s00015-007-1206-4>
- Jenkyns, H. C., Jones, C. E., Gröcke, D. R., Hesselbo, S. P. & Parkinson, D. N. 2002: Chemostratigraphy of the Jurassic System: applications, limitations, and implications for palaeoceanography. *Journal of the Geological Society*, 159/4: 351-378. <https://doi.org/10.1144/0016-764901-130>
- Kabal, Y. & Tasli, K. 2003: Biostratigraphy of the Lower Jurassic carbonates from the Aydinick area (Central Taurides, S. Turkey) and morphological analysis of *Lituolipora termieri* (Hottinger, 1967). *J. Foram. Res.*, 33: 338-351.
- Kim, S.T., Mucci, A. & Taylor, B.E. 2007: Phosphoric acid fractionation factors for calcite and aragonite between 25 and 75 °C: Revisited. *Chemical Geology*, 246: 135-146. <https://doi.org/10.1016/j.chemgeo.2007.08.005>
- Kramar, S., Bedjanič, M., Mirtič, B., Mladenovič, A., Rožič, B., Skaberne, D., Gutman, M.,

- Zupančič, N. & Cooper, B. J. 2015: Podpeč limestone: a heritage stone from Slovenia. In: Pereira, D. et al. (eds.): *Global heritage stone: towards international recognition of building and ornamental stones*, London, 219-231. <http://dx.doi.org/10.1144/SP407.2>
- Maritan, L., Mazzoli, C. & Melis, E. 2003: A multi-disciplinary approach to the characterization of Roman gravestones from Aquilea (Udine, Italy). *Archeometry*, 45/3: 363-74. <https://doi.org/10.1111/1475-4754.00114>
- Martinuš, M., Bucković, D. & Kukoč, D. 2012: Discontinuity surfaces recorded in shallow marine platform carbonates: an example from the Early Jurassic of the Velebit Mt. (Croatia). *Facies*, 58: 649-669. <https://doi.org/10.1007/s10347-011-0288-7>
- McArthur, J. M., Howarth R. J. & Shields, G. A. 2012a: Strontium isotope stratigraphy. In: Gradstein, F. M, Ogg, J. G., Schmitz, M. D. & Ogg G.M. (eds): *A Geologic Time Scale 2012*, Elsevier B.V., 1: 127-144. <https://doi.org/10.1016/C2011-1-08249-8>
- McArthur, J.M., Howarth, R.J. & Bailey, T.R. 2012b: Strontium Isotope Stratigraphy: LOWESS Version 3: Best Fit to the Marine Sr-Isotope Curve for 0-509 Ma and Accompanying Look-up Table for Deriving Numerical Age. *The Journal of Geology*, 109/2: 155-170. <https://doi.org/10.1086/319243>
- Miler, M. & Pavšič, J. 2008: Triassic and Jurassic beds in Krim Mountain area (Slovenia). *Geologija*, 51/1: 87-99. <https://doi.org/10.5474/geologija.2008.010>
- Miletić, S., Šmuc, A., Dolenc, M., Miler, M., Mladenovič, A., Gutman Levstik, M. & Dolenc, S. 2021: Identification and provenance determination of stone tesserae used in mosaics from Roman Celeia, Slovenia. *Archaeometry*, 64/3: 561-577. <https://doi.org/10.1111/arcm.12742>
- Mirtič, B., Mladenovič, A., Ramovš, A., Senegačnik, A., Vesel, J. & Vižintin, N. 1999: *Slovenski naravni kamen*. Geološki zavod Slovenije, Zavod za gradbeništvo Slovenije, Naravoslovnotehniška fakulteta, Oddelek za geologijo, Ljubljana: 131 p.
- Munsell color (Firm) 2010: *Munsell rock color charts: with genuine Munsell color chips*. MI: Munsell Color, Grand Rapids.
- Müllner, A. 1879: *Emona, archäologische Studien aus Krain*. I.V. Kleinmayr & F. Bamberg, Laibach.
- Novak, M. 2003: Upper Triassic and Lower Jurassic beds in the Podutik area near Ljubljana (Slovenia). *Geologija*, 46/1: 65-74. <https://doi.org/10.5474/geologija.2003.004>
- Ogorelec, B. & Rothe, P. 1993: Mikrofazies, Diagenese und Geochemie des Dachsteinkalkes und Hauptdolomits in Süd-West-Slowenien = Mikrofazies, diagenesa in geokemija dachsteinskega apnenca ter glavnega dolomita v jugozahodni Sloveniji. *Geologija*, 35: 81-181. <https://doi.org/10.5474/geologija.1992.005>
- Ogorelec, B. 2009: Spodnje jurske plasti v Preserju pri Borovnici. *Geologija*, 52/1: 193-204. <https://doi.org/10.5474/geologija.2009.019>
- Placer, L. 1999: Contribution to the macro-tectonic subdivision of the border region between southern Alps and External Dinarides. *Geologija*, 41: 223-255. <https://doi.org/10.5474/geologija.1998.013>
- Ramovš, A. 1990: *Gliničan od Emone do danes*. Odsek za geologijo, VTOZD Montanistika, Fakulteta za naravoslovje in tehnologijo, Ljubljana: 171 p.
- Ramovš, A. 2000: *Podpeški in črni ter pisani lesnobrajski apnenec skozi čas*. Mineral, Ljubljana: 115 p.
- Romaniello, S.J., Field, M.P., Smith, H.B., Gordon, G.W., Kim, M.H. & Anbar, A.D. 2015: Fully automated chromatographic purification of Sr and Ca for isotopic analysis *Journal of analytical atomic spectrometry*, 30/9: 1906-1912. <https://doi.org/10.1039/c5ja00205b>
- Rosenbaum, J. & Sheppard, S.M. 1986: An isotopic study of siderites, dolomites and ankerites at high temperatures. *Geochim. Cosmochim. Acta*, 50/6: 1147-1150. [https://doi.org/10.1016/0016-7037\(86\)90396-0](https://doi.org/10.1016/0016-7037(86)90396-0)
- Rožič, B., Gale, L., Brajkovič, R., Popit, T. & Žvab Rožič, P. 2018: Lower Jurassic succession at the site of potential Roman quarry Staje near Ig (central Slovenia). *Geologija*, 61/1: 49-71. <https://doi.org/10.5474/geologija.2018.004>
- Šašel Kos, M. 1997: *The Roman Inscriptions in the National Museum of Slovenia / Lapidarij Narodnega muzeja Slovenije*. Situla: razprave Narodnega muzeja Slovenije = dissertationes Musei nationalis Sloveniae, 35: 541 p.
- Šmuc, A., Dolenc, M., Lesar-Kikelj, M., Lux, J., Pflaum, M., Šeme, B., Županek, B., Gale, L., Kramar, S. 2016: Variety of Black and White Limestone Tesserae Used in Ancient Mosaics in Slovenia. *Archaeometry*, 59/2: 205-221. <https://doi.org/10.1111/arcm.12250>
- Veizer, J. 1983: Chemical diagenesis of carbonates: theory and application of trace element

- technique. In: Arthur, M.A., Anderson, T.F., Kaplan, I.R., Veizer, J. & Land, L.S. (eds.): *Stable Isotopes in Sedimentary Geology*. Society of Economic Palaeontologists and Mineralogists, 3-100. <https://doi.org/10.2110/scn.83.10>
- Veizer, J., Ala, D., Azmy, K., Bruckschen, P., Buhl, D., Bruhn, F., Carden, G.A.F., Diener, A., Ebner, S., Godderis, Y., Jasper, T., Korte, C., Pawellek, F., Podlaha, O.G. & Strauss, H. 1999:  $^{87}\text{Sr}/^{86}\text{Sr}$ ,  $\delta^{13}\text{C}$  and  $\delta^{18}\text{O}$  evolution of Phanerozoic seawater. *Chemical Geology*, 161/1-3: 59-88. [https://doi.org/10.1016/S0009-2541\(99\)00081-9](https://doi.org/10.1016/S0009-2541(99)00081-9)
- Velić, I. 2007: Stratigraphy and palaeobiogeography of Mesozoic benthic Foraminifera of the Karst Dinarides (SE Europe). *Geologija Croatica*, 60/1: 1-113.
- Vlahović, I., Tišljar, J., Velić, I. & Matičec, D. 2005: Evolution of the Adriatic Carbonate Platform: Palaeogeography, main events, and depositional dynamics. *Palaeogeography, Palaeoclimatology, Palaeoecology*, 220/3-4: 333-360. <https://doi.org/10.1016/j.palaeo.2005.01.011>
- Vodnik, P., Djurić, B. & Gale, L. 2017: Vrednotenje možnosti lokacije rimskega kamnoloma v Podutiku na podlagi sedimentološke analize. In: Rožič, B. (ed.): 23. posvetovanje slovenskih geologov = 23rd Meeting of Slovenian Geologists. Ljubljana, March 2017. Ljubljana: Univerza v Ljubljani, Naravoslovnotehniška fakulteta, Oddelek za geologijo.
- Vrabc, M. & Fodor, L. 2006: Late Cenozoic tectonics of Slovenia: structural styles at the Northeastern corner of the Adriatic microplate. In: Pinter, N., Greneczy, G., Weber, J., Stein, S. & Medek, D. (eds.): *The Adria microplate: GPS geodesy, tectonics, and hazards*. NATO Sei. Ser., IV, Earth Environ. Sei., 61: 151-168. [https://doi.org/10.1007/1-4020-4235-3\\_10](https://doi.org/10.1007/1-4020-4235-3_10)
- Weis, D., Kieffer, B., Maerschalk, C., Barling, J., de Jong, J., Williams, G.A., Hanano, D., Pretorius, W., Mattielli, N., Scoates, J.S., Goolaerts, G., Friedman, R.M. & Mahony, J.B. 2006: High-precision isotopic characterization of USGS reference materials by TIMS and MC-ICP-MS. *Geochemistry, Geophysics, Geosystems.*, 7/8: 1-30. <https://doi.org/10.1029/2006GC001283>
- Wright, V.P. 1992: A revised classification of limestones. *Sedimentary Geology*, 76/3-4: 177-185. [https://doi.org/10.1016/0037-0738\(92\)90082-3](https://doi.org/10.1016/0037-0738(92)90082-3)

## Navodila avtorjem

**GEOLOGIJA** objavlja znanstvene in strokovne članke s področja geologije in sorodnih ved. Revija izhaja dvakrat letno. Članke recenzirajo domači in tuji strokovnjaki z obravnavanega področja. Ob oddaji člankov avtorji lahko predlagajo **tri recenzente**, uredništvo pa si pridržuje pravico do izbire recenzentov po lastni presoji. Avtorji morajo članek popraviti v skladu z recenzentskimi pripombami ali utemeljiti zakaj se z njimi ne strinjajo.

**Avtorstvo:** Za izvirnost podatkov, predvsem pa mnenj, idej, sklepov in citirano literaturo so odgovorni avtorji. Z objavo v GEOLOGIJI se tudi obvežejo, da ne bodo drugje objavili prispevka z isto vsebino.

Avtorji z objavo prispevka v GEOLOGIJI potrjujejo, da se strinjajo, da je njihov prispevek odprto dostopen z izbrano licenco **CC-BY**.

**Jezik:** Članki naj bodo napisani v angleškem, izjemoma v slovenskem jeziku, vsi pa morajo imeti slovenski in angleški izvleček. Za prevod poskrbijo avtorji prispevkov sami.

### Vrste prispevkov:

#### Izvirni znanstveni članek

Izvirni znanstveni članek je prva objava originalnih raziskovalnih rezultatov v takšni obliki, da se raziskava lahko ponovi, ugotovitve pa preverijo. Praviloma je organiziran po shemi **IMRAD (Introduction, Methods, Results, And Discussion)**.

#### Pregledni znanstveni članek

Pregledni znanstveni članek je pregled najnovejših del o določenem predmetnem področju, del posameznega raziskovalca ali skupine raziskovalcev z namenom povzemanja, analiziranja, evalvirati ali sintetizirati informacije, ki so že bile publicirane. Prinaša nove sinteze, ki vključujejo tudi rezultate lastnega raziskovanja avtorja.

#### Strokovni članek

Strokovni članek je predstavitev že znanega, s poudarkom na uporabnosti rezultatov izvirnih raziskav in širjenju znanja.

#### Diskusija in polemika

Prispevek, v katerem avtor ocenjuje ali komentira neko delo, objavljeno v GEOLOGIJI, ali z avtorjem strokovno polemizira.

#### Recenzija, prikaz knjige

Prispevek, v katerem avtor predstavlja vsebino nove knjige.

**Oblika prispevka:** Besedilo pripravite v urejevalniku Microsoft Word. Prispevki naj praviloma ne bodo daljši od 20 strani formata A4, v kar so vštete tudi slike, tabele in table. Le v izjemnih primerih je možno, ob predhodnem dogovoru z uredništvom, tiskati tudi daljše prispevke.

Članek oddajte uredništvu vključno z vsemi slikami, tabelami in tablamami v elektronski obliki po naslednjem sistemu:

- Naslov članka (do 12 besed)
- Avtorji (ime in priimek, poštni in elektronski naslov)
- Ključne besede (do 7 besed)
- Izvleček (do 300 besed)
- Besedilo
- Literatura
- Podnaslovi slik in tabel
- Tabele, Slike, Table

**Citiranje:** V literaturi naj avtorji prispevkov praviloma upoštevajo le objavljene vire. Poročila in rokopise naj navajajo le v izjemnih primerih, z navedbo kje so shranjeni. V seznamu literature naj bodo navedena samo v članku omenjena dela. Citirana dela, ki imajo DOI identifikator (angl. Digital Object Identifier), morajo imeti ta identifikator izpisan na koncu citata. Za citiranje revije uporabljamo standardno okrajšavo naslova revije. Med besedilom prispevka citirajte samo avtorjev priimek, v oklepaju pa navajajte letnico izida navedenega dela in po potrebi tudi stran. Če navajate delo dveh avtorjev, izpišite med tekstom prispevka oba priimka (npr. Pleničar & Buser, 1967), pri treh ali več avtorjih pa napišite samo prvo ime in dodajte et al. z letnico (npr. Mlakar et al., 1992). Citiranje virov z medmrežja v primeru, kjer avtor ni poznan, zapišemo (Internet 1). V seznamu literaturo navajajte po abecednem redu avtorjev.

Imena fosilov (rod in vrsta) naj bodo napisana poševno, imena višjih taksonomskih enot (družina, razred, itn.) pa normalno. Imena avtorjev taksonov naj bodo prav tako napisana normalno, npr. *Clypeaster pyramidalis* Michelin, *Galeanella tollmanni* (Kristan), Echinoidea.

### Primeri citiranja članka:

Mali, N., Urbanc, J. & Leis, A. 2007: Tracing of water movement through the unsaturated zone of a coarse gravel aquifer by means of dye and deuterated water. *Environ. geol.*, 51/8: 1401–1412. <https://doi.org/10.1007/s00254-006-0437-4>

Pleničar, M. 1993: *Apricardia pachiniana* Sirna from lower part of Liburnian beds at Divača (Triest-Komen Plateau). *Geologija*, 35: 65–68

### Primer citirane knjige:

Flügel, E. 2004: *Mikrofacies of Carbonate Rocks*. Springer Verlag, Berlin: 976 p.

Jurkovič, B., Toman, M., Ogorelec, B., Šribar, L., Drobne, K., Poljak, M. & Šribar, Lj. 1996: Formacijska geološka karta južnega dela Tržaško-komenske planote – Kredne in paleogenske kamnine 1: 50.000 = Geological map of the southern part of the Trieste-Komen plateau – Cretaceous and Paleogene carbonate rocks. Geološki zavod Slovenije, Ljubljana: 143 p., incl. Pls. 23, 1 geol. map.

### Primer citiranja poglavja iz knjige:

Turnšek, D. & Drobne, K. 1998: Paleocene corals from the northern Adriatic platform. In: Hottinger, L. & Drobne, K. (eds.): *Paleogene Shallow Benthos of the Tethys*. Dela SAZU, IV. Razreda, 34/2: 129–154, incl. 10 Pls.

### Primer citiranja virov z medmrežja:

Če sta znana avtor in naslov citirane enote zapišemo:

Čarman, M. 2009: Priporočila lastnikom objektov, zgrajenih na nestabilnih območjih. Internet: [http://www.geo-zs.si/UserFiles/1/File/Nasveti\\_lastnikom\\_objektov\\_na\\_nestabilnih\\_tleh.pdf](http://www.geo-zs.si/UserFiles/1/File/Nasveti_lastnikom_objektov_na_nestabilnih_tleh.pdf) (17. 1. 2010)

Če avtor ni poznan zapišemo tako:

Internet: <http://www.geo-zs.si/> (22. 10. 2009)

Če se navaja več enot z medmrežja, jim dodamo še številko:

Internet 1: <http://www.geo-zs.si/> (15. 11. 2000)

Internet 2: <http://www.geo-zs.si/> (10. 12. 2009)

**Slike, tabele in table:** Slike (ilustracije in fotografije), tabele in table morajo biti zaporedno oštevilčene in označene kot sl. 1, sl. 2 itn., oddane v formatu TIFF, JPG, EPS ali PDF z ločljivostjo 300 dpi. Le izjemoma je možno objaviti tudi barvne slike, vendar samo po predhodnem dogovoru z uredništvom. Če avtorji oddajo barvne slike bodo te v barvah objavljene samo v spletni različici članka. Pazite, da bo tudi slika tiskana v sivi tehniki berljiva. Grafični materiali naj bodo usklajeni z zrcalom revije, kar pomeni, da so široki največ 172 mm (ena stran) ali 83 mm (pol strani, en stolpec) in visoki največ 235 mm. Večjih formatov od omenjenega zrcala GEOLOGIJE ne tiskamo na zgib, je pa možno, da večje oziroma daljše slike natisnemo na dveh straneh (skupaj na levi in desni strani) z vmesnim "rezom". V besedilu prispevka morate omeniti vsako sliko po številčnem vrstnem redu. Dovoljenja za objavo slikovnega gradiva iz drugih revij, publikacij in knjig, si pridobijo avtorji sami.

Če je članek napisan v slovenskem jeziku, mora imeti celotno besedilo, ki je na slikah in tabelah tudi v angleškem jeziku. Podnaslovi naj bodo čim krajši.

**Korekture:** Avtorji prejmejo po elektronski pošti članek v avtorski pregled. Popravijo lahko samo tiskarske napake. Krajši dodatki ali spremembe pri korekturah so možne samo na avtorjeve stroške.

Prispevki so prosto dostopni na spletnem mestu: <http://www.geologija-revija.si/>

### Oddaja prispevkov:

Avtorje prosimo, da prispevke oddajo v elektronski obliki na naslov uredništva:

### GEOLOGIJA

Geološki zavod Slovenije

Dimičeva ulica 14, SI-1000 Ljubljana

[bernarda.bole@geo-zs.si](mailto:bernarda.bole@geo-zs.si) ali [urednik@geologija-revija.si](mailto:urednik@geologija-revija.si)

## Instructions for authors

**Scope of the journal:** GEOLOGIJA publishes scientific papers which contribute to understanding of the geology of Slovenia or to general understanding of all fields of geology. Some shorter contributions on technical or conceptual issues are also welcome. Occasionally, a collection of symposia papers is also published.

All submitted manuscripts are peer-reviewed. When submitting paper, authors can suggest **three reviewers**. Note that the editorial office retains the sole right to decide whether or not the suggested reviewers are used. Authors should correct their papers according to the instructions given by the reviewers. Should you disagree with any part of the reviews, please explain why. Revised manuscript will be reconsidered for publication.

**Author's declaration:** Submission of a paper for publication in GEOLOGIJA implies that the work described has not been published previously, that it is not under consideration for publication elsewhere and that, if accepted, it will not be published elsewhere.

Authors agree that their contributions published in GEOLOGIJA are open access under the licence [CC-BY](#).

**Language:** Papers should be written in English or Slovene, and should have both English and Slovene abstracts.

### Types of papers:

#### Original scientific paper

In an original scientific paper, original research results are published for the first time and in such a form that the research can be repeated and the results checked. It should be organised according to the IMRAD scheme (Introduction, Methods, Results, And Discussion).

#### Review scientific paper

In a review scientific paper the newest published works on specific research field or works of a single researcher or a group of researchers are presented in order to summarise, analyse, evaluate or synthesise previously published information. However, it should contain new information and/or new interpretations.

#### Professional paper

Technical papers give information on research results that have already been published and emphasise their applicability.

#### Discussion paper

A discussion gives an evaluation of another paper, or parts of it, published in GEOLOGIJA or discusses its ideas.

#### Book review

This is a contribution that presents a content of a new book in the field of geology.

### Style guide:

Submitted manuscripts should not exceed 20 pages of A4 format including figures, tables and plates. Only exceptionally and in agreement with the editorial board longer contributions can also be accepted.

Manuscripts submitted to the editorial office should include figures, tables and plates in electronic format organized according to the following scheme:

- Title (*maximum 12 words*)
- Authors (*full name and family name, postal address and e-mail address*)
- Key words (*maximum 7 words*)
- Abstract (*maximum 300 words*)
- Text
- References
- Figure and Table Captions
- Tables, Figures, Plates

**References:** References should be cited in the text as follows: (Flügel, 2004) for a single author, (Pleničar & Buser, 1967) for two authors and (Mlakar et al., 1992) for multiple authors. Pages and figures should be cited as follows: (Pleničar, 1993, p. 67) and (Pleničar, 1993, fig. 1). Anonymous internet resources should be cited as (Internet 1). Only published references should be cited. Manuscripts should be cited only in some special cases in which it also has to be stated where they are kept. Cited reference list should include only publications that are mentioned in the paper. Authors should be listed alphabetically. Journal titles should be given in a standard abbreviated form. A DOI identifier, if there is any, should be placed at the end as shown in the first case below.

Taxonomic names should be in italics, while names of the authors of taxonomic names should be in normal, such as *Clypeaster pyramidalis* Michelin, *Galeanella tollmanni* (Kristan), Echinoidea.

### Articles should be listed as follows:

Mali, N., Urbanc, J. & Leis, A. 2007: Tracing of water movement through the unsaturated zone of a coarse gravel aquifer by means of dye and deuterated water. *Environ. geol.*, 51/8: 1401–1412. <https://doi.org/10.1007/s00254-006-0437-4>

Pleničar, M. 1993: *Apricardia pachiniana* Sirna from lower part of Liburnian beds at Divača (Triest-Komen Plateau). *Geologija*, 35: 65–68.

### Books should be listed as follows:

Flügel, E. 2004: *Mikrofacies of Carbonate Rocks*. Springer Verlag, Berlin: 976 p.

Jurkovšek, B., Toman, M., Ogorelec, B., Šribar, L., Drobne, K., Poljak, M. & Šribar, Lj. 1996: Formacijska geološka karta južnega dela Tržaško-komenske planote – Kredne in paleogenske kamnine 1: 50.000 = Geological map of the southern part of the Trieste-Komen plateau – Cretaceous and Paleogene carbonate rocks. Geološki zavod Slovenije, Ljubljana: 143 p., incl. Pls. 23, 1 geol. map.

### Book chapters should be listed as follows:

Turnšek, D. & Drobne, K. 1998: Paleocene corals from the northern Adriatic platform. In: Hottinger, L. & Drobne, K. (eds.): *Paleogene Shallow Benthos of the Tethys*. Dela SAZU, IV. Razreda, 34/2: 129–154, incl. 10 Pls.

### Internet sources should be listed as follows:

Known author and title:

Čarman, M. 2009: Priporočila lastnikom objektov, zgrajenih na nestabilnih območjih. Internet: [http://www.geo-zs.si/UserFiles/1/File/Nasveti\\_lastnikom\\_objektov\\_na\\_nestabilnih\\_tleh.pdf](http://www.geo-zs.si/UserFiles/1/File/Nasveti_lastnikom_objektov_na_nestabilnih_tleh.pdf) (17. 1. 2010)

Unknown authors and title:

Internet: <http://www.geo-zs.si/> (22.10.2009)

When more than one unit from the internet are cited they should be numbered:

Internet 1: <http://www.geo-zs.si/> (15.11. 2000)

Internet 2: <http://www.geo-zs.si/> (10.12. 2009)

**Figures, tables and plates:** Figures (illustrations and photographs), tables and plates should be numbered consecutively and marked as Fig. 1, Fig. 2 etc., and saved as TIFF, JPG, EPS or PDF files and submitted at 300 dpi. Colour pictures will be published only on the basis of previous agreement with the editorial office. If, together with the article, you submit colour figures then these figures will appear in colour only in the Website version of the article. Be careful that the grey scale printed version is also readable. Graphic materials should be adapted to the journal's format. They should be up to 172 mm (one page) or 83 mm wide (half page, one column), and up to 235 mm high. Larger formats can only be printed as a double-sided illustration (left and right) with a cut in the middle. All graphic materials should be referred to in the text and numbered in the sequence in which they are cited. The approval for using illustrations previously published in other journals or books should be obtained by each author.

When a paper is written in Slovene it has to have the entire text which accompanies illustrations and tables written both in Slovene and English. Figure and table captions should be kept as short as possible.

**Proofs:** Proofs (in pdf format) will be sent by e-mail to the corresponding author. Corrections are made by the authors. They should correct only typographical errors. Short additions and changes are possible, but they will be charged to the authors.

GEOLOGIJA is an open access journal; all pdfs can be downloaded from the website: <http://www.geologija-revija.si/en/>

**Submission:** Authors should submit their papers in electronic form to the address of the GEOLOGIJA editorial office:

### GEOLOGIJA

Geological Survey of Slovenia  
Dimičeva ulica 14, SI-1000 Ljubljana, Slovenia  
[bernarda.bole@geo-zs.si](mailto:bernarda.bole@geo-zs.si) or [urednik@geologija-revija.si](mailto:urednik@geologija-revija.si)

- 5 Žorž, M., Voudouris, P. & Rieck, B.  
Pyrite with lower cubic symmetry from Lavrion, Greece
- 21 Elster, D., Szócs, T., Gál, N., Hansen, B., Voutchkova, D.D., Schullehner, J., Lions, J. Martarelli, L., Giménez-Forcada, E., DÍaz-Muñoz, J.Á., Malcuit, E., Schubert, G., Hobiger, G. & Rman, N.  
Terminologies and characteristics of natural mineral and thermal waters in selected European countries
- 47 Ivšinović, J. & Malvić, T.  
Comparison of mapping efficiency for small datasets using inverse distance weighting vs. moving average, Northern Croatia Miocene hydrocarbon reservoir
- 59 Markič, M. & Kanduč, T.  
Carbon isotopic composition of methane and its origin in natural gas from the Petišovci-Dolina oil and gas field (Pannonian Basin System, NE Slovenia) – a preliminary study
- 73 Kralj, P.  
Rare earth elements and yttrium in cold mineral and thermal (Ö30-60 °C) waters from Tertiary aquifers in the Mura Basin, north-eastern Slovenia: A review
- 93 Diercks, M., Grützner, C., Vrabec, M. & Ustaszewski, K.  
Addendum to Diercks et al., 2021: A model for the formation of the Pradol (Pradolino) dry valley in W Slovenia and NE Italy
- 101 Brajkovič, R., Gale, L. & Djurić, B.  
Multi-method study of the Roman quarry at Podpeč sedimentary succession and stone products